eurad

**European Joint Programme
on Radioactive Waste Management**

Deliverable 17.7:

Synthesis report on Innovative and Enhanced Equipment for Repository Monitoring

Work Package 17

http://www.ejp-eurad.eu/

EURAD Deliverable 17.7 – Synthesis report on Innovative and Enhanced Equipment for Repository Monitoring

Document information.

Project Acronym	**EURAD**
Project Title	**European Joint Programme on Radioactive Waste Management**
Project Type	**European Joint Programme (EJP)**
EC grant agreement No.	**847593**
Project starting / end date	**1st June 2019 – 30 May 2024**
Work Package No.	**17**
Work Package Title	**Monitoring Equipment and Data Treatment for Safe Repository Operation and Staged Closure**
Work Package Acronym	**MODATS**
Deliverable No.	**17.7**
Deliverable Title	**Synthesis report on Innovative and Enhanced Equipment for Repository Monitoring**
Lead Beneficiary	**Andra**
Contractual Delivery Date	**30 May 2024**
Actual Delivery Date	**4 June 2024**
Type	**Report**
Dissemination level	**Public**
Authors	**Johan BERTRAND (Andra), Edgar MANUKYAN (Nagra), Pierre DICK (IRSN), Rüdiger GIESE (GFZ-Potsdam), Tommi PIRTTISALO (Posiva), Johanna HANSEN (Posiva), Jeremy PERROT (Université de Saint-Etienne), Denis DOIZI (CEA), Tobias VOGT (Nagra), Mykola SAPON (SSTC NRS), Sam PARSONS (NWS)**

To be cited as:

J. Bertrand, E. Manukyan, P Dick, R. Giese, To Pirttisalo, J. Hansen, J. Perrot, D. Doizi, T. Vogt, M. Sapon, S. Parsons (2024): Synthesis report on Innovative and Enhanced Equipment for Repository Monitoring. Final version as of MODATS of deliverable D17.7 of the HORIZON 2020 project EURAD. EC Grant agreement no: 847593.

Disclaimer

Acknowledgement

EURAD (Deliverable n° 17.7) - Synthesis report on Innovative and Enhanced Equipment for Repository Monitoring
Dissemination level: PUBLIC
Date of issue of this report: 04/06/2024

Page 1

Status of deliverable		
	By	Date
Delivered (Lead Beneficiary)	Johan BERTRAND (Andra)	31 /03/2024
Verified (WP Leader)	Edgar Bohner (VTT) Task 3 members	26/04/2024
Reviewed (Reviewers)	PART A :José-Luis Sineriz (Amphos21) Part B :	21/05/2024
Approved (PMO)	Bharti Reddy (NWS)	01/6/2024
Submitted to EC	Andra (Coordinator)	04/06/2024

![eurad logo] European Joint Programme on Radioactive Waste Management

EURAD (Deliverable n° 17.7) - Synthesis report on Innovative and Enhanced Equipment for Repository Monitoring
Dissemination level: PUBLIC
Date of issue of this report: 04**/06/2024**

Page 2

PART A: Synthesis report on Innovative and Enhanced Equipment for Repository Monitoring

EURAD (Deliverable n° 17.7) - Synthesis report on Innovative and Enhanced Equipment for Repository Monitoring
Dissemination level: PUBLIC
Date of issue of this report: 04/06/2024

Page 3

Executive Summary

The Monitoring Equipment and Data Treatment for Safe Repository Operation and Staged Closure (MODATS) work package (WP) of the European Joint Programme on Radioactive Waste Management (EURAD) is conducting research, development and demonstration (RD&D) into: monitoring data acquisition, treatment and management; use of monitoring data to enhance system understanding, including development of digital twins; interactions with civil society and other stakeholders; development of monitoring technologies; and development of knowledge regarding repository monitoring.

The focus of MODATS is monitoring during the operational phase of repository programmes to build further confidence in the long-term safety case. MODATS is focusing on confidence in monitoring data. There are challenges associated with monitoring data acquired during repository operations, including challenges associated with its management (including processing and storage), acquisition, modelling and visualisation.

For example, it should be demonstrated before deployment that monitoring equipment can operate in the environmental conditions in which it is being emplaced within the repository. These conditions may include high temperatures, high pressures, humidity and/or submersion, chemically aggressive environments, and levels of radiation that may degrade electrical and optical cables performances. The equipment may be required to operate for long periods (possibly without access for maintenance), with a high level of confidence in the signal, and without interfering with barrier performances, in particular as pertaining to long term safety.

In the Modern2020 and Modern projects, extensive research, development, and demonstration (RD&D) activities have been undertaken to increase the toolbox of monitoring techniques from which a monitoring programme can be developed, considering the above challenges. The ability to monitor the disposal system and the extent to which such monitoring can provide detailed understanding of the disposal system evolution can be enhanced through development of novel technologies, and there is a need to further develop the most promising novel technologies.

To monitor with confidence during the operational phase, there could be a requirement to develop remote monitoring technologies (non-invasive inspection, non-destructive methods techniques (NDT)) in combination with in-situ monitoring to have redundancy measurement without interaction with the engineered barrier.

There also could be requirement to develop monitoring technologies that can quantify parameters difficult to measure, such as water saturation, pH, corrosion rate. Accurate measurements of these parameters offer could offer a better understanding by reducing the uncertainty on the monitoring process. To monitor with confidence, there is a requirement to greater understanding of the interactions between monitoring sensors and the medium in which they are emplaced, to ensure the monitoring equipment is not impacting the performance of the multibarrier to an unacceptable level.

The work in Task 3 of MODATS was divided into three main themes main directions:

- Develop innovative sensors and geophysical techniques to measure and infer parameters that are difficult to obtain for long-term monitoring.
- Develop and qualify optical sensors to get them ready to be used in the initial phase of the development of the geological disposal for temperature and strain measurement.
- Develop a roadmap for technology development, to ensure that technologies can be used with confidence from the start of repository operations.

The main results obtained during the MODATS WP are important about the monitoring technologies perspectives because of at the first time, the importance of Artificial intelligence (AI) and machine learning (ML) to improve the measurement performance has been clearly highlighted. AI/ML facilitate the analyse of row data to monitoring parameters that are useful to evaluate the performance behaviour of the geological disposal. AI/ML have shown immense potential in understanding complex data like geophysical methods or image processing. In the same time, optical fibre sensor (OFS) technology has

EURAD (Deliverable n° 17.7) - Synthesis report on Innovative and Enhanced Equipment for Repository Monitoring
Dissemination level: PUBLIC
Date of issue of this report: 04**/06/2024**

Page 4

reached a new level of maturity: OFS are now ready for industrial geological disposal application with potential to have access to chemical parameters.

More detailed conclusions on monitoring technology developed during the MODATS WP are summarised below.

Geophysical methods

Geophysical methods can estimate material properties away from the sensors. However, geophysical methods also suffer from some deficiencies. Firstly, they are often ambiguous, that is, several subsurface models explain the data equally well. Depending on the method(s) employed, they can offer only limited spatial and/or temporal resolution. Finally, geophysical methods yield physical material properties, such as elasticity parameters, density, or electrical conductivities, and it is not straightforward to translate these material properties to parameters of interest (i.e., temperature, pressure, etc.).

One of the main advantages of geophysical technologies is the spatial information it could provide on relevant parameters (in contrast to point information, obtained with traditional point sensors). A combination of machine learning (ML), geophysical measurements and local water content information has been used in MODATS to demonstrate the feasibility of obtaining tomographic images of humidity distribution in a granular bentonite mixture.

Electrical methods

The Induced Polarization (IP) characterizes the ability of a medium to store charges reversibly under a slowly alternating electrical field. In MODATS, it was demonstrated that Spectral Induced Polarisation (SIP) is not only sensitive to variations in water content but also to the mineralogical and chemical variability of the water and bentonite Furthermore, it is feasible to relate parameters from the SIP technique to permeability and thus it offers a potential method to image in 4D the permeability of porous media. However, further RD&D is required before this technique can be confidently deployed for this purpose.

Automatic passive seismic monitoring

An algorithm was developed by Institute of Mine Seismology (IMS) to automatically classify seismic events. It utilizes ML algorithms and is used with their seismic analysis software "IMS Combined". In MODATS, the algorithm was evaluated based on selected data: It was able to correctly classify 97% of events from the ONKALO database of seismic events, occurring from 2021 to 2023. The number of false positives, i.e. falsely accepted events, was still quite high with only 77% of manually rejected events being correctly rejected by the algorithm.

Further training of the algorithm is still required before full integration in daily analysis routines. The results obtained so far, in the framework of MODATS WP, are promising and field use is expected soon.

Water leakage identification

A review of literature was undertaken in MODATS to identify the most promising technique for automatic mapping of underground water leakages. Standard thermal imaging provides the possibility to detect different type of inflows in conditions where different structures like shotcrete, steel mesh reinforcement and other tunnel infra may disturb the results and was therefore judged to be the most promising technique. The potential of the method has already been assessed in different studies (e.g. Neretnieks et al 2018), where the main conclusion was that thermal imaging (with an IR camera) can be used to locate and identify spots with even very low leakage flow rates in fractured crystalline rocks. This study was not directly used to repeated flow mapping but to characterise leaking fractures.

Even leakages of less than 1 ml/min were identified with this method. Thermal imaging alone only gives qualitative information, but together with fracture geometry and 3D fracture network models, it could give better understanding of inflows (Neretnieks et al 2018). The next phase is to conduct a ML exercise to distinguish different semiquantitative results on number of inflows.

EURAD (Deliverable n° 17.7) - Synthesis report on Innovative and Enhanced Equipment for Repository Monitoring
Dissemination level: PUBLIC
Date of issue of this report: 04/06/2024

Page 5

Even though thermal imaging has some challenges, it could be applied to assist in manual leakage mapping. Thermal images/recordings could be used to automatically identify the leakages and to digitize them. In practice, this would mean taking images and using photogrammetry (Huang et al. 2020) and pattern recognition to map the anomalies to the tunnel profile. After anomalies are digitized, the mapping personnel could then determine the amount of inflow in each anomaly by other means, for example by visual observation.

Radiation tolerant optical cables.

Optical fibers offer many advantages compared to point sensors. It offers distributed and time resolved measurements with high spatial resolution in harsh environments. It is possible to adapt its composition and structure to match the sensors capabilities to the desired requirements. In addition, optical fibers can be used to provide 3D maps of temperature and strain at the location of the optical fiber depending on the spatial resolution of the interrogation technique.

The study focused on the effects of gamma irradiation on radiation-hardened optical fibers. The RD&D will next consider the effects of neutrons, as well as the investigation of cable coatings. ANDRA is actively involved in developing new cables specifically designed for this application. It's important to note that this work is still in the development phase.

This irradiation campaign testing radiation tolerance of six optical cables under a mixed field neutron/gamma at low doses (~ 1.7Gy) has been conducted. Six cables with different structures have been investigated under and after irradiation. The results obtained in the irradiation campaign give good candidates to be used in strong nuclear environment and also external coating requirement for optical cable.

Optical pH sensor.

A proof-of-concept optical pH sensor has been developed. It is based on a simple concept involving the immobilization of a chemical recognition phase sensitive to pH variation on a surface part of the optical chain. This concept uses light to measure variations in optical properties resulting from interactions between the aqueous system to be analyzed and the chemical recognition phase of the probe. The immobilization technique for this chemical recognition phase, demonstrated in MODATS, is an important step in the development of these optical probes. A white light source is injected into a multimode optical fiber. The fiber carries the light to the measurement location. A mirror, positioned in front of the fiber, sends the light back on a multimode optical fiber to a spectrometer for spectral analysis. A computer software enables the spectral responses processing. The interaction of the immobilized organic layer with the protons contained in a given sample, in the presence of light, leads to variations in optical properties. The chemical recognition phase can be covalently immobilized on the end of the metallized optical fiber or on the 316L stainless steel mirror.

The first results obtained from testing in Bure for two different optical configurations lead to a measured value of pH~6 for poral water. These preliminary results are very encouraging because they are independent of the localization of the grafting (fiber or mirror) and are very close to the value pH ~7 measured by conventional on-site pH sensors. It is a promising technique, although further testing is required.

Strain measurement with optical fibre.

The understanding of ground response and induced strains in the tunnel lining, when tunnelling for a deep geology repository, is needed for the design of the construction technology to comply with operational and long-term safety requirements. To test different tunnel support systems in the sandy facies of the Swiss host rock Opalinus Clay, the TS Experiment at the Mont Terri underground research laboratory URL was initiated. The ground response and strains in the lining during and after excavation are monitored by conventional convergence measurements (3D-optical displacement measurements by means of total station and reflectors), as well as with different fibre-optic strain sensing methods.

EURAD (Deliverable n° 17.7) - Synthesis report on Innovative and Enhanced Equipment for Repository Monitoring
Dissemination level: PUBLIC
Date of issue of this report: 04/06/2024

Page 6

Different optical fiber techniques have been used to evaluate the performance of each technique. Distributed measurements based on Rayleigh and Brillouin were compared to Bragg fibre grating.

In general, Optical Backscatter Reflectometer (OBR) data provide the highest resolution deformation data in the tunnel lining, compared to the other monitoring techniques. The results also show that a high spatial resolution (in millimetre range) is required to characterize the behaviour of tunnel lining.

Source of hardness

In MODATS, RD&D was undertaken to examine sensor capabilities and to evaluate the impacts of repository-like harsh environment conditions on their performance. The monitoring system should be robust and durable as required, owing to the limited possibility for maintenance and repair for inaccessible sensors.

An analysis of literature data on environmental conditions was carried out, considering temperature, mechanical pressure, hydraulic pressure, salinity, radiation, displacement, etc. in different types of rocks (crystalline, argillaceous, salt) and different locations around the repository (from the waste package to the far-field rock).

Based on the results of the analysis, it was established that the maximum temperature, sensors, and other equipment could have to operate in, are in repositories hosted in salt rocks, where temperature of 200 ºC could be experienced adjacent to the waste package in the buffer and near-field rock. A maximum mechanical pressure of 42 MPa could be experienced in salt and crystalline host rocks, in the buffer adjacent to the waste package and in the near-field rock. Regarding hydraulic pressure and salinity (not expected in salt rock), up to 9.5 MPa and up to 70 g/l, respectively, could be expected for all locations in a repository in crystalline and argillaceous host rocks. But regarding radiation effects, the maximum impacts are expected in the buffer and waste package and will be as high as 10 Gy/h regardless of the type of rock.

Future needs

Work performed in MODATS aims to provide a monitoring technology RD&D roadmap that can be used to help plan research, targeted enhancements, and/or the development of novel technologies, tailored to the specific demands of the repository. By identifying the gaps between existing monitoring sensor/system capabilities and the technical requirements (expected in their deployment in the repository), this methodology aims to pave the way for the implementation of more robust, reliable, and tailored monitoring solutions.

The methodology employs a matrix approach, cross-comparing technology capabilities and limitations and technical requirements for 36 technology/parameter combinations. Identified developmental needs are grouped into 14 categories and aggregated into 3 families, forming the basis for a generic technology development roadmap.

The issues directly revealed by the matrices relate to the performance of the technology in harsh environmental conditions and its ability to fulfil the data quality objectives (DQOs). When the technology is unable to operate owing to physical conditions, it means that it lacks the necessary robustness. In this analysis such identified issues include:

- Unable to withstand high relative humidity.
- Unable to withstand high salinity.
- Unable to withstand high pressure.
- Unable to withstand high temperature.
- Suffering from radiation.

The matrix analysis also reveals issues relating to meeting DQOs, including:

- Cannot measure expected range.
- Insufficient lifetime.

EURAD (Deliverable n° 17.7) - Synthesis report on Innovative and Enhanced Equipment for Repository Monitoring
Dissemination level: PUBLIC
Date of issue of this report: 04/06/2024

Page 7

- Insufficient accuracy.
- Significant drift.

In addition, other specific issues are identified from a literature review, including:

- Unsatisfactory measurement repeatability.
- Unsatisfactory sensor attachment.
- Unsuitable power supply.
- Unsuitable sampling.
- Require calibration procedure and scaling relationships for the interpretation of signal.

The roadmap, which fits into the Modern2020 Screening Methodology, addresses the critical question of parameter feasibility. Its flexibility is evident in assessment gates and activities suggesting processes based on answers. An initial gate upstream of the proposed workflow, explores reasons for parking processes, parameters, and technologies resulting from the Modern2020 screening workflow, leading to four possible responses and specific activities. Assessment gates evaluate technology development based on three critical questions that would cover the three methods for identifying issues with existing technologies that include the 14 needs identified previously:

- Can the technology fulfil data quality objectives?
- Can the technology be installed and operated?
- Can the technology withstand relevant expected conditions within the repository?

These questions constitute an assessment common to three main such gate/activity couples that each act as sub-workflows; one devoted to standard laboratory testing of technology, one to demonstration in a repository-like environment (e.g., underground research laboratory), and one to demonstration in the site-specific repository, which is not always required. Positive responses to the assessment gates lead to next sub-workflow activities and eventually deployment, whereas negative responses initiate sub-activities, allowing for identification of reasons for failure, proposition and selection of development options, and actual development.

The roadmap's flexibility accommodates sequential or parallel undertaking of these sub-workflows and related activities based on ongoing technology developments, ensuring scalability and adaptability.

Acknowledging diverse technology development stages, the roadmap offers flexibility in workflow execution, incorporating assessment gates for evaluation and iterative development processes, and for continuous improvement. The absence of a fixed timeline underscores a commitment to practicality, allowing waste management organizations (WMOs) to tailor the roadmap to their unique needs, recognizing diverse contexts and programmatic intricacies. Addressing challenges corresponding to project size, WMOs can use the roadmap as a guideline, adapting the pace and intensity of each stage to their programmes. The study emphasizes a strategic and adaptable approach to monitoring technology development.

Confidence in monitoring data can be achieved if the acquisition, management and use of the data is appropriate for the purpose for which it has been acquired. Therefore, in terms of providing confidence in monitoring data associated with long-term safety, confidence in monitoring data can be built if the methods and technologies used to acquire, manage and use it contribute to meeting the purposes of monitoring identified by the IAEA-TECDOC 1208. MODATS contribute to use of novel technologies that can extend the current capabilities of monitoring technologies and allow additional information to be gained during repository operation.

EURAD (Deliverable n° 17.7) - Synthesis report on Innovative and Enhanced Equipment for Repository Monitoring
Dissemination level: PUBLIC
Date of issue of this report: 04/06/2024

Page 8

Table of Contents

EURAD (Deliverable n° 17.7) - Synthesis report on Innovative and Enhanced Equipment for Repository Monitoring
Dissemination level: PUBLIC
Date of issue of this report: 04/06/2024

Page 9

EURAD (Deliverable n° 17.7) - Synthesis report on Innovative and Enhanced Equipment for Repository Monitoring
Dissemination level: PUBLIC
Date of issue of this report: 04**/06/2024**

Page

EURAD (Deliverable n° 17.7) - Synthesis report on Innovative and Enhanced Equipment for Repository Monitoring
Dissemination level: PUBLIC
Date of issue of this report: 04**/06/2024**

Page

EURAD (Deliverable n° 17.7) - Synthesis report on Innovative and Enhanced Equipment for Repository Monitoring
Dissemination level: PUBLIC
Date of issue of this report: 04**/06/2024**

Page

List of figures

EURAD (Deliverable n° 17.7) - Synthesis report on Innovative and Enhanced Equipment for Repository Monitoring
Dissemination level: PUBLIC
Date of issue of this report: 04/06/2024

Page

EURAD (Deliverable n° 17.7) - Synthesis report on Innovative and Enhanced Equipment for Repository Monitoring
Dissemination level: PUBLIC
Date of issue of this report: 04/06/2024

Page

EURAD (Deliverable n° 17.7) - Synthesis report on Innovative and Enhanced Equipment for Repository Monitoring
Dissemination level: PUBLIC
Date of issue of this report: 04/06/2024

Page

EURAD (Deliverable n° 17.7) - Synthesis report on Innovative and Enhanced Equipment for Repository Monitoring
Dissemination level: PUBLIC
Date of issue of this report: 04/06/2024

Page

EURAD (Deliverable n° 17.7) - Synthesis report on Innovative and Enhanced Equipment for Repository Monitoring
Dissemination level: PUBLIC
Date of issue of this report: 04/06/2024

Page

EURAD (Deliverable n° 17.7) - Synthesis report on Innovative and Enhanced Equipment for Repository Monitoring
Dissemination level: PUBLIC
Date of issue of this report: 04/06/2024

Page

EURAD (Deliverable n° 17.7) - Synthesis report on Innovative and Enhanced Equipment for Repository Monitoring
Dissemination level: PUBLIC
Date of issue of this report: 04/06/2024

Page

List of Tables

EURAD (Deliverable n° 17.7) - Synthesis report on Innovative and Enhanced Equipment for Repository Monitoring
Dissemination level: PUBLIC
Date of issue of this report: 04/06/2024

Page

Glossary

ACA:	AusCultation Alvéole HA: (disposal cell monitoring experiment)
AE:	Acoustic Emission
ATR:	Total Attenuated Reflexion
BOTDA:	Brillouin Optical Time Domain Analyser
BOTDR:	Brillouin Optical Time-Domain Reflectometry (Brillouin Scattering)
Cox :	Callovo-Oxfordien
CV:	Cyclic Voltammetry
EBS:	Engineered Barrier System
EDZ:	Excavation disturbed zone
DMSO:	DiMethylSulfOxyde
GDF:	Geological Disposal Facility
FEPs:	Features, events, processes
FTIR:	Fourier Transform InfraRed Spectroscopy
HLW:	High level radioactive waste
ILW:	Intermediate level waste
NMR:	Nuclear Magnetic Resonance
NR:	Neutral Red
OBR:	Optical Backscatter Reflectometer
pH:	Hydrogen potential
PPP-BOTDA:	Pulse-prepump brillouin optical time domain analysis
SNF:	Spent nuclear fuel.
TW-COTDR:	Tunable Wavelength - Coherent Optical Time Domain Reflectometry
UV-Vis:	Ultra-violet- Visible Spectrometry
XPS:	X Photoelectron Spectroscopy

EURAD (Deliverable n° 17.7) - Synthesis report on Innovative and Enhanced Equipment for Repository Monitoring
Dissemination level: PUBLIC
Date of issue of this report: 04/06/2024

Page

PART A

EURAD (Deliverable n° 17.7) - Synthesis report on Innovative and Enhanced Equipment for Repository Monitoring
Dissemination level: PUBLIC
Date of issue of this report: 04/06/2024

Page

1. Introduction

1.1 Background

Monitoring and suitable management of the acquired data can also be used to support engagement with stakeholders. In this way, monitoring will support decision making, help to build further confidence in geological disposal, and contribute to optimisation of the disposal system.

The Monitoring Equipment and Data Treatment for Safe Repository Operation and Staged Closure (MODATS) work package (WP) of the European Joint Programme on Radioactive Waste Management (EURAD) is conducting research, development and demonstration (RD&D) into: monitoring data acquisition, treatment and management; use of monitoring data to enhance system understanding, including development of digital twins; interactions with Civil Society and other stakeholders; development of monitoring technologies; and development of knowledge regarding repository monitoring. MODATS is building on previous international collaborative RD&D activities, including a European Thematic Network[108] the MoDeRn [110].and Modern2020 [projects [109]

Monitoring of the geosphere during site investigations and disposal facility construction and monitoring of URL experiments have demonstrated that it is feasible to collect detailed information to support understanding of the evolution of the disposal system, and to use that understanding to support development of the long-term safety case.

A broad range of technologies exist for undertaking monitoring. However, monitoring of the disposal system during the operation period provides challenges, particularly associated with ensuring the passive safety of the disposal system. The ability to monitor the disposal system and the extent to which such monitoring can provide detailed understanding of the disposal system evolution can be enhanced through development of novel technologies, and there is a need to further develop the most promising novel technologies. These include mainly geophysical methods and fibre optic systems. In addition, to monitor with confidence, there is a requirement to develop greater understanding of the interactions between monitoring sensors and the medium in which they are emplaced.

1.2 Objectives

New and emerging sensing methods may change the paradigm of how to monitor waste repositories. To push forward what is possible in terms of monitoring, it is crucial to stay abreast with the technological development to apply and adapt emerging technologies to waste repository monitoring and develop new technologies that are suitable for the specific requirements of repository monitoring. In addition, new methods are developed that extract signals from the data through signal processing, joint inversion schemes and other techniques that are specific to the monitoring methods. The work in

The work in Task 3 of MODATS was divided into three main themes main directions:

- Develop innovative sensors and geophysical techniques to measure and infer parameters that are difficult to obtain for long-term monitoring.
- Develop and qualify optical sensors to get them ready to be used in the initial phase of the development of the geological disposal for temperature and strain measurement.
- Develop a roadmap for technology development, to ensure that technologies can be used with confidence from the start of repository operations.

1.3 Intended Scope and Audience

This report is dedicated to the comprehensive exploration and analysis of monitoring technologies in the context of the repository, with a primary focus on the underground locations and associated boreholes within the underground repository The content is intended primarily for people in charge of developing monitoring technologies to tell them the progress performed during the three years project of MODATS WP.

EURAD (Deliverable n° 17.7) - Synthesis report on Innovative and Enhanced Equipment for Repository Monitoring
Dissemination level: PUBLIC
Date of issue of this report: 04/06/2024

Page

1.4   Report structure

This report is presented in seven sections. Following this introduction (Section 1), separate sections (or sub-sections) are presented for monitoring technology types respectively (Sections 2-3). For monitoring technology development: an introduction, problem analysis, research objectives, overview of the development team, development steps follow during the MODATS project, Material and method, Description on the field test used during the project, Results, Discussion about the results obtained, References is provided.

Section 4 examine the sources of hardness and evaluate the impacts of the harsh environment on the requirements for long-term monitoring on sensor equipment based on literature reviews.

Section 5 provides the future needs from the MODATS work on monitoring technologies with the perspectives of monitoring data. The outcome from this activity is a generic RD&D roadmap. The methodology to create the generic roadmap has included an understanding of data requirements, current state of development of technologies, and non-comprehensive identification of outstanding technology issues that need to be addressed before implementation of repository monitoring programmes commence.

The appendix A provides a summary of the monitoring technology developed in MODATS through Technology Data sheet summary.

EURAD (Deliverable n° 17.7) - Synthesis report on Innovative and Enhanced Equipment for Repository Monitoring
Dissemination level: PUBLIC
Date of issue of this report: 04/06/2024

Page

2. Geophysics & Innovative Sensors

2.1 Introduction

For monitoring of radioactive waste repositories, knowledge of the spatial and temporal variations of key parameters, such as temperature, pressure, moisture, porosity, etc. is envisaged. In principle, this can be obtained with a sensor network, in which all these parameters can be measured directly. However, this imposes challenges. First, the placement of the sensors could have an impact on the passive safety of the multi-barrier system. Furthermore, the placement of a sensor may locally disturb the embedding material, and the measurements may be therefore not representative. Finally, the sensor data corresponds to point information only, which may be not representative for the entire volume of interest.

With geophysical methods the problems mentioned above can be addressed. They can be performed in a non-destructive fashion. Therefore, the integrity of the barriers remains unaffected, and the embedding material is not disturbed locally. Most importantly, repeated geophysical measurements allow spatial and temporal changes to be monitored over larger volumes.

Unfortunately, geophysical methods also suffer from some deficiencies. Firstly, they are often ambiguous, that is, several subsurface models explain the data equally well. Depending on the method(s) employed, they can offer only limited spatial and/or temporal resolution. Finally, geophysical methods yield physical material properties, such as elasticity parameters, density, or electrical conductivities, and it is not straightforward to translate these material properties to parameters of interest (i.e., temperature, pressure, etc.).

2.2 Geophysical monitoring

2.2.1 Introduction

It is commonly accepted that radioactive waste repositories must be constructed to be passively safe for a long time period, up to millions of years. Often, monitoring is requested to confirm that repository conditions are consistent with safety assessments. IAEA technical documents and safety standards compile current knowledge on monitoring purposes, goals and requirements [8][9][10][11][12](and serving as non-binding guideline in many disposal programmes.

International research further developed deduced workflows and methods for parameter selection to support development and implementation of monitoring projects that are consistent with the typically stepwise evolution of repository programmes (White & Scourfield, 2019; Farrow et al., 2019). In the case of repositories for high-level radioactive waste, knowledge of the spatial and temporal variations of parameters such as temperature, pressure or water content is considered important. In principle, this can be obtained with a dense sensor network, with which all these parameters can be measured directly. However, this imposes several problems. First, the placement of the sensors may affect the integrity of the repository barriers. Furthermore, the placement of a sensor may locally disturb the embedding material, and the measurements may therefore not be representative. Finally, the sensor data represent only point information, which may not be representative for the entire volume of interest.

With geophysical methods, the problems mentioned above can be addressed. They can be performed in a non-destructive and non-intrusive fashion. Therefore, the integrity of the barriers remains unaffected, and the embedding material is not disturbed locally. Most importantly, repeated geophysical measurements allow spatial and temporal changes to be monitored over larger volumes.

In the framework of earlier projects, possibilities, and limitations of geophysical monitoring of high-level radioactive repositories have been investigated. Geophysics offers a wide range of methods, ranging from potential field methods (gravity, magnetics, geoelectrics) over inductive electromagnetic methods to wave propagation methods (seismics and ground-penetrating-radar (GPR)). For monitoring radioactive waste repositories, geoelectrical, seismic and GPR techniques were judged to be most useful. Geoelectrical measurement arrays are relatively simple to install, and highly repeatable surveys can be carried out in an efficient manner. An example includes Yaramanci (2000) [30], and in the framework of the MODERN2020 project, extensive laboratory experiments were carried out (MODERN2020, 2020)[23].

EURAD (Deliverable n° 17.7) - Synthesis report on Innovative and Enhanced Equipment for Repository Monitoring
Dissemination level: PUBLIC
Date of issue of this report: 04/06/2024

Page

The potential of seismic methods was investigated in detail during MODATS WP predecessor projects ESDRED, MODERN and MODERN2020. As documented in various publications (Marelli et al., 2010 [18]; Manukyan, 2011[14]; Manukyan et al., 2012[16]; Marelli et al., 2012[19]; Tisato and Marelli, 2013[28]; Manukyan et al., 2017[17]; Manukyan and Maurer, 2020[15]), it could be shown that seismic methods, particularly full waveform inversions, can be a powerful option for monitoring. Likewise, the potential of GPR measurements has been explored. Maurer and Spillmann (2018)[22] have shown that such type of measurements can be useful.

Geophysical methods suffer from some deficiencies: First, they are often ambiguous, that is, several subsurface models explain the data equally well. Depending on the method(s) employed, they can offer only limited spatial and/or temporal resolution. Finally, geophysical methods yield physical material properties, such as elasticity parameters, density or electrical conductivities, and it is not straightforward to translate these material properties to parameters of interest (i.e., temperature, pressure, etc.) to evaluate repository performance.

In the framework of MODATS, the first (ambiguity) and the last (material properties of interest) problem will be addressed. As explained in more detail in the next section, this is achieved via joint inversions of several geophysical data types and data attributes, and by combining geophysical data with in-situ point measurements. Finally with the use of machine learning we demonstrate how geophysical methods can help to obtain tomographic images of moisture distribution.

2.2.2   Problem analysis

With geophysical methods one can non-intrusively obtain tomographic images of geophysical properties. However, these parameters cannot be directly used for assessing the state of repository. In the FE experiment, there are a large amount of point sensors within granulated bentonite mixture (GBM), two fibreglass pipes installed within GBM for geophysical measurements (cross-hole seismic and GPR measurements and single hole GPR, gamma-gamma and neutron log) and additional 3 seismic sources and 5 receivers attached at the floor and roof area within GBM. The aim of this work is to develop a methodology that allows obtaining spatial distributions of water content using geophysical information from geophysical measurements and local water content measurements.

2.2.3   Research Objectives

- The main objective of this research is to establish constitutive relationships that allow the physical material parameters, obtained from geophysical data, to be converted to geotechnical parameters, such as temperature, pressure, and water content.
- Additionally, the complementary nature of different geophysical data will be exploited. This will aid setting up optimized monitoring networks and will ultimately allow traditional sensor (point) data to be extrapolated to 3D volumes.

2.2.4   Overview of the development team

Most of the work was carried out by Dr. David Sollberger (ETH Zürich). He is an expert in algorithmic developments and seismic data processing. Additionally, Prof. Dr. Hansruedi Maurer (ETH Zürich) dedicated part of his time to the project. Dr. Edgar Manukyan (Nagra) led the collaboration on Nagra side and supported the project with his expertise in geophysics, in-depth knowledge of the FE experiment as well as by providing the necessary data.

2.2.5   Development steps followed during the MODATS project.

1.   **Identification of suitable geophysical methods**

The first phase of the project was dedicated to the identification of the set of geophysical methods that is best suited to characterize the geotechnical parameters of interest. The focus lies on seismic methods, which were identified to be the most promising for the characterization of radioactive waste repositories (Maurer and Greenhalgh, 2012[21]). Besides the analysis of seismic travel time and attenuation measurements, it is explored whether full waveform inversion (FWI) techniques are suitable to extract accurate, high-resolution information on temporal changes in the seismic velocity and attenuation distribution. Tests are conducted using both synthetic data and field data from the FE experiment.

EURAD (Deliverable n° 17.7) - Synthesis report on Innovative and Enhanced Equipment for Repository Monitoring
Dissemination level: PUBLIC
Date of issue of this report: 04/06/2024

Page

Synthetic data are generated based on models that are created using empirical relationships found in the literature (e.g., Tisato & Marelli, 2013[28]). If FWI turns out to be too challenging to be applied to the monitoring data (e.g. due to strong 3D effects, poor data quality, or data ambiguity), other methods might be explored that allow one to infer on weak temporal variations in the seismic properties. For example, coda wave interferometry was shown to be a highly sensitive technique to infer on weak changes in the medium using ultrasound (e.g., Planès & Larose, 2013[26]). Additionally, we expect that the inclusion of information from GPR measurements will provide crucial, independent constraints on the geotechnical parameters of interest. We also expect that the accuracy of the extracted parameter distribution inferred with the tomographic tools can highly benefit from joint inversion approaches using structural constraints. We therefore attempt a joint inversion of the cross-hole seismic and GPR data (travel times and amplitudes). This should ideally improve the spatial resolution of the estimated parameters, hopefully enabling us to better link the extracted geophysical parameters with the direct measurements of the water content at sparse locations.

2. **Determination of constitutive relationships between geotechnical and geophysical parameters**

In this phase of the project, the constitutive relationships between the measured geophysical parameters and the geotechnical parameters of interest are established. Some geotechnical parameters might be available from direct point measurements at sparse locations. It is explored whether these parameters can be accurately extrapolated to larger volumes using either modelling (e.g., for the extrapolation of temperature measurements) or reconstruction techniques such as compressive sensing, which enable the accurate recovery of information from severely under-sampled data.

It is expected that the relationships between the geophysical parameters and the geotechnical parameters are highly non-linear. If enough calibration data are available (e.g., from the extrapolated point measurement data) these non-linear relationships could potentially be learned from the data using supervised machine learning techniques as recently shown by Klessens et al. (2021)[13].

2.2.6 Material and method

In this work we used geophysical measurements performed within the FE experiment that were performed from 2015 until 2021. These data were used to check eligibility of full waveform inversion and coda wave interferometry. Furthermore, we developed structurally constrained joint inversion code of seismic and GPR travel times and amplitudes. The code was applied to FE data sets to obtain velocity and attenuation tomograms. Finally, to obtain a relationship between geophysical and geotechnical properties we applied XGBoost algorithm. Details on the individual method developments and corresponding results are provided in the Results chapter.

2.2.7 Description on the on-field test used during the project.

Since 2015, the FE Experiment is running in the Mont Terri Rock Laboratory. Its main objective is to demonstrate that high-level radioactive waste can be stored safely in a deep geological repository (Müller et al. 2017 [24], Fisch et al. 2019[6]). For that purpose, a 50-m-long, 3 m diameter tunnel was excavated (*Figure 1*) that should mimic a full-scale repository. High-level radioactive waste canisters are simulated by placing three heaters within the tunnel. After their installation, the tunnel was backfilled with a granulated bentonite mixture (GBM) using a backfilling machine with five screw conveyors. The installation and backfilling of FE Experiment was done step wise. After each step of backfill the GBM slope was scanned, and average backfilling densities were estimated. The heaters were then switched on, and temperatures reached approximately 130 °C on the heater surfaces, and, depending on the position, 45 °C to 60 °C at the tunnel walls. Finally, the tunnel was sealed with a shotcrete plug.

As described in Müller et al. (2017) [24], more than 1'500 sensors were installed for monitoring relevant physical parameters (temperature, pressure, relative humidity, etc.). For geophysical monitoring of temporal changes of the GBM, two fiberglass pipes were inserted prior to the installation of the shotcrete plug. As shown in *Figure 1*, these pipes extend beyond the heater H3. They were employed for a variety of borehole logging surveys (gamma-gamma and neutron logs) and cross-hole measurements (seismics, GPR).

EURAD (Deliverable n° 17.7) - Synthesis report on Innovative and Enhanced Equipment for Repository Monitoring
Dissemination level: PUBLIC
Date of issue of this report: 04/06/2024

Page

<div align="center">2.2.1   Results</div>

Full Waveform Inversion

To translate geophysical parameters to geotechnical parameters (the main objective of this project), it is crucial to estimate the geophysical parameters as accurately as possible and at a high spatial resolution. Full waveform inversion was therefore identified at an early stage as a method of primary interest to be applied to the FE data. However, a key disadvantage of FWI is that it constitutes an attempt to solve a highly non-linear, and non-convex optimization problem that can easily get trapped in local optima. This problem is especially severe if the observed experimental data is complex (i.e., due to 3D effects, low data quality, complex heterogeneous media, etc.)

We made use of the software package Salvus (Afanasiev et al., 2019 [1]), developed by Mondaic AG to try and apply FWI to the cross-hole seismic data collected during the FE experiment. Salvus relies on the spectral element method to solve the forward problem (i.e., the solution of the elastic wave equation). The initial model is then iteratively updated using an optimization scheme that is based on the adjoint method (Fichtner et al., 2006) by minimizing the difference between the observed data and the simulated data. The difference can be formulated using different misfit functionals, where typically an L2 misfit is used.
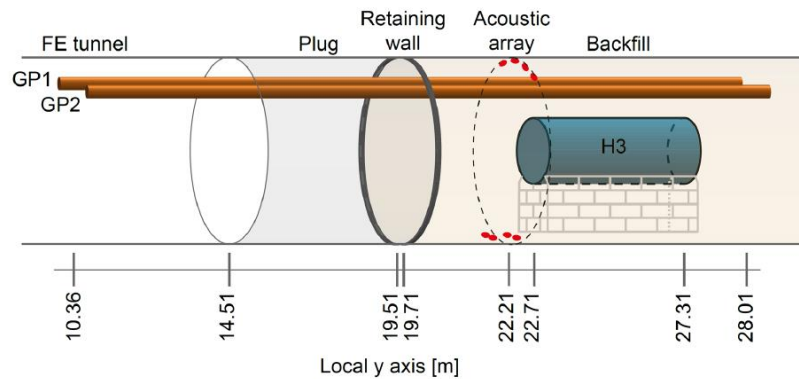
Figure 1: Side-view of the FE experiment. GP1 and GP2 are the two geophysical pipes within which crosshole seismic and GPR data is acquired. H3 marks the position of the third heater. Permanently installed acoustic sensors are marked in red.
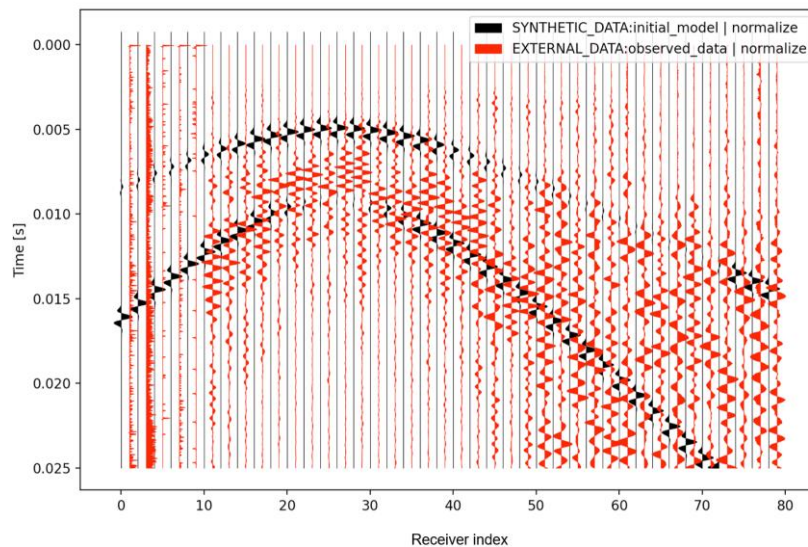
Figure 2: Attempt to apply full waveform inversion to the FE cross-hole seismic data. Shown is data from a single source location, recorded on 80 receivers. Simulated data obtained using the spectral element method in an initial model is shown in black and is interleaved with the observed data shown in red. Note the complexity of the observed data.

EURAD (Deliverable n° 17.7) - Synthesis report on Innovative and Enhanced Equipment for Repository Monitoring
Dissemination level: PUBLIC
Date of issue of this report: 04/06/2024

Page

We tried to apply the following full waveform inversion strategy:

- Data filtering to remove undesired ringing.
- 3D to 2D conversion of the data (since the simulations are done in 2D, leading to amplitude differences).
- Data windowing to suppress energy arriving before the first arrival. Initially, only a short time window around the first arriving energy is sought to be fitted, the window is then subsequently opened to include more data).
- Estimation of source-time-function and receiver-coupling factors.
- Inversion was performed by initially only fitting the low-frequency content and subsequently gradually adding higher frequencies.

  - L2-misfit functional was used for the solution of the optimization problem.

A comparison between the observed data (in red), and the modelled data (in black) obtained using an initial guess (starting model) is shown in *Figure 2*. The Figure illustrates that the observed data is characterized by a relatively low signal-to-noise ratio and is dominated by ringing reverberations and 3D effects (energy arriving from outside the source-receiver plane). A significant amount of energy seems to arrive earlier than the expected P-wave first arrival (the two events seen in the synthetic data mark the P- and S-wave first arrivals). We interpret this energy to be related to refracted waves originating from the tunnel walls.

Due to the low signal-to-noise-ratio and the pronounced 3D artefacts, it was not possible to obtain reliable velocity models by means of seismic full waveform inversions. However, it is important to note that this is rather a problem of the FE seismic data set and not the full waveform inversion technique in general. Its usefulness has been demonstrated in many other projects (e.g. Manukyan et al. 2012, [16]).

Coda wave interferometry

Unlike full waveform inversion, Coda wave interferometry (CWI) is a purely comparative technique, meaning that it can only be used to infer on relative changes in the medium instead of delivering absolute values of the geophysical parameters. However, these changes can be inferred even if the perturbations in the medium are very small (e.g., fractions of a percent of perturbation in the seismic velocities), providing significant improvements in both accuracy and precision compared to conventional methods. This makes it a very valuable and sensitive tool for real-time monitoring.

Another key advantage of CWI is that it benefits from data complexity due to 3D effects and multiple scattering, since these are exactly the phases that are exploited due to their increased sensitivity to medium perturbations. Additionally, CWI can be applied to data with a relatively low signal to noise ratio since CWI is generally less susceptible to the presence of noise, as it uses many more data points (the full signal), providing more robust estimates (Singh et al., 2019 [27]).

For these reasons, we identified CWI as a potentially beneficial method for long-term monitoring of radioactive waste repositories. Especially given the challenges encountered when trying to apply full waveform inversion to the FE data (3D effects and low signal-to-noise ratio). To evaluate the potential of the method, we tested it on the semi-continuous seismic data recorded during the FE experiment. The semi-continuous recording is done by automatic activation of 4 sources one by one and recording of the resulting signal by an array of 13 receivers. 3 of the sources and 5 of the receivers are permanently installed in GBM. One source and 8 receivers are installed in GP1 and GP2 (see *Figure 1*), respectively. They are removed before every geophysical campaign and reinserted afterwards.

The semicontinuous seismic measurements were carried out daily between 22:00 and 06:00 of the next day. The selection of this time interval allows one to minimize seismic noise coming from human activities in Mont Terri. Each seismic source is activated once per hour to generate 1'024 repeatable signals one after another. The waves reaching the receivers are then stacked and recorded.

Semi-continuous data for two different source and receiver pairs are displayed in *Figure 3*. Note the long reverberating coda following the first-arriving energy, suggesting that this data can potentially be used

EURAD (Deliverable n° 17.7) - Synthesis report on Innovative and Enhanced Equipment for Repository Monitoring
Dissemination level: PUBLIC
Date of issue of this report: 04/06/2024

Page

to apply coda wave interferometry. The apparent decrease in the travel time of the first-arriving energy over the years indicate that the seismic velocities are increasing as the GBM expands during saturation. An abrupt decrease in the signal-to-noise ratio can be observed for both receivers (occurring in May 2019 for receiver 1 and in October 2018 for receiver 4). The reason for the sudden drop in the data quality is not entirely clear but is likely linked to the deterioration of the sensors over time. Note that the signal to noise ratio of the more distant receiver 4 is significantly lower than the one of receiver 1, making it impossible to pick accurate first arrivals for conventional travel-time analysis.

We implemented CWI in MATLAB and attempted to apply it to the semicontinuous seismic data. The result for the same two source-receiver pairs as in *Figure 3* is shown in *Figure 4*.
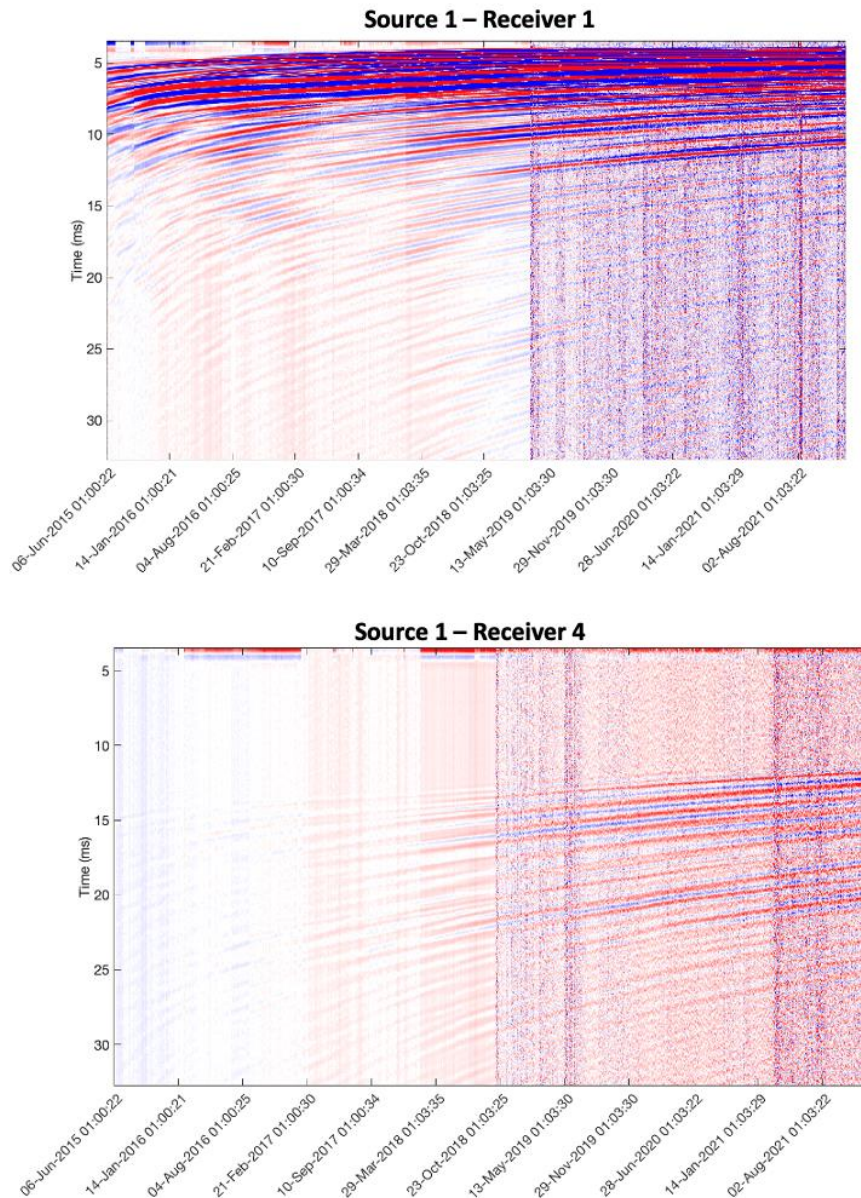
Figure 3: Semi-continuous data for two source-receiver pairs. The top panel shows data for source 1 (located at the top) and receiver 1 (located at the top). The bottom panel shows data for source 1 and receiver 4 (located on the floor).

For the high-quality data (Source 1 – Receiver 1), the continuous velocity increase of the GBM is retrieved with high accuracy and precision. The rate of velocity increase seems to be slowing down over time. Yet, today the seismic velocities still seem to be increasing more than 6 years after the tunnel was backfilled.

EURAD (Deliverable n° 17.7) - Synthesis report on Innovative and Enhanced Equipment for Repository Monitoring
Dissemination level: PUBLIC
Date of issue of this report: 04**/06/2024**

Page

Interestingly, the increase in seismic velocities can also be inferred from the lower quality data (Source 1 – Receiver 4) despite the very low signal-to-noise ratio, which at times even makes it difficult to visually identify the signal. This indicates that coda wave interferometry is indeed very robust towards high levels of noise and is therefore a suitable method to be applied to the challenging FE dataset. There are certain time periods, where coda wave interferometry seems to yield unreliable results (marked in red in *Figure 4*). Here, the signal-to-noise ratio appears to be too low for the method to work reliably. We expect that the results can be further improved by stacking multiple repeated signals each night (here, we only looked at the data recorded around midnight). Additionally, increasing the recording time beyond the ~35 ms used so far and thereby increasing the number of data points that go into the analysis might help to improve the robustness towards noise.
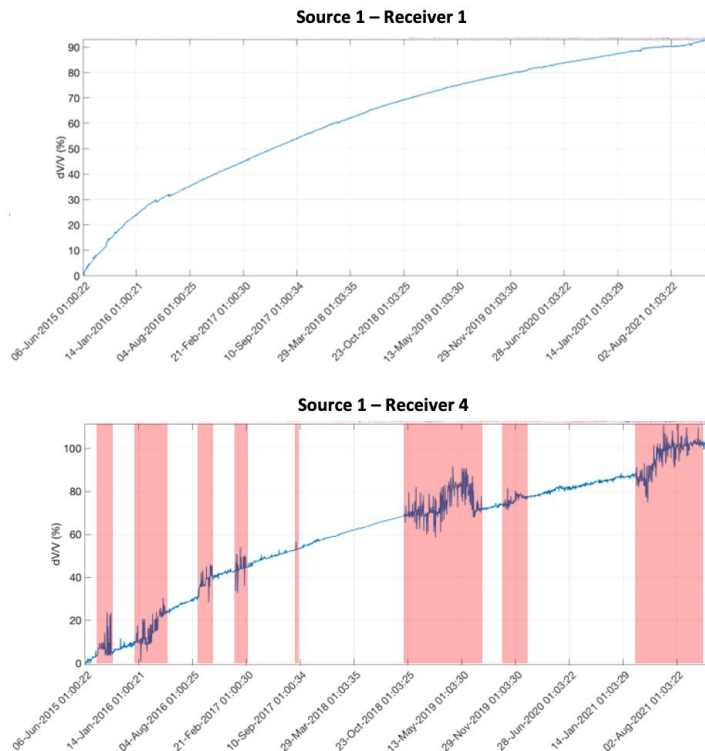
Figure 4: Inferred velocity increase of bulk seismic velocity of the FE GBM obtained by applying coda wave interferometry to the semi-continuous seismic data. Time periods where no stable results could be obtained are marked by red rectangles.

Joint inversion

Due to the lack of a suitable public software package, we have implemented our own joint inversion tomography code for cross-hole seismic and GPR data based on structural coupling with cross-gradient constraints.

Figure 5 shows a synthetic data test of our newly developed code. We used a source and receiver geometry that resembles the geometry of the FE experiment. We first generated a synthetic traveltime and GPR amplitude dataset using a velocity and attenuation model that includes two rectangular anomalies that should mimic a dry (low seismic velocities, high GPR velocities and low GPR attenuation) and a wet zone (high seismic, low GPR velocities and high GPR attenuation). We then tried to reconstruct this model by travel time and amplitude tomography. We first inverted the seismic and GPR data individually (middle panels in *Figure 5*) and then attempted to jointly invert the datasets with our structurally-coupled joint inversion code (bottom panels in *Figure 5*). The results show that the joint inversion approach helps to better reconstruct the true location, shape, and velocity of the two anomalies.

EURAD (Deliverable n° 17.7) - Synthesis report on Innovative and Enhanced Equipment for Repository Monitoring
Dissemination level: PUBLIC
Date of issue of this report: 04**/06/2024**

Page
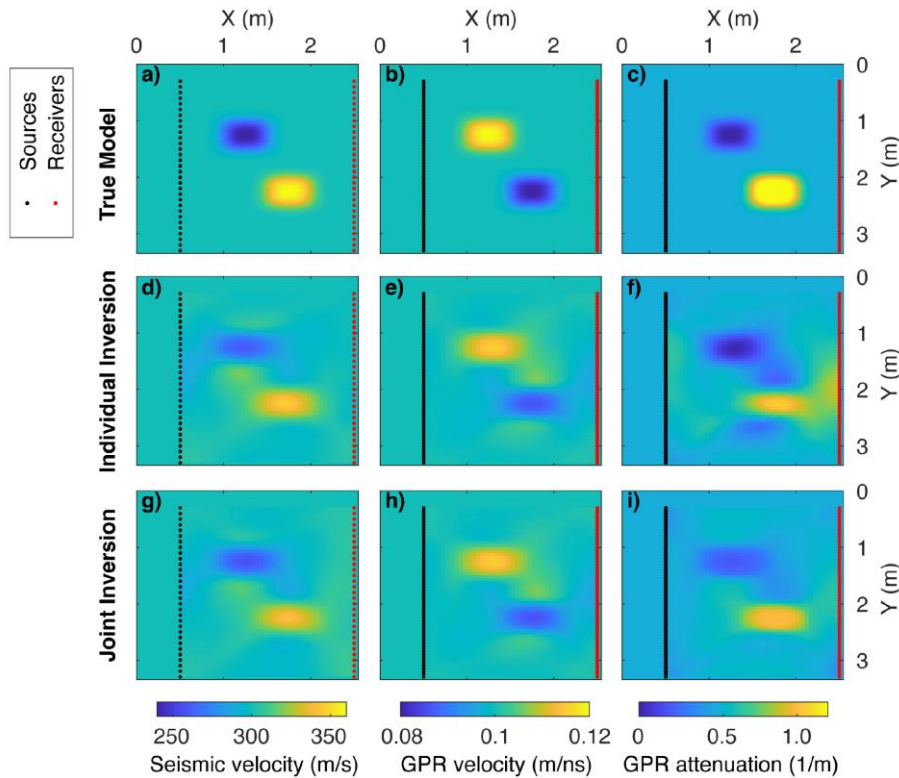
Figure 5: Test of the joint inversion code that was developed within MODATS. Top: True seismic and GPR velocities and GPR attenuation models used to generate a synthetic dataset. Middle: Inversion obtained by individual inversion of the seismic and GPR dataset. Bottom: Inversion obtained using a structurally-coupled joint inversion with cross-gradient constraints.

We jointly invert seismic and GPR data for the 10 consecutive crosshole experiments listed in *Table 1*. GPR and seismic first-arrival travel times were manually picked in an initial step and subsequently refined using a cross-correlation procedure. GPR amplitudes were determined by picking the maximum amplitude in a 3 ns time window around the manually picked first breaks. No amplitudes could be picked for the seismic data due to the very poor data quality, which is likely caused by poor coupling of the piezoelectric sensors to the granulated bentonite mixture. While seismic data quality seems to have significantly improved over time, the quality of the GPR data deteriorated over time so that no travel times could be picked for an additional 11th experiment that was conducted in the summer of 2022.

Jointly inverted tomographic images of GPR velocity, GPR attenuation, and seismic velocity are shown in *Figure 6* for each of the ten consecutive experiments. Results are shown after 10 Gauss-Newton iterations. We observe a general decrease in GPR velocity and a simultaneous increase in GPR attenuation and seismic velocity over time. This meets the expected behaviour of the geophysical parameters as the granular bentonite mixture gets more and more saturated with water as time progresses. From experiment 4 onward, two zones exhibiting significantly increased radar attenuation and seismic velocity and decreased radar velocity appear to form close to the two fibreglass pipes in the region of the heater at around 23–25 m, marking a zone of potentially significantly increased humidity. Sandwiched in between these potential wet zones is a region with significantly decreased radar attenuation and seismic velocity, and increased radar velocity.

Table 1: Dates of consecutive cross-hole GPR, cross-hole seismic, and single-hole neutron log experiments used in this study.

Experiment number	Acquisition dates

EURAD (Deliverable n° 17.7) - Synthesis report on Innovative and Enhanced Equipment for Repository Monitoring
Dissemination level: PUBLIC
Date of issue of this report: 04/06/2024

Page

	GPR	Seismic	Neutron log
1	2015/02/17	2015/02/18	2015/02/16
2	2015/05/19	2015/05/28	2015/05/27
3	2015/09/03	2015/08/27	2015/08/29
4	2016/02/03	2016/02/05	2016/02/04
5	2016/08/26	2016/08/30	2016/08/25
6	2017/05/17	2017/02/24	2017/02/21
7	2018/05/24	2018/02/09	2018/05/28
8	2019/03/26	2019/03/27	2019/03/23
9	2020/09/24	2020/09/29	2020/09/26
10	2021/06/01	2021/06/10	2021/06/05

Machine Learning

While the tomograms presented in *Figure 6* contain a rich amount of information on the spatial variations of the geophysical properties of the granulated bentonite mixture within the repository, they are not particularly easy to interpret. It would be advantageous to translate the geophysical properties to geotechnical parameters – such as water content, temperature, and pressure – that are of direct interest for the evaluation of the repository state. From direct temperature measurements in the FE experiment we know that the temperature distribution quickly reaches quasi-steady state after the heaters are turned on. Hence, after the quasi-steady state is reached, we do not expect that temperature plays a significant role in the observed temporal evolution of the geophysical parameters. Water saturation, on the other hand, seems to be a key factor driving the evolution of the geophysical parameters. Experimental data from laboratory measurements directly linking the water content in bentonite to geophysical parameters are only available for seismic velocities of pressed bentonite blocks, for which a non-linear relationship was observed (Tisato & Marelli, 2013 [28]). A direct translation of the tomographic images to an image of water content based on empirical relationships is thus not possible.

EURAD (Deliverable n° 17.7) - Synthesis report on Innovative and Enhanced Equipment for Repository Monitoring
Dissemination level: PUBLIC
Date of issue of this report: 04/06/2024

Page
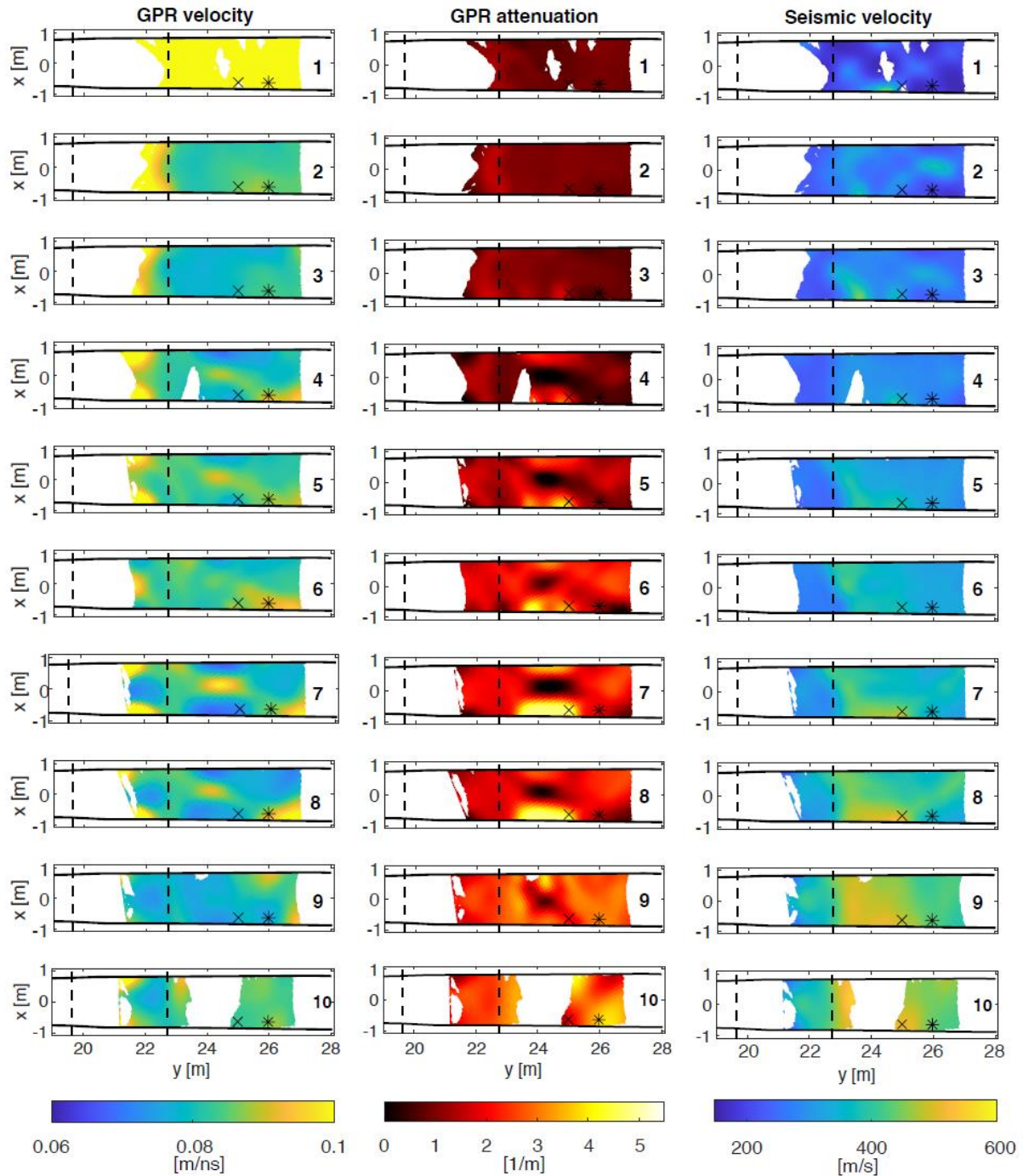
Figure 6: Joint tomography results for 10 consecutive crosshole GPR and seismic surveys in the FE experiment. Note the increase in GPR attenuation and seismic velocity over time, and the decrease in GPR velocity, as the granulated bentonite mixture gets saturated with water. Vertical dashed lines mark the back of the concrete plug and the front of the third heater, respectively (see Figure 1). The cross and the asterisk mark two positions where direct water content sensors were installed. Results are only plotted in regions with significant ray coverage (>50 rays) in order to avoid interpreting results in regions with low sensitivity.

We therefore pursue a fully data-driven approach where we use direct measurements of relative humidity available from sparse point sensors to establish constitutive relationships with the geophysical parameters by employing a machine-learning model. Machine-learning has been widely proven as a powerful tool for non-linear regression tasks such as the one at hand. Here, we use the supervised machine-learning technique of gradient tree boosting (Friedman, 2001 [7]), specifically the open source package XGBoost (Chen & Guestrin, 2016) to train an ensemble of weak learners (shallow decision trees) that enable us to predict the relative humidity given tomographically estimated geophysical

EURAD (Deliverable n° 17.7) - Synthesis report on Innovative and Enhanced Equipment for Repository Monitoring
Dissemination level: PUBLIC
Date of issue of this report: 04**/06/2024**

Page

properties (Note that *any machine learning technique could be applied for this regression task. Here we choose gradient-boosted trees since they have proven to be accurate for non-linear regression tasks, they train fast, and allow us to evaluate feature importance. Gradient-boosting has been shown to usually outperform random forests (e.g., Piryonesi & El-Diraby, 2020 [25]). As input features for training, we use the geophysical parameters (seismic velocity, radar velocity, and radar attenuation)* extracted from the tomographic images at the point that lies closest to a given point sensor that directly measures relative humidity. We then attempt to fit a gradient-boosted tree model that enables the prediction of the relative humidity based on these features. Unfortunately, only two functioning water content sensors lie reasonably close to the tomographic plane (<30 cm away). The locations of these two sensors are marked by a cross and an asterisk in *Figure 6*. The resulting training data set of only 20 samples is thus too small to fit a meaningful machine learning model that enables a reliable prediction of the relative humidity in a quantitative fashion.

Hence, since neutron logs are sensitive to the amount of hydrogen atoms in surrounding environment, we attempt to use neutron logging data as a second, alternative direct measurement that is indicative of the water content. As neutron logging data is available every 5 cm along the two fiberglass pipes, that largely increases the data pool that can be used to train a machine learning model and to establish a constitutive relationship with the geophysical parameters. The larger data pool also enables us to evaluate the performance of the gradient-boosted tree model on independent test data.

We trained independent gradient-boosted tree models to directly predict water content (trained using the only 20 data points from direct water content sensors) and to predict neutron log units (a total of 1187 data points were available from which 80 % were randomly selected for training and 20 % were randomly selected to test the performance of the model). Optimal hyperparameters for the latter XGBoost model were determined using an optimization procedure that maximizes the model score on the independent test data (Bergstra et al., 2013 [2]). Default hyperparameters were used for the first model due to the lack of available test data.

Figure 7 shows a scatter plot of the predicted neutron log value versus the true neutron log value for all samples of the independent test dataset. Results are shown for two models using different input features: the first model uses the tomographic images obtained by joint inversion, whereas the second uses the images from individual inversions. In the case of a perfect prediction, all samples would fall onto a line of unit slope. Since there are uncertainties in both the input features (tomographic images) and the output labels (neutron log data), a perfect prediction is not desired since that would indicate over-fitting. Both models fit the data well, indicating that the neutron log values can indeed be quantitatively predicted from the geophysical parameters. With a correlation coefficient of R = 0.93, the predictions based on joint inversions match the true values slightly better than the predictions based on individual inversions (R = 0.90).

After training, we applied the machine learning models to the tomograms in *Figure 6*, yielding predictions of the water content and neutron log units at each pixel of the geophysical inversion grid. The results are displayed in *Figure 8*.

Generally, both predictions show the expected increase in water content and decrease in neutron log units over time with specific regions of increased humidity forming early on close to the two fiberglass pipes, where wet spots (previously known from tunnel mapping) exist. Due to the limited amount of data that could be used in the training of the model for the direct prediction of the water content, a quantitative interpretation of the values of the predicted water content distribution should be avoided but, interestingly, a good qualitative match of the overall estimated humidity distribution can be observed for the two independently trained models.

EURAD (Deliverable n° 17.7) - Synthesis report on Innovative and Enhanced Equipment for Repository Monitoring
Dissemination level: PUBLIC
Date of issue of this report: 04/06/2024

Page
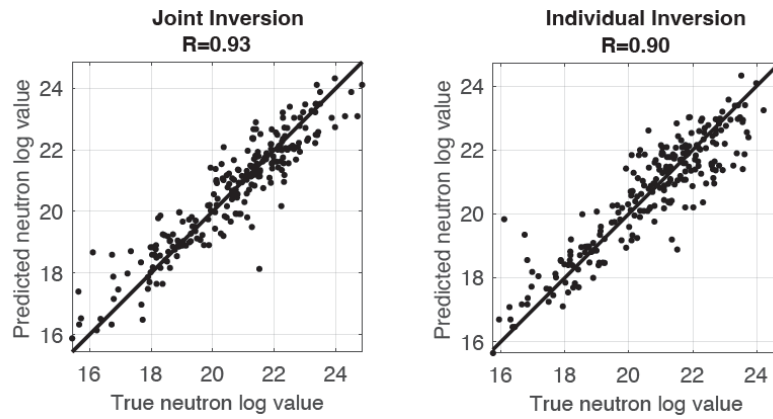
Figure 7: Evaluation of the performance of the trained machine learning model for the geophysical prediction of neutron log values. Note that the model that is trained using the joint inversion results as input features appears to outperform the model that is trained on results from individual inversions.
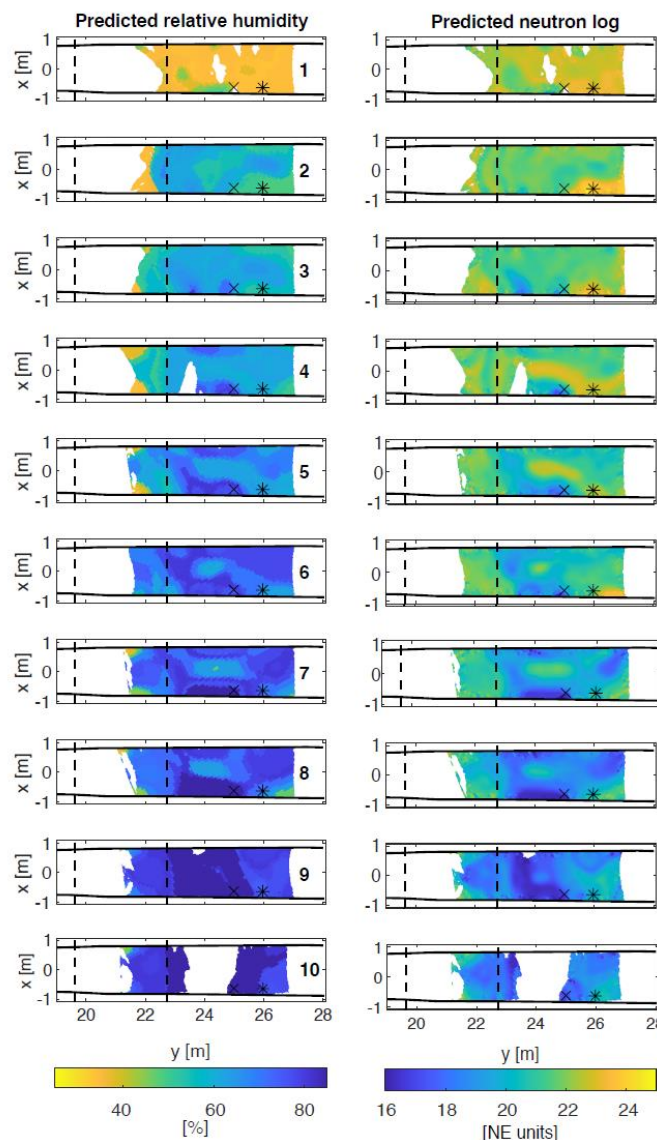
Figure 8: Estimated distribution of relative humidity (left) and virtual neutron log measurements (right) predicted from jointly inverted geophysical tomograms using a machine learning model.

EURAD (Deliverable n° 17.7) - Synthesis report on Innovative and Enhanced Equipment for Repository Monitoring
Dissemination level: PUBLIC
Date of issue of this report: 04/06/2024

Page

2.2.2 Discussion about the results obtained.

Full waveform inversion

Even with the conservative full waveform inversion strategy outlined in the previous section, we could not obtain any reasonable model updates and the inversion algorithm kept getting trapped in local minima. This ultimately led us to the conclusion that FWI is not a suitable method to be applied to the FE experiment data, requiring the search for alternative methods. The primary reasons for this are the low signal-to-noise-ratio and substantial off-plane effects that deteriorate 2D inversions.

Coda wave interferometry

We have demonstrated that coda wave interferometry can be used to efficiently track small perturbations in the seismic velocity that cannot be observed with other geophysical methods. The main limitation of coda wave interferometry compared to tomographic methods such as travel time tomography or full waveform inversion is that it only enables the estimation of a bulk increase or decrease of the seismic velocity. It is difficult to extract information on where exactly this velocity change occurs since the scattered coda waves sample a much larger volume of the medium than the direct waves that are typically used in tomographic methods. It is expected that the sensitivity is restricted to a volume surrounding the source and receiver pair, where the sensitivity is highest close to the acquisition hardware (see sensitivity kernels in Margerin et al., 2016 [20]). An additional limitation of the method is that it requires that the analyzed signals are highly repeatable. This repeatability might not be guaranteed if the coupling of both the sources and the receivers varies over time. This makes it difficult to apply the technique to the cross-hole measurements in the FE experiment where significant waveform differences can be observed after each reinsertion of the source and the receivers due to geophysical campaigns. In the current state, CWI is likely not a suitable technique for the accurate inference of the spatial distribution of seismic velocities inside a repository. However, given the results obtained during this study, we expect that CWI could be used in the future to refine the temporal resolution of the geophysical parameter distribution obtained by tomographic methods that depend on a more time-consuming acquisition process and, therefore, are typically only obtained periodically (i.e., with a low temporal resolution).

Joint Inversion

We have developed a structurally constrained joint inversion algorithm for the simultaneous inversion of seismic and GPR traveltime and attenuation data. The algorithm was checked on a synthetic data set and then was applied to the data collected within FE experiment. Results suggest that such an approach allows us to better constrain the location, shape, and values of anomalies.

Machine Learning

To further evaluate the quality of the images of predicted neutron log values that we obtained from the geophysical tomograms, we extract the values at the pixels that lie closest to the location of the two direct water content sensors for each of 10 repeated experiments. *Figure 9* shows a comparison of the directly measured relative humidity with the negative value of the predicted neutron log at these two locations. Due to the direct link of neutron log units with water content, we expect to see a correlation between these two parameters. However, the former is obtained in a purely non-invasive fashion by geophysical tomography, while the latter is intrusively measured in-situ. For the predicted neutron logs, we again show two independently obtained results, where the first was obtained using the geophysical tomograms from joint inversion and the second was obtained using geophysical tomograms from individual inversions (in both cases, machine learning models were trained using the respective tomograms as input features). At sensor location 1 (asterisk in *Figure 9*, a generally lower water content is observed than at sensor location 2 (cross). The independently obtained, estimated neutron log values appear to clearly resolve this difference in humidity (i.e., lower neutron log values are predicted at sensor 2). The overall increase in water content over time is reflected well by the decrease of predicted neutron log values at both sensor locations. Interestingly, the true evolution of the water content seems to be

EURAD (Deliverable n° 17.7) - Synthesis report on Innovative and Enhanced Equipment for Repository Monitoring
Dissemination level: PUBLIC
Date of issue of this report: 04/06/2024

Page

better recovered when using a joint inversion approach rather than performing individual inversions of the three datasets.

Other considerations / Applicability

This work has shown that geophysical monitoring has the potential to extract tomographic images of water content information of bentonite. Further research is needed to check the applicability and limitations of the method for the cases when geophysical sensors are located further away from the repository tunnel.
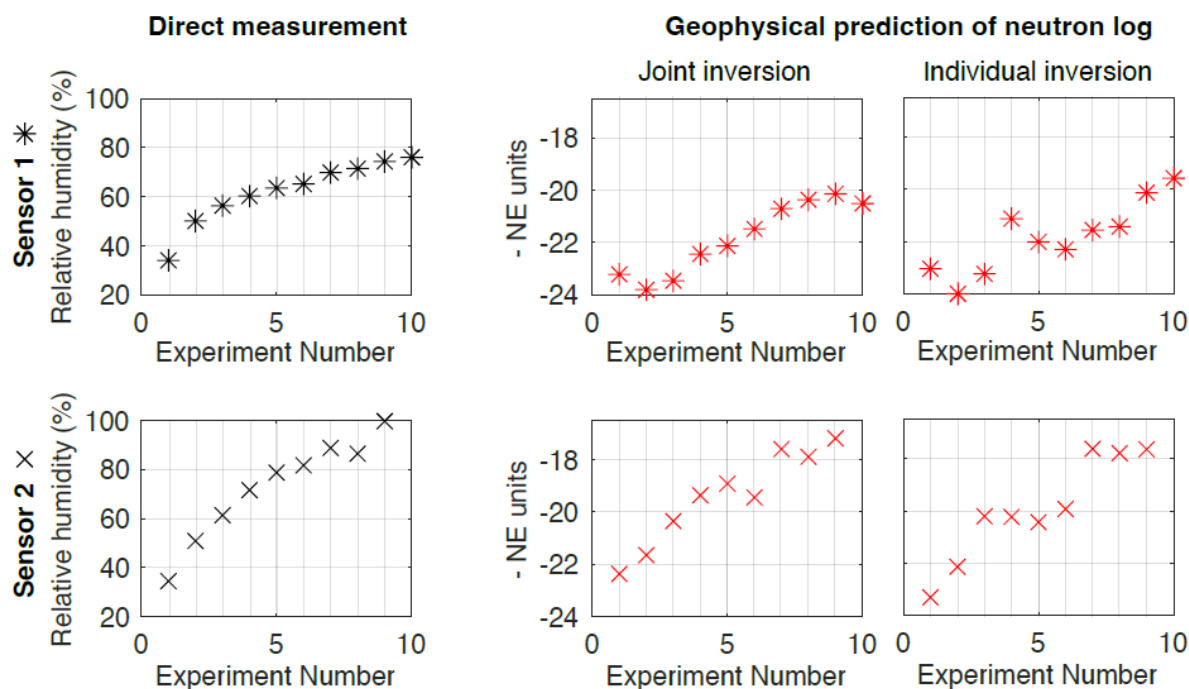
Figure 9: Comparison of directly measured relative humidity at two-point sensors with completely independently obtained geophysical predictions of the neutron log values.

2.2.3   References

[1]. Afanasiev, M., Boehm, C., Van Driel, M., Krischer, L., Rietmann, M., May, D. A., Knepley M.G., Fichtner, A. (2019). Modular and flexible spectral-element waveform modelling in two and three dimensions. *Geophysical Journal International*, *216*(3), 1675–1692.

[2]. Bergstra, J., Yamins, D., & Cox, D., 2013. Making a science of model search: Hyperparameter optimization in hundreds of dimensions for vision architectures, in Proceedings of the 30th International Conference on Machine Learning, vol. 28 of Proceedings of Machine Learning Research, pp. 115–123, PMLR, Atlanta, Georgia, USA.

[3]. Chen, T. & Guestrin, C., 2016. Xgboost: A scalable tree boosting system, in Proceedings of the 22nd ACM SIGKDD International Conference on Knowledge Discovery and Data Mining, KDD '16, p. 785–794, Association for Computing Machinery, New York, NY, USA.

[4]. Farrow, J., White, M., Scourfield, S., Chabiron, A., Jobmann, M., Gazul, R., Frieg, B., Hart, J., Rosca-Bocancea E., Schröder, T., Wildenborg, A., Karvonen, T., Pere, T., Hansen, J., Reijonen, H., Morosini, M., Luterkort, D. & Vokal, A. (2019): Monitoring Parameter Screening: Test Cases. – Modern2020, European Commission, Euratom Research and Training Programme on Nuclear Energy, Horizon 2020 Framework Programme, Contract Number: 622177, Deliverable D2.2; 26 March 2019.

[5]. Fichtner, A., Bunge, H. P., & Igel, H. (2006). The adjoint method in seismology. I. Theory. *Physics of the Earth and Planetary Interiors*, *157*(1–2), 86–104.

[6]. Fisch, H.R., Firat Lüthi, B., Reinicke, A. & Sakaki, T. (2019): Modern2020 WP 4.4 Full-Scale Emplacement (FE) Experiemnt, Mont Terri (Switzerland) – Field realization. Nagra Arbeitsbericht NAB 19-32.

[7]. Friedman, J. H., 2001. Greedy function approximation: A gradient boosting machine, The Annals of Statistics, 29(5), 1189–1232.

EURAD (Deliverable n° 17.7) - Synthesis report on Innovative and Enhanced Equipment for Repository Monitoring
Dissemination level: PUBLIC
Date of issue of this report: 04/06/2024

Page

[8]. IAEA (2001): Monitoring of geological repositories for high level radioactive waste. - IAEA-TECDOC-1208, International Atomic Energy Agency (IAEA).

[9]. IAEA (2011a): IAEA Safety Standards: Disposal of Radioactive Waste. – IAEA Specific Safety Requirements SSR-5.

[10]. IAEA (2011b): IAEA Safety Standards: Geological Disposal Facilities for Radioactive Waste. – IAEA Specific Safety Guide SSG-14.

[11]. IAEA (2012): IAEA Safety Standards: The Safety Case and Safety Assessment for the Disposal of Radioactive Waste. – IAEA Specific Safety Guide SSG-23.

[12]. IAEA (2014): Monitoring and Surveillance of Radioactive Waste Disposal Facilities. - Specific Safety Guide. No. SSG-31. International Atomic Energy Agency (IAEA).

[13]. Klessens, W., Vasconcelos, I. and Y. Jiao (2021). AI-driven Bayesian inference of statistical microstructure descriptors from finite-frequency waves, Arxiv.

[14]. Manukyan, E. (2011), Seismic monitoring and elastic full waveform inversion investigations applied to the radioactive waste disposal issue, PhD thesis, ETH Zurich, Switzerland

[15]. Manukyan, E. and H. Maurer (2020). Elastic vertically transversely isotropic full-waveform inversion using cross-gradient constraints—An application toward high-level radioactive waste repository monitoring. Geophysics **85**(4): R313-R323.

[16]. Manukyan, E., H. Maurer, S. Marelli, S. A. Greenhalgh and A. G. Green (2012). Seismic monitoring of radioactive waste repositories. Geophysics **77**(6): En73-En83.

[17]. Manukyan, E., H. Maurer and A. Nuber (2017). Improvements to elastic full waveform inversion using cross-gradient constraints. Geophysics **83**(2): 1-46.

[18]. Marelli, S., E. Manukyan, H. R. Maurer, S. A. Greenhalgh and A. G. Green (2010). Appraisal of waveform repeatability and reliability for crosshole and hole-to-tunnel seismic monitoring of radioactive waste repositories. Geophysics **75(5)**: Q21-Q34.

[19]. Marelli, S., H. Maurer and E. Manukyan (2012). Validity of the acoustic approximation in full-waveform seismic crosshole tomography. Geophysics **77**(3): R129-R139.

[20]. Margerin, L., Planès, T., Mayor, J., & Calvet, M. (2016). Sensitivity kernels for coda-wave interferometry and scattering tomography: theory and numerical evaluation in two-dimensional anisotropically scattering media. *Geophysical Journal International*, *204*(1), 650–666.

[21]. Maurer, H. and S.A. Greenhalgh (2012 Application of seismic waveform inversions for monitoring radioactive waste repositories and their surroundings: state-of-the-art and future challenges. Nagra work report NAB 12-46.

[22]. Maurer, H. and T. Spillmann (2018). Novel-refinement procedures for differential traveltime tomography. SEG Technical Program Expanded Abstracts 2018, Society of Exploration Geophysicists.

[23]. MODERN2020 (2020).Deliverable D3.5: Geophysical Methods for Repository Monitoring. http://www.modern2020.eu/deliverables.html

[24]. Müller, H.R., Garitte, B., Vogt, T., Köhler, S., Sakaki, T., Weber, H., Spillmann, T., Hertrich, M., Becker, J.K., Giroud, Nl., Cloet, V., Diomidis, N. & Vietor, T. (2017): Implementation of the full-scale emplacement (FE) experiment at the Mont Terri rock laboratory. Swiss Journal of Geosciences 110 (1), pp. 287-306.

[25]. Piryonesi, S. M. & El-Diraby, T. E., 2020. Data analytics in asset management: Cost-effective prediction of the pavement condition index, Journal of Infrastructure Systems, 26(1), 04019036.

[26]. Planès, T, and E. Larose (2013). A review of ultrasonic Coda Wave Interferometry in concrete. Cement and Concrete Research **53**: 248-255.

[27]. Singh, J., Curtis, A., Zhao, Y., Cartwright-Taylor, A., & Main, I. (2019). Coda Wave Interferometry for Accurate Simultaneous Monitoring of Velocity and Acoustic Source Locations in Experimental Rock Physics. *Journal of Geophysical Research: Solid Earth*, *124*(6), 5629–5655. https://doi.org/10.1029/2019JB017577/FORMAT/PDF

[28]. Tisato, N. and S. Marelli (2013). Laboratory measurements of the longitudinal and transverse wave velocities of compacted bentonite as a function of water content, temperature, and confining pressure. Journal of Geophysical Research: Solid Earth **118**(7): 3380-3393.

[29]. White, M. & Scourfield, S. (2019): Modern2020 Project Synthesis Repository Monitoring: Strategies, Technologies and Implementation. - Modern2020, European Commission, Euratom Research and Training Programme on Nuclear Energy, Horizon 2020 Framework Programme, Contract Number: 622177, Deliverable D6.5; 9. September 2019.

[30]. Yaramanci, U. (2000). Geoelectric exploration and monitoring in rock salt for the safety assessment of underground waste disposal sites. Journal of Applied Geophysics **44**(2-3): 181-196.

EURAD (Deliverable n° 17.7) - Synthesis report on Innovative and Enhanced Equipment for Repository Monitoring
Dissemination level: PUBLIC
Date of issue of this report: 04/06/2024

Page

2.3   Spectral Induced Polarization

2.3.1   Introduction

Deep geological disposal facilities under development or being planned in many countries will rely on plugs and seals to isolate and contain sections of the repository during the operation phase and for the whole repository at closure. The plug and sealing systems that will be used in the facilities have typically two roles: (i) to restrict material movement, and (ii) to control water flow. The design of these seals often includes the installation of a bentonite-based swelling clay core. The overall performance of these clay cores will depend on their characteristics and immediate environment (degree of saturation, heterogeneity, water chemistry, permeability, presence of a damaged zone) as well as on the stresses to which they are likely to be subjected to (saturation defect, sliding of the support masses). Therefore, the monitoring of these different physical and petrophysical parameters during the operating phase appears to be a key element in supporting post-closure safety, as it must ensure that the behaviour of these components evolves favourably towards the desired final state.

Nevertheless, there are technical problems in monitoring these seals, such as ensuring a global monitoring of these structures without jeopardizing their confining properties. Geophysics, particularly electrical geophysics, is potentially an ideal way to overcome this problem as: (i) it can be designed in a non-intrusive manner; (ii) it is sensitive to variations in water and clay content; (iii) it allows dynamic phenomena to be monitored over time and (iv) it allows local anomalies to be captured those isolated sensors cannot detect.

Among the electrical methods available, Spectral Induced Polarisation (SIP) appears to be the most suitable, as it is not only sensitive to variations in water content but also to the mineralogical and chemical variability of the water. Moreover, this non-intrusive monitoring method has made a spectacular leap forward during the last decade, with regards to geophysical imaging and petrophysical analysis of sedimentary rocks. Indeed, thanks to new physical models (Revil, 2012[42], 2013[43]), it is possible to relate the parameters from SIP to permeability (Revil and Florsch, 2010[45]; Revil et al., 2015[46]), which constitutes a completely new method for imaging the permeability of porous/fractured media. For comparison, this is not possible with the conventional electrical resistivity imaging method, which includes two contributions (volume and surface) that cannot be separated.

SIP could thus broaden the range of non-destructive methods usually used (acoustic, electrical resistivity, etc.) for large sealing structures and consequently complete the range of innovative sensors previously used and developed in the in-situ tests of the European Modern2020 project to monitor and characterise the saturation of a swelling clay seal.

2.3.2   Problem analysis

The main petrophysical parameters that were investigated are: Water content, saturation, dry and bulk density, bentonite and sand ratios, pore water chemistry.

2.3.3   Research Objectives

- Extend the studies carried out during the Modern2020 project on innovative non-intrusive monitoring techniques for engineered barrier systems.
- Build a spectral induced polarised (SIP) model for bentonite swelling clays for different hydric, chemical and mechanical environments.

2.3.4   Overview of the development team

Most of the work will be carried out by Jad El Alam (IRSN). He is a PhD student at the University Savoie Mont-Blanc (USMB) and IRSN. His supervisors are André Revil (USMB), Alessandro Tarantino (University of Strathclyde) and Pierre Dick (IRSN). His allocation for the project is 36 months (50% workload on MODATS). Pierre Dick is the project manager of this project. He is responsible for the project management and reporting.

EURAD (Deliverable n° 17.7) - Synthesis report on Innovative and Enhanced Equipment for Repository Monitoring
Dissemination level: PUBLIC
Date of issue of this report: 04/06/2024

Page

2.3.5 Development steps follow during the MODATS project.

- Bibliography
- Determination of a SIP model for pure bentonite (MX80)
- Determination of a SIP model for bentonite (MX80) and sand mixtures with deionised water
- Determination of a SIP model for bentonite (MX80) and sand mixtures with an hyperalkaline solution (pH 13.5)
- Drafting PhD manuscript

Activity	Q4 2021	Q1 2022	Q2 2022	Q3 2022	Q4 2022	Q1 2023	Q2 2023	Q3 2023	Q4 2023	Q1 2024
1. Bibliography	■									
2. SIP model for pure bentonite		■	■	■						
3. SIP model for bentonite and sand mixtures with deionised water					■	■				
4. SIP model for bentonite and sand mixtures with an hyperalkaline solution (pH 13.5)						■	■			
5. PhD manuscript							■	■	■	

2.3.6 Material and method

The raw materials used in manufacturing the samples are MX80 bentonite powder, Fontainebleau sand, de-ionised water, saline solutions (NaCl) and hyperalkaline (high pH) solutions. The samples manufactured from these materials are compacted in the form of cylindrical mixture (*Figure 10*) at a wide range of hydration states (gravimetric water content, volumetric water content and saturation), compaction states (bulk density, dry density and porosity), bentonite to sand ratios and pore water chemistry (de-ionised water, variations in NaCl concentration and hyperalkaline solution).
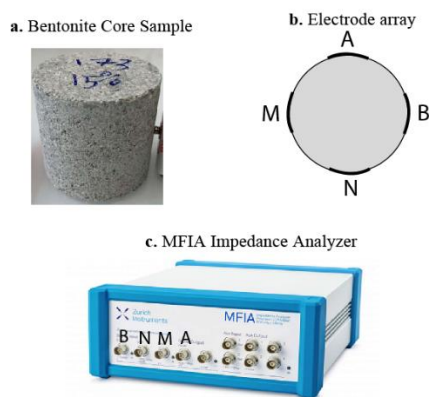
Figure 10: Sample and impedance meter. a. Picture of a fabricated sample (the sample is 5 cm in diameter and 6 or 8 cm in length). b. Position of the electrodes (A and B are the current electrodes and M and N are the voltage electrodes). c. Zurich Instruments MFIA Impedance Analyzer used to measure the complex conductivity spectra.

EURAD (Deliverable n° 17.7) - Synthesis report on Innovative and Enhanced Equipment for Repository Monitoring
Dissemination level: PUBLIC
Date of issue of this report: 04/06/2024

Page

Once each sample is ready, 4 pre-gelled and disposable Ag-AgCl ECG (electro-cardiogram) medical electrodes are attached to the sample in a radial configuration (at 90° offsets from one another) (Jougnot et al., 2010a). Two electrodes (A and B) impose the current and two other electrodes (M and N) measure the potential at two points (**Figure 10**). The measurements are made right after the sample is made to minimize the effects of drying.

Most of the measurements were done in the 1 Hz to 45 kHz range with a sampling rate of 100 which allows to capture the dependance of amplitude and phase on frequency at a high resolution. The measurement time highly depends on the frequency range and sampling rate. The frequency range 1 Hz to 45 kHz was chosen because (i) smectite particles are relatively small and polarize at higher frequencies, (ii) field work with time-domain induced polarization is done at 1 Hz and (iii) at lower frequencies electrode drift affects the measurement accuracy more significantly.

2.3.7 Results

SIP results for pure bentonite.

The result on pure MX-80 bentonite covers 69 samples made from two types of bentonites: one in the form of powder made from crushed pellets (Type I) with a homogenous grain size distribution (0.2 to 2 mm) and the other in the form of a granular bentonite mixture (GBM, type II) with a wider grain size distribution comprised between 0.1 and 7 mm, at different compaction and saturations (with de-ionised water) states.

The SIP measurements were performed using the high-precision MFIA Impedance Analyzer manufactured by Zurich Instruments. As expected, an increase was observed in both in-phase (representing electromigration of charge carriers) and quadrature (representing the ability of the material to hold charge) conductivities with higher volumetric water contents (θ). Preliminary results indicate for a wide range of volumetric water content (16 – 60%) the measured conductivity values span between two orders of magnitude for the in-phase and quadrature conductivities, indicating that such a difference is detectable using the SIP method (**Figure 11**).
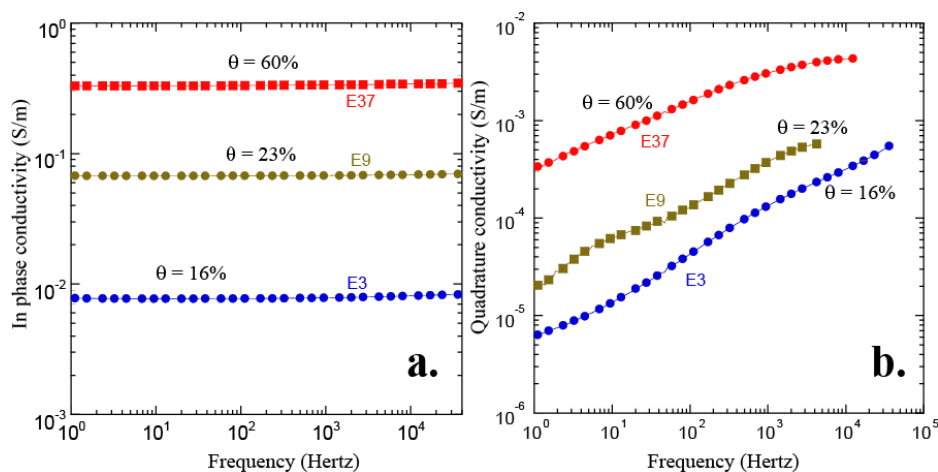
Figure 11: *In-phase and quadrature conductivity spectra of three core samples characterized by distinct water contents (here expressed in Vol.%). a. In phase conductivity spectra. b. Quadrature conductivity spectra.*

The CEC of the two bentonites were measured using the cobaltihexamine method (Guillaume 2002 [36]). A CEC of 81.9 ± 0.64 cmol(+)/kg (81.9 meq/100 g) was obtained for the crushed pellets MX80 (Type I) and 87.2 ± 0.64 cmol(+)/kg (87.2 meq/100 g) for the GBM (Type II).

The surface conductivity (σ_s) representing the conduction along the surface of the grains and the formation factor (F) were calculated using a linear conductivity model and samples made with solutions at controlled conductivities (NaCl, 25°C) (**Figure 11**). The conductivity of the saturated samples (mixed with the saline solution) is plotted against the conductivity of the pore water at saturation. Using the linear conductivity model (represented by the best fit on **Figure 12**), we obtained values of σ_s=0.26 S m-

EURAD (Deliverable n° 17.7) - Synthesis report on Innovative and Enhanced Equipment for Repository Monitoring
Dissemination level: PUBLIC
Date of issue of this report: 04/06/2024

Page

1 and F=14 at a porosity of around 53±2%. Then, using Archie's law, we obtained the cementation exponent m, which was determined at 4.5. Finally, we used sample E28 to estimate the pore water conductivity of our database as it is fully saturated and has a similar porosity.

An induced polarization model based on the dynamic Stern layer model is used to explain this dataset. We obtained a new relationship that links the petrophysical parameters to both in-phase and quadrature conductivities as well as normalized chargeability values, which were obtained by calculating the difference of in-phase conductivity between 10 kHz and 1 Hz:

$$\sigma' = \theta^m \sigma_w + \theta^p \Sigma_S \qquad (7)$$

$$\sigma'' = \theta^p \frac{\Sigma_S R}{\alpha} \qquad (8)$$

$$M_n = \theta^p R \Sigma_S \qquad (9)$$

$$\Sigma_S \equiv \rho_g B\,\mathrm{CEC} \qquad (10)$$

Where σ' and σ'' are in-phase and quadrature conductivities, Θ is volumetric water content, ρ_g is grain density, R is a dimensionless ratio of apparent mobilities (surface conduction vs. polarization), p is the saturation exponent, M_n denotes normalized chargeability, CEC is the cation exchange capacity and Σ_S is a constant for the studied material representing the characteristics responsible for charge accumulation along its grain surfaces with *B* representing the apparent mobility of counterions for surface conduction (the higher its value, the more mobile the counterions).
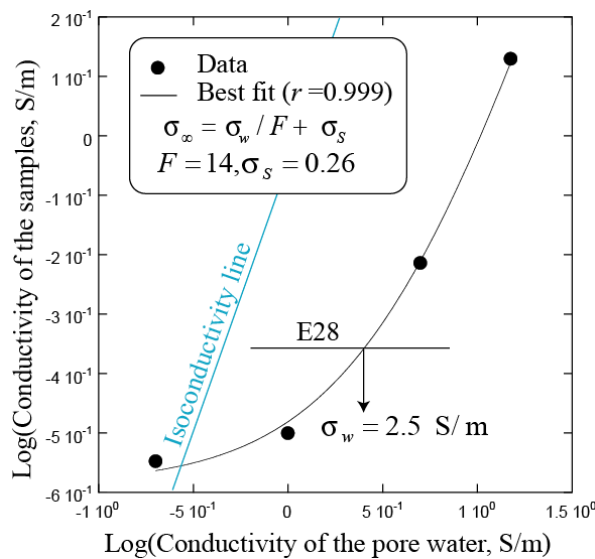
Figure 12: *Conductivity of the saturated samples (mixed with saline solution) versus the conductivity of the pore water at saturation and for a porosity of 0.53±0.02. Sample E28 (also fully water- saturated) is saturated with distilled water and has the same porosity than the other core samples (around 0.52), which indicates that the real conductivity of the pore water is around 2.5 S m-1 (25°C). The value of the formation factor and the porosity (0.53±0.02) yields a porosity exponent m = 4.5. The iso-conductivity line is the line for which the conductivity of the core sample is equal to the conductivity of the pore water.*

These models allow to predict the value of the hydration state of pure bentonite (Θ) purely from the three electrical parameters (σ', σ'' or M_n) (***Figure 12***).

Preliminary results indicate that the two types of bentonites evolve in the same way but have a slight offset which could be linked to their grain size distribution (***Figure 13***).

EURAD (Deliverable n° 17.7) - Synthesis report on Innovative and Enhanced Equipment for Repository Monitoring
Dissemination level: PUBLIC
Date of issue of this report: 04/06/2024

Page

Furthermore, to understand the behaviour of the surface and pore water conductivities, we compared the normalized "chargeabilities" of the samples to their in-phase conductivities (**Figure 14**). The first results show that samples are either dominated by the surface or bulk conductivity. Currently, no clear relation can be found to explain why the measured samples are dominated by the surface or bulk conductivity. Nevertheless, the relation between these two conductivities must be determined, as they are linearly dependent on the formation factors (e.g., cementation exponent) and in-phase conductivities of our samples.

When we compare our results to other materials in terms of its surface conductivities and reduced CEC **Figure 15**), we observe that the results from this study represents one of the highest values. This is due to the high montmorillonite content in our samples (> 70).

In addition to the model obtained allowing to predict volumetric water content, we obtained a relationship between saturation (Sr) and in-phase conductivity for pure bentonites. The use of linear and non-linear regression analysis enabled to predict the saturation and in-phase conductivity. Since both parameters can be obtained it is possible to calculate the porosity for each sample and estimate the dry density of the samples with an error of 12% between predicted and measured values.
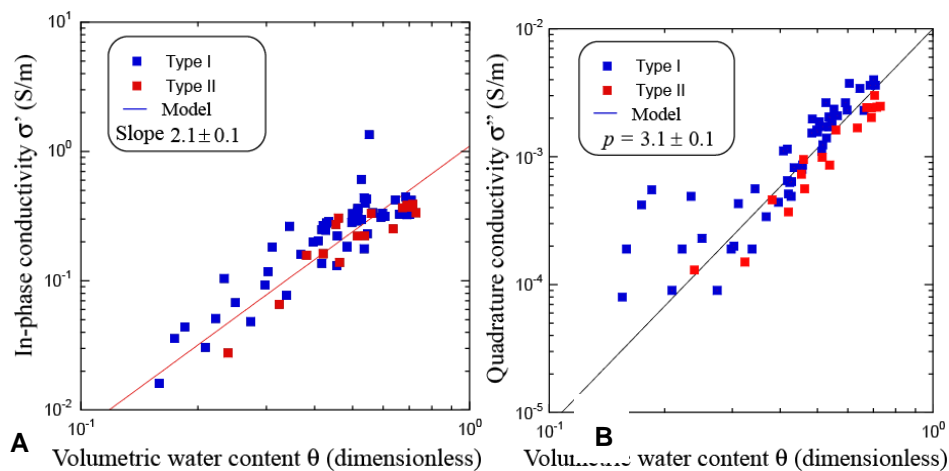
Figure 13: *Dependence of the in-phase (A) and quadrature conductivities (B) on the Vol. water content for bentonite types I and II (plotted at 345 Hz). The data are fitted with power law functions which are described in the above text. The pre-factor is determined from the linear regressions.*
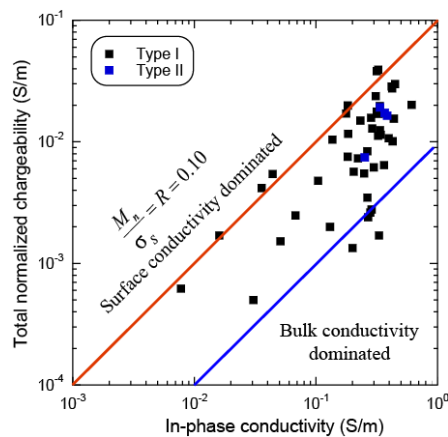
Figure 14: *Normalized chargeability versus the in-phase conductivity (at 345 Hz). The red and blue lines represent the domination of surface and bulk conductivities, respectively. Since normalized chargeability is directly dependent on the ability of a material to hold charge (and thus CEC) and in-phase conductivity has both surface and bulk porewater conductivity components, this plot allows us to determine how our porous material is conducting current through both the pore and surface contributions. The results closer to the blue line are consistent with a high value of pore water conductivity.*

EURAD (Deliverable n° 17.7) - Synthesis report on Innovative and Enhanced Equipment for Repository Monitoring
Dissemination level: PUBLIC
Date of issue of this report: 04/06/2024

Page
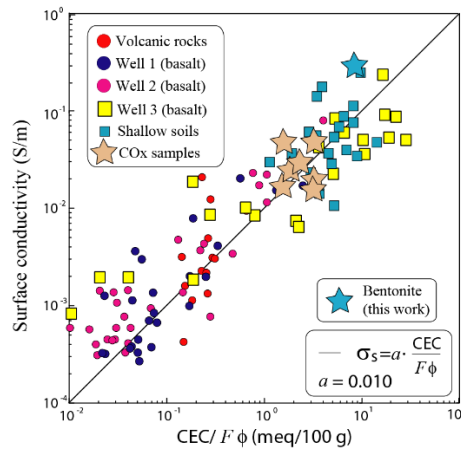
Figure 15: Surface conductivity versus the reduced CEC (CEC divided by the bulk tortuosity defined by the product of the formation factor and the connected porosity). COx stands for Callovo-Oxfordian clayrocks from the Paris Basin. The data on the volcanic rocks are from Revil et al. (2018)[47], Ghorbani et al. (2018)[35], and Revil et al. (2021)[48]. The MX80 bentonite in our database is characterized by the highest surface conductivity of all other materials. This is in line with what is expected by a material with a very high montmorillonite content, as surface conductivity is linearly related to CEC (model linking the two parameters illustrated with black line).

SIP results for bentonite/sand mixtures

The dataset of bentonite/sand mixtures is composed of a total of 45 samples. We used the type I Wyoming MX80 bentonite and Fontainebleau sand. The Fontainebleau sand is a quartz sand (99.98% silica) with a narrow grain size distribution and a mean grain diameter of ~250 µm (Bourbie and Zinszner, 1985 [31]; Doyen, 1988 [32]).

The dataset of complex conductivity spectra covers different mass fractions of bentonite content (10% to 90%), dry density (0.97 to 1.64), temperature (in the range 10-60°C), and volumetric water contents (19 % to 76%). The polarization is mainly dominated by surface conductivity.

We compared the experimental data with the dynamic Stern layer model to explain the observed trends found between the complex conductivity spectra and the mass fraction of bentonite at different hydration states. The results show that the relationship between the in-phase and quadrature conductivities does not agree with the prediction of the classical dynamic Stern layer model. Therefore, we propose a modified version of the dynamic Stern layer model that is consistent with the experimental data and could be used to interpret field data.

The parametric model that can be used to interpret our observations can be summarized by two equations for the electrical conductivity and the normalized chargeability according to

$$\sigma_\infty = \theta^{2.3}\left(\sigma_w + \gamma_B \Sigma_S\right) \qquad (11)$$

$$M_n = \theta^{3.3} R \Sigma_S \qquad (12)$$

where $\Sigma_S \equiv \rho_g B \mathrm{CEC}_B$ and the exponents are used to fit the experimental trends. With this parametric model, the surface conductivity linearly depends on the bentonite content but not the normalized chargeability or the quadrature conductivity. Between 100 Hertz and 1 kHz, the simplified expressions for the in-phase and quadrature conductivities $\sigma^* = \sigma' + i\sigma''$ can be written as,

$$\sigma' = \theta^{2.3}\left(\sigma_w + \gamma_B \Sigma_S\right), \qquad (13)$$

$$\sigma'' = \theta^{3.3}\frac{\Sigma_S R}{\alpha}. \qquad (14)$$

EURAD (Deliverable n° 17.7) - Synthesis report on Innovative and Enhanced Equipment for Repository Monitoring
Dissemination level: PUBLIC
Date of issue of this report: 04/06/2024

Page

Using ρ_g = 2800 kg m^{-3}, B (Na+, 25°C) =3.1×10^{-9} m^{2}s^{-1}V^{-1}, and CEC$_B$ = 90 meq/100 g = 87×10^3 C kg^{-1} yields Σ_S = 0.75 S m^{-1}. As the pore water conductivity is σ_w =0.21 S m^{-1}, the prefactor for the in-phase conductivity is $\sigma' = \sigma'_0 \theta^{2.3}$ with σ'_0 = 0.96 S m^{-1} for pure bentonite. **Figure 16** shows that the prefactor is σ'_0 =1.1±0.2 S m^{-1} from the experimental data therefore in close agreement with the predicted value. Now we turn our attention to the prefactor for the quadrature conductivity. With α = 8 (based on the grain size distribution covering 4 orders of magnitude) and the value of the dimensionless number R = 0.10, the prefactor of the power law relationship for the quadrature conductivity is $\sigma''_0 = \Sigma_S R/\alpha$ = 0.0095 S m^{-1}. The observed prefactor is as $\sigma'' = \sigma''_0 \theta^{3.3}$ with σ''_0 =0.0124 S m^{-1} (see **Figure 17**) in agreement with the prediction.
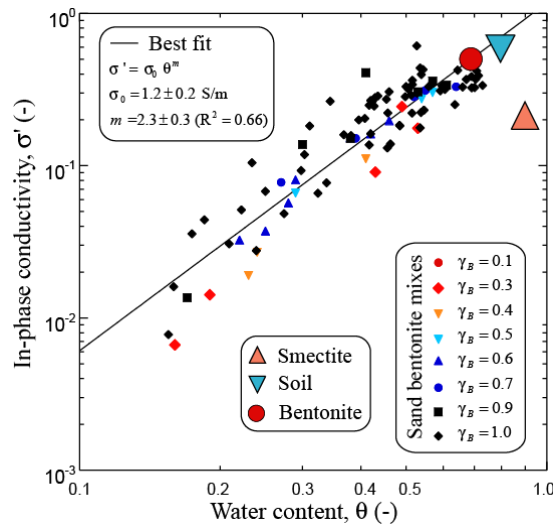
Figure 16: *In-phase conductivity (345 Hz, 25°C) versus water content in volume for the entire collection of experiments reported in Table 1 (saturated and unsaturated samples). The data from the study of El Alam et al (2023)[34] have been added for the pure bentonite samples (γ_B =1). The power-law fit is used to obtain the value of the exponent m. The pure smectite data point (very high porosity of the gel of 0.90) is from Revil et al. (2018)[47]. The soil is the CG soil sample from the study of Revil et al. (2017)[46] (porosity 0.78, CEC 19 meq/100 g). The bentonite corresponding to the large red circle is sample B2 from Okay et al. (2014) (porosity 0.67, CEC 44.2 meq/100g).*

EURAD (Deliverable n° 17.7) - Synthesis report on Innovative and Enhanced Equipment for Repository Monitoring
Dissemination level: PUBLIC
Date of issue of this report: 04/06/2024

Page
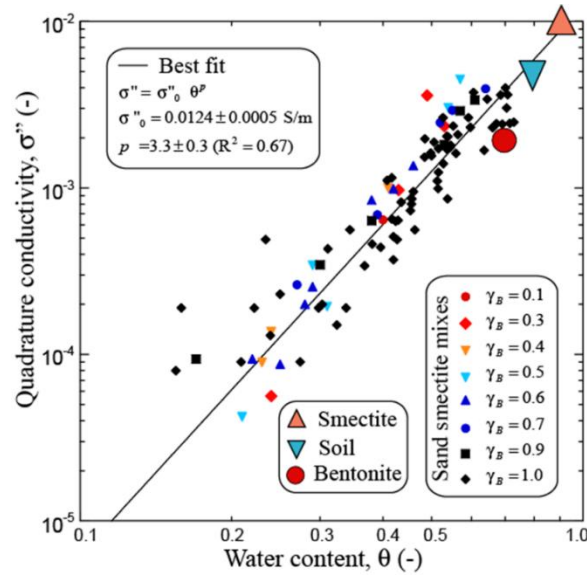
Figure 17: *Quadrature conductivity (345 Hz, 25°C) versus water content in volume for the entire collection of experiments reported in Table 1 (saturated and unsaturated samples). The data from the study of El Alam et al. (2023) have been added for the pure bentonite samples gB =1). The power-law fit is used to obtain the value of the exponent p. The pure smectite data point (porosity 0.90, fully saturated) is from Revil et al. (2018). The soil is the CG soil sample from the study of Revil et al. (2017)[46] (porosity 0.78, CEC 19 meq/100 g). The bentonite corresponding to the large red circle is sample B2 from Okay et al. (2014) (porosity 0.67, CEC 44.2 meq/100g).*

The dry density is also an important parameter to understand and monitor as it affects the swelling pressure of smectite-rich materials. In saturated conditions, the quadrature conductivity can be written as,

$$\log \sigma'' = 3.3 \log \phi + \log\left(\frac{\Sigma_S R}{\alpha}\right). \qquad (15)$$

Since the dry density can be written as $\rho_d = (1-\phi)\rho_g$ and therefore $\phi = (\rho_g - \rho_d)/\rho_g$. Inserting this relationship into equation (15), we obtain,

$$\log \sigma'' = 3.3 \log\left(\frac{\rho_g - \rho_d}{\rho_g}\right) + \log\left(\frac{\Sigma_S R}{\alpha}\right). \quad (16)$$

In **Figure 18**, we plot the quadrature conductivity versus the dry density ρ_d (at constant temperature) and we observe a relationship consistent with the form of equation (16). The data can be fitted with the following relationship:

$$\log \sigma'' = 2.6 \log\left(\frac{2.65 - \rho_d}{2.65}\right) - 2.02. \qquad (17)$$

Taking $\Sigma_S R/\alpha = 0.0124$ (see above), we have log($\Sigma_S R/\alpha$)≈-1.9 consistent with the estimate given above.

EURAD (Deliverable n° 17.7) - Synthesis report on Innovative and Enhanced Equipment for Repository Monitoring
Dissemination level: PUBLIC
Date of issue of this report: 04/06/2024

Page
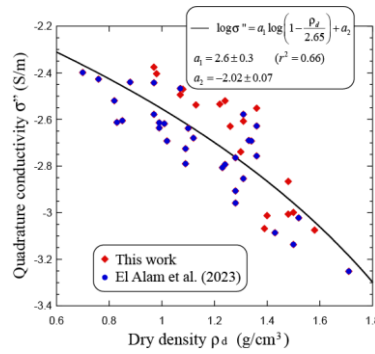
Figure 18: *Quadrature conductivity (345 Hz, 25°C) versus dry density (saturated and nearly saturated samples with saturation >0.90). The data from the study of El Alam et al. (2023)[34] have been added (gB =1) also using only the saturated sample. The plain line corresponds to the fit of the data according to the relationship discussed in the main text with the dry density in g cm^{-3}.*

SIP results for bentonite/sand mixtures with an hyperalkaline fluid

A total of 54 experiments were conducted to analyse the effect of an hyperalkaline solution on the induced polarization response of MX80 bentonite and sand mixtures. We first measured the complex conductivity spectra 10 minutes after the preparation of the core samples (**Figure 19**) and then carried out 29 experiments on 29 new samples to analyse the evolution of the complex conductivity spectra over time (**Figure 20**).
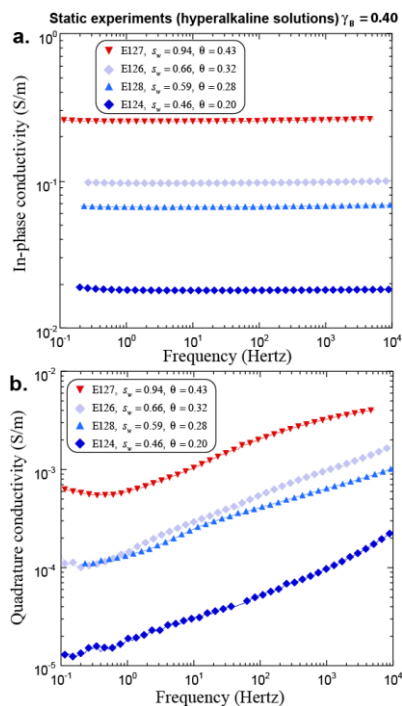
Figure 19: *Complex conductivity spectra of 4 samples at the same bentonite mass fraction ($\gamma_B = 0.4$) and at a range of hydration states (saturations s_w ranging from 0.46 to 0.94 and volumetric fluid content θ ranging from 0.20 to 0.43) saturated with the same hyperalkaline solution. a. In-phase conductivity spectra. b. Quadrature conductivity spectra*
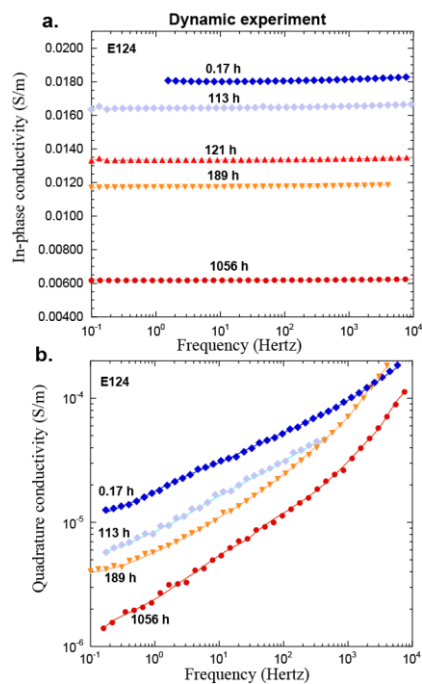
Figure 20: *Example of time-lapse experiment. In-phase and quadrature conductivity spectra for sample E124 (bentonite content $\gamma_B = 0.4$ and saturation $s_w = 0.46$), with measurements taken at different time steps, ranging from 10 minutes to 1056 hours. a. In-phase conductivity spectrum. b. Quadrature conductivity spectrum. The times are provided in hours from the assemblage of the samples.*

We assumed that the samples are isotropic and time-invariant during the time needed to perform each complex conductivity spectrum. Furthermore, as mentioned previously we have assumed that the smectite polarizes above 1 Hertz and the sand grains polarize below 1 Hertz.

EURAD (Deliverable n° 17.7) - Synthesis report on Innovative and Enhanced Equipment for Repository Monitoring
Dissemination level: PUBLIC
Date of issue of this report: 04/06/2024

Page

For the static experiments, we note an increase of the in-phase and quadrature conductivity with the presence of the hyperalkaline solutions with respect to the spectra at near-neutral pH conditions. These changes are observed to be associated with the high conductivity of the hyperalkaline solution with respect to the experiment carried out on pure bentonite. The relationships established for pure bentonite regarding the dependence of the in-phase and quadrature conductivity with respect to the water content and saturation remains however valid.

For the time-lapse experiments, we observed at the opposite with respect to the static experiments a decrease of both the in-phase and quadrature conductivities over time. These data can be fitted using an exponential decay function (**Figure 21**).
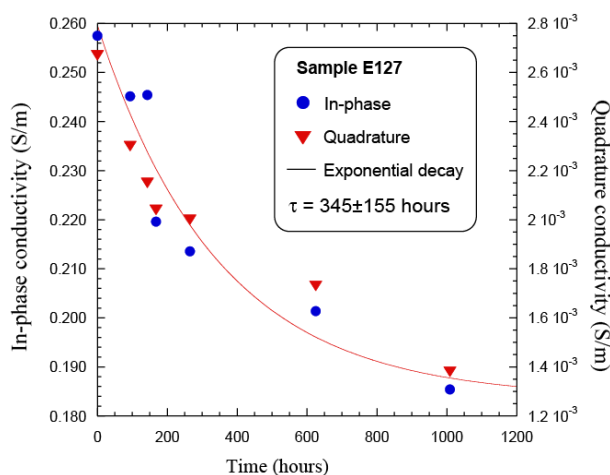
Figure 21: In-phase and quadrature conductivity data at 345 Hz of one bentonite sample E127 (gB = 0.40) versus time (time-lapse experiment). The exponential decay was observed for the two components of the complex conductivity indicating the same process affecting the in-phase and quadrature conductivities. The relaxation time t results from the best fit of the exponential decay. A possible mechanism could correspond to the dissolution of some of the smectite within the samples due to the hyperalkaline solution and its transformation in illite. This illitization process releases also fresh water in the pore space, reducing the pore water conductivity.

This evolution may be explained by the illitization process of the smectite contained in the bentonite thanks to the presence of potassium in the pore water solution (**Figure 22**). A small decrease of the CEC can be inferred from the quadrature conductivity while the in-phase conductivity values are consistent with a decrease of the ionic strength of the pore water (**Figure 23**). Indeed, illite is characterized by a smaller CEC than smectite and this CEC change explains the decrease of the quadrature conductivity. Furthermore, the illitization process is responsible for the release of fresh water (associated with the dehydration of smectite). This fresh-water release explains the decrease of the in-phase conductivity.

EURAD (Deliverable n° 17.7) - Synthesis report on Innovative and Enhanced Equipment for Repository Monitoring
Dissemination level: PUBLIC
Date of issue of this report: 04/06/2024

Page
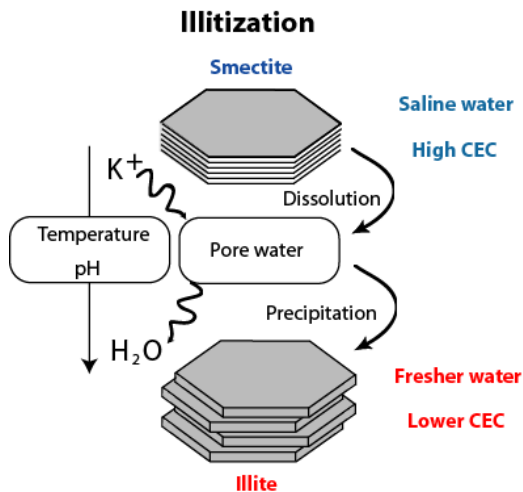
Figure 22: *Illitization process of smectite in the bentonite because of temperature and pH conditions in presence of potassium. The process leads to a decrease of the CEC (the CEC of illite is substantially smaller than the CEC of smectite) and a decrease of the conductivity of the pore water since illitization releases water molecules from the dehydration of smectite.*
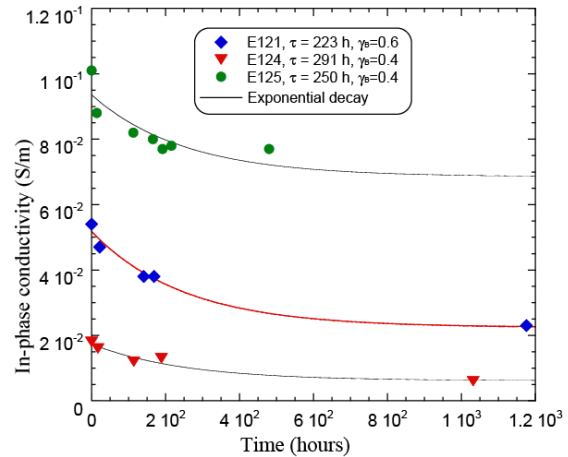
Figure 23: *Evolution of the in-phase conductivity with time for three samples characterized by two values of the bentonite content. The relaxation time of the exponential decay remains in the range 220-290 hours.*

2.3.8   Discussion about the results obtained.

In this study we have developed power-law saturation models based on the dynamic Stern layer model that quantitatively and accurately determine the volumetric water content in our samples using laboratory measurements between 1 Hz and 45 kHz of in-phase and quadrature conductivity as well as normalized chargeability. The power-law models include relatively few parameters: the bulk conductivity (through the pores), the cation exchange capacity, the grain density, the apparent mobility of counterions for surface conduction and the cementation and saturation exponents (m and p, see Archie's law).

The parametric model can also be used for bentonite and sand mixtures and allows to determine the bentonite mass fraction of each sample. We also find satisfactory correlations between the electrical parameters and temperature at all saturations and bentonite fractions, meaning that if variations in temperature were to occur, with all other variables held constant, the effect of temperature on the IP response can be quantified.

Furthermore, we observe a strong dependence of in-phase and quadrature conductivity on saturation when the mass fraction of bentonite is kept constant. Hence, the evolution of saturation in bentonite and sand mixtures can be monitored if the mass of the melange stays constant.

Finally, we investigated the effects of dry density of samples that are saturated or at near saturated conditions ($s_w > 0.9$) and found that this parameter obeys an inverse logarithmic behaviour with quadrature conductivity using a non-linear regression. We find that higher dry densities lead to lower values of the imaginary component. Similarly, to the lack of link between this component and clay fraction, no direct explanation can be given yet and a more in-depth study needs to be done.

The petrophysical investigations and results presented in this study can be applied to time-domain induced polarization data obtained in field conditions. Indeed, in the field tomography of time-domain induced polarization data can be performed to obtain tomograms of the conductivity and normalized chargeability. Theoretically, we could apply our models to field data to determine the water content and CEC tomograms. The conductivity of the pore water can be obtained using a speciation model

EURAD (Deliverable n° 17.7) - Synthesis report on Innovative and Enhanced Equipment for Repository Monitoring
Dissemination level: PUBLIC
Date of issue of this report: 04**/06/2024**

Page

accounting for the solubility of the minerals (see as an example for the Callovo-Oxfordian formation, Leroy et al., 2007).

However, field results using the models built within this project have yet to deliver satisfactory results. Nevertheless, induced polarization already appears as a promising method to monitor indirectly, through time and space, the petrophysical characteristics of sealing bentonites. From the lab to the field measurement there is a volume that should be investigated.

2.3.9 References

[31]. Bourbie, T. & Zinszner, B., 1985. Hydraulic and acoustic properties as a function of porosity in Fontainebleau Sandstone, Journal of Geophysical Research: Solid Earth, 90, 11524–11532, doi:10.1029/JB090iB13p11524.

[32]. Doyen, P.M., 1988. Permeability, conductivity, and pore geometry of sandstone, Journal of Geophysical Research: Solid Earth, 93, 7729–7740, doi:10.1029/JB093iB07p07729.

[33]. Duvillard P.A., Revil A., Soueid Ahmed A., Qi Y., Coperey A., Ravanel L., 2018, Three-dimensional electrical conductivity and induced polarization tomography of a rock glacier. Journal of Geophysical Research, 123. https://doi.org/10.1029/2018JB015965.

[34]. El Alam J., Revil A., Dick P., 2023. Influence of the water content on the complex conductivity of bentonite. Eng. Geol., 322 (2023), Article 107183, 10.1016/j.enggeo.2023.107183.

[35]. Ghorbani A., Revil A., Coperey A., Soueid Ahmed A., Roque S., Heap M.J., Grandis H., Viveiros F., 2018. Complex conductivity of volcanic rocks and the geophysical mapping of alteration in volcanoes. J. Volcanol. Geotherm. Res., 357 (2018), pp. 106-127.

[36]. Guillaume, G., 2002. Etude expérimentale du système fer - smectite en présence de solution à 80°C et 300°C. Géochimie. Université Henri Poincaré - Nancy I. PHD thesis, P217.

[37]. Leroy, P. & Revil, A., 2009. A mechanistic model for the spectral induced polarization of clay materials, Journal of Geophysical Research: Solid Earth, 114, B10202, doi:10.1029/2008JB006114.

[38]. Madsen, F. T., 1998, Clay Mineralogical investigations related to nuclear waste disposal: Clay Minerals, 33 (1), 109–29. https://doi.org/10.1180/000985598545318.

[39]. Okay, G., Leroy, P., Ghorbani, A., Cosenza, P., Camerlynck, C., Cabrera, J., Florsch, N. & Revil, A., 2014. Spectral induced polarization of clay-sand mixtures: Experiments and modeling, Geophysics, 79, E353–E375, doi: 10.1190/geo2013-0347.1.

[40]. Proix, N., Cleret, L., Viart, G., Ducristel, D., & Guerin, A., 2015. Mesure de CEC et de cations échangeables par une solution de cobaltihexamine saturée en carbonate. COMIFER.

[41]. Promentilla, M. A. B., & Sugiyama, T., 2010. X-ray microtomography of mortars exposed to freezing-thawing action. Journal of Advanced Concrete Technology, 8(2), 97-11201.

[42]. Revil, A., 2012. Spectral induced polarization of shaly sands: Influence of the electrical double layer. Water Resour. Res., 48, W02517.

[43]. Revil, A., 2013. Effective conductivity and permittivity of unsaturated porous materials in the frequency range 1 mHz–1GHz, Water Resources Research, 49, 306-327.

[44]. Revil, A., Cathles III, L. M., Losh, S., & Nunn, J. A., 1998. Electrical conductivity in shaly sands with geophysical applications. Journal of Geophysical Research: Solid Earth, 103(B10), 23925-23936.

[45]. Revil, A., and N. Florsch, 2010. Determination of permeability from spectral induced polarization data in granular media, Geophysical Journal International, 181, 1480-1498.

[46]. Revil, A., A. Binley, L. Mejus, and P. Kessouri, 2015. Predicting permeability from the characteristic relaxation time and intrinsic formation factor of complex conductivity spectra, Water Resour. Res., 51 Revil, A., Coperey, A., Shao, Z., Florsch, N., Fabricius, I.L., Deng, Y., Delsman, J.R., Pauw, P.S., Karaoulis, M., de Louw, P.G.B., van Baaren, E.S., Dabekaussen, W., Menkovic, A., Gunnink, J.L., 2017. Complex conductivity of soils, Water Resources Research, 53, 7121–7147, doi:10.1002/2017WR020655.

[47]. Revil, A., Coperey, A., Deng, Y., Cerepi, A., Seleznev, N., 2018. Complex conductivity of tight sandstones, Geophysics, 83, E55–E74, doi:10.1190/geo2017-0096.1.

[48]. Revil A., Schmutz M., Abdulsamad F., Balde A., Beck C., Ghorbani A. Hubbard S. S., 2021. Field-scale estimation of soil properties from spectral induced polarization tomography. Geoderma, 403, 115380. https://doi.org/10.1016/j.geoderma.2021.115380.

EURAD (Deliverable n° 17.7) - Synthesis report on Innovative and Enhanced Equipment for Repository Monitoring
Dissemination level: PUBLIC
Date of issue of this report: 04/06/2024

Page

2.4 CHENILLE: Coupled beHaviour undErstaNdIng of fauLts: from the Laboratory to the fiEld

2.4.1 Introduction

The project realized in the frame of the EURAD consortium consists in the monitoring of an in-situ heating experiment in the URL of Tournemire, southern France. The overall objective of this project is to create a dataset that will allow to study the physical processes resulting from thermal and fluid loading on an existing, identified and characterized, fault zone. The idea here is to carry out a thermally controlled (with temperatures ranging from 15 to 150°C) in situ gas injection experiment in one of the faults accessible from the galleries. A heating system was installed in two boreholes close to the injection borehole (injection_1) to allow a precise and controlled incremental increase of the thermal load. The monitoring system of this experiment consists of borehole-supported temperature, pressure and seismic/acoustic observation shown in *Figure 24*.
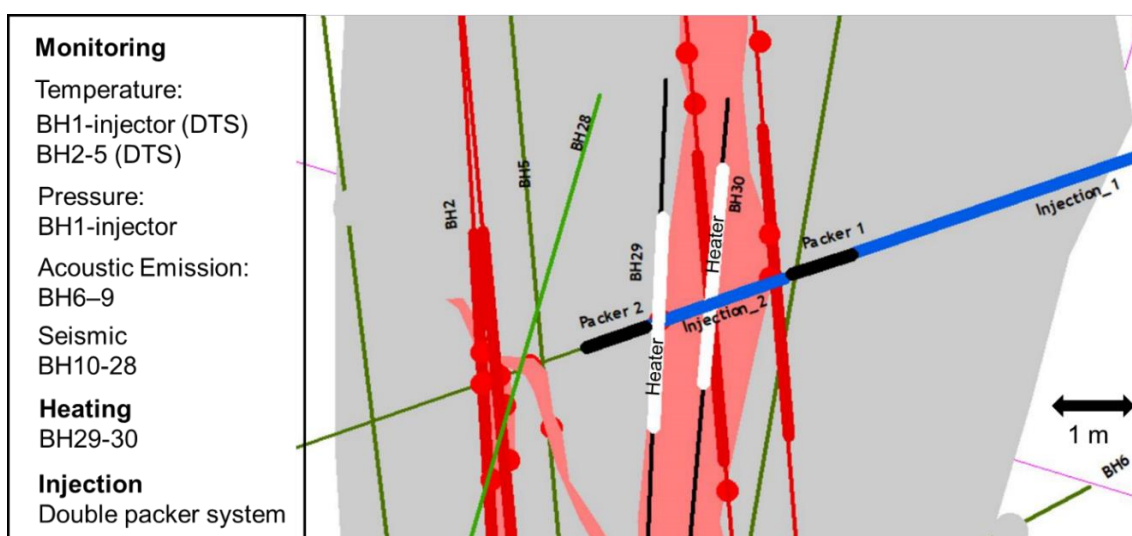
Figure 24: Top view of the Chenille experimental setup realized in boreholes (BH) at the URL Tournemire. Grey shaded areas include the damage and light red the fault core zone.

2.4.2 Problem analysis

The project aims at carrying out a thermally controlled (with temperatures ranging from 15 to 150°C) in situ gas injection experiment in one fault core zone accessible from the galleries. Two three-meter-long heaters were installed in aluminium cased boreholes (BH 29-30) about 1 m distance above and below the injection chamber (injector_1 in Figure 1) to allow a precise and controlled incremental increase of the thermal load. Fibre optic monitoring (DTS) was installed in four boreholes (BH2-5) of 20 m length and in the 30 m long injection borehole (BH1, see *Figure 25*). DTS technology enables borehole temperature monitoring to study hydrogeological processes at a frequency of about 4.5 minutes and a spatial resolution of about 0.5 m. The objective of this sub-task was to test our ability to install DTS equipment, perform this measurement type under extreme conditions, including the complete temperature range from 15 to 150°C, and compare the results to other techniques. In addition to the fundamental knowledge that this project will provide, it will lead to a significant improvement in current measurement methods in clay-rich material thanks to the combination of several geophysical techniques and complementary sensors, and more broadly in the context of monitoring underground installations at high temperature levels in complex geological environments.

EURAD (Deliverable n° 17.7) - Synthesis report on Innovative and Enhanced Equipment for Repository Monitoring
Dissemination level: PUBLIC
Date of issue of this report: 04/06/2024

Page
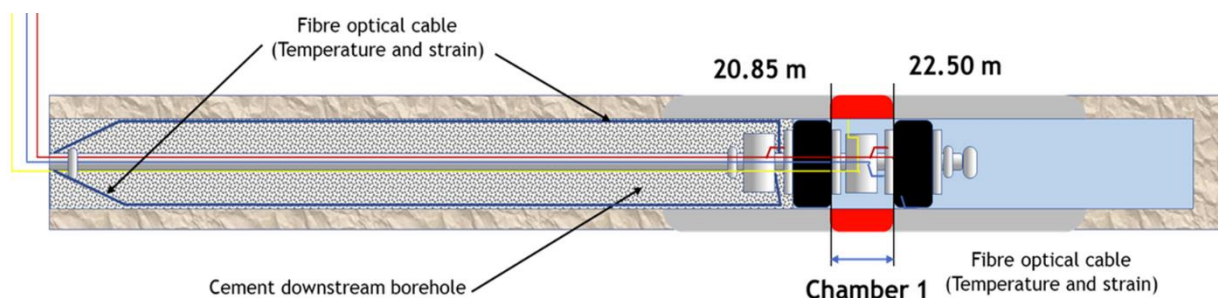
Figure 25: *Multipacker system installed in the injection borehole BH1 isolating the fault core zone. The chamber length is 1.85 m. Pressure and temperature sensors are in the chamber and at the packers (black). Fibre optical cable is installed in up-(0 to 19.85 m) und downstream parts of the borehole (24.5 to 29.93 m). For further details see also **Figure 27**.*

2.4.3   Research Objectives

The objectives of our work in the frame of the MODATS project are to:

- Create a dataset that will enable identification and characterization of the physical processes resulting from thermal and fluid loading on a pre-existing fault zone.
- Install the combination of heaters and optical fiber (FO) for distributed temperature measurements in boreholes in fractured medium (fault zone)
- Investigate the thermal diffusion in a fault zone.

In order to fulfil these objectives our work was divided into 3 sub-tasks that are related to the different monitoring and imaging techniques that we decided to use in order to monitor our THM experiment.

2.4.4   Overview of the development team

Carolin Böse, GFZ Potsdam,

Dr. Carolin Böse is a scientist and seismologist with an extensive background in borehole- and URL-based Acoustic Emission studies. She lead several passive seismic monitoring projects at the field scale in New Zealand (ICDP Alpine Fault Drilling Project, Contact Energy Wairakei Geothermal field), Germany (GEOREAL Kontinentale Tiefbohrung Project) and the decameter scale (STIMTEC-X hydraulic stimulation experiment at Reiche Zeche URL Freiberg, Germany). She has established the seismological skill set and tools for a comprehensive analysis of the seismic event data including stress field determination at various scales.

Sven Fuchs, GFZ Potsdam

Dr. Sven Fuchs is a senior scientist in Section 4.8 Geoenergy at GFZ, and is contact person for the reservoir monitoring. He holds a PhD in Geology from the University of Potsdam, Germany, and a Diploma in Hydrogeology from the Technical University of Berlin, Germany. His research is focused on the Earths thermal field and its relevance for geodynamic processes as well as for the technological utilization of the subsurface (exploration of resources, geothermal production, geological storage of energy and waste, etc.). This includes detailed studies of the heat flow evolution and associated rock thermal properties, considering the effects of geoscientific processes across scales and time. He has been principle investigator (PI), work package, and task leader in several major DFG, BGE and EU funded projects, e.g. WHDB project, ThermoBase, ITHERLAB, GeoPuR.

Stefan Lüth, GFZ Potsdam

Dr. Stefan Lüth is a senior researcher and group leader at GFZ. He has been working on active seismic imaging projects in various fields of application, including tectonic studies, underground storage of carbon dioxide, tunnel construction and characterization of geological formations for nuclear waste disposal. He has been the project coordinator for the seismic characterization and monitoring activities at the Ketzin Pilot Site for CO2 Storage throughout the operational phases until the final closure of the site. Within the EU funded projects CO2Sink and CO2Care, he has been working as the task and work package leader in the site monitoring work packages. He is currently also active as the PI of a seismic imaging experiment in the Mont Terri clay rock laboratory which is focusing at tomographic and reflection seismic imaging at the scale of an Underground Rock Laboratory (URL).

EURAD (Deliverable n° 17.7) - Synthesis report on Innovative and Enhanced Equipment for Repository Monitoring
Dissemination level: PUBLIC
Date of issue of this report: 04**/06/2024**

Page

Audrey Bonnelye, Université de Lorraine

Dr. Audrey Bonnelye Ass. Prof in Université de Lorraine. She is an experimental rock physicist with a strong interest on mechanisms of deformation at different scales (from µm to m scale) on complex materials (complex geometries, anisotropy). She is one of the co-PI of the CHENILLE (Coupled beHaviour undErstaNdIng of fauLts: from the Laboratory to the field, (Bonnelye et al., 2023)) project in Tournemire URL.

Rüdiger Giese, GFZ Potsdam

Dr. Rüdiger Giese is a senior scientist in geophysics at the GFZ-German Research Centre for Geosciences in Potsdam. His research interests include development of high-resolution seismic exploration and monitoring systems for the application in tunnels and boreholes, VSP and MSP, mining geophysics, and scientific drilling. He is heading the underground seismic working group and Helmholtz Innovation Lab "3D-Underground Seismics" at GFZ. He is responsible for the GFZ-Underground-Lab in the Research and Education Mine "Reiche Zeche" in Freiberg. Dr. Giese has mainly worked together with industry partners in the development of seismic hard- and software tools e.g. for tunnel and borehole seismic prediction. His works have resulted in a significant number of patents.

2.4.5   Development steps follow during the MODATS project.

I.   Design of the experimental setup and of the monitoring systems according to their spatial and temporal resolution and range

II.   Installation of the monitoring sensor network and remote data transmission system

III.   Create baseline surveys as a basis for modelling of different scenarios of pressure, temperature evolution, crack formation and fluid movement along and through the different fault zones

IV.   Comparison with measured data and adaption of the THM model to reproduce this data

Activity	Q4 2021	Q1 2022	Q2 2022	Q3 2022	Q4 2022	Q1 2023	Q2 2023	Q3 2023	Q4 2023	Q1 2024	Q2 2024
1. Preparation of experimental test site and of measuring devices	■	■									
2 Active seismic surveys, data analysis & imaging			■	■	■	■					■
3. Installation of DTS network in BH2-5, start of continuous temperature monitoring				■	■	■	■	■	■	■	■
4. Installation of AE-sensors in BH6-9, start of continuous acoustic monitoring				■	■	■	■	■	■	■	■
5. Installation of the injection system and FO-sensors in BH1, start monitoring						■	■	■	■	■	■

EURAD (Deliverable n° 17.7) - Synthesis report on Innovative and Enhanced Equipment for Repository Monitoring
Dissemination level: PUBLIC
Date of issue of this report: 04**/06/2024**

Page

of pressures and temperatures												
6. Installation of two new borehole heaters, start of heating												

2.4.6   Material and method

Fibre optic monitoring under extreme conditions

The former heating boreholes (BH2-5, Figure 1) house a 4 m long stainless-steel heating canister. The heaters contain spiral resistors enabling a heating power of 4000 W at 230 V. The heating canisters were designed to generate, incrementally, temperatures in the order of 150 °C in and around the vicinity of the injection interval.

It was intended to monitor the temperature evolution along the four heating boreholes using distributed temperature sensing (DTS), which is placed according to the scheme presented in *Figure 26*. This is probably the most frequently applied fibre-optic sensing method, which has also been used with increasing success for geophysical applications in boreholes during the past 30 years (Henninges and Masoudi, 2020).
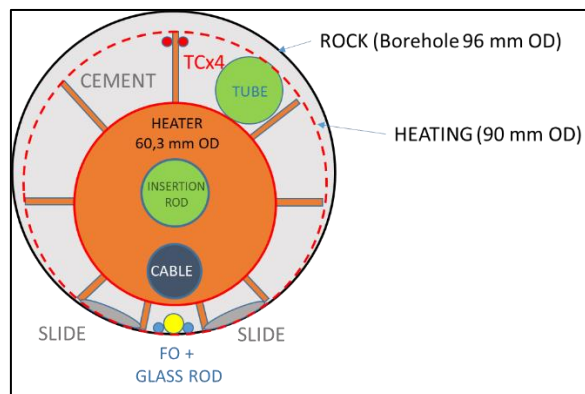
Figure 26: Cross section of the insertion of the FO cables together with the heaters and tubes for cementation after installation in BH2-5.

Using DTS technology, an optical fibre acts as the sensing element. As there are no electronic parts required, fibre-optic sensors have some advantages over conventional sensors, including ruggedness, flexibility and ease of deployment, high temperature tolerance, and immunity to electromagnetic interference. With a proper DTS installation and system, a measurement accuracy of +/- 0.3 °C can be achieved (e.g. (Henninges et al., 2005a)[59]). The resolution or repeatability of the measurement depends on a number of factors including the length of the fibre, and the integration time over which the data is averaged. As an example, for a fibre length of 1000 m and 10 minutes integration time, an RMS error of 0.02 °C has been reported (Voigt et al., 2011, [72]). For the DTS monitoring at Tournemire, an interrogator from Sensa is used, which enables measurements with a spatial resolution of 1 m and a sampling space which can be selected between 0.25 m and 1 m.

Under harsh environmental conditions such as high temperature and excessive pressure, the fiber attenuation can be altered through a process known as hydrogen ingression or darkening, which can lead to a rapid degradation of the measurement data (e.g. (Smithpeter et al., 1999) [71]). The coating material protects the optical fibre against adverse chemical influences and primarily determines the temperature tolerance. Metal-coated fibres have the highest temperature tolerances, but usually also

EURAD (Deliverable n° 17.7) - Synthesis report on Innovative and Enhanced Equipment for Repository Monitoring
Dissemination level: PUBLIC
Date of issue of this report: 04/06/2024

Page

exhibit high attenuation, especially at low temperatures (Reinsch and Henninges, 2010, [67]), which limits their use to very short sensing ranges. A coating comprised of an outer high-temperature tolerant polyimide layer and an additional carbon layer, which offers some protection against hydrogen ingression, is referred to as hermetic coating. During a field test in a high-temperature geothermal well in Iceland, (Reinsch et al., 2013, [68]) have successfully deployed hermetic coating fibres at temperatures up to 230 °C over a period of 14 days, but reported different signs of degradation occurring after exposure to temperatures above 300 °C. As this is within the expected temperature range of 200-250 °C for the heating boreholes, such fibres will also be used for the current experiment.

For deployment in boreholes, sensor cables must be designed to protect the optical fibers against mechanical stress, and to withstand the environmental conditions like temperature, pressure, and corrosive fluids. For installation in the four heating boreholes, a sensor cable design with an inner stainless-steel tubing hosting the optical fibres and an outer steel wire jacket for additional mechanical strength and protection has been chosen. The fibre-optic sensor cables were installed in a loop configuration, allowing to interrogate the optical fibre from both sides. They were fixed to the outside of the heater elements, extending as long as possible towards the tip of the borehole, using suitable devices to protect the cables from mechanical damage during installation.

For these reasons, two kinds of arrays were deployed: in the Tournemire URL one allowing for the temperature distributed monitoring (Raman) (Henninges et al., 2005b,[60]), and one for deformation measurement (Brillouin).The first array provide accurate information on the temperature evolution along the heating boreholes. The DTS data allows to derive petrophysical properties such as thermal conductivity and heat capacity of the surrounding host rocks. The second array is an essential tool to understand the influence of thermal loading on a fault zone.

<u>Passive seismic monitoring</u>

Crack formation detection is challenging in clay rich material due to high attenuation of the media. Monitoring seismic deformation and resulting high-frequency signals in clay rich rocks is challenging due to strong attenuation and anisotropy present in the rock mass (e.g. (Plenkers et al., 2022 [66]; Kwiatek et al., 2011[62]; Bohnhoff et al., 2009 [52])). During the Faults&Fluids (De Barros et al., 2016 [55]) project at the Tournemire URL, accelerometers sensitive in a frequency range between 2 Hz and 4 kHz were installed in boreholes within the same fault zone. These allowed for the detection of 32 events with magnitudes ranging between M -4.3 and M -3.7. Within this project, we intent to further extend the observed frequency range both to higher and lower frequencies by using the AE sensors and broadband seismometers, respectively. It is anticipated that the AE sensors that are sensitive between 1-60 kHz will be capable to detect seismic events of sub-dm size (see earlier successful monitoring campaigns in crystalline and metamorphic rocks, e.g. (Boese et al., 2022 [51]; Kwiatek et al., 2011[62], 2018, Plenkers et al., 2011[65]) with magnitudes down to M -6.0. The key element of success is to overcome the attenuation by installation of AE sensors close to the expected seismic sources and ensure good coupling of the sensors. We installed 12 AE sensors in the boreholes BH6-9 at distances up to 5 meters from the stimulated intervals to limit the effect of strong attenuation expected in shales (see also part dedicated to active seismic monitoring. The AE sensors were installed as perpendicular to the borehole trace and anchored against the borehole wall to optimize the coupling quality. The network layout was optimized for the 3D coverage of the injection interval, enabling more accurate location of seismic events and estimation of focal mechanisms (cf. Boese et al., 2022[51]; Kwiatek et al., 2018[63]). The acquisition system now records full waveforms in continuous mode at 200 kHz sampling rate. Triggering-mode recordings turned out to be unfavourable due to strong specific noise condition on site. The passive measurements have been supplemented with active ultrasonic transmission measurements and hammer/centre punch hits. The ultrasonic transmitter was located at 12 positions in borehole BH8 to generate high-frequency impulsive signals that were recorded by the majority of the AE sensors. This allowed to (i) measure the P-wave velocity and its 3D anisotropy in the direct proximity of stimulation site (as derived for crystalline rocks by Boese et al., 2022 [51]), (ii) assess the attenuation through analysis of frequency-dependent amplitude decay (Blanke et al., 2023 [49]), (iii) test and further improve the coupling of AE sensors to the borehole walls. Active measurements using

EURAD (Deliverable n° 17.7) - Synthesis report on Innovative and Enhanced Equipment for Repository Monitoring
Dissemination level: PUBLIC
Date of issue of this report: 04/06/2024

Page

sledgehammer and centre-punch tools (Boese et al., 2022 [51]) were additionally used along the tunnel walls to increase the ray path coverage at the site.

<u>Active seismic monitoring</u>

Controlled seismic experiments were performed in 2021 and 2022, using coupled magnetostrictive vibrators and impact hammer sources (Richter et al., 2018 [69]) along the East gallery and the main tunnel as well as between boreholes to investigate the structural environment in particular the complex fault network surrounding the tunnel lab. The experiment consists of two baseline surveys and repeated acquisition using the same survey layout during and after the heating and stimulation activities. The fault structure is composed of a main brecciated and foliated core zone of up to 2 m thickness and a damage zone of complex geometry made up of subsidiary faults. The results of the seismic underground survey allow to assess the position of eventual damage occurrence and to detect potential time-lapse effects in comparison with observations from fibre-optic and passive seismic surveying.

The 3D-imaging techniques combining tomographic and migration inversion techniques using wave polarization attributes (Richter et al. 2022 [69]) are applied to gain images for P- and S- waves in the area of about 50 m around the tunnel with a resolution of about 0.5 m (Giese et al., 2005 [57]; Lüth et al., 2008 [64]). Recent experiments performed with the same system in the Mount Terri URL (Switzerland) revealed a transmissivity of seismic waves for frequencies of up to 1000 Hz. The concept of seismic imaging for Tournemire will be completed by tomographic inversion of attenuation values (Krauß et al., 2014 [61]). The seismic attenuation is a valuable parameter to understand the rocks mechanical behaviour during hydraulic stimulation experiments.

2.4.7 Description on the field test used during the project.

The CHENILLE experiment was set up in the following steps:

- 2020: Drilling of a first set of injection and monitoring wells BH1-9
- 2021: Drilling of additional monitoring wells BH10-26 for active seismic experiment; first
- baseline active seismic survey along the Gallery East 03 and the main tunnel
- 2022: Second baseline active seismic survey including a crosshole survey in two newly drilled
- monitoring wells BH27-28; Installation of DTS and AE sensor network in BH2-9
- 2023: Installation of injection system and FO-cables in BH1; Installation of two new heaters in
- BH29-30; start of heating 20th of November.

Major delays in the execution of the CHENILLE experiment were caused by defects of the borehole heating systems first installed in boreholes BH2-5. It was not possible to initiate five of the eight heater elements. It was therefore decided to build two new 3 m long borehole heating systems with the same output as the previously installed systems. To ensure the functionality of the new borehole heating systems, it was decided to equip the two new boreholes with an aluminum casing which was cemented by IRSN. This allowed the recovery of the heaters in the case of malfunctions. No fiber-optics were installed in the new wells. Temperature monitoring is realized by two sensors in the middle of the heaters. The heating has been started on the 20th of November 2023. The heaters gradually reached a temperature of 245 °C, which has been kept constant ever since.

<u>Multipacker equipment</u>

We installed one multipacker system (***Figure 27***) in BH1 to monitor measure the spatiotemporal evolution of temperature and pore-pressure fields caused by induced heating of a sound, damaged and intensely deformed shale formation crossed by a tectonic fault. The multipacker system was installed in borehole BH1 which crosscuts perpendicularly the studied fault zone. It consists of a set of steel tubes equipped with water-inflated packers. The packers prevent any flow from the injection interval when they have a minimum pressure difference of +15 bars with regards to the injection interval. The system is composed of two hydraulic packers, each with an anchoring length of 1 m. The external diameter of the unanchored packer is 89 mm. The packers are dimensioned for a pressure of 120 bar for a 96 mm diameter borehole

EURAD (Deliverable n° 17.7) - Synthesis report on Innovative and Enhanced Equipment for Repository Monitoring
Dissemination level: PUBLIC
Date of issue of this report: 04**/06/2024**

Page

and for a maximum temperature of 120°C. The packers are anchored separately by injecting water into 4/2.4 mm steel lines.

The injection interval 1 is defined by the bottom of the borehole and packer 1. At the base of interval 1 is a stainless-steel end cap with a 30% porosity sinter (OD 70 mm, ID 66 mm) surrounding a stainless-steel inner tube and a hydrostatic pressure measurement line (4/2.4 mm).

The injection interval 2 is delimited by packer 1 and 2. It is fitted with a 30% porosity sinter (OD 70 mm, ID 66 mm) surrounding a stainless-steel inner tube. Three steel lines (4/2.4 mm) at the level of the interval allow hydrostatic pressure measurement as well as injection and circulation.

Furthermore, a PT1000 temperature sensor (range -23°C; +77°C) was also installed in interval 2.
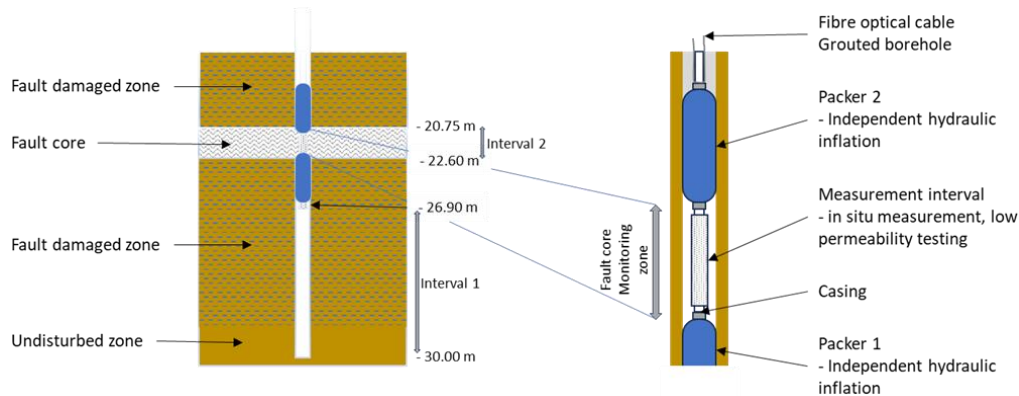
Figure 27: *Schematic diagram of the multipacker system in BH1*

Temperature variations in the fault core zone

The temperature sensor in interval 2 is located at a depth of 21 m. The sensor records the air temperature of a 1.85 m long interval which also corresponds to an estimated volume of 929 cm3 for the interval measurement. The injection borehole and the temperature sensor are located between 0.8 and 1.1 m from the two heating boreholes (***Figure 24***). The temperature and pressure evolution during the heating is shown in ***Figure 28***. The heat power steps were increase gradually to reach a maximum temperature on the heaters of 245°C. The maximum temperature has not yet been recorded as the temperature in the borehole continues to rise 3 months after the heaters were switched on. An electrical incident occurred during the first week of January which caused a power shut down of the experiment. After the heaters were turned back it has taken another month to reach the temperature before the power cut. The temperature today in the injection 2 interval is 32.25°C, the average increase in temperature is around 0.5°C/week.
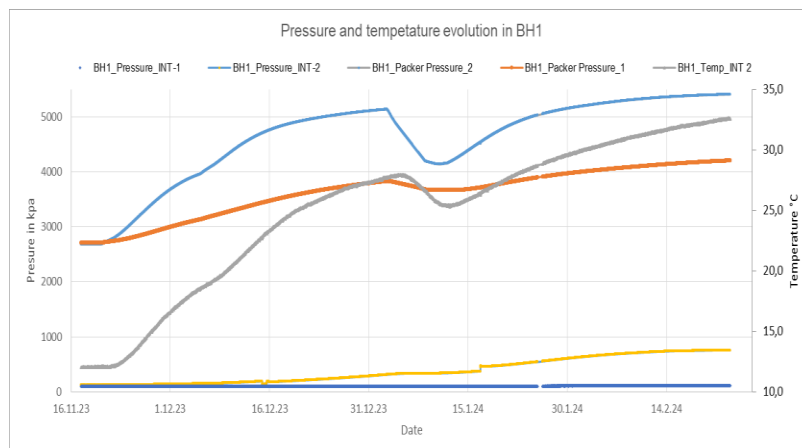
Figure 28: *Pressure and temperature curve in the injection well since the start of heating on 20th of November.*

EURAD (Deliverable n° 17.7) - Synthesis report on Innovative and Enhanced Equipment for Repository Monitoring
Dissemination level: PUBLIC
Date of issue of this report: 04/06/2024

Page

2.4.8   Results

Passive seismic monitoring

Several natural Acoustic Emission (AE) events were recorded in triggering-mode during closure of operations at the Tournemire URL over Christmas (***Figure 29*** and ***Figure 30***). These events originate in the direct vicinity of the installed AE system as can be seen by the almost simultaneous arrival at several AE sensors. These events will be used to tune the detection system and train a convolutional neural network for characterization of recorded signals. By switching to continuous recording since 23 December 2023, triggering of events will be performed during postprocessing of the data, which allows to suppress noise spikes frequently seen in the data. Using the continuous wavelet transform the frequency content of regularly occurring noise spikes can be characterized and suppressed by a special way of filtering as shown in Figure 8. This facilitates detection of small events otherwise indistinct from the noise for common triggering methods.
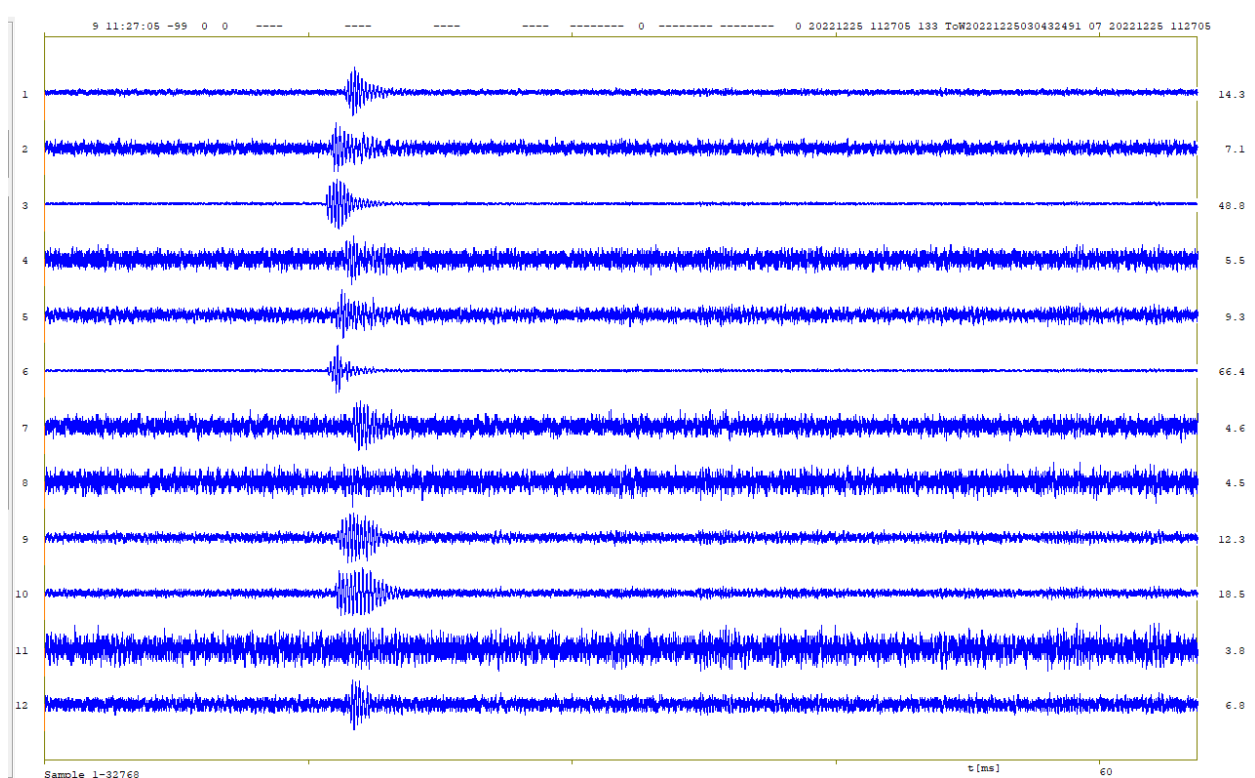
Figure 29 : *Waveform example of a natural AE event recorded on 25 December 2023 (11:27:05) by all 12 channels (as indicated by labels on the left) with good signal to noise ratio. The traces are normalised with maximum raw amplitude in mV shown by the labels on the right.*

EURAD (Deliverable n° 17.7) - Synthesis report on Innovative and Enhanced Equipment for Repository Monitoring
Dissemination level: PUBLIC
Date of issue of this report: 04/06/2024

Page
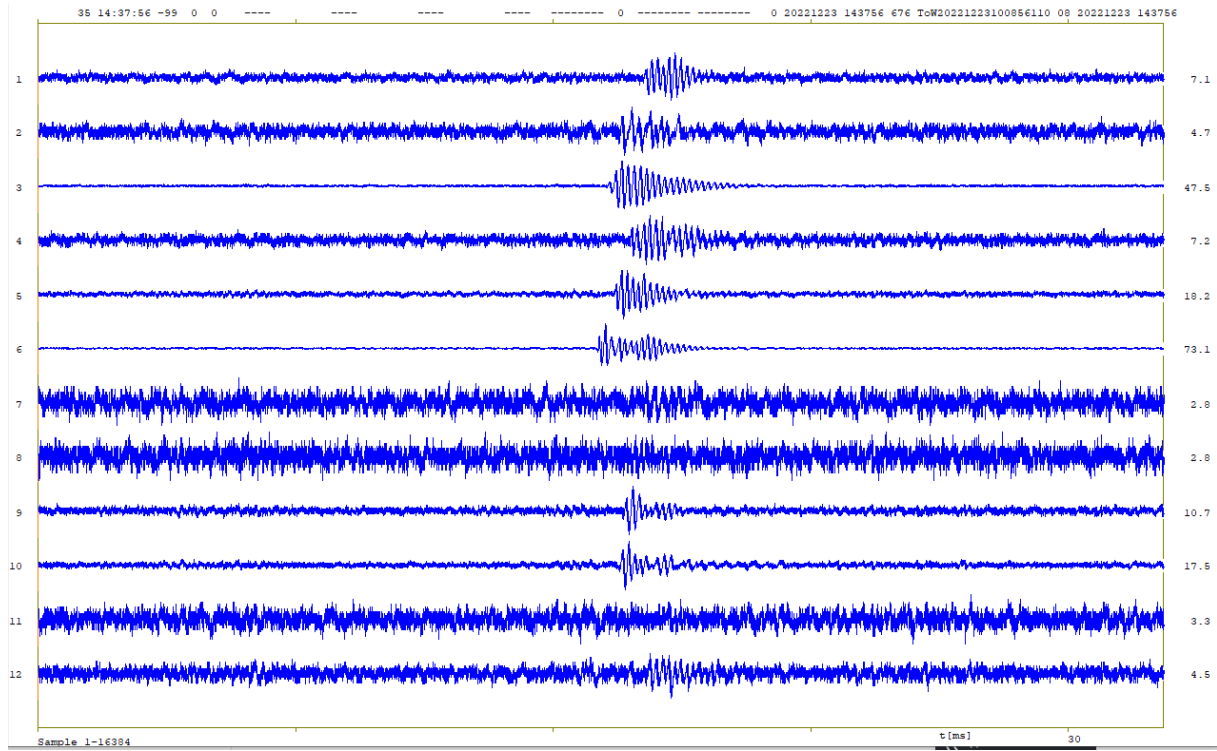
*Figure 30: Another waveform example of a smaller natural AE event recorded on 23 December 2023 (14:37:56) by a subset of channels (as indicated by labels on the left). The traces are normalised with maximum raw amplitude in mV shown by the labels on the right. Note that the time window shown is halved compared to that in **Figure 29**Spectra of the raw signal for channel 3 and 6 are shown in the corresponding technology data sheet, indicating that the dominant frequency content of the event is around 10 kHz.*
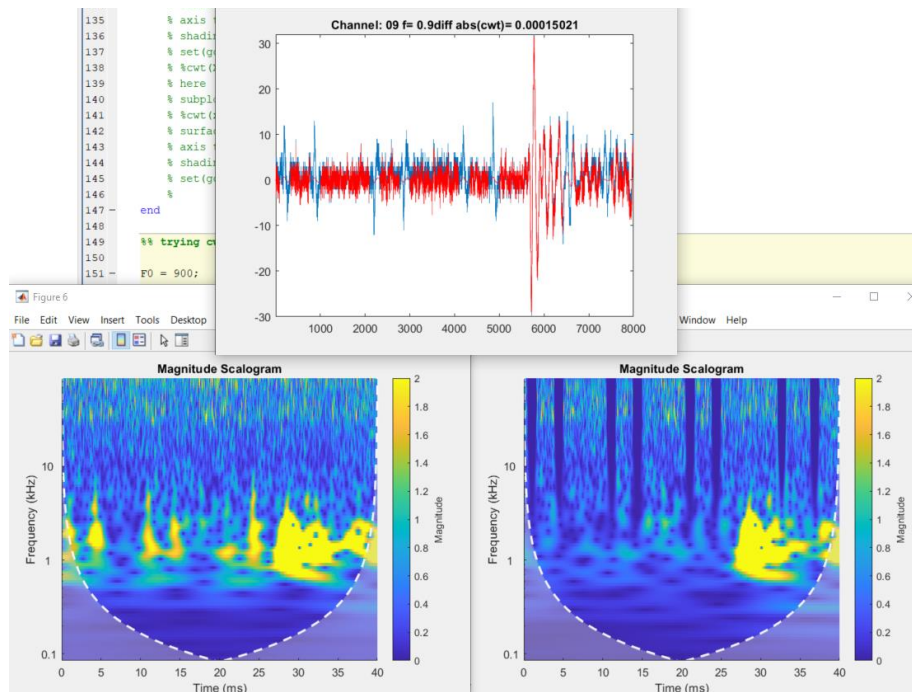
Figure 31: Waveform example of a small AE event masked by noise spikes of similar amplitude as the event (top). Using the continuous wavelet transform the frequency content of the recurring spikes (bottom left) is filtered out as shown in the scalogram on the right, which allows for processing with common AE event detection algorithms (courtesy of M. Rosskopf)

Active seismic monitoring

EURAD (Deliverable n° 17.7) - Synthesis report on Innovative and Enhanced Equipment for Repository Monitoring
Dissemination level: PUBLIC
Date of issue of this report: 04/06/2024

Page

Controlled seismic experiments are part of the monitoring concept, using different types of seismic sources (Richter et al., 2018 [69]) to investigate the structural environment in particular the complex fault network within the Tournemire URL. The results of the seismic underground survey are complementary to the geological mapping of the core samples and aim to improve the background geological model for later time lapse investigations. A baseline seismic survey along the main tunnel and Gallery East-03 was performed in June 2021 to explore the structures and to map the seismic rock conditions before the hydraulic stimulation experiment will be started. The survey length is about 100 m with a source point interval of 0.5 m. Two different pneumatically driven impact sources were used in a comparative test in 1 m intervals each (*Figure 32*). To prove the repeatability of the sources and to increase the signal-noise ratio by vertical stacking three and five shots were fired per source point. In total, 821 shots were recorded by 15 three-component geophone receivers (28 Hz) of about 6 to 7 m interval installed in 2 m deep boreholes (BH10 to BH26 in *Figure 31*). The selection of the source type for the baseline Tournemire survey is based on a previous seismic experiment conducted in the Mont Terri URL (Wawerzinek et al., 2022 [73]).
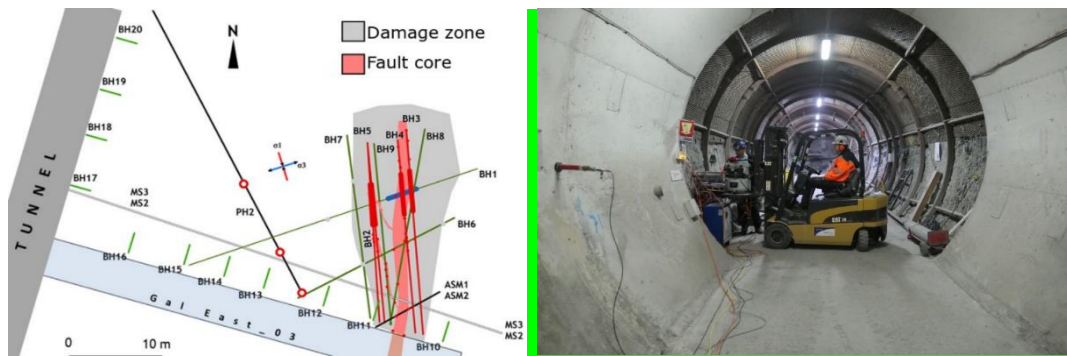
Figure 32: map view of the experiment. The short boreholes dedicated to the active seismic activity are denoted in green (from BH10 to BH20). Right: View into the Gallery East-03 from the main tunnel showing the impact seismic source mounted onto a forklift. In the foreground the tail end of a seismic receiver is visible on the left tunnel wall.

Raw data recordings are characterized by P-, S-, and surface waves in the frequency range of 30 to 1000 Hz up to about 5 m offset. Beyond this range, the maximum signal frequencies decrease quickly below 500 Hz. Figure 10 depicts a raw data example of the radial component of the receiver in borehole BH14 Figure 9. The fault core zone (see *Figure 32*) is characterized by later arrival times of the direct waves and back-propagated surface waves (arrows in *Figure 33*). These later arrival times can be observed also at other locations along gallery East-03 which indicates the complexity of the fault zone.
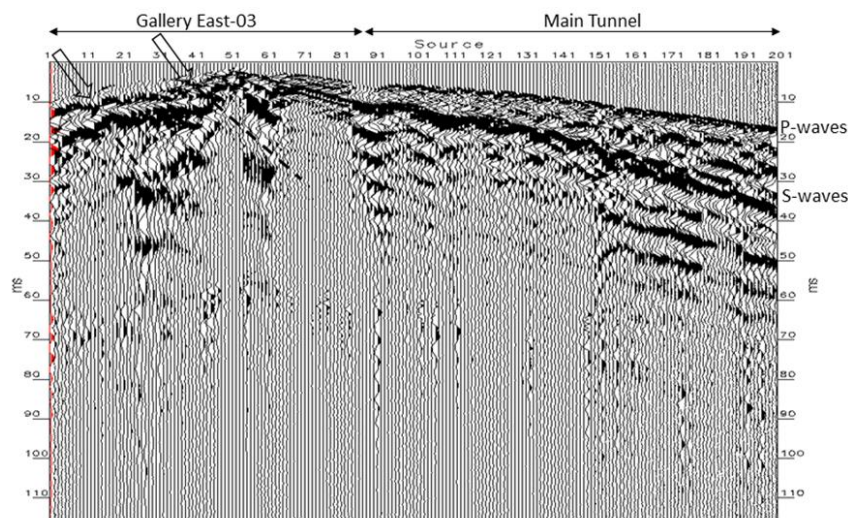
Figure 33: Raw data example of seismograms recorded by the radial component in BH14. Arrows mark later P-wave arrival times which indicates the location of the fault core and possible fractured zones within the damaged zone crossing the Gallery East-03

EURAD (Deliverable n° 17.7) - Synthesis report on Innovative and Enhanced Equipment for Repository Monitoring
Dissemination level: PUBLIC
Date of issue of this report: 04**/06/2024**

Page

Different seismic imaging approaches have been applied to image the fault zone and the tunnel surrounding area. *Figure 34* shows the imaging results of different 3C-Kirchhoff migration types using selected phase signals and different signal frequency bands. It was possible to trace the outlines of the fault zone up to 30 m into the rock mass (*Figure 34*). Major challenges occurred in the data processing and imaging due to the high amplitude-level of direct and reflected surface waves and the measurement setup surrounding the fault zone from two sides only.

To improve the imaging quality of the second baseline seismic survey, which was acquired in June 2022, it was decided to drill two additional wells at both sides of the fault zone. The 30 m long well at the end of Gallery East-03 enables a better ray coverage for the tomographic inversion, whereas the 15 m long well on the other side allows a cross-hole tomography with higher signal frequencies and a denser source and receiver spacing. To increase the data quality for reflection imaging, a magnetostrictive vibration source was applied in addition to the impact source along the tunnel surface.
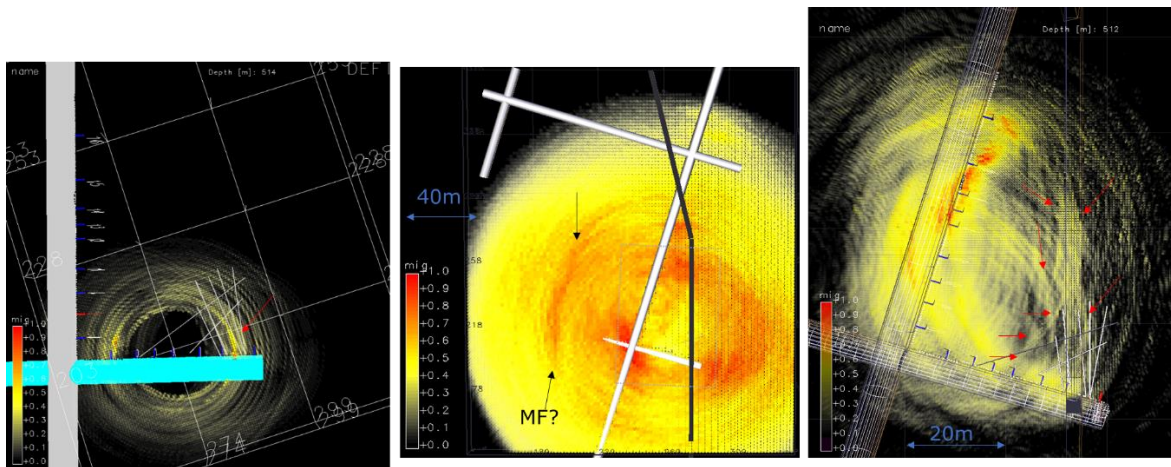
Figure 34: Seismic imaging of the reflected wavefield applying a signal-phase selected 3C-Kirchhoff Migration (left) and a Fresnel-Volume Migration (FVM) for low-frequency surface and shear waves (middle) and for high-frequency polarization filtered shear waves (right). The used constant seismic velocities range from 1950 to 2050 m/s. MF: Arrows point to potential reflection image of the Main Fault ~50 m west of the main tunnel.

Figure 35 shows the magnetostrictive vibration source shooting in Gallery East-03. The source signal was a linear sweep with frequencies from 350 to 2.000 Hz and with a length of 22 s. The lower frequency limit was at a relatively high level to reduce the energy of the exited low-frequency surface waves. *Figure 36* depicts receiver gather examples of impact and vibro sources recorded by one borehole geophone chain level. Due to its larger coupling area and the higher contact pressure the number of source points in particular in Gallery East-03 was lower for the vibration source than for the impact source.

Figure 35: Magnetostrictive vibration system applied on the side wall of Gallery East-03. The source is equipped with four magnetostrictive actuators which work simultaneously using a real-time control system.

EURAD (Deliverable n° 17.7) - Synthesis report on Innovative and Enhanced Equipment for Repository Monitoring
Dissemination level: PUBLIC
Date of issue of this report: 04/06/2024

Page
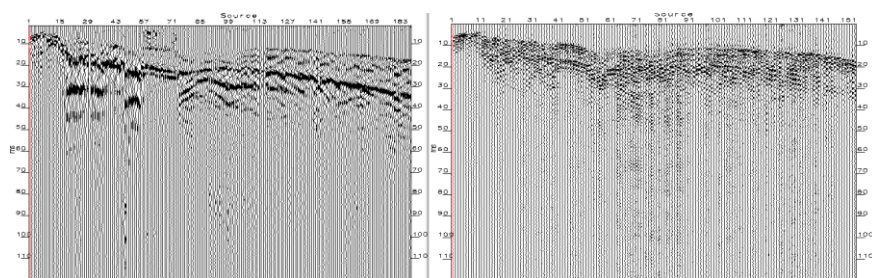
Figure 36: *Receiver gathers of the impact (left panel) and vibration source (right panel) operating on the side walls of the Gallery East-03 and the main tunnel. The borehole receiver was located in the receiver borehole at the far end of the Gallery East-03.*

For the cross-hole tomography a newly developed seismic borehole vibration source was applied (***Figure 37***)The borehole source was driven with a linear sweep with frequencies of 350 to 3000 Hz and a length of 22 s. A geophone chain consisting of eight 3C-levels with a spacing of 3.5 m was used as receiver array (Figure 14). The borehole source and the receivers were moved in both wells so that a nominal point spacing of 0.5 m for source and receiver positions was obtained.

The tomographic traveltime inversion of the second baseline survey was performed using the pyGIMLi (Rücker et al., 2017 [74]) package. P- and S-wave traveltimes were picked in the receiver gathers of impact and vibro source operation. We focus here on the results of the impact source traveltime data. Because of the small tilt of the bedding (5°) and the isotropic plane parallel to the bedding, the anisotropy of the clay stone can be ignored (Bretaudeau et al., 2014 [54]). The results of the seismic tomography (***Figure 37***) measured from the tunnel walls show that the fault can be resolved to a depth of ~30 m with P-wave travel time inversion (Esefelder et al., 2023 [56]). The S-wave tomography has resolved the fault to a depth of ~15 m. The Vp/Vs ratio seems to be reduced within and around the fault, compared to the surrounding rock mass, but this signature is less clear than the velocity distribution derived from the tomographic inversion (***Figure 38***).
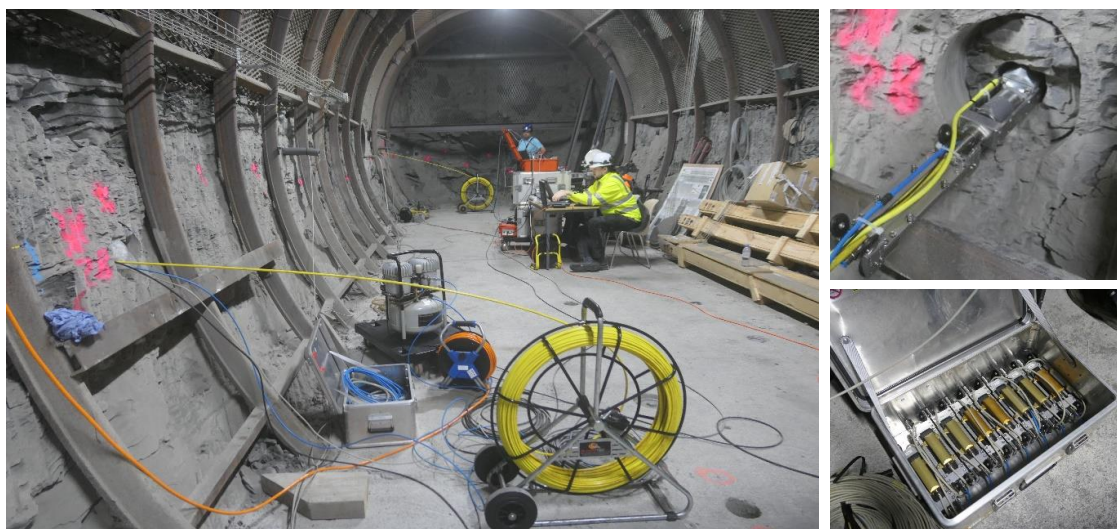
Figure 37: *Seismic cross-hole tomography in Gallery East-03 during the second baseline seismic survey (large picture). A prototype of a newly developed borehole vibration system was used as seismic source (upper-right picture). A borehole geophone chain consisting of eight 3C-levels with a spacing of 3.5 m was applied as receivers (lower-right picture).*

One of the main objectives of the seismic tomography measurements was to deliver baseline data representing the state before heating and injection experiments start. Repeated seismic measurements are planned to investigate changes of rock physical properties due to the temperature and/or pressure changes caused by the experiments. A seismic modelling study was performed as a recovery test, based on a simple thermal model simulating the predicted temperature increase in the final stage of the active heating phase. A maximum temperature increases of 150 °C was assumed and, based on rock

EURAD (Deliverable n° 17.7) - Synthesis report on Innovative and Enhanced Equipment for Repository Monitoring
Dissemination level: PUBLIC
Date of issue of this report: 04/06/2024

Page

physical experiments performed on rock samples from Tournemire (Masri et al., 2014), changes of elastic properties (Young's modulus and Poisson's ratio) were computed depending on the temperature increase.

The changed elastic properties were then applied to a baseline model including the fault zone. The forward travel times were calculated and 3% noise was added. These data were then inverted. ***Figure 39*** shows the simulated temperature increase (with 150 °C maximum temperature in the centre), the derived change of P-wave velocity and the tomographic inversion of the simulated P-wave traveltimes (from left to right). Despite the noise added to the data, the predicted P-wave velocity anomaly could be recovered by the tomographic inversion in terms of the absolute value of the velocity change. The shape of the anomaly was slightly modified, compared to the predicted shape, which is a result of the limited aperture of the tomographic acquisition geometry.
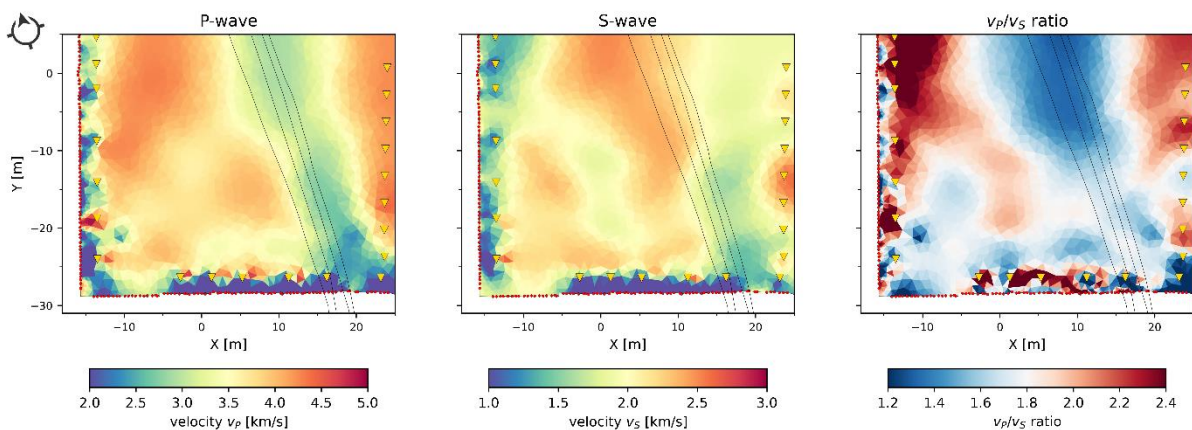
Figure 38: *Tomographic inversion results for P- and S-wave velocities (left, center), and Vp/Vs ratio (right). The black lines indicate the fault zone. Yellow triangles mark the positions of the receivers and red dots those of the source points.*
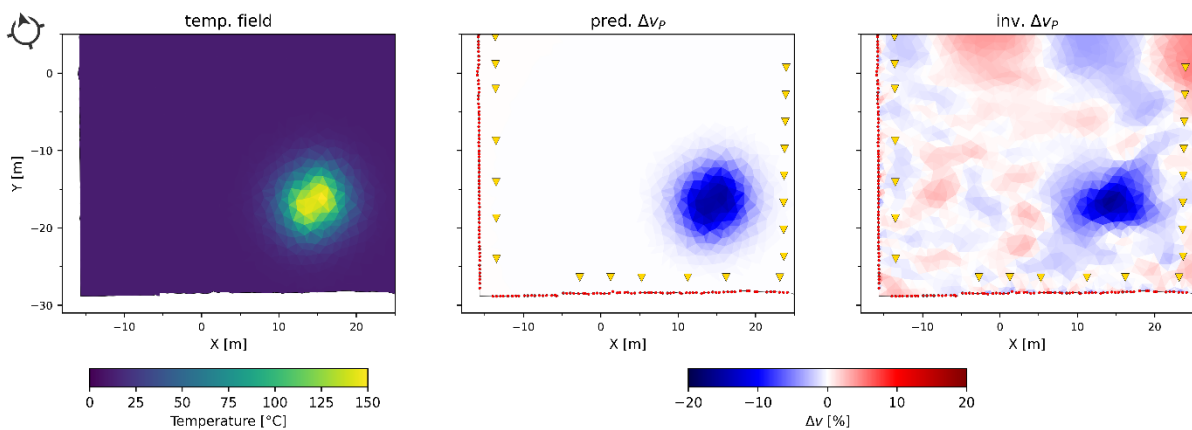
Figure 39: *Temperature simulation and tomographic recovery test. From left to right: Simulated temperature field after heating, change of P-wave velocity due to temperature increase, tomographic inversion result from traveltimes simulated using the modified P-wave velocities due to the temperature increase.*

Distributed Temperature Sensing

Monitoring with FO along the heaters will provide accurate information on temperature evolution in the medium and allow to infer on the properties such as thermal diffusion. The FO were installed in 09/2022 and continuously recorded data since then, providing a long-running baseline for the actual heating experiment. Every T-profile has an integration time of ~67s. As the wells are measured one after another, new T-profiles are recorded every 4:30min for every borehole. A 100 m-breakout cable was connected before and after every well to have a proper connection to the interrogator. To perform a length correlation on the fibre traces, reference temperature spots were set at the well entrance. DTS

EURAD (Deliverable n° 17.7) - Synthesis report on Innovative and Enhanced Equipment for Repository Monitoring
Dissemination level: PUBLIC
Date of issue of this report: 04**/06/2024**

Page

(distributed temperature sensing) Interrogator, readout computer and an Uninterruptable Power Supply (UPS) were installed in a small cabinet that protects the electronics. Examples of the visualized data for borehole BH2 are shown in Figure 18. Beside of the preparation of the FO monitoring, we took samples for laboratory measurements of thermal rock properties and conducted in-situ measurements of thermal conductivity with a needle probe at the gallery walls. The high-T laboratory measurements are still running.
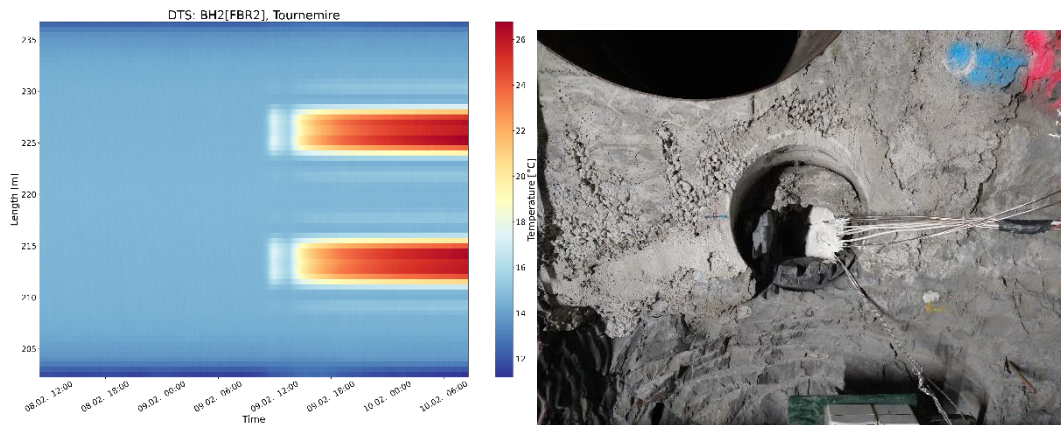
Figure 40: *Colour plot of time-length temperature signal in borehole BH2 for February 2023 (left) and example of FO implementation in borehole.*

Figure 18: Colour plot of time-length temperature signal in borehole BH2 for February 2023 (left) and example of FO implementation in borehole.

<u>Thermal Rock Property Measurements</u>

In a first step, we have measured thermal conductivity at 77 locations directly at the tunnel wall/gallery under in-situ conditions. We used a needle probe (transient line source) with different orientations to the wall (horizontal and vertical) both in the fault zone and at beside the fault zone.

In the GFZ laboratory, we have measured thermal conductivity and diffusivity (using optical scanning) under laboratory ambient pT conditions on 38 oven-dried core samples of different drillings (BH2, BH3, BH4, BH5, BH27, BH28, T01, T02, T03, T04, G5M180). For some samples (7 core samples of different drillings: BH2, BH3, BH5, BH27, BH28, T01, T03), we extended the measurements to elevated temperature conditions using a transient plane source up to 245 °C. The dry measured data were corrected for the water effect (geometric mean approach) using a 10% assumption for total porosity from the IRSN info sheet (Le Toarcien du LRS de Tournemire).

The main results are that (1) rocks from fault zone (FZ) and non-FZ show different behavior; (2) there is no different anisotropy in the horizontal plane (along the tunnel or horizontally perpendicular to it); (3) there is a significant anisotropy parallel (higher values horizontally) to perpendicular (lower values vertically) to rock bedding; (4) the fault zone shows a lower anisotropy (A ~ 1.15) than non-FZ (A ~ 1.5). Results are summarized in **Table** 2.

Date from the DTS monitoring and from the thermal property characterization were implemented into a subsurface thermal model to simulate the subsurface temperature field in comparison to the measured temperatures. The detailed analysis is work in progress since the experiment is still running.

Table 2**:** Summary of thermal properties

	Location	Orientation	Thermal Conductivity			Anisotropy
			W/(mK)			-
Dry measured			mean	min	max	A

EURAD (Deliverable n° 17.7) - Synthesis report on Innovative and Enhanced Equipment for Repository Monitoring
Dissemination level: PUBLIC
Date of issue of this report: 04/06/2024

Page

			mean	min	max	
	FZ	vertical	1.3	1.1	1.5	
		horizontal	1.3	1.1	1.5	1
	non-FZ	vertical	2.3	1.9	2.5	
		horizontal	1.6	1.4	1.8	1.43
Saturated calculated			mean	min	max	
	FZ	vertical	1.79	1.51	2.06	
		horizontal	1.79	1.51	2.06	
	non-FZ	vertical	3.16	2.61	3.44	
		horizontal	2.20	1.93	2.48	
Matrix			mean	min	max	
	FZ	vertical	1.88	1.59	2.17	
		horizontal	1.88	1.59	2.17	
	non-FZ	vertical	3.33	2.75	3.62	
		horizontal	2.31	2.02	2.60	
		Diffusivity	mm²/s			
			mean	min	max	
		vertical	0.75	0.6	1	
		SHC	J/(kgK)			
			mean	min	max	
Dry measured			850	680	960	
Matrix			944.3	755.4	1066.5	
Saturated calculated			850.3	680.3	960.3	

2.4.9   Discussion about the results obtained.

Two seismic baseline surveys have provided valuable data for a reflection imaging and tomography-based characterization of the fault zone and surrounding undisturbed rock mass. Some of the limitations posed by the acquisition restricted to the Main Tunnel and the Gallery East03 were overcome by adding receiver positions in an additional borehole at the far end of the Gallery East03 and by adding a high-resolution cross-hole acquisition close to the fault zone. The fault zone has been detected by slightly enhanced reflectivity and is characterized by reduced P- and S-wave velocities. Of particular interest here is a zone of enhanced Vp/Vs ratio within the fault zone which seems to coincide with fluid-filled fractures in the fault zone. All results shown so far are still preliminary and need validation by synthetic modelling. The upcoming repeat survey will provide the opportunity to investigate potential time-lapse effects due to temperature and pressure changes around the injection and heating installation.

Several natural AE events were already recorded during closure of operations at the Tournemire URL. These events will be used to tune the detection system and train a convolutional neural network for characterization of recorded signals. A master's thesis on this has just begun.

The DTS equipment was set up in September 2022. Several baselines were recorded before the experiments started in 2023. Since then, continuous recording of temperature evolution has taken place. Data are generally looking reasonable. The different fibres record a variation of temperature responses with different time-dependent features. The nature of these features is currently under investigation.

EURAD (Deliverable n° 17.7) - Synthesis report on Innovative and Enhanced Equipment for Repository Monitoring
Dissemination level: PUBLIC
Date of issue of this report: 04/06/2024

Page

2.4.10 References

[49]. Blanke, A., Boese, C. M., Dresen, G., Bohnhoff, M., & Kwiatek, G. (2023). Metre-scale damage zone characterization using S-coda waves from active ultrasonic transmission measurements in the STIMTEC project, URL Reiche Zeche, Germany. Geophysical Journal International, 233(2), 1339–1355. https://doi.org/10.1093/gji/ggad003

[50]. Boese, C.M., Kwiatek, G., Plenkers, K. et al. Performance Evaluation of AE Sensors Installed Like Hydrophones in Adaptive Monitoring Networks During a Decametre-Scale Hydraulic Stimula-tion Experiment. Rock Mech Rock Eng (2023). https://doi.org/10.1007/s00603-023-03418-9

[51]. Boese, C. M., Kwiatek, G., Fischer, T., Plenkers, K., Starke, J., Blümle, F., Janssen, C., and Dresen, G.: Seismic monitoring of the STIMTEC hydraulic stimulation experiment in anisotropic metamorphic gneiss, Crustal structure and composition/Seismics, seismology, geoelectrics, and electromagnetics/Seismology, https://doi.org/10.5194/se-2021-84, 2021.

[52]. Bohnhoff, M., Dresen, G., Ellsworth, W. L., and Ito, H.: Passive Seismic Monitoring of Natural and Induced Earthquakes: Case Studies, Future Directions and Socio-Economic Relevance, in: New Frontiers in Integrated Solid Earth Sciences, edited by: Cloetingh, S. and Negendank, J., Springer Netherlands, Dordrecht, 261–285, https://doi.org/10.1007/978-90-481-2737-5_7, 2009.

[53]. Bonnelye, A., Dick, P., Bohnhoff, M., Cotton, F., Giese, R., Henninges, J., Jougnot, D., Kwiatek, G., and Lüth, S.: CHENILLE: Coupled Behavior Understanding of Faults: from the Laboratory to the Field, Adv. Geosci., 58, 177–188, https://doi.org/10.5194/adgeo-58-177-2023, 2023.

[54]. Bretaudeau, F., Gélis, C., Leparoux, D., Brossier, R., Cabrera, J., & Côte, P. (2014). High-resolution quantitative seismic imaging of a strike-slip fault with small vertical offset in clay rocks from underground galleries: Experimental platform of Tournemire, France. Geophysics, 79(1), B1-B18.

[55]. De Barros, L., Daniel, G., Guglielmi, Y., Rivet, D., Caron, H., Payre, X., Bergery, G., Henry, P., Castilla, R., Dick, P., Barbieri, E., and Gourlay, M.: Fault structure, stress, or pressure control of the seismicity in shale? Insights from a controlled experiment of fluid-induced fault reactivation: Seismicity Controlling Factors in Shale, Journal of Geophysical Research: Solid Earth, 121, 4506–4522, https://doi.org/10.1002/2015JB012633, 2016.

[56]. Esefelder, R., Lüth, S., Giese, R., Bonnelye, A., Dick, P., & Krawczyk, C.M. (2023). Seismic imaging of a fault zone in shale – baseline characterization for monitoring a heating and diffusion experiment. DGG Annual Meeting Conference Abstracts, Bremen.

[57]. Giese, R., Klose, C., and Borm, G.: In situ seismic investigations of fault zones in the Leventina Gneiss Complex of the Swiss Central Alps, Geological Society, London, Special Publications, 240, 15–24, https://doi.org/10.1144/GSL.SP.2005.240.01.02, 2005.

[58]. Henninges, J. and Masoudi, A.: Fiber-Optic Sensing in Geophysics, Temperature Measurements, in: Encyclopedia of Solid Earth Geophysics, edited by: Gupta, H. K., Springer International Publishing, Cham, 1–12, https://doi.org/10.1007/978-3-030-10475-7_281-1, 2020.

[59]. Henninges, J., Huenges, E., and Burkhardt, H.: In situ thermal conductivity of gas-hydrate-bearing sediments of the Mallik 5L-38 well: CONDUCTIVITY OF HYDRATE-BEARING SEDIMENT, J. Geophys. Res., 110, https://doi.org/10.1029/2005JB003734, 2005a.

[60]. Henninges, J., Zimmermann, G., Büttner, G., Schrötter, J., Erbas, K., and Huenges, E.: Wireline Distributed Temperature Measurements and Permanent Installations Behind Casing, 5, 2005b.

[61]. Krauß, F., Giese, R., Alexandrakis, C., and Buske, S.: Seismic travel-time and attenuation tomography to characterize the excavation damaged zone and the surrounding rock mass of a newly excavated ramp and chamber, International Journal of Rock Mechanics and Mining Sciences, 70, 524–532, https://doi.org/10.1016/j.ijrmms.2014.06.010, 2014.

[62]. Kwiatek, G., Plenkers, K., Dresen, G., and JAGUARS Research Group: Source Parameters of Picoseismicity Recorded at Mponeng Deep Gold Mine, South Africa: Implications for Scaling Relations, Bulletin of the Seismological Society of America, 101, 2592–2608, https://doi.org/10.1785/0120110094, 2011.

[63]. Kwiatek, G., Martínez-Garzón, P., Plenkers, K., Leonhardt, M., Zang, A., von Specht, S., Dresen, G., and Bohnhoff, M.: Insights Into Complex Subdecimeter Fracturing Processes Occurring During a Water Injection Experiment at Depth in Äspö Hard Rock Laboratory, Sweden, Journal of Geophysical Research: Solid Earth, https://doi.org/10.1029/2017JB014715, 2018.

EURAD (Deliverable n° 17.7) - Synthesis report on Innovative and Enhanced Equipment for Repository Monitoring
Dissemination level: PUBLIC
Date of issue of this report: 04/06/2024

Page

[64]. Lüth, S., Giese, R., Otto, P., Krüger, K., Mielitz, S., Bohlen, T., and Dickmann, T.: Seismic investigations of the Piora Basin using S-wave conversions at the tunnel face of the Piora adit (Gotthard Base Tunnel), International Journal of Rock Mechanics and Mining Sciences, 45, 86–93, https://doi.org/10.1016/j.ijrmms.2007.03.003, 2008.

[65]. Plenkers, K., Schorlemmer, D., Kwiatek, G., and JAGUARS Research Group: On the Probability of Detecting Picoseismicity, Bulletin of the Seismological Society of America, 101, 2579–2591, https://doi.org/10.1785/0120110017, 2011.

[66]. Plenkers, K., Manthei, G., and Kwiatek, G.: Underground In-situ Acoustic Emission in Study of Rock Stability and Earthquake Physics, in: Acoustic Emission Testing: Basics for Research – Applications in Engineering, edited by: Grosse, C. U., Ohtsu, M., Aggelis, D. G., and Shiotani, T., Springer International Publishing, Cham, 403–476, https://doi.org/10.1007/978-3-030-67936-1_16, 2022.

[67]. Reinsch, T. and Henninges, J.: Temperature-dependent characterization of optical fibres for distributed temperature sensing in hot geothermal wells, Meas. Sci. Technol., 21, 094022, https://doi.org/10.1088/0957-0233/21/9/094022, 2010.

[68]. Reinsch, T., Henninges, J., and Ásmundsson, R.: Thermal, mechanical and chemical influences on the performance of optical fibres for distributed temperature sensing in a hot geothermal well, Environ Earth Sci, 70, 3465–3480, https://doi.org/10.1007/s12665-013-2248-8, 2013.

[69]. Richter, H., Hock, S., Mikulla, S., Krüger, K., Lüth, S., Polom, U., Dickmann, T., and Giese, R.: Comparison of pneumatic impact and magnetostrictive vibrator sources for near surface seismic imaging in geotechnical environments, Journal of Applied Geophysics, 159, 173–185, https://doi.org/10.1016/j.jappgeo.2018.08.010, 2018.

[70]. Richter, H., Jaksch, K., Zirkler, A., Giese, R., Krawczyk, C. (2023): Use of polarization properties of seismic waves to improve Fresnel Volume Migration of three-component subsurface seismic data. - International Journal of Rock Mechanics and Mining Sciences, 170, 105449.

https://doi.org/10.1016/j.ijrmms.2023.105449.

[71]. Smithpeter, C., Normann, R., Krumhansl, J., and Thompson, D. B. S.: EVALUATION OF A DISTRIBUTED FIBER-OPTIC TEMPERATURE SENSOR FOR LOGGING WELLBORE TEMPERATURE AT THE BEOWAWE AND DIXIE VALLEY GEOTHE~AL FIELDS, 9, 1999.

[72]. Voigt, D., van Geel, J. L. W. A., and Kerkhof, O.: Spatio-temporal noise and drift in fiber optic distributed temperature sensing, Meas. Sci. Technol., 22, 085203, https://doi.org/10.1088/0957-0233/22/8/085203, 2011.

[73]. Wawerzinek, B., Lüth, S., Esefelder, R., Giese, R., and Krawczyk, C. M.: Performance of high-resolution impact and vibration sources for underground seismic exploration of clay formations at the scale of a rock laboratory, Geophysical Journal International, 231, 1750–1766, https://doi.org/10.1093/gji/ggac283, 2022.

[74]. [Rücker, C., Günther, T., & Wagner, F. M. (2017). pyGIMLi: An open-source library for modelling and inversion in geophysics. Computers & Geosciences, 109, 106-123. doi: 10.1016/j.cageo.2017.07.011.

[75]. Schoenball, M., Ajo-Franklin, J. B., Blankenship, D., Chai, C., Chakravarty, A., Dobson, P., et al. (2020). Creation of a mixed-mode fracture network at mesoscale through hydraulic fracturing and shear stimulation. Journal of Geophysical Research: Solid Earth, 125, e2020JB019807. https://doi.org/10.1029/2020JB019807

EURAD (Deliverable n° 17.7) - Synthesis report on Innovative and Enhanced Equipment for Repository Monitoring
Dissemination level: PUBLIC
Date of issue of this report: 04/06/2024

Page

2.5 Automatic passive seismic monitoring (POSIVA°)

2.5.1 Introduction

Microseismic monitoring is widely used to ensure operational safety of mining operations. It allows for locating and analysis of e.g., fault zone movements, bedrock fracturing and rockfalls. Within context of geological final disposal, microseismic monitoring aims at detecting seismic events in the "ONKALO block to confirm long term safety of the facility, as well as guard it from malicious actors. For example, excavation of unlawful infiltration tunnels lead to the facility would be detected via microseismic monitoring.

Posiva has performed microseismic monitoring of the final disposal facility ONKALO® since 2002. The precise setup and layout of the seismic monitoring network has evolved over the years, to accommodate the progress of the facility's excavation. The network consists of borehole installed triaxial geophones that are located inside the disposal facility, as well as surface mounted geophones and accelerometers on the ground surface. Most of the devices are located near or inside the facility, focused on monitoring what is known as the "ONKALO block" (*Figure 41*) and in addition there are four long period geophones located approximately 5 kilometers from the facility, monitoring the surrounding area of ONKALO-block known as the "semi-regional area" (*Figure 42*). All regional earthquakes originating from outside the aforementioned areas are recorded and monitored as well.
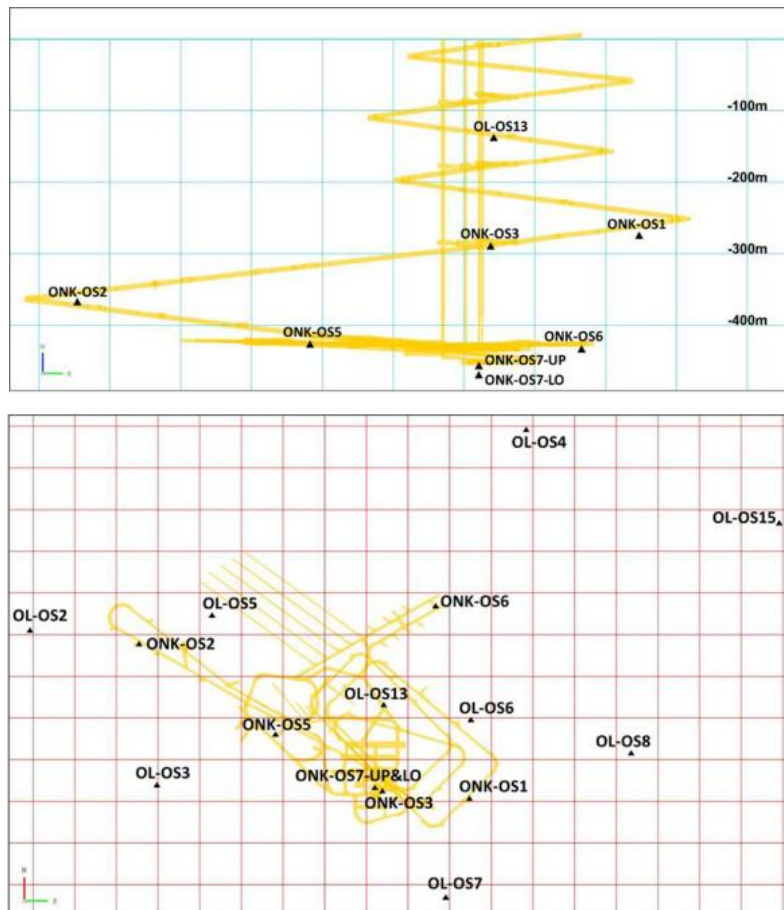
Figure 41: *Seismic stations (19) inside the seismic ONKALO block in 2023. Up: view from above, the distance between the grid lines is 100 m. Below: view from south, the distance between the grid lines is 100 m. Stations OL-OS2 … OL-OS8 and OL-OS15 are on the ground surface OL-OS13 in a borehole and stations ONK-OS1 … ONK-OS3 and ONK-OS5 … ONK-OS7 in ONKALO. (Kuusisto et al, 2022[76])*

EURAD (Deliverable n° 17.7) - Synthesis report on Innovative and Enhanced Equipment for Repository Monitoring
Dissemination level: PUBLIC
Date of issue of this report: 04/06/2024

Page
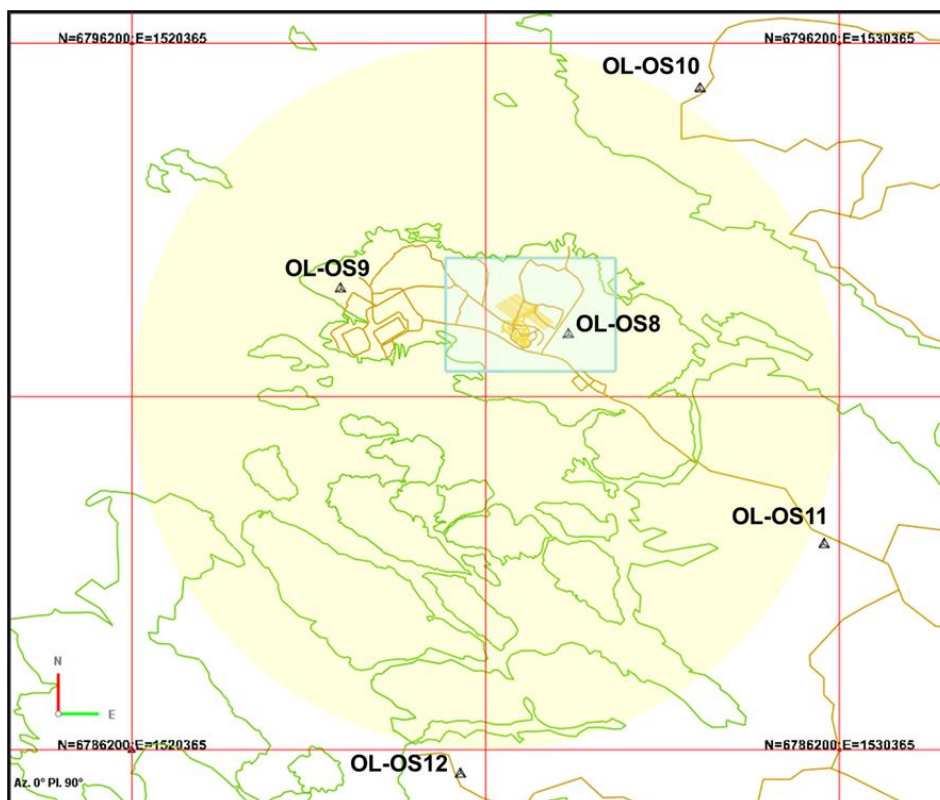
Figure 42: *Seismic stations for monitoring semi-regional seismicity (OL-OS8 … OL-OS12). The seismic semi-regional area is marked with yellow and the seismic ONKALO block with light blue colour. The distance between the grid lines is 5 km. (Kuusisto et al, 2022 [76])*

Unlike in a standard mining operation, seismic events of interest for geological final disposal facilities should not be limited to fault movements, rockfalls or excavation blasts. In addition to those, attention should also be paid to other types of spatially and temporarily isolated seismic sources. Even though these sources may be related to scheduled construction work, the safeguarding principles mandate that the seismic signals from these events should be accounted for.

The following classifications for seismic events in Olkiluoto are used (Kaisko et al, 2019 [77]):

- **Microearthquakes:** Small earthquake inside the seismic ONKALO block. Location within the rock mass. Origin time separated from construction operations (e.g., occurrence during a ventilation break after a blast). Potentially creeping type first particle motion. Energy only at low frequencies (microearthquakes close to tunnels) or evenly up to high frequencies (microearthquakes within bedrock). Radiation pattern indicating a source mechanism which cannot be originated from human activities. S/P-ratios varying with azimuth seen from the source. Efficient coupling of signal to bedrock when compared to other small events or blasts. At least 3 reliable P-picks required.
- **Unidentified small events (UI):** Small event with clear seismic signal, which could fulfil the criteria of a microearthquake. Inadequate number of stations for defining a source mechanism or accurate location. Origin cannot be verified. Separated from reported construction operations. At least 3 reliable P-picks required. Separated from other construction signals also in continuous seismogram.
- **Miscellaneous small events:** Small event caused by human activity. Does not resemble an earthquake. Probable origin can be verified from daily reports. At least 3 reliable P-picks required. Separated from other construction signals also in continuous seismogram.
- **Explosions**: Blast inside seismic ONKALO block or semi-regional area. First P-arrival outwards from the source. Uneven frequency spectra.
- **Nordic earthquakes:** Natural earthquake outside the seismic ONKALO block. Origin in Finland, Sweden, Norway or Estonia. Origin verified by Institute of Seismology, University of Helsinki.

Not all seismic events recorded by the network and stored into database are considered for the above-mentioned classifications. Events that do not fulfill any of the criteria are considered "rejected". Events

EURAD (Deliverable n° 17.7) - Synthesis report on Innovative and Enhanced Equipment for Repository Monitoring
Dissemination level: PUBLIC
Date of issue of this report: 04/06/2024

Page

that are not rejected and are then given a classification are considered "accepted". A seismic event is rejected if one of the following criteria are met:

- The event is located outside the semi-regional area and cannot be classified as a Nordic earthquake.
- The event is part of a continuous work-related signals and is not spatially or temporarily isolated from the surrounding noise.
- The event is caused by electrical disturbances, and not by ground motion.
- Less than 3 reliable P-picks can be determined from the seismograms.

2.5.2 Problem analysis- (key parameter you want to measure).

Due to the required sensitivity of sensors deployed for microseismic monitoring, it is inevitable that the monitoring network will detect tens of thousands of seismic signals annually, out of which only hundreds are of real interest. Whether or not a seismic event is considered subject of further analysis is up to a trained seismologist. Seismic signals which are not of interest are mainly caused by continuous work, such as grinding, drilling or bolting. These are typically simple to recognize by observing a sufficient time window around the triggered event (e.g., 60 seconds).

To ease the workload of human analysts, a tool for automated seismic event rejection is needed. This tool will use machine learning to recognize and differentiate between seismic waveforms.

2.5.3 Research objectives.

The main objective for the research is to develop an automatic seismic event classifier system. The most important function of the system is to reliably accept or reject seismic events in real time, based on same criteria that are used by human experts. The initial main goal of the research project was to develop a system for automated event location. However, as the project progressed, it was realised that an automatic event classifier would be more efficient for easening the workload for human analysts, and thus the focus and scope of the project was adjusted accordingly.

Another objective during the project is to improve ONKALO's seismic velocity model for more reliable seismic event location. ONKALO's seismic velocity model prior to MODATS is homogeneous, based on empirical analysis of known seismic sources. While the homogeneous model has served its purpose relatively well, it has the tendency to overestimate source depths at deeper parts of the final disposal facility. This is in part also because Olkiluoto's seismic sensor geometry does not cover enough area below the facility.

2.5.4 Overview of the development team

Automatic classifier technology used for the project is created and owned by Institute of Mine Seismology (IMS). The technology is part of seismic analysis service widely provided by IMS. Training of the algorithm has been performed by Dr. Ernest Lotter (IMS). Coordination and feedback regarding the technology's desired performance is provided by MSc. Tommi Pirttisalo (Posiva) and MSc. Minna Kuusisto (Posiva).

Upgraded seismic velocity model was developed by Dr. Martin Gal (IMS) and Dr. Ernest Lotter (IMS). Data for the development of the velocity model was curated and provided by MSc. Tommi Pirttisalo (Posiva), MSc. Minna Kuusisto (Posiva) with assistance from MSc. Marianne Malm (AFRY), MSc. Lauri Rinne (AFRY) and MSc. Outi Kaisko (AFRY)

2.5.5 Development steps follow during the MODATS project.

- Updating ONKALO: seismic velocity model
- Deciding and collection of the data to be used for automatic classifier training.
- Training the automatic classifier

2.5.6 Material and method

Initially the automatic classifier was trained Posiva's seismic dataset ranging from January 1st, 2022, to November 8th 2023 (Run 1). The time frame was chosen because it best represents the current state of the seismic monitoring network (as of the end of 2023). Optimally, the training set for the automatic

EURAD (Deliverable n° 17.7) - Synthesis report on Innovative and Enhanced Equipment for Repository Monitoring
Dissemination level: PUBLIC
Date of issue of this report: 04/06/2024

Page

classifier should have rejected to accepted events ratio of 1:1. This unfortunately doesn't apply to the set of events recorded by Posiva's database, instead the amount of rejected events heavily outweighs the number of accepted events (838:46138). A second training set included events from the January 1st 2021 to September 30th 2023 (Run 2). The additional accepted events from 2021 were expected to help the recognition of events of interest, and additionally a subset of rejected events was chosen to make the populations of accepted and rejected events roughly the same size. However, Run 2 included a very large cluster of rejected events in August of 2021. The cluster was caused by a wall construction work, and it introduced an anomalous number of rejections which do not represent typical activity of the final disposal site. Because of this a third training set (Run 3) was introduced that excluded August of 2021.

For the creation of an updated seismic velocity model, a list of excavation blasts with known coordinates and times were compiled by members of Posiva and AFRY. Blasts were selected from years 2006-2022, covering as much of the ONKALO's volume as possible. Single blasts were selected, instead series of multiple blasts. The decision was made to avoid cases where two or more locations have been excavated simultaneously. Also, focusing on seismograms with single explosion events decreases risk of confusing phases of multiple explosions. In total, 54 blasts were chosen for the calibration.

Due to mostly planar sensor layout, lack of seismic sensors below the monitoring area of interest and very small amplitude of most of the seismic events of interest, it was deemed that a true 3D mesh velocity model was not ideal for ONKALO. Instead, an adaptive apparent velocity (AAV) model was created, with a prior probability function at open tunnels.

2.5.7   Results of automatic classifier test runs

Training set for Run 1 included some events from October and November 2023 that were not completely analysed by human experts due to their recency, so the training set cannot be considered fully representative. The relatively large number of false negatives (72) may be partially related to this fact.

RUN1 (events from 2022-2023)		
Manually prosessed	Automatically processed compared to manually processed	
	Accepted	Rejected
Accepted (921)	849	72
Rejected (51207)	12304	38903
Total	False positives	False negatives
52128	0.240	0.078

Adding data from year 2021 and omitting non-processed events from October and November of 2023 yielded noticeably less false negatives in Run 2. However, the large rejection cluster in August seems to have introduced a large number of false positives (45062).

RUN2 (events from 2021-2023)		
Manually prosessed	Automatically processed compared to manually processed	
	Accepted	Rejected
Accepted (1798)	1745	53
Rejected (114945)	45062	69883
Total	False positives	False negatives
116743	0.392	0.029

Leaving out the rejection cluster produced much less false positives, as well as lowering the amount of false negatives by one. This is also partly due to the fact for Run 3 the whole month of August in 2021 was omitted, even though the rejection cluster was concentrated only within two days of the month.

EURAD (Deliverable n° 17.7) - Synthesis report on Innovative and Enhanced Equipment for Repository Monitoring
Dissemination level: PUBLIC
Date of issue of this report: 04/06/2024

Page

RUN3 (events from 2021-2023, excluding August 2021)		
Manually prosessed	Automatically processed compared to manually processed	
	Accepted	Rejected
Accepted (1715)	1663	52
Rejected (65408)	15024	50384
Total	False positives	False negatives
67123	0.230	0.030

Considering Run 3 for further analysis, relatively most false negatives are produced by Nordic earthquakes. This is to be expected, since events with such classification are very rare in the database that was used for training. Therefore, the automatic classifier does not have enough data regarding Nordic earthquakes to learn how to correctly distinguish them. Adding to the challenge of correctly classifying Nordic earthquakes, it is common for human analysts to require external sources for confirming the classification themselves. While the waveform for these earthquakes is typically distinct, it is important to consider that ONKALO's seismic network is not primarily designed for analysis of events that are further than 5 km away from the final disposal facility.

While the automatic classifier fared well with small UIs in general, the relative number of false negatives in that category for year's 2022 data was quite high.

Automatic classifier's ability to correctly accept excavation blasts was very good, with the percentage of false negatives being < 1% for each individual year as well as for the total of 2021 – 2023. All blasts from ground surface were correctly accepted.

Table 3: Automatic classification results.

	MQ	Small	Small, UI	Nordic EQ	Blast
Manually accepted					
2021	113	59	200	6	538
2022	43	40	72	11	352
2023	3	8	16	6	3
Total	*159*	*107*	*288*	*23*	*893*
False negatives					
2021	5	3	9	1	5
2022	3	4	16	4	1
2023	0	0	0	1	0
Total	*8*	*7*	*25*	*6*	*6*
False Negatives (%)					
2021	4.42	5.08	4.5	16.67	0.93
2022	6.98	10	22.22	36.36	0.28
2023	0	0	0	16.67	0
Total	**5.03**	**6.54**	**8.68**	**26.09**	**0.67**

2.5.8   Discussion about the results obtained.

Machine learning classifier algorithm produced and trained by Institute of Mine Seismology shows promise for geological disposal monitoring applications. Currently, the biggest challenge is minimizing

EURAD (Deliverable n° 17.7) - Synthesis report on Innovative and Enhanced Equipment for Repository Monitoring
Dissemination level: PUBLIC
Date of issue of this report: 04/06/2024

Page

the number of false positives (events that have been automatically accepted, even though they should have been rejected). The high number of false positives is largely because amplitudes of events of interest mostly coincide with those of rejectable events. Therefore, it is difficult to set a strict PGV (peak ground velocity) threshold for rejection criteria. To mimic the workflow of current human analysts, the algorithm should make use of untriggered seismic data from around the signals of interest. Utilizing untriggered waveforms for algorithm training poses its own challenges however due to the amount of storage space required to store that kind of data. In standard operation of Posiva's seismic monitoring, untriggered data is stored for 40 days, and is automatically deleted by FIFO principle. Therefore, to have suitable training data available, manual processing of seismic events needs to be done with faster pace than normal. Although not impossible, this requires careful coordination between seismologists and programmers.

Another source of error for the machine learning algorithm is the existence of duplicate events in the training dataset. When a human analyst takes a seismic event in for further analysis, it is a common practice to create a duplicate of the event. This is done to a.) include more seismograms that may not have been automatically associated in the original event file due to poor SNR, and/or b.) to include a wider time window for observation of different wave phases. After duplication, the original event is rejected, which is likely to confuse the algorithm. Luckily the vast majority of rejected events are not duplicates of accepted events, so the effect of this is not extremely drastic.

After further training of the algorithm, the next step will be using the tool parallel with human experts. This way, the actual functionality of the classifier can be confidently determined, and remaining issues can be observed and fixed. These future plans are outside the scope of the MODATS work package.

2.5.9   References

[76].   Kuusisto, M. (ed.), Malm, M., Kaisko, O., Rinne, R., Lahtinen, S., Saaranen, Pirttisalo, T. 2022. Results of Monitoring at Olkiluoto in 2021, Rock Mechanics. Posiva Working Report 2022-47, Posiva Oy, Olkiluoto, Finland

[77].   Kaisko, O. & Malm M., 2019. Microearthquakes During the Construction and Excavation of the Final Repository for the Spent Nuclear Fuel at Olkiluoto in 2002-2018. Working Report 2019-05, Posiva Oy, Olkiluoto, Finland.

EURAD (Deliverable n° 17.7) - Synthesis report on Innovative and Enhanced Equipment for Repository Monitoring
Dissemination level: PUBLIC
Date of issue of this report: 04/06/2024

Page

2.6   Water leakage mapping

2.6.1   Introduction

As a part of hydrological and hydrogeological monitoring of Olkiluoto (Finland), Posiva has monitored the inflows after sealing actions into the underground facility ONKALO® since the beginning of its construction in 2004. The inflows are measured with measuring weirs and collectors. In addition to continuous inflow measurements in tunnels, a visual leakage mapping survey has been regularly conducted since 2005.

It is envisaged that water inflow will be monitored over long periods in crystalline rock environments The facility will be in parts open over 100 years (access routes and technical area), while some parts (deposition tunnels) will be open only for a few years, but still the detailed information of location and amount of leakages are important to be able to assess the condition and evolution of hydrological conditions prior closure of the tunnels.

The leakage maps are used for monitoring the surface area and location of leakages in the underground facilities. The time-dependent observation data is typically used together with other hydrogeological monitoring data to observe and analyse possible changes in tunnel inflow and changes in flow and pressure conditions of the bedrock and hydrogeological zones (hydraulically conductive brittle fault zone) intersecting the tunnels. Observation and monitoring of leakages into the underground facilities also provides feedback for construction as it enables evaluation of the success of sealing operations implemented by grouting.

The demand for leakage mapping survey comes from the need to observe and monitor local leakages in the underground facilities. Along with the underground leakage measurement network, leakage mapping provides more detailed information about the surface area and location of leakages. Monitoring of local small leakages in relatively dry tunnels is often more reasonable with combination of visual leakage mapping and manual leakage measurements rather than establishing fracture specific automatic measurement stations or utilizing tunnel-scale leakage measurements. In Posiva's underground disposal facility, there are some tunnel sections at the disposal depth (ca. -420 m) that are relatively dry and in which the visual leakage mapping is the primary method for monitoring tunnel leakages.

From the perspective of method validation, a transparent and reproducible mapping method is easier to validate in comparison to a visual observation that is, at some level, always a subjective interpretation done by the person performing the mapping. In addition, visual leakage mapping does not follow similar universal classification systems, which are available for example for rock masses with respect to stability of underground openings (e.g. Q-system). In order to develop a mobile functional method for mapping leakages in tunnel walls and roof, a Task for Automatic Digital Mapping of Leakages were initiated.

2.6.2   Water mapping data in monitoring programme of Olkiluoto

The survey is based on visual observation of groundwater leakage on tunnel walls and roof (*Figure 43*). The tunnel surface is mapped using five different "moisture condition" classes, ranging from dry to flowing surface (dry, damp, wet, dripping and flowing). The mapping observations are later digitised into tunnel layout with other relevant data including bolts, fractures (mapped by geologists), shotcrete areas and covered drainage systems under the shotcrete. Dripping or flowing fractures or fracture sets can also be selected to undergo more specific and regular leakage measurements (by using local collectors or manual measurements) based on mapping observations.

EURAD (Deliverable n° 17.7) - Synthesis report on Innovative and Enhanced Equipment for Repository Monitoring
Dissemination level: PUBLIC
Date of issue of this report: 04/**06/2024**

Page
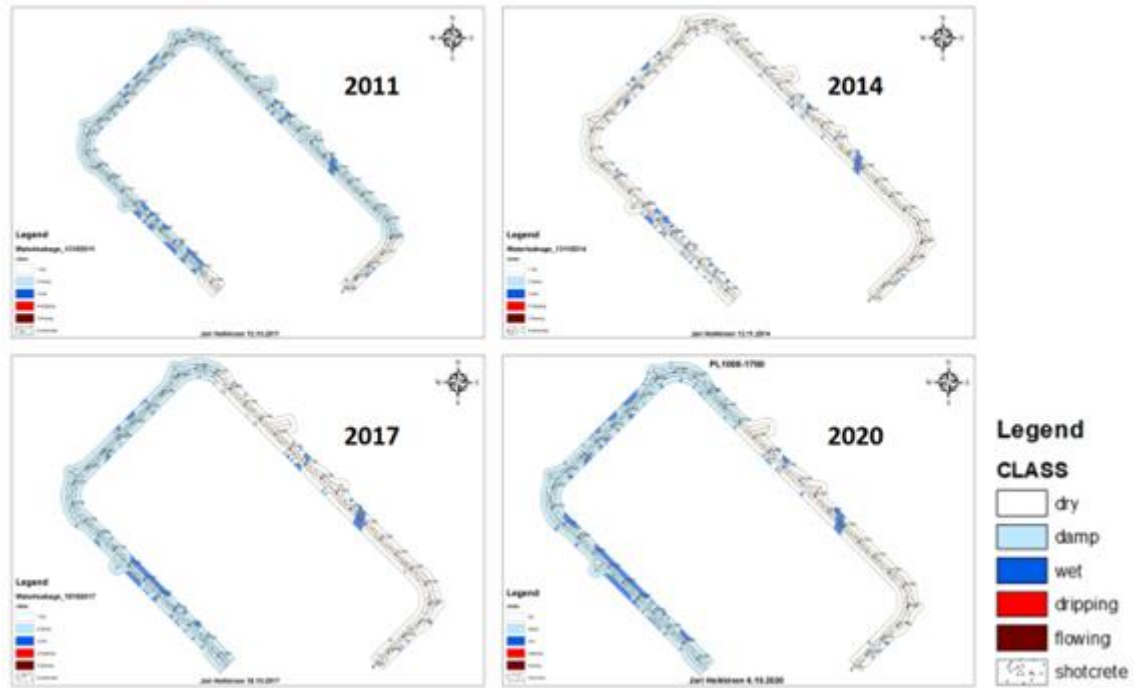
Figure 43: Leakege maps representing observations from same tunnel location in ONKALO® through years 2011, 2014, 2017 and 2018 as example.
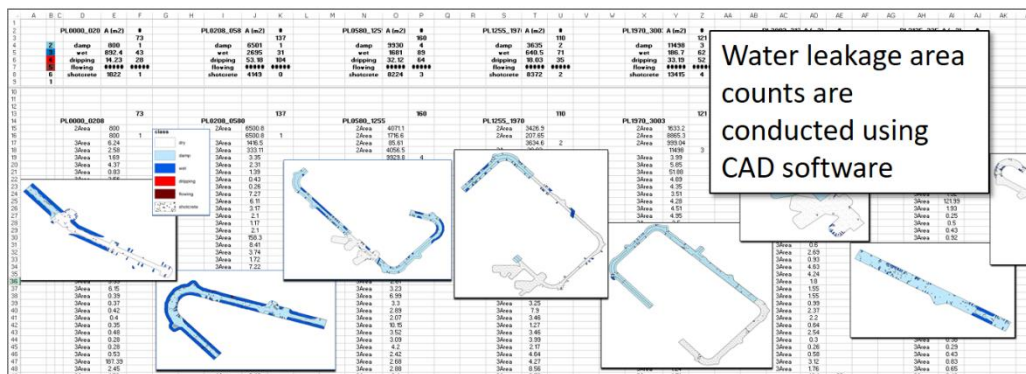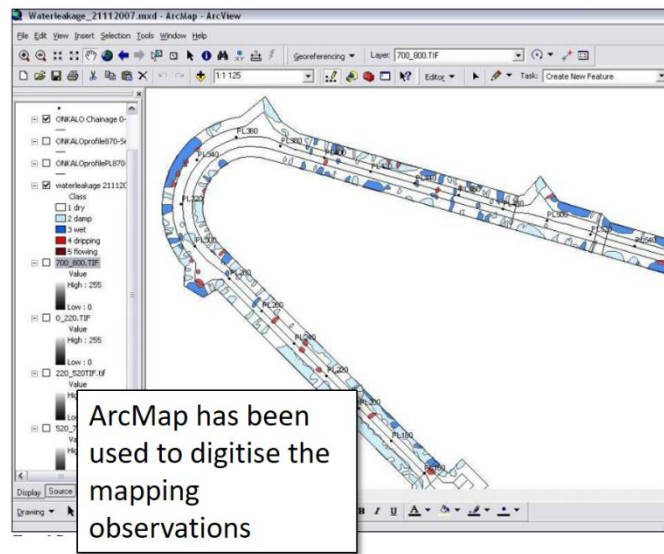
Figure 44: The figure is showing the current method of leakage mapping with digitation with ArcMap software.

EURAD (Deliverable n° 17.7) - Synthesis report on Innovative and Enhanced Equipment for Repository Monitoring
Dissemination level: PUBLIC
Date of issue of this report: 04/06/2024

Page
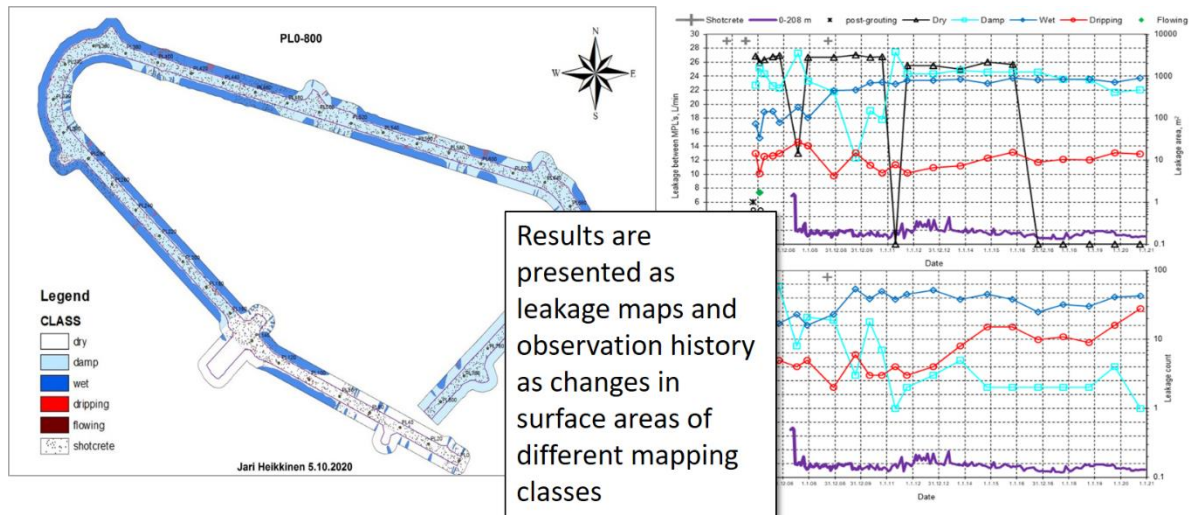
Figure 45: *An example how the results are presented and reported.*

Water leakage counting is then conducted to calculate total surface area of each moisture content class in each tunnel section (*Figure 44*). Water leakage area counting enables statistical examination of the data, making interpretation of long-term changes easier. Results of visual leakage mapping (*Figure 45*) and other inflow analysis are reported annually in Posiva Working report *Results of monitoring at Olkiluoto, Hydrology and hydrogeology* (cf. Vaittinen et al. 2020 [89][83] and Laakso et al. 2021[83]).

2.6.3 Objectives

Current leakage mapping methods are based on manual acquisition and analysis. Consequently, results may be subject to bias. In addition, the work is time consuming and cannot be undertaken frequently, which restricts in-depth analysis of, for example, the annual variation in response to changes of weather and ventilation. The disposal facility construction and operation activities may also change the hydrogeological conditions rapidly. In addition, the commissioning of disposal facility set new and more strict requirements on leakages in deposition tunnels. It is essential to know how the amount of the leakages and their location will evolve during the short (couple of years) opening time of the tunnel prior its closure. Therefore, a rapid, efficient, and reliable method is needed to be able to conduct leakage surveys. In addition, the use of data could be combined to the models and the visualisation methods could be improved. POSIVA conducted a literature survey on different methods and selected the most appropriate method to be tested in ONKALO® in Olkiluoto and analyse the outcome.

Main goal for task Automatic Digital Mapping of Leakages were to develop and test a semi-automatic (or automatic) method for tunnel leakage mapping, that is, to identify and separate tunnel surface areas with different moisture conditions (eg. dry, damp, wet, dripping and flowing). The task aims to find a technical application that could simplify or replace the present visual & manual mapping survey. The technical objectives of the development are that the application should be able to:

- Detect and separate tunnel surface areas with different moisture conditions. The requirements concerning the reliability and performance for the developed technical application are to be determined during Activity. For example:

    o Mobility of the application (used on foot, on a car roof etc.)

    o Moisture condition classes to detect and separate (same 5-class classification as in Posiva's visual leakage mapping or something else)

    o Ability to perform in different tunnel conditions such as a) well lighted and dim tunnels b) rock, shotcrete and concrete surfaces c) low and high relative air humidity.

    o Requirements for data handling and analysis

EURAD (Deliverable n° 17.7) - Synthesis report on Innovative and Enhanced Equipment for Repository Monitoring
Dissemination level: PUBLIC
Date of issue of this report: 04**/06/2024**

Page

2.6.4   Activities

 The main goal of the task is to describe the possibilities for future related to the method development. It was obvious that within this specific task the outcome serves the basis for continuation and not a ready-made solution. The work was initiated by hydrogeological staff of Posiva but soon it was realized that this specific issue would require support from geophysical staff, while planned methods for analyzing the issue is more physical in nature and the end user of the selected method is the hydrogeological staff. The main research personnel in this task were:

- Jyri Laakso, M.Sc. in Geology from the University of Helsinki. He has been working at Posiva since 2016 and is currently working as hydrogeologist and developing the hydrogeological investigation methods. The role of Jyri Laakso was planning the task and be as an expert in hydrogeology to provide the information and needs to the development team.
- Tommi Pirttisalo M.Sc. in Geophysics from the University of Oulu. He has been working as a geophysicist at Posiva since 2021. He's main responsibilities include rock mechanical monitoring and geophysical surveys. For automatic leakage mapping, he has provided support with field experimentation and method investigation.
- Henrik Jänkävaara M.Sc. in Geophysics from the University of Oulu. He has been working as a Research Engineer at Posiva since 2020 with main focus being automatic flow logging measurements (PFL) in boreholes. For automatic leakage mapping his role has been to search for and to test potential measurement methods and technologies.
- Sami Kivistö M.Sc. in Engineering Physics from Aalto University, Espoo. He has been working as an automation engineer and instrumentation specialist for Teollisuuden Voima Oyj since 2021.
- Johanna Hansen M.Sc. in Geology and Mineralogy from the Åbo Akademi University. She has been working at Posiva since 1997 both with site investigations and currently with development of disposal technology and EBS concept. She works as R&D coordinator in Engineered barrier unit. She coordinated the FP7 project DOPAS 323273 and she acts as a Finnish WMO mandated actor deputy contact in Eurad programme.

The new hydrogeologist M.Sc. in geology from the University of Turku Ville Paalumäki reviewed the memorandum in January 2024.

The workflow for the leakage mapping method development did consist of following subtasks:

- January – June 2022 Search for potential technologies for leakage mapping and review of the latest innovations (Tommi Pirttisalo & Henrik Jänkävaara)
- June – September 2022 Selection of method type and contractor for co-operation to conduct method development (Henrik Jänkävaara).
- November 2022 – January 2023 Method development and testing in different tunnel conditions, (e.g. well lighted and dry tunnels vs dim and damp tunnel conditions) in Olkiluoto. (Jänkävaara and Kivistö)
- February 2023 – January 2024 Assessment of performance and suitability of the method to replace conventional visual leakage mapping (Jänkävaara, Pirttisalo, Kivistö, Hansen)

2.6.5   Technology description and literature survey during the MODATS project

The work started by literature survey of different methodology used for analysis of water leakages and limit the work scope. It was obvious that a method just for imaging the leakages and inflows is not enough and there will be needs also for positioning the location of images to be able to use automatized systems (in underground conditions the normal GPS signal is not available, and the positioning requires a different approach.

At first, different possible measurement methods and corresponding physical quantities were discussed. Such include for example, radiometry and different electromagnetic methods. One proposed method was a kind of electromagnetic rake that could scan the conductivity of tunnel walls. Quite promptly methods based on near and mid infrared regions of electromagnetic spectrum were seen as the most promising.

Inspiration was taken from automatic tunnel scanning solutions (Xue et al. 2021 [90], Huang et al. 2020 [80]) and construction inspections (e.g., Resende et al. 2022 [88]) and combining laser scanning interpretation with verifying the possible leakages with thermal camera (Yu et al. 2018). The different methods combining laser scanning information with photogrammetry or with automated water leakage

EURAD (Deliverable n° 17.7) - Synthesis report on Innovative and Enhanced Equipment for Repository Monitoring
Dissemination level: PUBLIC
Date of issue of this report: 04/06/2024

Page

detection with Mask-R CNN algorithm also give an understandings of leakage locations. Still these methods seem to be more characterisation methods or they are time consuming and the resolution of the method is not known or not suitable for required in disposal facility conditions. From literature it is not always obvious how intense leakages can be analysed with these methods. The inflows into the underground disposal facility at different locations vary from few ml/min up to 300 ml/min except the few larger structures along the access tunnel. The main need still is to analyse the leakages around, with inflow 100 ml/min or less.

Hyperspectral imaging, utilizing the absorption spectrum water, was one method that was further investigated. For example, Specim, Spectral Imaging Ltd. (specim.com) provides hyperspectral imaging solutions and their products include short wave infrared SWIR (1000–2500 nm) and FX17 (900-1700 nm) cameras. These are line scanners if specific wavelength band is not selected, which is not optimal. The bigger problem is the amount of external lighting that the cameras require.

The selection criteria for methodology selected for field test was based on the practical aspects: economically feasible, fast and easy to use, suitability in underground conditions.

The most promising and feasible for underground field testing was judged to be standard thermal imaging to start with to be able to see the possibility to detect different type of inflows in conditions where different structures like shotcrete, steel mesh reinforcement and other tunnel infra may disturb the results. The potential of the method was already studied in different studies like one done by SKB (Neretnieks et al 2018 [86]) where the main conclusions was that thermal imaging (with an IR camera) can be used to locate and identify spots with even very low leakage flowrates of water in fractured crystalline rocks. This study was not directly used to repeated flow mapping but more or less to characterise leaking fractures. Even the leakages less than 1 ml/min were able to be identified with this method. It was obvious that alone the IR imaging gives only qualitative information but together with fracture geometry and 3D modelling of fracture network it could give better understanding of inflows (Neretnieks et al 2018).

If the method is feasible the next phase is to conduct a machine learning exercise to distinguish different type of inflows and inflow area to receive semiquantitative results on number of inflows. According to the literature (Huang et al. 2021) the machine learning methods have been tested on inflow locations. The different type of AI and machine learning services are available as well in commercial and scientific means. As part of the Task 3 there were a short review of available services and one demonstration was done with Aiforia, which is a Finnish private enterprise providing AI analysis services mainly to the medical analytics, but also for other fields. It was decided that due the limited scope in this task there is no need to develop methods further and when implementing a technology, a commercial analyse method can be utilised for creating the library to classify the type of inflows. The creation of library is site dependent and requires a big set of pictures to make the machine learning exercise possible. There are some calibration needs also to consider the different structures like reinforcement, the tunnel infrastructure, the possible temperature deviation in groundwater depending on the water source (there might be some drawdown and upconing) during the possible disturbances related to the excavation period.

2.6.6   Description on the field test implemented during the project.

In December 2022, a field test was conducted in ONKALO® (*Figure 46*). An IR-camera was used to scan tunnels and to detect water leakages.

EURAD (Deliverable n° 17.7) - Synthesis report on Innovative and Enhanced Equipment for Repository Monitoring
Dissemination level: PUBLIC
Date of issue of this report: 04/06/2024

Page
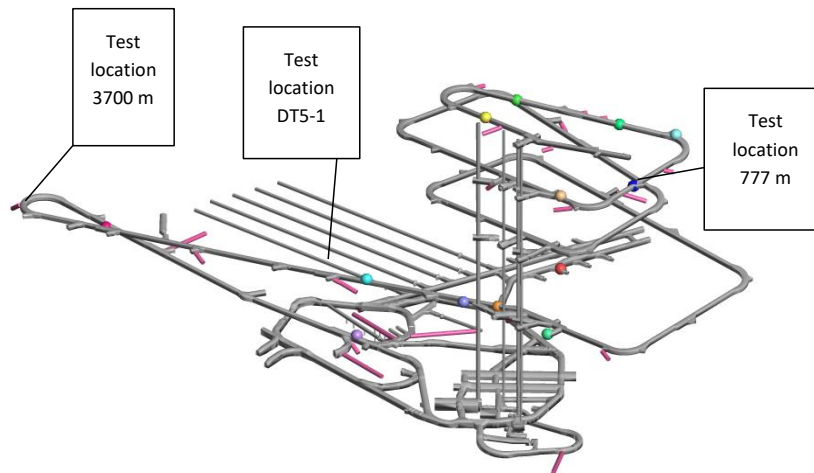
Figure 46: The test locations in ONKALO®

The method was tested during two days in December 2022. The timing was agreed to present the time slot when the visual mapping is done as well to be able compare the results. Infradex (infradex.com) provided to the test a T865 high-end infrared (IR) camera (wavelength range 7.5 - 13 μm). The specifications of the IR camera are presented in Appendix. Both shotcrete and rock surfaces were filmed. Water in ONKALO® is cooler than the surrounding rock and shotcrete. Most anomalies that were included were 'wet'. One 'flowing' anomaly at PL777 was included as well.

In *Figure 47* and *Figure 48* is a series of images from around PL660 to PL777 in ONKALO® access tunnel. Otherwise, the images could be used for mapping the anomalies, except the 'flowing' anomaly at PL777 doesn't look any different from other 'wet' anomalies. The image of the anomaly included in the series is also one of the best IR-images of the PL777 anomaly we managed to take. Corresponding water leakage mapping can be seen in Figure 49. The location of this leaking point is most probably a rock bolt hole due the fact that in this current location there are no signs of fracture flowing into the tunnel (in very accurate Posiva flow flog or geophysical measurements) according to the drilling report (Öhberg et al. 2006 [92]). The flowing point is located at the drilled pilot hole ONK-PH3 in 80,16 meters when comparing the tunnel chainage toward the pilot hole length.
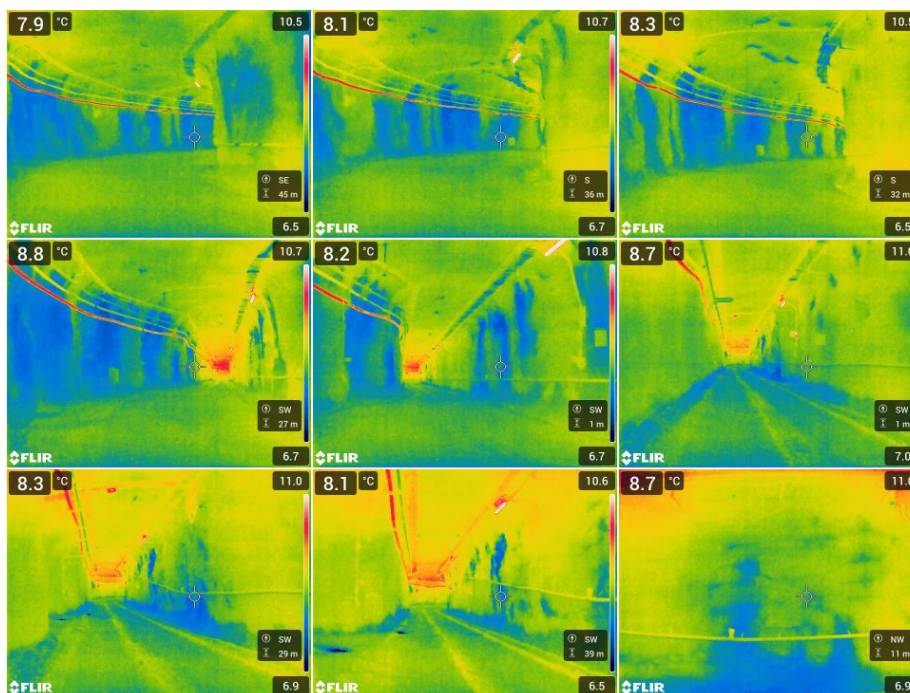
Figure 47: Series of IR-images between PL660 and PL777 (in order). At PL777 (the last image) there is a feature with high water flow. 15.12.2022.

EURAD (Deliverable n° 17.7) - Synthesis report on Innovative and Enhanced Equipment for Repository Monitoring
Dissemination level: PUBLIC
Date of issue of this report: 04/06/2024

Page
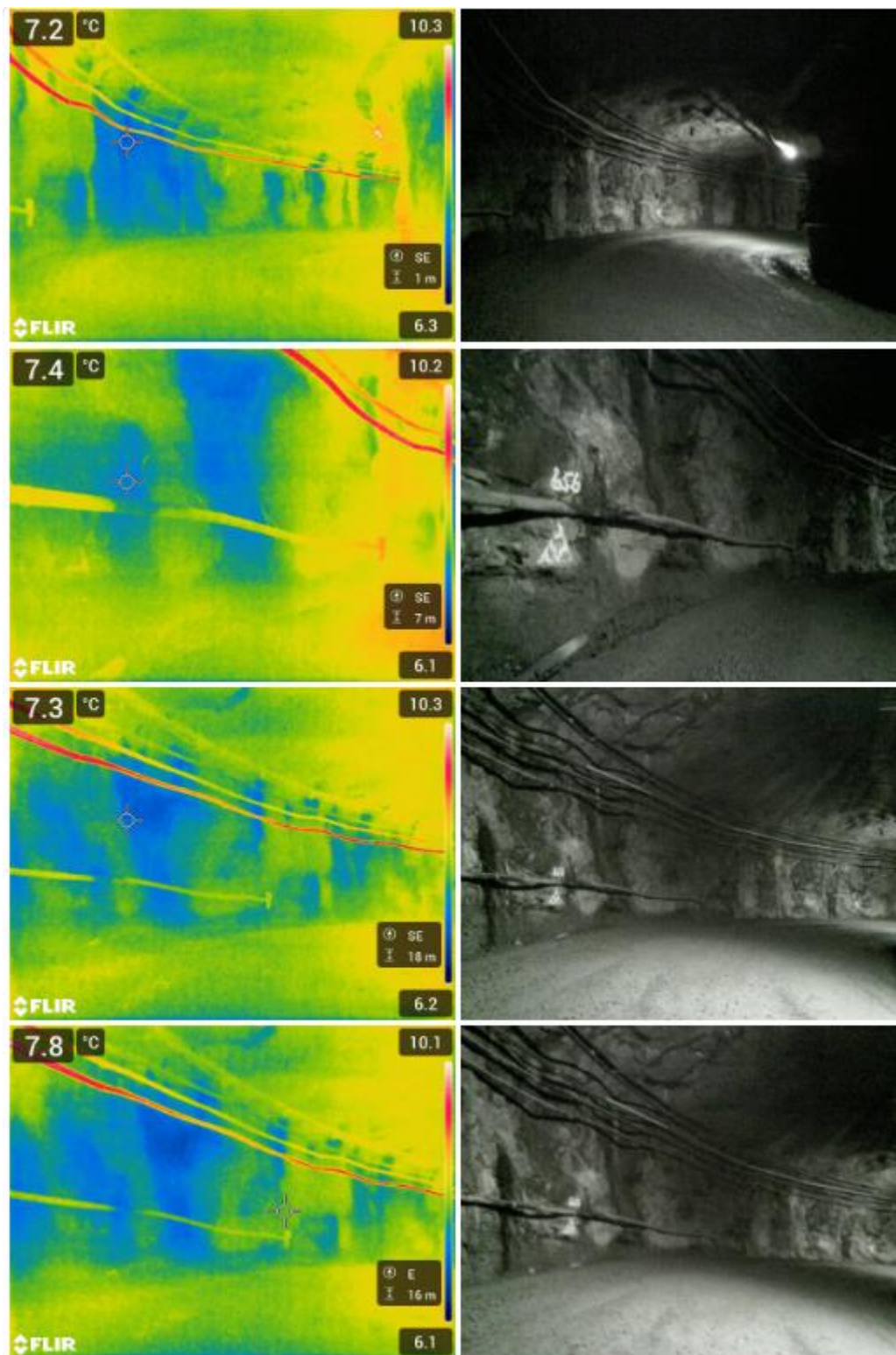
Figure 48: *Comparison between IR-images and visual images at around PL656. 15.12.2022.*

EURAD (Deliverable n° 17.7) - Synthesis report on Innovative and Enhanced Equipment for Repository Monitoring
Dissemination level: PUBLIC
Date of issue of this report: 04/06/2024

Page
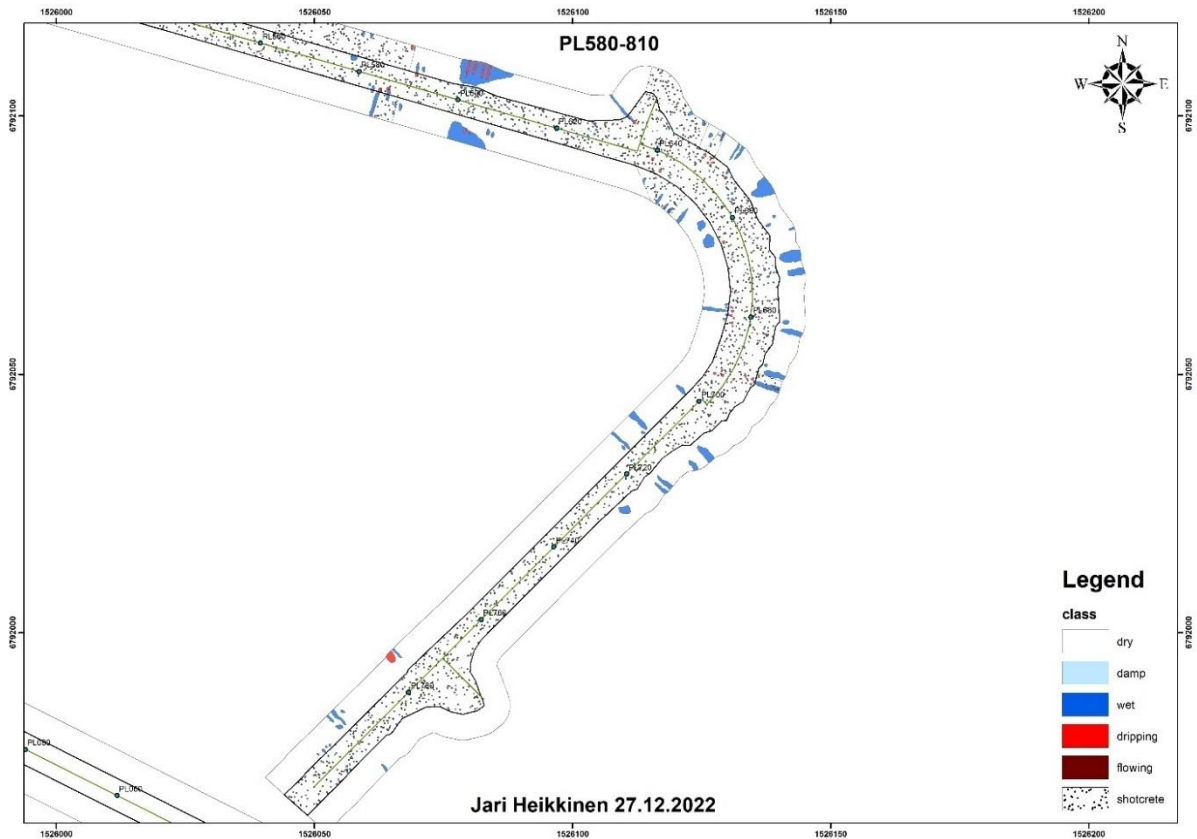
Figure 49: *Water logging map of PL580-810. The map corresponds to IR-image series in Figure 47 and Figure 48. Red 'dripping' anomaly is recorded at PL777.*

IR-images in Figure 50 and Figure 52 are taken in deposition tunnel 5-1. Corresponding water logging map in **Figure 51**. The tunnel is straight, and walls and floor are exposed rock. In Figure **52**, wet anomalies at tunnel roof. Anomalies in this case are quite visible, but it was not the case most of the time. The metal net covering the roof is also visible. Especially hard to distinguish point like anomalies are present in the roof.
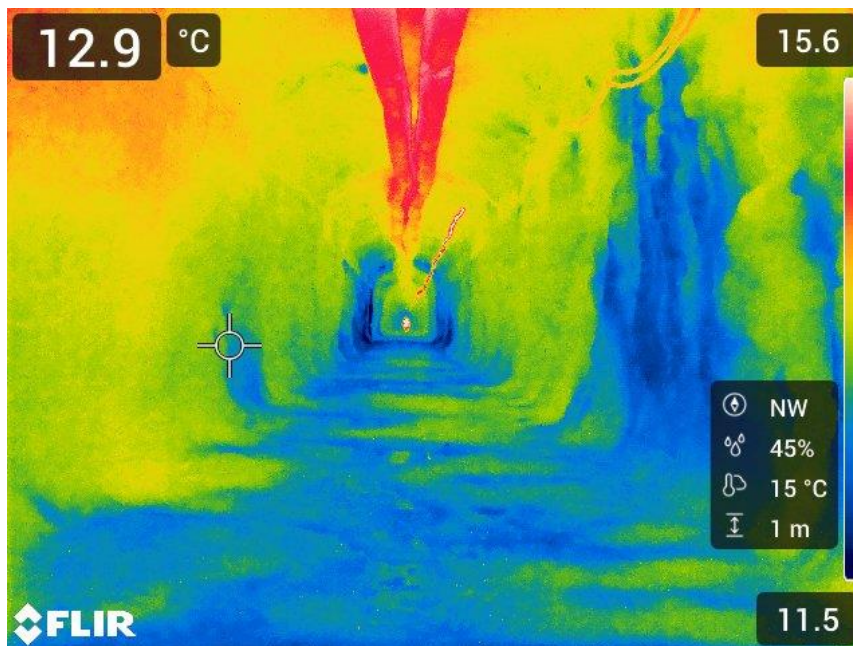
Figure 50: *IR-image at the start of the deposition tunnel 5-1 (DT5-1). Floor and walls are exposed rock, roof is covered with steel mesh reinforcement 16.12.2022.*

EURAD (Deliverable n° 17.7) - Synthesis report on Innovative and Enhanced Equipment for Repository Monitoring
Dissemination level: PUBLIC
Date of issue of this report: 04/06/2024

Page
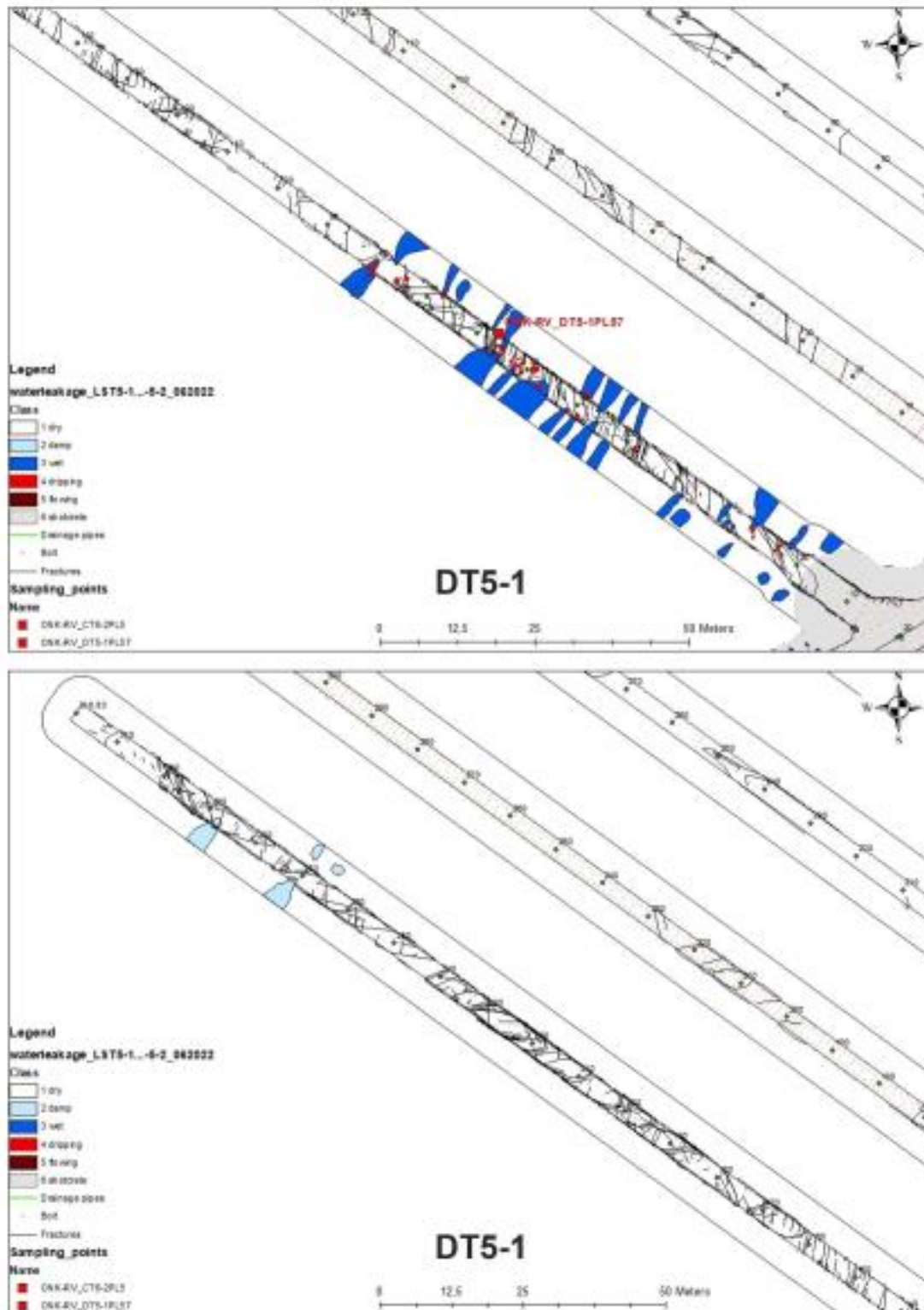
Figure 51: *Water logging map of deposition tunnel 5-1.*

EURAD (Deliverable n° 17.7) - Synthesis report on Innovative and Enhanced Equipment for Repository Monitoring
Dissemination level: PUBLIC
Date of issue of this report: 04/06/2024

Page
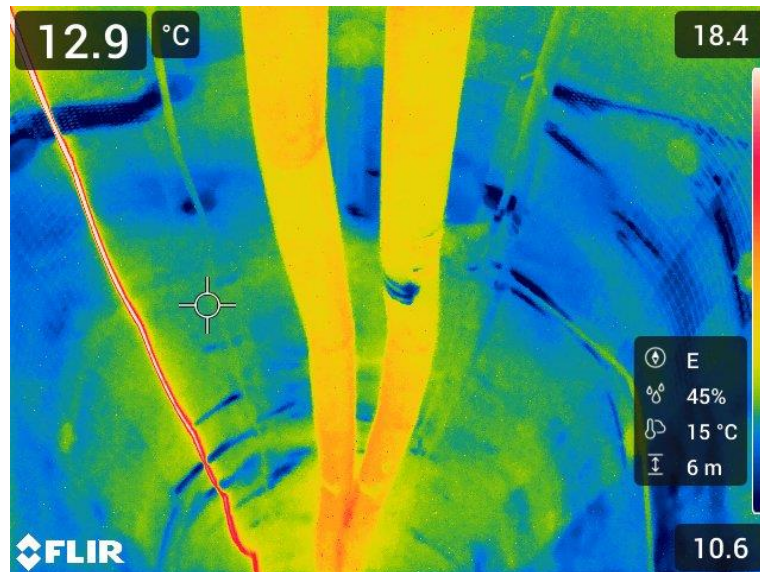
Figure 52: IR-image of the roof at the deposition tunnel 5-1 (DT5-1). The roof is covered with metal net. 16.12.2022.

Figure 53 and Figure 54 are from PL3700 in ONKALO® driving tunnel. Anomalies are on shotcrete and are more pronounced than on exposed rock. In Figure *54* is a comparison between IR and visible light images. The same anomaly can be seen on the right in Figure 53. Corresponding waterlogging map in *Figure 55*.

Figure 53: IR-image at around PL3830. Roof and walls are covered with shotcrete. 15.12.2022.
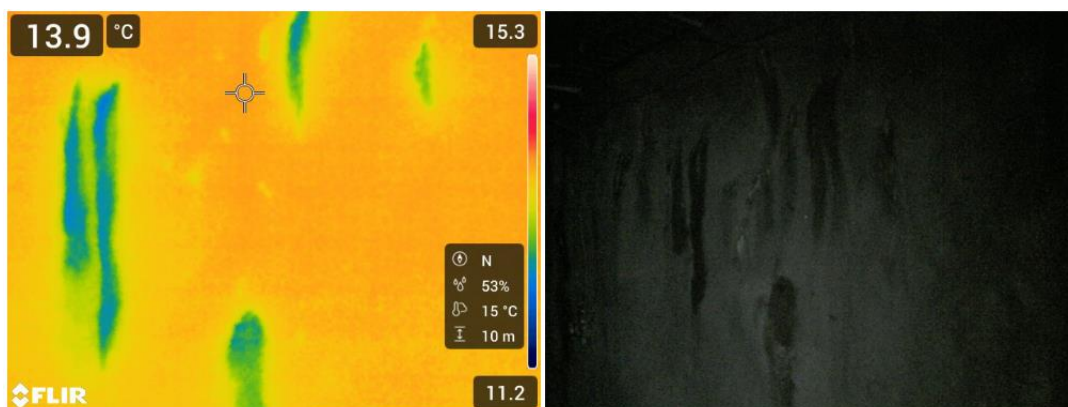
Figure 54: IR and visible light images at around PL3830. The same anomalies on shotcrete. 16.12.2022.

EURAD (Deliverable n° 17.7) - Synthesis report on Innovative and Enhanced Equipment for Repository Monitoring
Dissemination level: PUBLIC
Date of issue of this report: 04/06/2024

Page

Figure 55: Water logging map of PL3800-PL3980. The map corresponds to images in Figure 53 and Figure 54.

2.6.7   Results

The IR-imaging results from ONKALO® were promising in that at least the anomalies were detected. The amount of water on the other hand could not be determined solely from the IR-image. Anomalies obscured by different objects and constructions are also hard to detect. This is especially true in case of the tunnel roof since in the tunnels the roof area is filled with pipes etc. In addition, roof anomalies are mostly point-like which make them even harder to detect. The fact could be that the point wise leakages are usually connected to the rock bolt holes.

On shotcrete the anomalies were a little bit more pronounced and easier to detect. On exposed rock the anomalies are more blurred. Comparing Figures 47 and 49, anomalies logged by human logger are much sharper.

It must be noted that the accurate and absolute temperature values were not measured. Only the temperature differences were of interest as it is enough to detect the anomalies. For more accurate temperature measurements, surface emissivity as well as the humidity and temperature of air must be considered.

Even though the thermal imaging has some challenges, it could be applied to assist human logger. IR-image/recording could be used to automatically identify the leakages and to digitize them. In practice, this would mean taking IR-images and using photogrammetry (Huang et al. 2020 [80]) and pattern recognition to map the anomalies to tunnel profile. Even this would provide significant help, though. After anomalies are digitized, the logging personnel could then determine the amount of water (five different classes) in each anomaly by other means, for example by visual observation (which is the procedure currently anyway).

2.6.8   Discussion about the results obtained.

The more automatized method to map the leakages into the disposal facility would save the hydrogeologist working time to another scientific topic. Posiva estimated, for the current extend of tunnel, that with current manual method one sheet (800 meter of tunnel) would take around 1 day in the field and 1 day to create the digitalisation, which approximately means for whole facility 1 person month/year. In addition, the interpretation takes additional time. With thermal camera the same work can be done within couple of days. This enables the possibility to repeat the measurements more often and get

EURAD (Deliverable n° 17.7) - Synthesis report on Innovative and Enhanced Equipment for Repository Monitoring
Dissemination level: PUBLIC
Date of issue of this report: 04/06/2024

Page

information for example from operational period what happens in neighbouring tunnels when one tunnel is backfilled and plugged.

Also, the work phase is time consuming and cannot be done very often. The results are also dependent on the annual variation and ventilation. Therefore, a quick and efficient and reliable method is needed to be able to make the work. In addition, the use of data could be combined to the models and the visualisation methods could be improved. This topic could be useful for all WMO's having crystalline host rock.

An automatic water leakage digitizing system is possible to develop but achieving accuracy on par with human will be challenging.

Some problems include achieving accurate location information especially in variable tunnel profiles, determining the amount of water, detecting point like anomalies and detecting anomalies behind objects. Also the fact that water temperature varies depending on the depth in ONKALO® and also the temperature increase is expected during the operational phase it might be difficult to achieve a library which can take into account these facts.

If the accuracy cannot be compromised, replacing human as the leakage mapper is not that simple. Developing methods to automate parts of the process would be worth considering, though.

2.6.9 Upcoming plans

Even though the hyperspectral imaging was ruled out for the time being, the near infrared (NIR) methods are still considered promising. One future focus of interest is to create a small scale (hand-held) test detector consisting of emitter and receiver NIR-LEDs. Prominent peaks in NIR region of water absorption spectrum are located at around 950 nm, 1400 nm, and 1900 nm (*Figure 56* ref. Fig 3, data from Kou et al. 1993). At least 950 nm, 1210 nm, 1445 nm, and 1885 nm wavelength LEDs were readily available for testing. The test meter of at least two LEDs (lighting and recording of one frequency) would be used to scan water leakages from a close range which would provide an estimation about the water film thickness. Of course, multiple frequencies can be combined in pairs of two LEDs, for example four frequency meter with 8 LEDs.
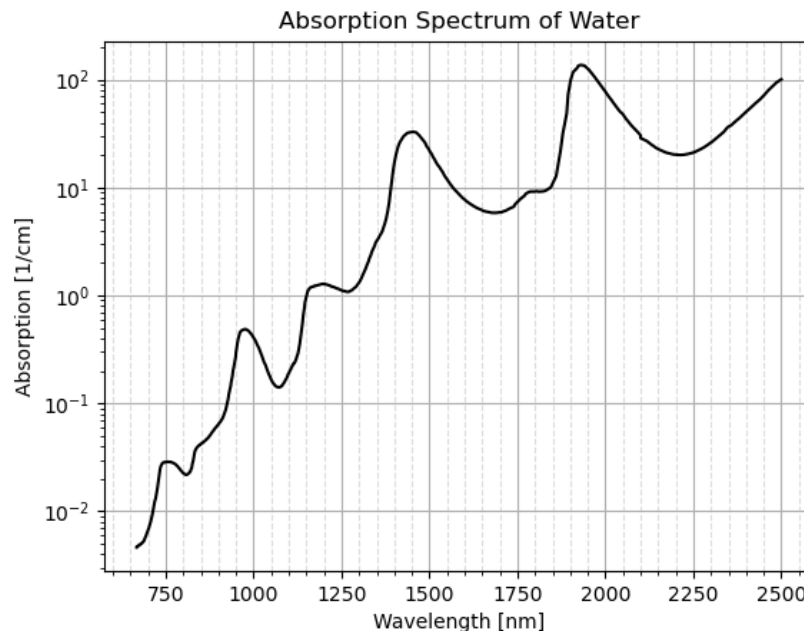
Figure 56: *Water Absorption Spectrum at NIR and SWIR region, data from Kou et al. 1993*

Another absorption-based method could be lighting up the tunnels with specific frequency band sources e.g., LEDs, and recording the result with suitable camera or with other sensor solution.

In the solution, the wall is illuminated with a sinusoidal profile and only this frequency is selected from the received signal. In this case, the flat background does not affect so much. Of course, the frequency should be chosen so that it is not a multiple of the 50 Hz of the electricity grid.

EURAD (Deliverable n° 17.7) - Synthesis report on Innovative and Enhanced Equipment for Repository Monitoring
Dissemination level: PUBLIC
Date of issue of this report: 04/06/2024

Page

It is possible to optimize the resistance values according to the situation. For this, it would be advisable to order a selection of resistors of different values. There should always be 10 of them of the same value and the tolerance may be 5%. Each resistance is measured separately with a multimeter, so by combining 2 or 3 in series or in parallel in a different way, a dense comb of different resistance values is obtained, even if the selection only consists of, for example, 6 values per decade.

Automatic scanning of leakage anomalies could be done using some kind of trolley or drone where the thermal imaging equipment would be mounted. Odometer and accelerometer could help the localization of the scanning records/images and some kind of yardstick system around the tunnel could make the photogrammetry easier. The use of GPS is not possible underground. On the other hand, indoor magnetic positioning systems might be of use. One such technology is provided by IndoorAtlas (indooratlas.com).

For the IR-scanning trolley, interesting solutions available on the market include FLIR A50 and A70 thermal image streaming cameras, streaming, recording, and analysis software FLIR Research Studio (paid licence), and the FLIR Desktop Atlas SDK (free) development kit.

2.6.10   Summary

Task for Automatic Digital Mapping of Leakages is initiated to develop and test a technical application that could be used to ease the present mapping method that is time-consuming and hard to validate, as visual mapping is always a subjective interpretation of the performing person.

After determination of specific requirements for reliability and performance of the technology, a search for potential technologies and contractors were carried out. Selection of method type and contractor for co-operation to conduct method development were completed by November 2022. Method development continued to test of the technology in various tunnel conditions in Olkiluoto, Finland.

The most promising and feasible for underground field testing was judged to be standard thermal imaging to start with to be able to see the possibility to detect different type of inflows in conditions where different structures like shotcrete, steel mesh reinforcement and other tunnel infra may disturb the results.

The IR-imaging results from ONKALO® were promising in that at least the anomalies were detected. The amount of water on the other hand could not be determined solely from the IR-image. Anomalies obscured by different objects and constructions are also hard to detect. This is especially true in case of the tunnel roof since in the tunnels the roof area is filled with pipes etc. In addition, roof anomalies are mostly point-like which make them even harder to detect.

The different type of AI and machine learning services are available as well in commercial and scientific means. It was decided that due the limited scope in this task there is no need to develop methods further and when implementing a technology, a commercial analyse method can be utilised for creating the library to classify the type of inflows. The creation of library is site dependent and requires a big set of pictures to make the machine learning exercise possible.

2.6.11   References

[78].   Cuiuli, E.; Procopio, S.Hydrogeological Survey, Radiometric Analysis and Field Parametric Measurements:A Combined Tool for the Study of Porous Aquifers. Water2022, 14, 2173. https://doi.org/10.3390/w14142173

[79].   Guerin, A., Jaboyedoff, M., Collins, B.D. et al. Detection of rock bridges by infrared thermal imaging and modeling. Sci Rep 9, 13138 (2019). https://doi.org/10.1038/s41598-019-49336-1

[80].   Huang H, Cheng W, Zhou M, Chen J, Zhao S. Towards Automated 3D Inspection of Water Leakages in Shield Tunnel Linings Using Mobile Laser Scanning Data. Sensors (Basel). 2020 Nov 21;20(22):6669. doi: 10.3390/s20226669. PMID: 33233387; PMCID: PMC7700199.

[81].   Kou, L., Labrie, D., Chylek, P., 1993. Refractive indices of water and ice in the 0.65-2.5µm spectral range.

EURAD (Deliverable n° 17.7) - Synthesis report on Innovative and Enhanced Equipment for Repository Monitoring
Dissemination level: PUBLIC
Date of issue of this report: 04/06/2024

Page

[82].   Krapez, J.-C.; SanchisMuñoz, J.; Mazel, C.; Chatelard, C.; Déliot, P.; Frédéric, Y.-M.; Barillot, P.; Hélias, F.; Barba Polo, J.; Olichon, V. 2022. Multispectral Optical Remote Sensing for Water-Leak Detection. Sensors 2022, 22, 1057. https://doi.org/10.3390/s22031057

[83].   Laakso, J., Junnila, J., Tapiola I., Vaittinen, T., Hurmerinta, E., Nummela, J., Pentti, E., Tammisto, E., Turku, J. and Karvonen, T. 2021. Olkiluoto – Hydrology and Hydrogeology. Eurajoki, Finland: Posiva Oy. 142 p. Working Report 2021-43.

[84].   Monerris, A., Vall-llossera, M., Camps, A., Sabia, R., Villarino, R., Cardona, M., Alvarez, E. and Sosa, S."Soil Moisture Retrieval Using L-band Radiometry: Dependence on Soil Type and Moisture Profiles," *2006 IEEE MicroRad*, San Juan, PR, USA, 2006, pp. 171-175, doi: 10.1109/MICRAD.2006.1677083.

[85].   Monerris, A., Cardona, M. and Vall-llossera, M. and Camps, A. and Sabia, R. and Villarino, R. and Alvarez, E. and Sosa, S "Soil moisture retrieval errors using l-band radiometry induced by the soil type variability," *Proceedings. 2005 IEEE International Geoscience and Remote Sensing Symposium, 2005. IGARSS '05.*, Seoul, Korea (South), 2005, pp. 1123-1126, doi: 10.1109/IGARSS.2005.1525313.

[86].   Neretnieks, I., Moreno, L., Liu, L., Mahmoudzadeh, B., Shahkarami, P., Maskenskya, O., Kinnbom, P. 2018. Use of infrared pictures to assess flowing channel frequencies and flowrates in fractured rocks. SKB R-17-04.

[87].   Q. Feng, G.W.K.R., 2006. Detection of water leakage using laser images from 3D laser scanning data, Proceedings of IAEG 10th Congress. London: The Geological Society of London, London.

[88].   Resende, M. M., Gambare, E. B., Silva, L. A., Cordeiro, Y. de S., Almeida, E., Salvador, R. P., 2022. Infrared thermal imaging to inspect pathologies on façades of historical buildings: A case study on the Municipal Market of São Paulo, Brazil. Case Studies in Construction Materials. https://doi.org/10.1016/j.cscm.2022.e01122

[89].   Vaittinen, T., Hurmerinta, E., Nummela, J., Pentti, E., Tammisto, E., Turku, J. & Karvonen, T. 2020. Results of Monitoring at Olkiluoto – Hydrology and Hydrogeology. Eurajoki, Finland: Posiva Oy. 704 p. Working Report 2020-43.

[90].   Xue, Y., Zhang, S., Zhou, M., 2021. Novel SfM-DLT method for metro tunnel 3D reconstruction and Visualization. Underground Space. https://doi.org/10.1016/j.undsp.2020.01.002.

[91].   Yu, P., Wu, H., Liu, C., Xu, Z. 2018. Water leakage diagnosis in metro tunnels by intergration of laser point cloud and infrared thermal imaging. The International Archives of the Photogrammetry, Remote Sensing and Spatial Information Sciences, Volume XLII-3, 2018 ISPRS TC III Mid-term Symposium "Developments, Technologies and Applications in Remote Sensing", 7–10 May, Beijing, China

[92].   Öhberg, A., Heikkinen, E., Hirvonen, H., Kemppainen, K., Majapuro, J., Niemonen, J., Pöllänen, J. & Rouhiainen, P. 2006. Drilling and the Associated Borehole Measurements of the Pilot Hole ONK-PH3. Working Report 2006-20. Posiva Oy, Eurajoki. 175 p

EURAD (Deliverable n° 17.7) - Synthesis report on Innovative and Enhanced Equipment for Repository Monitoring
Dissemination level: PUBLIC
Date of issue of this report: 04/06/2024

Page

3.   Advancement of Fibre-Optic Method

3.1   introduction

Optical fibre sensors (OFS) are exceptional tools, as they enable distributed measurements, providing data over their entire extent. Moreover, optical fibre's small size reduces the invasiveness of measurements. Furthermore, the sensing units do not contain electronics and can be exposed to the harsh repository conditions during the operating period. The promising developments seen in the application of fibre optic sensing methods will be further developed. While some of these techniques have already been explored successfully for repository monitoring in MoDeRn and Modern2020, fibre optic sensing sees a fast-paced development and a continuous stream of innovation. Here we focus on new sensing capability, qualifying optical fibres for various monitoring technologies and gleaning additional insights from distributed measurements of temperature and deformation.

3.2   Qualification of Radiation Tolerant Sensors

3.2.1   Introduction

The Industrial geologic storage centre (Cigéo) is conceived to store High Activity (HA) and Medium Activity - Long life (MA-VL) wastes from French nuclear facilities. The reversible underground storage centre is located at a 500m depth and will be operational for 100 years and from 2035 in Meuse/Haute-Marne area. Cigéo is planning on storing 3% of French nuclear wastes. Facilities are composed of: a descending area to ensure radioactive waste reception, a dedicated area for underground galleries construction and a waste storage area. HA wastes will be contained in 70cm diameter and 100m long cells whereas MA-VL wastes will be stored in 10m diameter and 100m long cells. The storage area elected by ANDRA is made of homogeneous hard rock and clayey layers with a low permeability and stable. The site is so a good candidate to welcome this storing facility for a long-term project such as Cigéo. The observation and monitoring of the storage area will allow to monitor the state of wastes and the quality of the confinement during the project. ANDRA aims at monitoring the site instrumenting the nuclear cells to follow physical measurements such as dose, temperature and strain. This is also motivated by acquiring real time data to confirm phenomenological models that can be used for further projects or in EURAD project. This PhD thesis work is part of the EURAD program in the MODATS (Monitoring equipment and Data Treatment for Safe repository operation and staged closure) work package. The main goal of this work in the subtask 3.2 (Task 3: Novel and Optimised Monitoring Technology for Repository Monitoring) is to qualify radiation tolerant optical fibres sensors used for distributed temperature and strain sensing.

ANDRA aims at monitoring the site instrumenting nuclear cells to follow physical measurands such as temperature and strain along the canister length. Optical fiber-based technologies offer many advantages compared to previous used point sensors such as thermocouples or extensometers. Optical fibers sensors can offer:

- Distributed measurement with high spatial resolutions (mm to m).
- Deported measurement allowing to perform measurement in harsh environments.
- Real-time sensing with a time resolution up to the second.
- Tuning the sensor to fit the required application.

Optical fiber-based monitoring technologies for temperature and strain monitoring offer real time measurements of both T and ε with a cm spatial resolution along nuclear waste cell. In addition, optical fiber sensor design through its composition, manufacturing process and interrogation techniques, offers a high variety of monitoring application to either perform dose-deposition measurement with radio-sensitive fibers or other monitoring processes (temperature, strain, gas concentrations, etc.) using radiation hardened optical fibers.

3.2.2   Problem analysis- (key parameter you want to measure).

Measuring temperature and strain around the radioactive waste cells with accuracies of < 1 °C and 20 με are the two parameters measured by this fiber optic application. Key parameters to develop such

EURAD (Deliverable n° 17.7) - Synthesis report on Innovative and Enhanced Equipment for Repository Monitoring
Dissemination level: PUBLIC
Date of issue of this report: 04/06/2024

Page

sensors under irradiation are Radiation Induced Attenuation (RIA) levels and kinetics determining the sensing length and the lifetime of the sensing capabilities. In addition, we look at: Radiation Induced Brillouin Gain Attenuation, Radiation Induced Brillouin Frequency Shift (RI-BFS) and radiation induced temperature and strain sensitivity changes, before during and after irradiation and Radiation Induced Rayleigh Frequency Shift (RI-RFS). The latter parameters provide information on the measurement lifetime, sensing length, temperature and strain accuracies, and radiation induced measurement errors. Other parameters are considered linked to coatings of the fiber cable: fiber permeability to H_2 diffusion, cable resistance to gamma and neutron exposures and cable structure influence on the measurement.

3.2.3   Research Objectives

The objective of this work is to analyse the influence of radiation on a distributed optical fiber sensor and to propose a measurement strategy for monitoring a structure hosting radioactive waste over a period of 100 years. Under irradiation, one of the main observed effects is an increase, sometimes abrupt, in the attenuation of optical fibers. This macroscopic degradation is explained by the generation of microscopic point defects induced by radiation in the pure or doped amorphous silica constituting the core and cladding of the optical fibers (S. Girard, et al, 2019[93]). These defects have distinct characteristics: optical (absorption bands), structural, and energetic, explaining that each defect will have a unique contribution to the response of a given fiber in a radiative environment. For Gamma irradiation, the observed degradations are solely caused by ionization mechanisms, and mitigation techniques have been implemented at the material, component, or system level to reduce the risk associated with high cumulative doses.

Under neutron radiation, the mechanisms become more complex, as atomic displacement effects are added to the ionization mechanisms. The impact of these new mechanisms, especially from the perspective of measurement and optical fiber sensors, remains to be explored for the neutron fluxes and fluences considered for Cigéo. Indeed, some waste families can emit neutrons. The impact of this radiation must be studied and modeled to characterize the sensor in its overall environment. During this study, the impact of neutrons on the optical and structural properties of the glass constituting the optical fiber is studied, which is the basis of the measurement. It is also essential to include the role of different layers of protective polymers surrounding the silica fiber. These layers, while not directly influencing the light propagation within the optical fiber, play a crucial role in transferring the deformations to be measured. Their degradation will, therefore, directly affect the operation of these sensors. This work through Jeremy Perrot's Thesis should enable the qualification of candidate sensor cables for the instrumentation of the initial phases of the Cigéo project.

3.2.4   Overview of the development team

This work is being conducted as part of Jeremy Perrot's (PhD student) thesis at the Hubert Curien Laboratory in Saint Etienne, France, within the MOPERE research group. Sylvain Girard (Full Professor and Head of the MOPERE team) is the thesis director, with co-direction by Youcef Ouerdane (Professor, MOPERE team), and supervision by Johan Bertrand (Research Engineer in Instrumentation, ANDRA, DISTEC). Jeremy Perrot initiated his PhD thesis in January 2022 and is entering his third and final year, focusing on the "Neutronic irradiation influence on fiber optic sensor performances." Sylvain Girard and Youcef Ouerdane are professors in the MOPERE team, specializing in optical fibers and radiation effects on materials. Johan Bertrand is an instrumentation expert at ANDRA, concentrating on the Cigéo project instrumentation, and leading the MODATS WP in the EURAD program.

Development steps followed during the MODATS project

I.   Identifying key parameters to deal with to fit the Cigéo requirements through a state of the art of this technology.
II.   Research studies conducted on optical fiber sensing and light scattering properties under irradiation.
III.   Qualifying optical fiber cables through irradiation campaigns.

![eurad logo] European Joint Programme on Radioactive Waste Management

EURAD (Deliverable n° 17.7) - Synthesis report on Innovative and Enhanced Equipment for Repository Monitoring
Dissemination level: PUBLIC
Date of issue of this report: 04/06/2024

Page

IV. Establishing optical cable discrimination through previous studies criteria to draw the best candidate for underground monitoring.
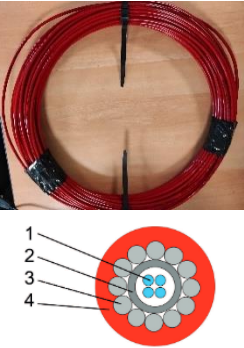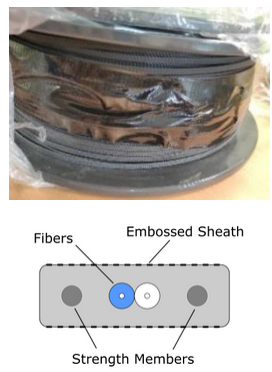
Activity	Q4 2021	Q1 2022	Q2 2022	Q3 2022	Q4 2022	Q1 2023	Q2 2023	Q3 2023	Q4 2023	Q1 2024
1. Identifying Keys parameters to deal with to fit the Cigéo requirements through a state of the art of this technology.	▉	▉								
2. Research studies conducted on optical fiber sensing and light scattering properties under irradiation.			▉	▉	▉	▉	▉	▉	▉	▉
3. Qualifying optical fiber cables through irradiation campaigns.				▉	▉			▉	▉	
4. Establishing optical cable discrimination through previous studies criteria to draw the best candidate for underground monitoring.									▉	▉

3.2.5   Material and method

3.2.5.1   Investigated samples.

Seven different optical cable were investigated during this irradiation campaign arbitrary named: CBT, CBS, CFB, NE, FN1, FN2 and PEEK and presented in the *Table 4*. All of tested cables present different structures and compositions represent a large panel of what is commercially available for optical fiber sensing application.

EURAD (Deliverable n° 17.7) - Synthesis report on Innovative and Enhanced Equipment for Repository Monitoring
Dissemination level: PUBLIC
Date of issue of this report: 04/06/2024

Page

***Table** 4: Test optical fiber cable specifications:*

BRUsens DTS STL PA **(CBT)** (1) FO Solifos type BruSens DTS 4 FO (2 mono and 2 multi). Primary coating with polyacrylate (2) Steel tube (3) Metallic protection layers (4) Polyamide sheath	**BRUsens DSS 3.2mm V9 grip (CBS)** (1) Step index glass/glass optical fiber E9/125 (G657 standard) (2) Polyamide sheath of 3.2 mm in diameter, (3) a steel tube (FIMT) of ~0.9 mm in diameter, a (4) Multi-layer buffer, which helps the strain transfer	**Fujikura blue loose Tube** **(CFB)**
		PEEK Cable (Neubrex) **(PEEK)** (1) 1 standard SM optical fiber (2) Accrylate coating (3) PEEK sheath
BRUsteel **(NE)** FO Solifos type Brusteel with 2 FO (1 mono and 1 multi) toron steel.	**Neubrex FN-SSL-3 white** **(FN1)**	**Neubrex FN-SILL-3 noir** **(FN2)** The outer sheath is made from olefin-type elastomer

3.2.5.2 CVRez Neutron irradiation

The main goal of this irradiation campaign is to qualify radiation tolerant optical fiber sensors and optical cables used for distributed sensing using Brillouin and Rayleigh scattering for temperature and strain monitoring. The irradiation facility is based in Czech Republic providing a ^{252}Cf source and in represented by Evzen Novak in the MODATS WP. This campaign aims at qualifying optical sensor cables to monitor geological disposal during the pilot phase of the underground geological nuclear waste repository Cigéo (Delepine-Lesoille et al, 2017 [94]).

EURAD (Deliverable n° 17.7) - Synthesis report on Innovative and Enhanced Equipment for Repository Monitoring
Dissemination level: PUBLIC
Date of issue of this report: 04/06/2024

Page

The experimentation plan has been established in June 2022 and sums-up which samples are tested, which configuration is used for online measurements and passive samples, at which dose and with which instrument. The irradiation started the 26th of August 2022 at 10h00 a.m. and stopped the 29th of October 2022 at 9h22 p.m. The irradiation campaign lasted a total of 1526 hours. The goal is also to help setting up the experiment when installing it in the irradiation chamber. Two fibers were tested and interrogated by an OTDR (Optical Time Domain Reflectometer) at 1310nm and 1550nm. The "F" fiber is fluorine-doped in the cladding, polyimide coated, single mode, furnished by ANDRA manufactured by iXblue under the reference: CUST-OPP31697-2.1-SMF (N° fiber B2363M1F2C010R02). This fiber is expected to be radiation tolerant with pure silica core and F-doped (1% weight around the core) and polyimide coated, 200 m were placed to expect a measurable effect of the irradiation for the entire campaign. Online with this fiber a phosphorus doped fiber "P" is placed after "F" since "P" is known to be radiation sensitive and have a linear RIA response with dose. For dosimetry purposes, 30 m of this fiber were placed inside the cable coil to monitor the deposited dose during the irradiation. A raspberry
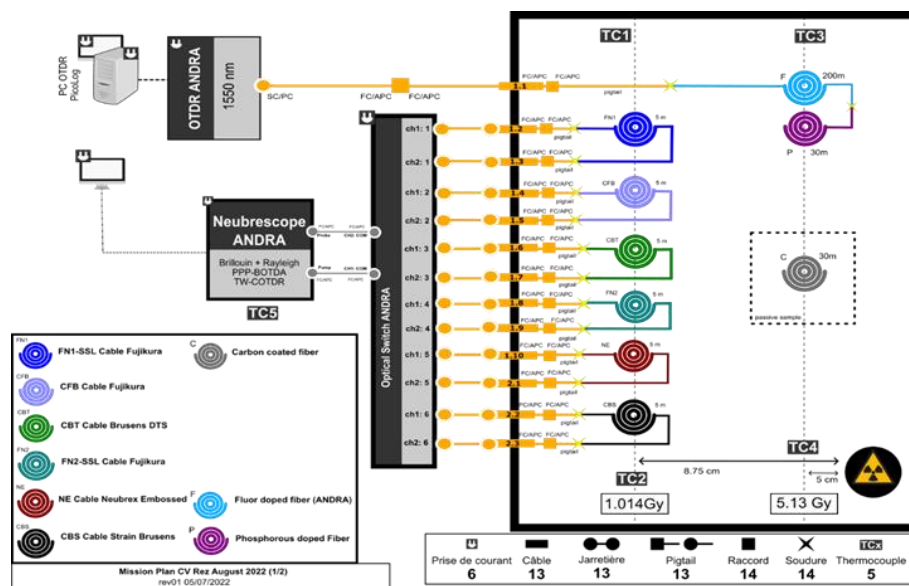
Figure 57: Experimentation plan established for CVRez neutron irradiation summer 2022.

monitored the OTDR to alternate between the two probed wavelengths to ensure a measurement every 30 min. The raspberry also monitored and stored thermocouples values. Four thermocouples were placed around and inside the optical cable coil in the irradiation chamber and one thermocouple was placed in the instrument room. Both F and P samples were placed at a distance of 5 cm from the source tube with a passive carbon coating sample "C" of 30m.

All optical cable samples were probed using Brillouin and Rayleigh scatterings via the Neubrescope interrogator furnished by ANDRA using PPP-BOTDA and TW-COTDR [4] respectively as described in *Figure 57* and *Figure 58* An optical switch helped ensuring the distributed measurement in all samples with both techniques consecutively. The coil containing each 5m of each cable sample has been placed around the source tube with a radius of 8.75cm from the surface. All sequences have been tested before the installation on the Neubrescope as well as the session sequence runner program with the optical switch. For each optical cable sample, both PPP-BOTDA and TW-COTDR techniques are used consequently by one port of the optical switch. Once both measurements are finished on one sample, the next port is selected to perform the same measurement. A loop configuration is performed to repeat this procedure during the entire irradiation campaign.

EURAD (Deliverable n° 17.7) - Synthesis report on Innovative and Enhanced Equipment for Repository Monitoring
Dissemination level: PUBLIC
Date of issue of this report: 04/06/2024

Page
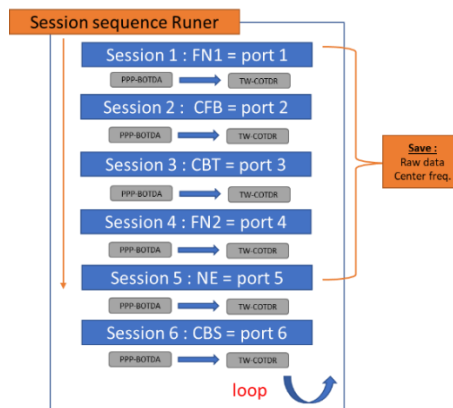
Figure 58: *Scheme of the Session sequence runner parameter on the Neubrescope to the optical switch.*

The installation process started from 23rd to the 26th of August 2022 with the help of Evzen Novak and Thomas Cernousek from CVRez [95]
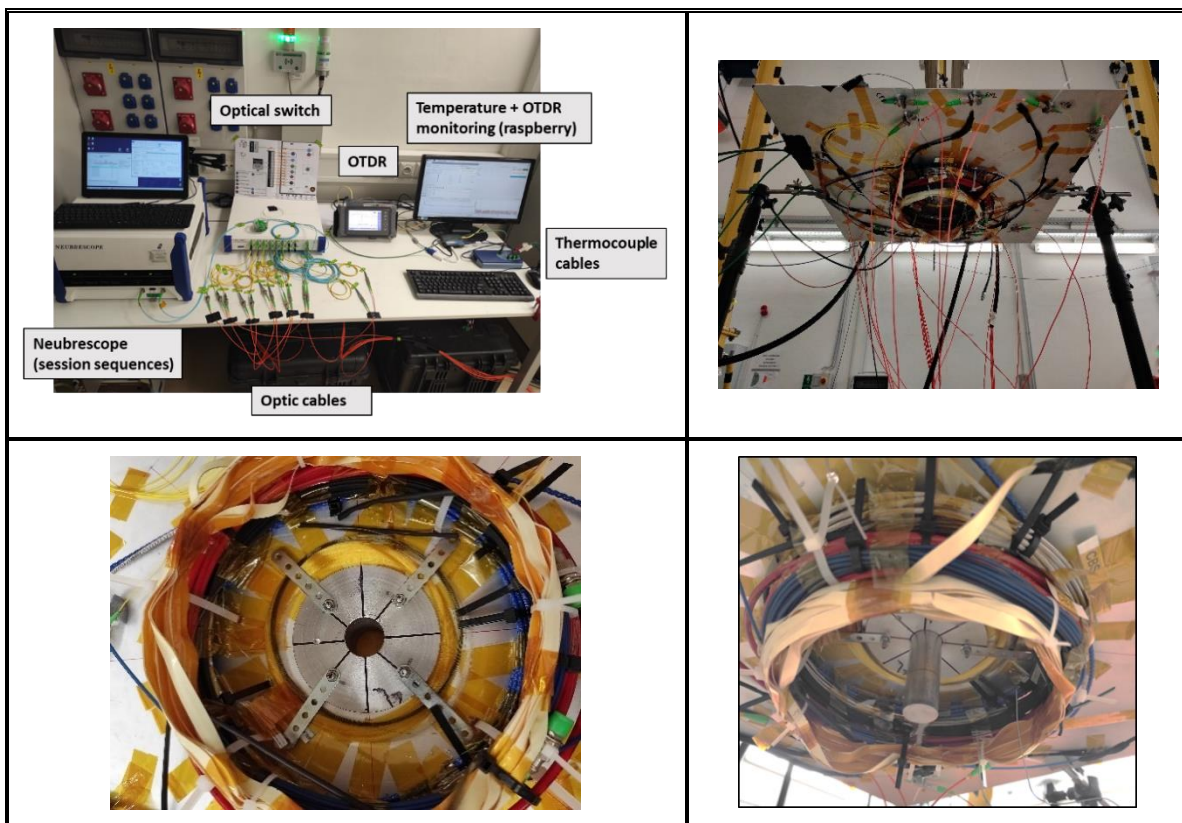
Figure 59: *Photos of the installation of: (top left) instrument room, (top right) upside-down sample holder, thermocouples and transport fiber cables connection, (bottom left) core of the optical cable sample coil with optical fiber samples in the centre, (bottom right) the sample coil and the source tube installed in the middle.*

During the installation, the instrument room has been set-up (Neubrescope, optical switch, OTDR, raspberry), then optical cables have been installed between the irradiation chamber and the instrument room, the sample holder have been placed and maintained in the irradiation chamber. Finally, thermocouples have been installed around and inside the sample coil and one in the instrument room, near the Neubrescope. The 20 cm diameter sample coil is maintained on an aluminium plate turned upside-down with a 12 cm diameter OTDR sample coil placed in the centre around the source tube shown in the ***Figure 59***. Transport fiber cables were used to transport light-waves from the instrument to the irradiation chamber and the samples out/in the optical switch and out of the OTDR. Thermocouple cables have also been used to connect the thermocouple from the irradiation chamber to the PicoLog

EURAD (Deliverable n° 17.7) - Synthesis report on Innovative and Enhanced Equipment for Repository Monitoring
Dissemination level: PUBLIC
Date of issue of this report: 04/06/2024

Page

recorder installed in the instrument room. Each transport cable is about 20 m long. The last two days were dedicated for reference measurements on Neubrescope and OTDR.

During the campaign a distance monitoring of the Neubrescope activity was setup with TeamViewer. On site, a visual monitoring of the irradiation chamber was available with an in-situ support from Evzen Novak. The source is a ^{252}Cf rod providing a 1/3.8 neutron and gamma irradiation at 2Mev with simulated spectrum shown *Figure 60* [95]. The source is transferred from its container to a source tube in the centre of the sample holder via a pneumatic system which sets the beginning of the irradiation. Given the calculation table with the neutron source emission obtain by MCNP calculations provided by CVR, a neutron source emission of 1.75e+8 n.s^{-1} is considered at 2 cm of the source tube surface [95].
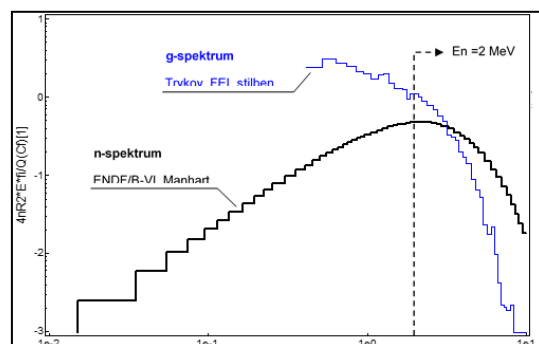
Figure 60: Simulated Neutron and gamma spectrum of ^{252}Cf isotopic source. [3]

From this value, the equivalent dose has been estimated on Si based material such as optical fibers. From this emission source the fluence is calculated from a source having a spherical isotropic emission leading to a fluence of 1.75*10^{+8}/(4*pi) = 1.392*10^{+7} n.s^{-1}.cm^{-2}, which is equal to 5.0134*10^{+10} n.h^{-1}.cm^{-2}. Knowing that the total irradiation lasted 1526 hours, 7.6504*10+13 n.cm-2 for the entire irradiation time. Thanks to the equivalent dose to fluence coefficient of 1*10+10 n.cm-2 for 1 rad(Si), the total estimated dose is estimated at 76,5 Gy(Si) à 2cm from the tube source surface. From a problematic of minimizing the curvature radius of the cable coil due to the radial tension and the signal loss, the cable coil was placed at 8.75 cm from the tube source with a 10 cm radius. The cable coil is then placed at a distance of 10 cm from the centre of the source. At this position, the total dose expected (neutron contribution only) according to the calculation results presented is about 1.6791 Gy (Si).

3.2.5.3 IRMA-IRSN Gamma irradiation

This irradiation campaign aims at investigating High dose/dose-rate Gamma irradiation effects on optical fibers cable sensing capabilities using Brillouin and Rayleigh scattering. It took place in CEA-IRSN (Institute of Nuclear Protection and Safety – France) at the IRMA facility in September 2023. The experimentation plan sums-up which samples are tested, which configuration is used for online measurements. The previously presented seven cables were tested for online measurements with the Neubrescope instrument (NBX-7020). An optical switch as for the previous irradiation campaign help sequencing channels in all tested cable sample and perform all the desired measurement sequentially. Three interrogators were used to perform online losses, Brillouin Frequency Shift (BFS) and Rayleigh Frequency Shift (RFS) measurements. The COTDR (Coherent Optical Time Domain Reflectometer), PPP-BOTDA (Pre-Pulse Pump Brillouin Optical Time Domain Analyser) and TW-COTDR Tunable Wavelength Coherent Time Domain Reflectometer) that offer the Neubrescope instrument have been used respectively (see *Figure 61*). The cables were place as a coil around the Gamma source holder to obtain a homogeneous irradiation inside the cables (10 m each). The mean dose-rate in the middle height of the cable coil have been evaluated by the IRSN-IRMA team as of 979 kGy(SiO2) accumulated dose and a mean dose-rate of 1.7865e+03 Gy/h. The IRMA facility provides a ^{60}Co source that is placed in the middle of the sample and source holder (see *Figure 62*). The irradiation has started on the 13 Sept. 2023 @14h18 and stopped on the 06 Oct. 2023 @10h00.

![eurad logo] EURAD (Deliverable n° 17.7) - Synthesis report on Innovative and Enhanced Equipment for Repository Monitoring
Dissemination level: PUBLIC
Date of issue of this report: 04/06/2024

Page

Associated with this cable coil, two thermocouples have been placed to monitor the temperature of the irradiation chamber. The seven optical cable samples have been connected to the optical switch (itself connected to the Neubrescope) via optical transport cable linking the instruments through the irradiation chamber. This deported and online measurement enables the real time monitoring of the dose deposition effect on the optical Losses, BFS and RFS (see *Figure 63*).
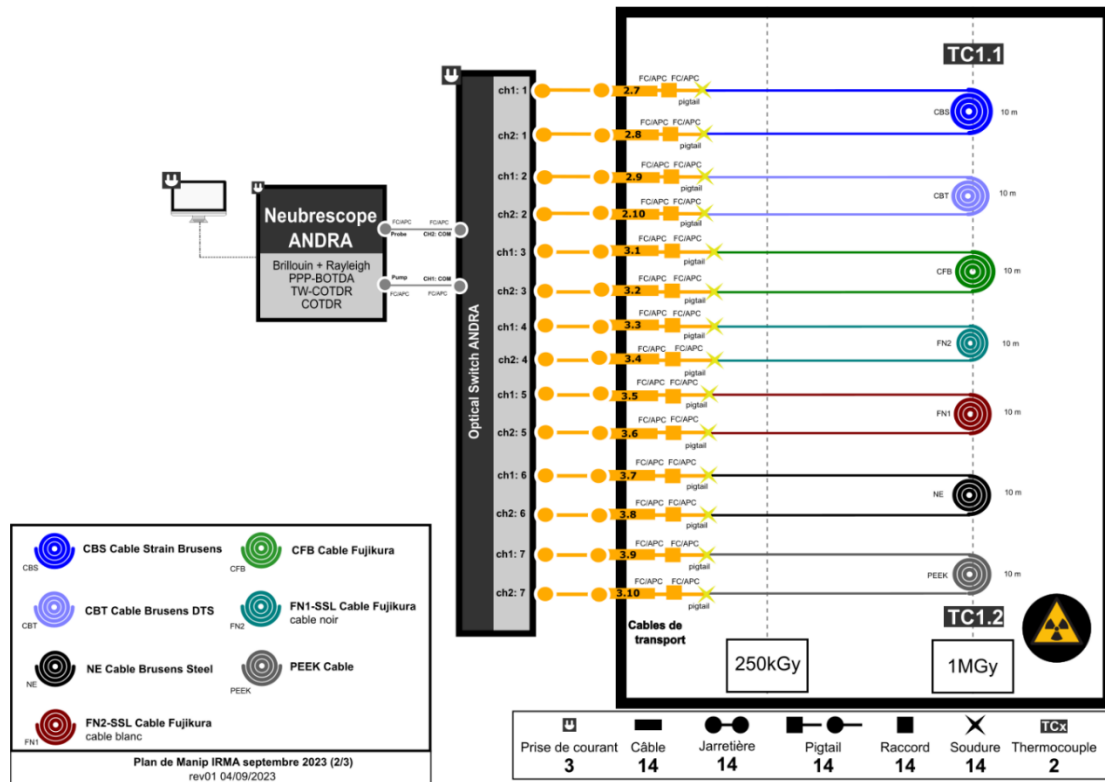
Figure 61: Experimentation Plan of the IRMA-IRSN Gamma irradiation campaign in September 2023
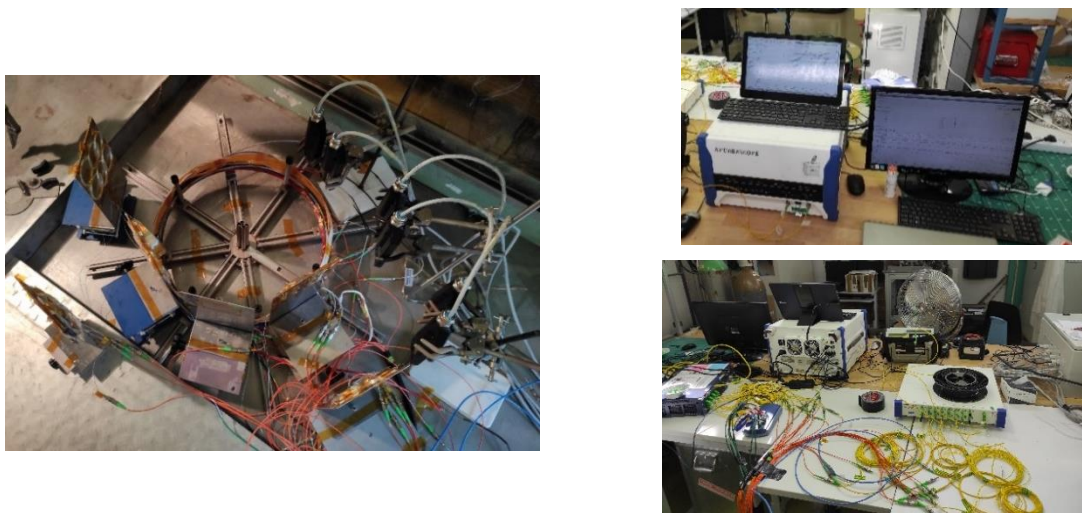
Figure 62: Installation set-up of cable samples on the left and instruments on the right at the IRMA-IRSN irradiation facility

EURAD (Deliverable n° 17.7) - Synthesis report on Innovative and Enhanced Equipment for Repository Monitoring
Dissemination level: PUBLIC
Date of issue of this report: 04/06/2024

Page
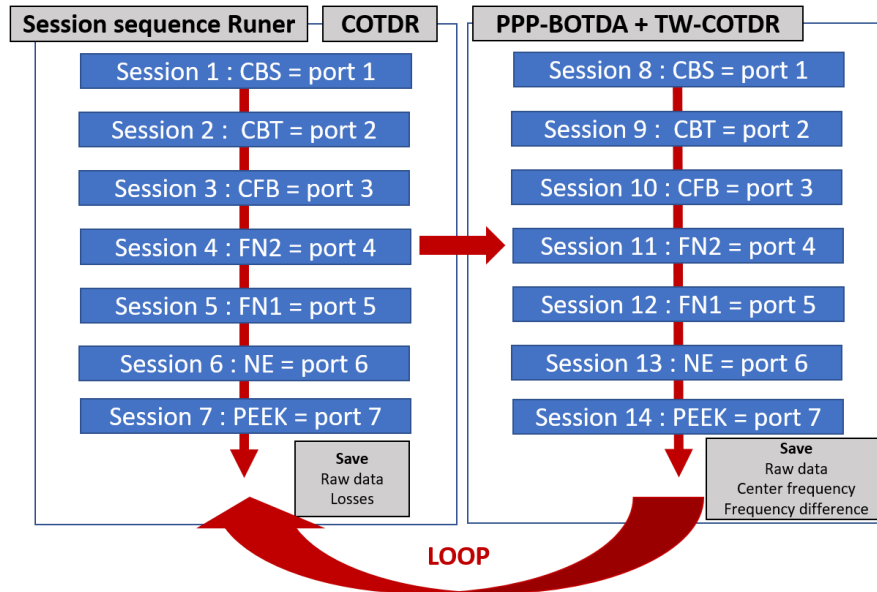
Figure 63: Scheme of the Session sequence runner parameter on the Neubrescope to the optical switch.

3.2.6 Results

3.2.6.1 CVRez neutron irradiation

From the OTDR trace measured (see *Figure 64*), the RIA (dB/km) can be obtained during the irradiation campaign at both 1310nm and 1550nm wavelengths. On every measured trace (every 30 min) the slope of the concerned fiber OTDR trace is calculated from a linear fit and subtracted by the reference slope. The measured RIA levels for both F-doped and P-doped fibers at both wavelengths are shown in *Figure 65*.
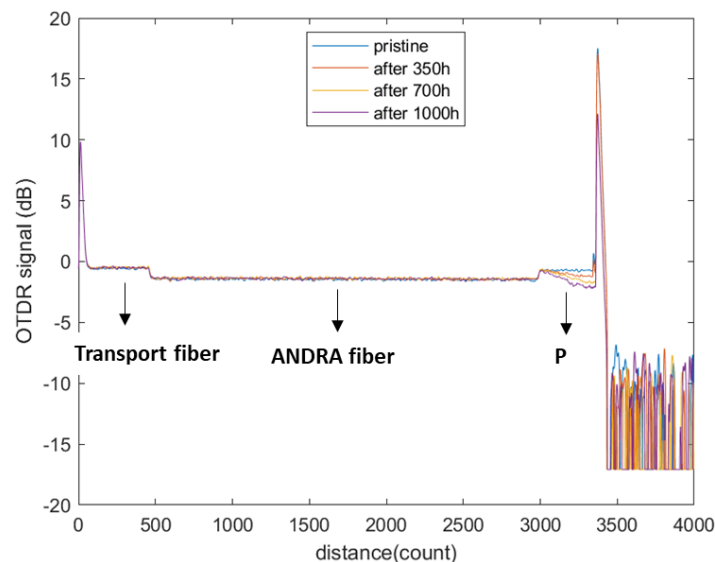
Figure 64: OTDR Trace before irradiation, after 350h, 700h and 1000h of irradiation. Containing traces of about 20m of the transport fiber, 200m of the F-fiber (ANDRA) and 30m of the phosphorus-doped fiber.

The P-doped fiber has been used for dosimetry purposes since it has a linear RIA response to absorbed dose. This radiation sensitive optical fiber is known to have a sensitivity to radiation about 4 dB/km/Gy at 1550nm. On the 30 m coil, the accumulated dose after 1526 hours of irradiation has been measured at 87 dB/km which is equivalent to a cumulated dose of 22 Gy received at 5 cm from the tube source by the P-doped fiber.

EURAD (Deliverable n° 17.7) - Synthesis report on Innovative and Enhanced Equipment for Repository Monitoring
Dissemination level: PUBLIC
Date of issue of this report: 04/06/2024

Page
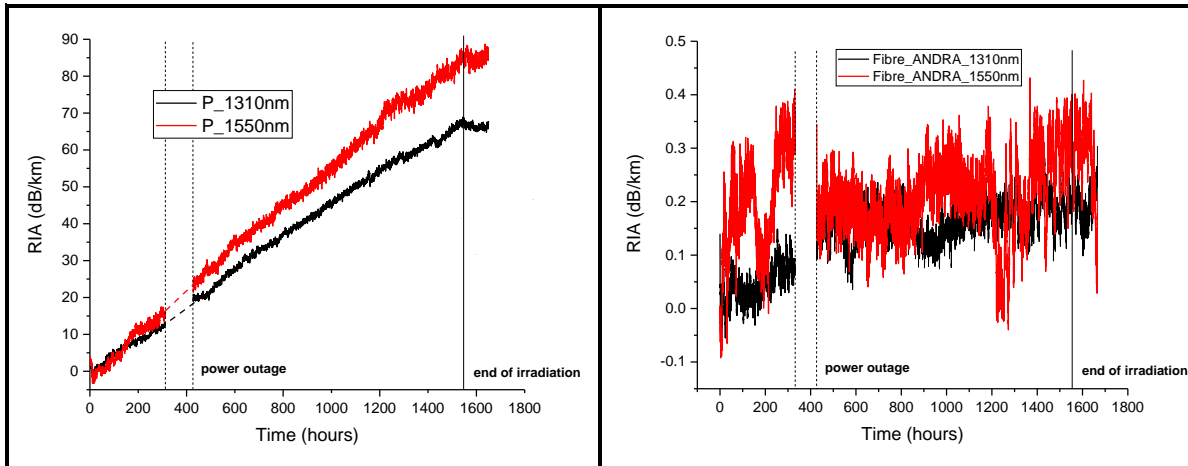
***Figure 65**: Measured RIA levels at 1310nm and 1550nm of (left) Phosphorus doped fiber and (right) fluorine doped fiber.*

From calculation, the expected dose at this distance from the tube surface is 8.5 Gy(Si) (neutron contribution only). In addition, the source is known to emit 1 neutron per 3.8 gammas. The calculated dose, considering only the neutron contribution, lacks of the gamma contribution to be compared to the measured dose of 22Gy. The order is the same but it also has to be considered that the fiber is made of SiO_2 and P-doped, since the calculation has been performed on Gy(Si), the conversion coefficient may differ from the one used. The F-doped fiber, contrary to P-doped fiber, exhibits a low RIA sensitivity to dose with an RIA level of 0.4 dB/km at 1550 nm after 1526 hours of irradiation. The measured attenuation for F-doped fiber at 1550 nm was about 0.48 dB/km. After the irradiation campaign, the total attenuation reached is about 0.9 dB/km at 1550 nm. For both fibers, RIA levels increase with wavelength. The temperature profile during the irradiation has been measured by four thermocouples placed on the sample holder and one thermocouple in the instrument room presented in ***Figure 66***.
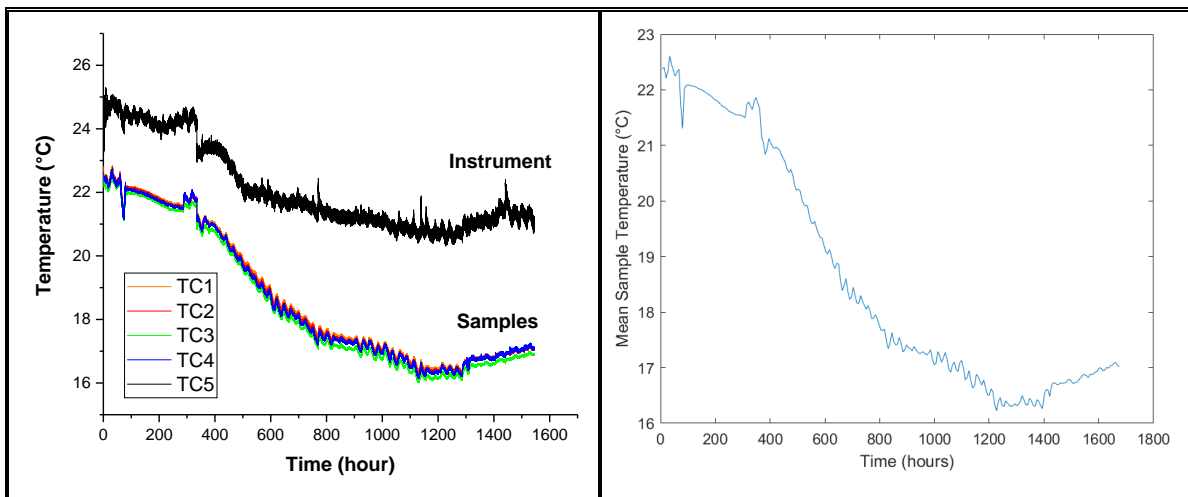
***Figure 66:** Measured temperature profile during the irradiation. (right) Samples coil temperature profile during the irradiation campaign.*

The temperature profile of the sample coil is obtained from a mean of the four sample thermocouples, this profile is presented ***Figure 66***. The noticeable decrease of the temperature is due to the weather condition going from a summer weather (26th August) to autumn (29th October) inducing a 6°C drop of the irradiation chamber temperature. In addition, it is possible to see the influence of day/night temperatures with periodic fluctuations of the measurement. This temperature profile will be useful for the temperature correction of the Brillouin Frequency Shift (BFS) and Rayleigh Frequency Shift (RFS) described below. BFS and RFS have been obtained using PPP-BOTDA and TW-COTDR techniques respectively provided by Neubrescope NBX-7020F (Piccolo, A., et al, 2019 [96], Kishida, Kinzo, et al.2017[97]. The BFS is obtained acquiring the Brillouin Gain Spectrum (BGS) along the optical path

EURAD (Deliverable n° 17.7) - Synthesis report on Innovative and Enhanced Equipment for Repository Monitoring
Dissemination level: PUBLIC
Date of issue of this report: 04/06/2024

Page

(transport cable sample, transport cable) to track the Brillouin frequency of the main peak of the sample of concern during the irradiation. The RFS is also acquired during the irradiation campaign using the reference measurement compared to the actual measured spectrum and deduce a frequency difference resulting in a frequency shift. Since BFS and RFS are both temperature and strain dependent, they mainly contain the temperature contribution since the sample coil is maintained at the same position during the entire campaign. A dose contribution can also occur and contribute to BFS and RFS via RI-BFS (Radiation Induced BFS) (Piccolo, A., et al, 2017 [98], Piccolo, A., et al, 2020[99]) and RI-RFS (Radiation Induced RFS). To obtain the BFS in one sample, the centre frequency measured (CF) (Z-axis) from the Neubrescope is displayed along the entire optical fiber path (X-axis) during the entire irradiation (Y-axis). An example is displayed **Figure 67** on the Rayleigh FD measurement for the "NE" cable.
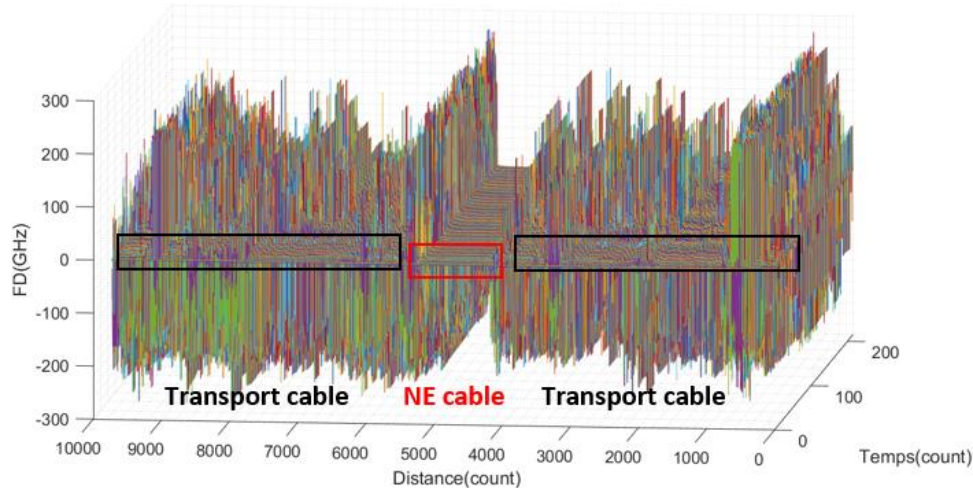
Figure 67: *Measured Distributed Rayleigh Frequency Difference (Z-axis) along the optical fiber path (X-axis) for the "NE" optical cable sample during the irradiation campaign (Y-axis).*

From this **Figure 67**, the indexes corresponding to the cable sample position in the optical path are selected to locate the sample in the optical path. Each position during the entire irradiation is subtracted by its reference measurement at the same position. The result of this subtraction is the Frequency Difference between the reference measurement and the measurement during irradiation. Then, a mean of the FD between all positions in the sample is performed. Each mean corresponds to a resulting value of BFS in the cable at a certain time during the irradiation. **Figure 68** is the result of the BFS displayed from this procedure during the entire irradiation time and recovery. The same procedure is applied to plot RFS but instead of CF the FD is measured by Neubrescope a mean on all location inside the cable is applied but on the FD. The RFS is then displayed for the entire irradiation time.
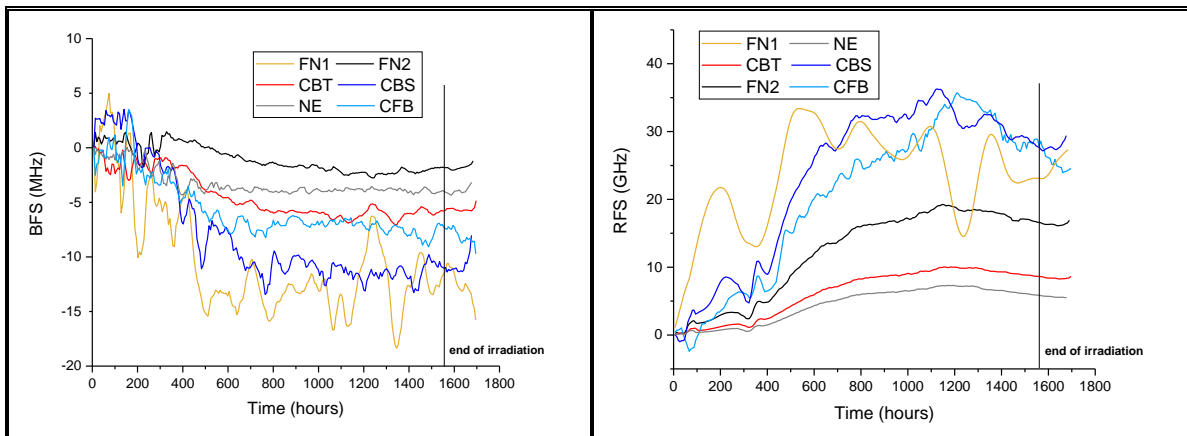
Figure 68: *Measured (left) Brillouin Frequency Shift and (right) Rayleigh Frequency shift during the irradiation.*

From **Figure 68**, BFS and RFS have been tracked during the entire irradiation campaign and exhibit the

EURAD (Deliverable n° 17.7) - Synthesis report on Innovative and Enhanced Equipment for Repository Monitoring
Dissemination level: PUBLIC
Date of issue of this report: 04/06/2024

Page

same tendency than the temperature profile. In fact, BFS and RFS are mainly affected by temperature. To extract the RI-BFS and RI-RFS, a temperature correction procedure is necessary. To do that, Brillouin and Rayleigh temperature sensitivity coefficients (C_{T_R} and C_{T_B} coefficients, respectively) are measured on the non-irradiated samples. BFS is known to be linear with temperature and strain from -40°C to +80°C and from $0\mu\varepsilon$ to $5000\ \mu\varepsilon$ respectively. Temperature steps are uniformly performed all over the cable coil, thanks to the BINDER MK115 heating and cooling chamber. While the Brillouin frequencies are tracked along the temperature evolution with the BOTDA interrogator from OzOptics. Rayleigh temperature sensitivity coefficients are measured with the OFDR interrogator OBR from Luna Technologies. Temperature steps have been performed on six pristine optical fiber cable samples with both interrogators.

Table 5: Brillouin and Rayleigh temperature sensitivity coefficients for the six optical sample used for the first temperature correction from one temperature cycle measurement.

Cable sample	FN1	CFB	CBT	CBS	FN2	NE
C_{T_B} (MHz/°C)	2.119	2.528	0.949	2.409	1.557	1.117
C_{T_R} (GHz/°C)	-2.747	-5.006	-1.605	-5.443	-2.281	-1.357

This irradiation campaign testing radiation tolerance of six optical cables under a mixed field neutron/gamma at low doses (~ 1.7Gy) has been conducted at CVRez in Czech Republic. Six cables with different structures have been investigated under and after irradiation. Characteristics of the six probed cables are summed-up along:

- The robustness mainly tested during the installation and preparation of the sample coil and strain tests. This characteristic is important since no break is allowed with the two-ended interrogation technique (PPP-BOTDA) and should be installed on hundred meters long coils. The fragility of FN1 and the impact of the coil holder on the measurement made it very sensitive to unwanted perturbations and not robust to shocks or local stresses. Thin layers of surrounding materials on FN1, FN2 and CFB (compared to other cables) makes these cables more likely to break.
- The temperature sensitivity has been tested on both pristine and irradiated cables exhibiting no major radiation induced change but mainly strain induced change. A higher temperature sensitivity can induce higher measurement dynamics and a possible improvement of temperature and strain discrimination capability.
- The stability of the temperature coefficient has been investigated in the cables exhibiting FN1 and CFB as two bad candidates showing the highest temperature coefficient margins and FN2 the highest temperature coefficient stability over six temperature cycles.
- Strain sensitivity has been tested for both pristine and irradiated samples exhibiting very low sensitivities with NE and CBT cables not making theses cables for strain sensing. On the other hand, no strain sensitivity coefficient radiation induce change has been noticed after irradiation for all cables.
- Due to the nature of some cable structures (CBT, NE, CBS) their robustness is also inducing strain while bended changing both temperature and strain sensitivities when installed. It can be problematic during the calibration phase. Temperature sensitivity measurement have to be performed with the same bending radius than the future installation.

Finally, both BFS and RFS tolerance to this irradiation have been tested with PPP-BOTDA and TW-COTDR exhibiting no detectable contribution of the accumulated dose on RFS and on CBT's BFS. Brillouin temperature correction has been impacted by the strain induced by the bending radius of the cable. No major effect of the accumulated dose on BFS on all six cable is so expected like CBT but some further experiment should testify.

3.2.6.2   IRMA-IRSN Gamma irradiation

RIA level and kinetic measurements have been performed by the COTDR interrogator from the NBX-7020 instrument as described in section 1.1.6.3. Results are presented below in *Figure 69*.

EURAD (Deliverable n° 17.7) - Synthesis report on Innovative and Enhanced Equipment for Repository Monitoring
Dissemination level: PUBLIC
Date of issue of this report: 04**/06/2024**

Page
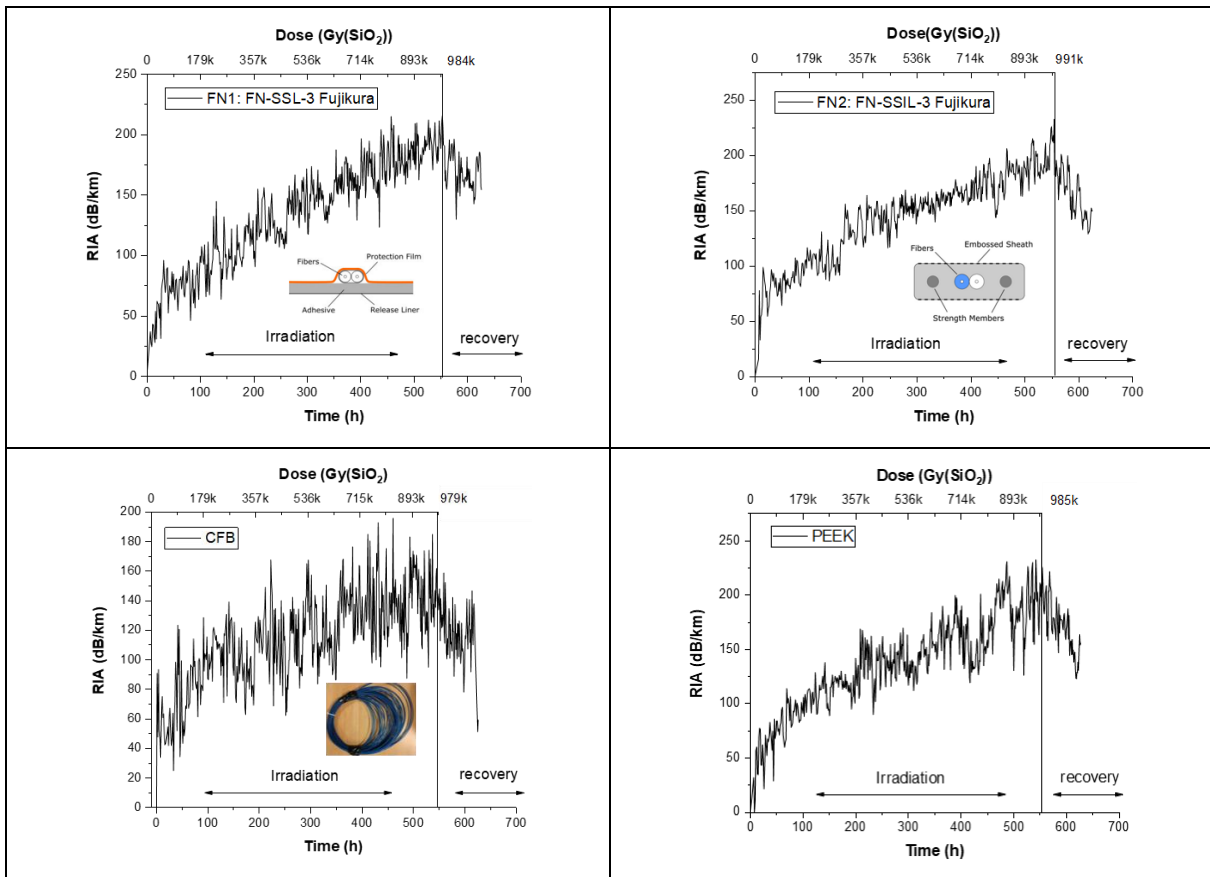
Figure 69: *RIA online measurement results from the IRSN-IRMA irradiation campaign on FN1, FN2, CFB and PEEK cables.*

RIA levels and kinetics exhibited in FN1, FN2, CFB and PEEK cables show equivalent results of standard Ge-doped silica-based optical fibers reaching levels of 200 dB/km, 200 dB/km, 160 dB/km and 200 dB/km respectively after 1 MGy gamma-accumulated dose (see ***Figure 70***). No effect from the cable influences significantly the RIA behaviour at high doses for all above cables. However, not all tested cables presented fiber related RIA levels and kinetics. In fact, CBT and CBS cables presented Ge-doped RIA levels up to 100 hours and 300 hours respectively. Then RIA levels drastically increase reaching 2500 dB/km and 1200 dB/km respectively after 1 MGy accumulated dose. In fact, this phenomenon is due to the H_2 diffusion inside the fiber core from the outer coatings of each cable. Some gel has been found inside these cables after irradiation. Under irradiation the gel releases gaz H_2 through radiolysis effect when gamma rays deposit energy in the material. This process results in a diffusion of this gas in the fiber core introducing additive OH-related optical defects presenting spectral absorption bands in the NIR domain increasing RIA levels at 1550 nm. The diffusion time differs from CBT to CBS cables (100 h to 300 h respectively). In fact, outer coatings composition and structure differ from one to another. The gel is also a different type. NE cable also reaches high RIA levels up to 2500 dB/km but no gas diffusion inside the cable can be noticed. Some investigation is undergoing to explain the origin of this behaviour. A proposal concerns the nature of the fiber itself. In fact, it is known that Phosphorus doped fiber exhibit comparable RIA levels. The investigation aims at identifying the fiber composition in the NE cable. Brillouin and Rayleigh frequency shifts have been measured with the NBX-7020 instrument using both PPP-BOTDA and TW-COTDR interrogators respectively.

EURAD (Deliverable n° 17.7) - Synthesis report on Innovative and Enhanced Equipment for Repository Monitoring
Dissemination level: PUBLIC
Date of issue of this report: 04/06/2024

Page
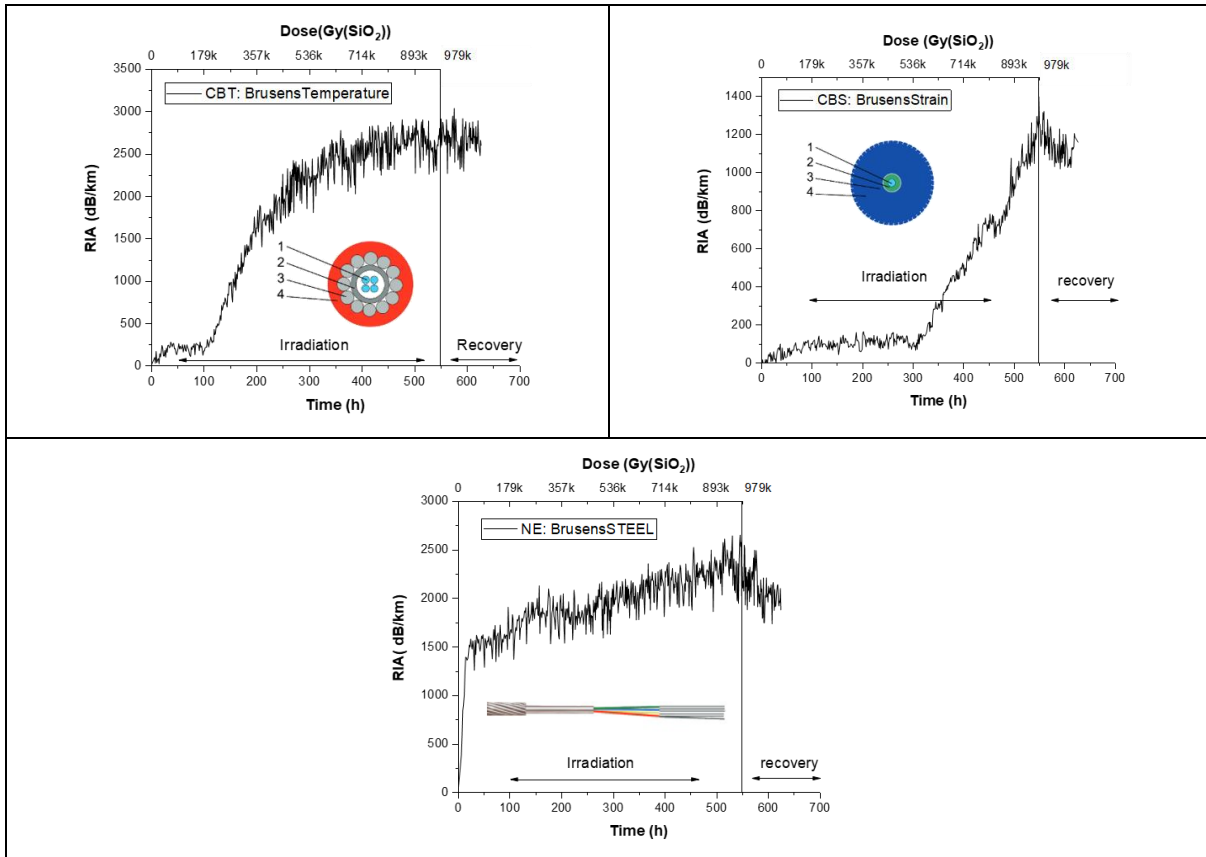
Figure 70: *RIA online measurement results from the IRSN-IRMA irradiation campaign on CBT, CBS, NE cables.*

After a temperature correction process of the measured BFS (Brillouin Frequency Shift) and RFS (Rayleigh Frequency Shift) eliminating the temperature contribution we have isolated both RI-BFS and RI-RFS measured during the irradiation. Results are presented in **Table 6** This table sums-up both RI-BFS and RI-RFS obtained after 1 MGy accumulated dose at IRMA-IRSN.

Table 6: *RI-BFS and RI-RFS levels obtained from the online PPP-BOTDA and TW-COTDR measurements during the IRMA-IRSN irradiation up to 1 MGy.*

	CBT	CBS	NE	FN1	FN2	CFB	PEEK
RI-BFS		+6 MHz		+7 MHz	+7 MHz	+14 MHz	+10 MHz
RI-RFS		-20 GHz		-5 GHz	-20 GHz	-14 GHz	+5 GHz

For both NE and CBT cables, it has been shown that the measurement exhibits high RIA levels. After the drastic increase of RIA in each cable, the instrument considered that both CBT and NE related lines were broken due to the very low Signal to Noise Ratio when incident light is absorbed by radiation-related defects. No PPP-BOTDA and TW-COTDR were performed after 250h and 100h of irradiation for CBT and NE respectively.

3.2.7 Discussion about the results obtained.

All the results obtained cannot be fully summarized in this document but are partially presented in the "Technology Data Sheet", outlining the evaluation criteria for selecting the optimal optical fiber candidate for temperature and strain monitoring in the Cigéo project. As of this stage in the study, PEEK and FN2 cables exhibit the most favorable characteristics. The samples underwent testing under mixed field neutron/gamma conditions for low neutron-related accumulated doses at CVRez and high gamma dose rates at IRMA-IRSN. New data will be continually added to this database. Specifically, post-irradiation

EURAD (Deliverable n° 17.7) - Synthesis report on Innovative and Enhanced Equipment for Repository Monitoring
Dissemination level: PUBLIC
Date of issue of this report: 04/06/2024

Page

results for the IRSN-IRMA irradiated cables will be included to assess possible temperature and strain sensitivity coefficient changes induced by high gamma doses in both Brillouin and Rayleigh scattering. Furthermore, the top four optical cables (FN1, FN2, CFB, PEEK) will undergo neutron/gamma irradiation at the NEAR facility at CERN in 2024. This will facilitate post-irradiation analysis to examine mechanical deterioration of coatings at high neutron fluences and modifications in light scattering properties, investigating higher neutron fluences compared to the initial campaign at CVRez.

3.2.8 References

[93]. **S**. Girard, et al. "Overview of radiation induced point defects in silica-based optical fibers", Reviews in Physics, 4, 100032 (2019).

[94]. Delepine-Lesoille, Sylvie, et al. "France's state of the art distributed optical fibre sensors qualified for the monitoring of the French underground repository for high level and intermediate level long lived radioactive wastes." Sensors 17.6 (2017): 1377.

[95]. Johan BERTRAND (ANDRA), Evzen NOVAK (CVRez), Research collaboration agreement for performance of irradiation of the sensors, Agreement no. 20086436, 2022.

[96]. Piccolo, A., et al. "Distributed optical fiber strain and temperature sensing system performances: Brillouin vs Rayleigh." Seventh European Workshop on Optical Fibre Sensors. Vol. 11199. SPIE, 2019.

[97]. Kishida, Kinzo, et al. "Monitoring of tunnel shape using distributed optical fiber sensing techniques." Proceedings of the 4th Conference on Smart Monitoring, Assessment and Rehabilitation of Civil Structures SMAR. 2017.

[98]. Piccolo, A., et al. "Coupled temperature and γ-radiation effect on silica-based optical fiber strain sensors based on Rayleigh and Brillouin scatterings." Optics Express 27.15 (2019): 21608-21621.

[99]. Piccolo, Arianna, et al. "Mechanical properties of optical fiber strain sensing cables under γ-ray irradiation and large strain influence." Sensors 20.3 (2020): 696**.**

EURAD (Deliverable n° 17.7) - Synthesis report on Innovative and Enhanced Equipment for Repository Monitoring
Dissemination level: PUBLIC
Date of issue of this report: 04/06/2024

Page

3.3 Advancement of Fibre-Optic Strain Sensing Methods for Monitoring Tunnel Linings in Clay Rocks

3.3.1 Introduction

The understanding of ground response and induced strains in the tunnel lining, when tunnelling for a deep geology repository, is needed for the design of the construction technology to comply with operational and long-term safety requirements. To test different tunnel support systems in the sandy facies of the Swiss host rock Opalinus Clay, the TS Experiment at the Mont Terri URL was initiated. The ground response and strains in the lining during and after excavation are monitored by conventional convergence measurements (3D-optical displacement measurements by means of total station and reflectors) as well as with different fibre-optic strain sensing methods. Whereas the engineering objective of the experiment is to analyse and understand the effect of support type, gallery orientation and facies on ground response with the scope on construction technology, the monitoring objective is the advancement of fibre-optic strain sensing methods for monitoring different tunnel linings in clay rocks.

Fibre-optic strain sensing was already identified in the MoDeRn project as a suitable monitoring technique and first tests were performed in the Modern2020 project. Aspects that could not be covered yet and will be the focus of our work are advanced analysis techniques, detailed comparisons of different sensor types and measurement techniques, and the evaluation of possible time-dependent effects of the sensor performance from aging.

We plan to use the existing instrumentation of the TS Experiment at the Mont Terri URL to further improve the application and analysis of fibre-optic strain sensing under repository-like conditions. Two shotcrete-supported sections and one steel-supported section were instrumented with 3 different types of fibre-optic strain sensors. We will continue the periodic measurements of circumferential strains in three cross-sections of different tunnel support systems, which are performed since late 2018. The following measurement methods will be applied, analysed, and compared to each other:

- BOTDA = Brillouin Optical Time-Domain Analysis (Brillouin Scattering)
- BOTDR = Brillouin Optical Time-Domain Reflectometry (Brillouin Scattering)
- OBR = Optical backscatter Reflectometry (Rayleigh Scattering)
- FBG = Fibre-Bragg Gratings
- Conventional convergence measurements.

3.3.2 Objectives

The main objectives of this project are:

- Use the existing instrumentation of the TS experiment at the Mont Terri URL to further improve the application and analysis of fibre-optic strain sensing under repository-like conditions.
- Develop and apply advanced data processing and analysis techniques for detailed quantification of the high-resolution strain distribution in the tunnel support and evaluation of different sensors and different sensing technologies.
- Assessment of the tunnel deformation in space and time under conditions representative of a repository.
- Recommendations for the selection of adequate fibre-optic strain monitoring methods for tunnel support monitoring that can be used by other monitoring experts (WMO, TSO or research organisations).

3.3.3 Overview of the development team

Tobias Vogt from Nagra (Switzerland) is the project manager of this project. He is responsible for the project management, conceptualisation and planning, parts of the analysis, and reporting.

The Swiss company Marmota is Subcontractor for the fibre-optic strain measurements in the framework of the TS-Experiment at the Mont Terri URL as well as for parts of the development of the advanced data processing and analysis techniques under the lead of Nagra. The key personal of Marmota for this project is Michael Iten and Frank Fischli.

EURAD (Deliverable n° 17.7) - Synthesis report on Innovative and Enhanced Equipment for Repository Monitoring
Dissemination level: PUBLIC
Date of issue of this report: 04/06/2024

Page

3.3.4 Technology description

Fiber-optic strain and temperature sensing can be performed as distributed or point sensing (**Table** 7). Point sensing means measuring at discrete locations with short gauges. The main point sensing technology is called Fiber-Bragg Grating (FBG). Distributed sensing implies that sensor data is obtained spatially continuous, over the full length of a sensor cable. This can be idealized as a gapless array of numerous point or short-gauge sensors aligned in series one after another. Continuous strain along optical fibres can be measured using several techniques based on two different scattering effects: Brillouin and Rayleigh. When simultaneous strain and temperature changes shall be measured, a loose fibre for temperature compensation must be placed next to a tightly fixed strain fibre.

FBG, inscribed at predefined locations along the fibre, reflect a specific wavelength. The reflected wavelength at the FBG changes with strain and/or temperature changes. Depending on the application and the packing of the sensor, the strain and temperature condition can be measured using FBG sensors.

Rayleigh scattering occurs because of small random variations in fibre density and refractive index, which are the cause of manufacturing imperfections. The Rayleigh backscatter can be analysed, resulting in a distributed sensor of high spatial resolution in the centimetre range (e.g., Samiec, 2011,[101]). When analysed, the backscatter signal exhibits a random but stationary pattern. This pattern can be regarded as a fingerprint (e.g., Samiec, 2011,[101]), which can shift due to strain and/or temperature variations.

Rayleigh scattering (OBR) offers high spatial and measuring resolution. In addition, it requires only access from one end of the sensor cable (the light pulses are sent in from the same end where also the reflection is recorded). The somewhat limiting factor is the maximum sensing length of 70 m including any possible lead-in that current state-of-the-art measurement units are offering.

Spontaneous Brillouin scattering occurs when a light pulse guided through a silica fibre is backscattered by a nonlinear interaction with thermally excited acoustic waves (Tkach et al., 1986, [102]). The scattered light undergoes a frequency shift, which is directly related to the strain and temperature in the medium at the scattering position. The backscatter is recorded in the time domain to obtain information of the scattering location. The frequency shift of the signal can then be analysed and converted into strain and temperature data. When using spontaneous Brillouin scattering (Brillouin Optical Time Domain Reflectometry - BOTDR), the resulting signal is weak, therefore, the frequency shift information is not very accurate, and the possible distance of signal transfer is limited.

In a more refined stimulated Brillouin setup (Brillouin Optical Time Domain Analysis - BOTDA), two counter-propagating light waves at different frequencies interact via stimulated acoustic waves (Horiguchi & Tateda, 1989 [100]). The interaction results in energy transfer which amplifies the signal. This leads to higher accuracy of the measured strain as well as longer possible sensor lengths.

Contrary to the Rayleigh scattering, the Brillouin technology allows for much longer sensor lengths of up to a few tens of kilometres. In exchange, the spatial resolution is in the meter range.

For the BOTDA technology, both cable ends need to be connected to the measuring device, forming a loop configuration. BOTDR allows measurements with access from one side only. This makes it a valuable alternative in case of broken embedded sensors. However, the BOTDR readout accuracy is about 10 times lower than the BOTDA.

Table 7**:** *Specifications of the different measurement technologies*

Technology	Spatial resolution	Measurement resolution	Measurement repeatability	Range / Limitations
FBG	Point sensor	0.1 °C / 0.8 µε	0.1 °C / 0.8 µε	Limited number of FBG per cable

EURAD (Deliverable n° 17.7) - Synthesis report on Innovative and Enhanced Equipment for Repository Monitoring
Dissemination level: PUBLIC
Date of issue of this report: 04/06/2024

Page

OBR	0.01 m	0.1 °C / 1 µε	To be assessed	70 m
BOTR	1.0 m	0.1 °C / 2 µε	<1 °C / <20 µε	Up to 40 km
BOTDA	0.5 m	0.1 °C / 2 µε	<0.1 °C / <2 µε	Up to 60 km

Table 8**:** shows the sensors that are used in the TS experiment.

Name	Type	Diameter	Manufacturer
V0	Strain	0.9 mm	Huber & Suhner AG
V3	Strain	7.2 mm	Solifos AG
V9	Strain	3.2 mm	Solifos AG
BruSens Temperature	Temperature	4.8 mm	Solifos AG
Loose Tube Temp	Temperature	0.9 mm	Huber & Suhner AG

Table 9: *Specifications of the different fibre-optic sensors*

3.3.5   Material and method

Three sections (TS-1 and TS-3, *Figure 71*) with different tunnel support of the Gallery 18 were instrumented directly after excavation and during support installation in October and November 2018 with several different fibre-optic strain sensors. In addition, sensors for temperature compensation were installed. Sections TS-1 and TS-3 are supported by different shotcrete applications and TS-2 by steel linings (TS-2) as supportive elements.
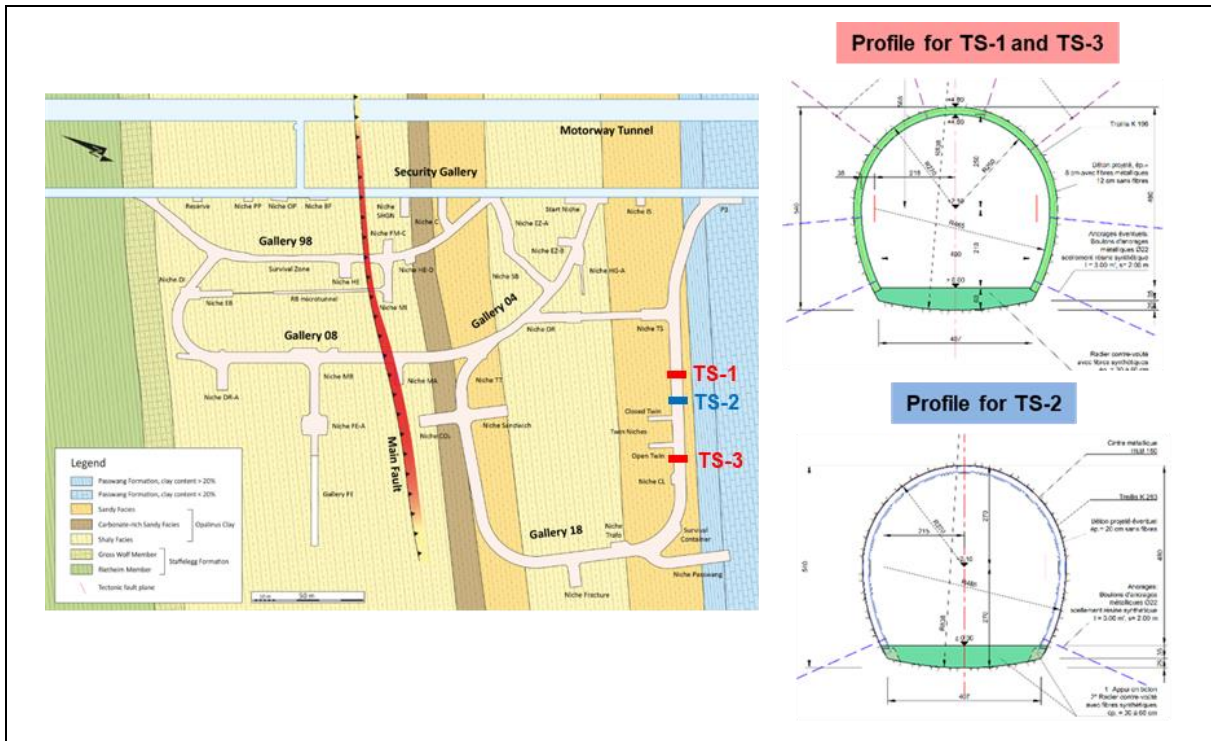
Figure 71: Map of Mont Terri URL (Switzerland) with the locations and the type of tunnel support used of the three cross-sections where fibre-optic sensors were installed.

EURAD (Deliverable n° 17.7) - Synthesis report on Innovative and Enhanced Equipment for Repository Monitoring
Dissemination level: PUBLIC
Date of issue of this report: 04**/06/2024**

Page

The fibre-optic cables were installed along the entire circumferential cross-sections in loop configuration so that they can be measured from both ends.

For the shotcrete-supported cross-sections TS-1 and TS-3, two robust strain sensors (V3 and V9) were installed in the heading and the invert of the tunnel. The separation into a heading section (overhead) and an invert section (floor) was due to construction boundary conditions, which did not allow to instrument a full cross-section at once. After installation the sensors were poured over with shotcrete. The loop layout results in an outer arch (Extra) close to the bedrock and an inner arch (Intra) with a distance of approximately 8 cm to the bedrock (*Figure 72*). Additionally, in the cross-section TS-3, an open-ended temperature compensation cable was installed running along the outer arch (Extra) in the heading and invert.

For instrumentation of the steel arche section the sensors were glued on the steel arches (*Figure 73*).
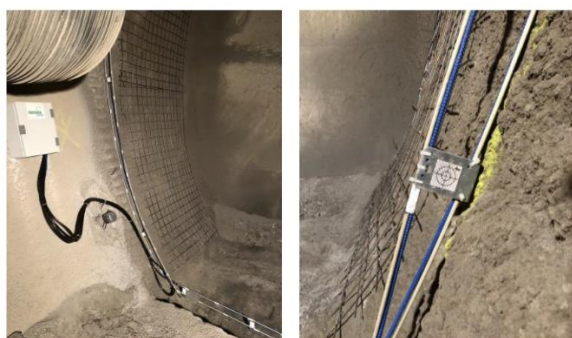
Figure 72: Installation of Extra and Intra sensors in a shotcrete section.

Figure 73: Installation of the sensors for the steel arche section.

3.3.6   Activities

The following activities were carried out:

- Measurements
  - Measurements of the different fibre-optic strain sensors (distributed/cables and point measurement) in the different cross-sections by means of different fibre-optic measurement technologies, namely based on Brillouin scattering (BOTDA, BOTDR) and based on Rayleigh scattering (OBR) as well as Fibre-Bragg Gratings (FBG).
  - The cross sections will be also monitored by conventional convergence measurements.
- Data processing and analysis.
  - The measurement technologies have different spatial resolution and different sensitivities.
  - Measurement results and performance of the different strain sensing technologies will be compared in detail for (a) total strain, (b) qualitative patterns of distributed strain, (c) spatial resolution, (d) overall functionality and (e) effects particular to each sensing technology. For these tasks data processing and analysis tools need to be developed.
  - Identification of advantages and challenges of different distributed sensor designs including a comparison of the obtained strain results.
  - Comparison of general performance between distributed sensors (Brillouin and Rayleigh) vs. point sensors (FBG). In addition, a comparison of the fibre-optic results with the conventional convergence measurements will be done.
  - Evaluation of possible time-dependent effects and properties of the sensors regarding long-term performance for repository monitoring.
- Reporting
  - MODATS report and publication

3.3.7   Results

The measurements of the TS-Experiment started already in autumn 2018. Within MODATS, three measurement campaigns were performed so far on 03.-04.09.2021, 10.-11.02.2022, and 26.-

EURAD (Deliverable n° 17.7) - Synthesis report on Innovative and Enhanced Equipment for Repository Monitoring
Dissemination level: PUBLIC
Date of issue of this report: 04/06/2024

Page

29.09.2022. The campaigns included measurements of the different fibre-optic strain sensors (distributed/cables and point measurement) in the different cross-sections by means of different fibre-optic measurement technologies, namely based on Brillouin scattering (BOTDA, BOTDR) and based on Rayleigh scattering (OBR) as well as Fibre-Bragg Gratings (FBG). In addition, the cross sections were also monitored by conventional convergence measurements.

The work on data processing and analysis started. The focus was on finding visualisation tools and useful graphs for data comparison and evaluation of strain distribution. **Figure 74** shows an example of a graph type that was identified as promising.
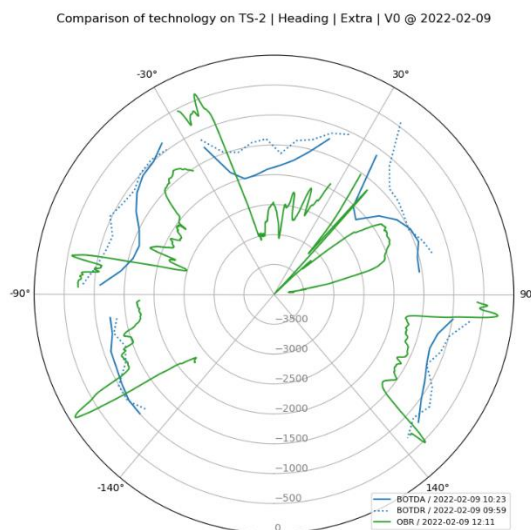
Figure 74: *Graph of different fibre-optic strain data of section TS2. The data of the floor of the cross-section is not shown (floor corresponds to -140° to 0° and 0° to 140°).*

3.3.8   Discussion about the results obtained.

No more distributed sensors failed, and measurements could be continued. However, the FBG sensors could not be measured during the last campaign. Their functionality will be checked during the next measurement campaign. If possible, they will be repaired. The different fibre-optic strain data show in some section consistent behaviour, in some section differences exist. The reason for that will be analysed in more detail.

In general, OBR data reveal more high-resolution details about deformation in the tunnel lining that would remain undetected with the other monitoring techniques.

In addition, the interpretation of the strain distribution and the resulting deformation pattern require more work in the next months.

3.3.9   References

[100].   Horiguchi, T. and Tateda, M., 1989, "Optical-fiber-attenuation investigation using stimulated Brillouin scattering between a pulse and a continuous wave", Optics Letters, Vol. 14, n° 8, Optical Society of America, pp. 408-410

[101].   Samiec, D., 2011, "Verteilte faseroptische Temperatur- und Dehnungsmessung mit sehr hoher Ortsauflösung", Photonik, No. 6, pp. 34-37.

[102].   Tkach, R. W., Chraplyvy, A. R. and Derosier R. M. (1986) Spontaneous Brillouin scattering for single-mode optical-fibre characterisation in Electronics Letters, vol. 22, no. 19, pp. 1011-1013, 11 September 1986. doi: 10.1049/el:19860691

EURAD (Deliverable n° 17.7) - Synthesis report on Innovative and Enhanced Equipment for Repository Monitoring
Dissemination level: PUBLIC
Date of issue of this report: 04/06/2024

Page

3.4 Development of an optical pH sensor for porewater monitoring

3.4.1 Introduction

The development and use of analytical tools for on-site measurements are of major importance in several applications (Daoudi, 2017, [103], in particular for environmental water quality monitoring in complex aqueous systems. Among measurable quantities, knowledge of pH value is fundamental because it governs a lot of chemical reactions that can induce important modifications in a complex aqueous system. pH measurement is generally performed either by electrochemical (pH electrode) or optical (pH optode) methods. Electrochemical methods are ideal for measurements in research laboratories but are limited for on-site measurements. They are fragile and require calibration with a reference electrode before measurement, they suffer from acid and alkaline errors. Optical methods offer advantages in terms of cost and simplicity of use, they do not require a reference electrode. They are not sensitive to electrical interferences and can address several measurement channels through multiplexing configuration. They can be used for remote, continuous, real-time, in situ measurements and can operate in hostile environments. The development of these optical probes is based on a simple concept involving the immobilization of a chemical recognition phase sensitive to pH variation on a surface part of the optical chain. These methods use light to measure variations in optical properties resulting from interaction between the aqueous system to be analyzed and the chemical recognition phase of the probe. The immobilization technique for this chemical recognition phase is an important step in the development of these optical probes. The immobilized chemical layer will determine the nature of the chemical species to be measured, the optical characteristics of the probe and its stability. The literature lists three main methods for immobilizing colored pH indicators on the surface of a stable solid support that is permeable to the diffusion of hydronium and hydroxide ions: these are adsorption, entrapment, and covalent immobilizations. Several optical probes based on the adsorption of pH indicator molecules are described in the literature. Other optical pH probes based on the adsorption of indicator molecules on a Bragg grating are also mentioned. Optical sensors based on the use of pH indicator molecules trapped in a polymer matrix are also described. The literature highlights those methods based on adsorption and trapping leads to a poor robustness of the probe because the pH-sensitive phase undergoes a temporal degradation of its response. Covalent immobilization reduces the problems associated with degradation of the chemical recognition phase. It can be achieved by either chemical or electrochemical grafting. The literature lists countless optical pH probes published using chemical grafting. The literature shows that the design process for these pH sensors based on chemical grafting requires a substrate surface activation step by various chemical methods (silanization, epoxidation, urea, formaldehyde). The chemical recognition phase is simply performed by immersing the surface of the activated substrate in a solution containing the colored pH indicator having a specific function (e.g. an aromatic primary amine function) capable of reacting with the surface to bind covalently. The development of this chemical recognition phase by the chemical grafting process is much slower and results from a delicate balance between activated substrate/pH indicator interactions. This chemical grafting process leads to the formation of a monolayer.

However, it is important to immobilize a sufficiently thick organic layer to obtain an optical pH sensor that delivers a valuable spectral response. Electrochemical grafting involves the establishment of a covalent bond between the substrate surface and the chemical recognition phase, and generally leads to the formation of a thick organic layer. The thickness of the electro grafted organic layer can reach several hundred nanometers. The thick film formed is stable and resistant in many solvents and even in the presence of ultrasounds.

Redox grafting of NR onto a solid surface using the Graftfast™ process has been reported in the literature (Mohr, 1994 [104],Fages,2015 [105] but this process is not reproducible and does not allow control of the thickness of the chemical recognition phase.

To the best of our knowledge, no study has been reported on the electrochemical grafting of the acid-base indicator, chosen for this work, NR, by cathodic reduction of aryl diazonium salts to realize an optical pH probe. The major advantages of electrochemical grafting under conductive surface

EURAD (Deliverable n° 17.7) - Synthesis report on Innovative and Enhanced Equipment for Repository Monitoring
Dissemination level: PUBLIC
Date of issue of this report: 04/06/2024

Page

polarization lie in its simplicity, its rapidity in generating radicals in a gentle and gradual manner. The thickness of the organic layer formed can be controlled by the concentration of aryl diazonium salts used, the amount of charge consumed and the main electrochemical parameters.

The aim of this work is to covalently immobilize NR on the end of a metallized optical fiber and on a stainless-steel mirror part of the optical chain in order to choose the best location for the chemical recognition phase. For this purpose, the metallized optical fiber and the 316L stainless steel mirror are modelized by a metallized glass plate and a 316L stainless steel plate respectively, in order to optimize the electro-grafting process and make analytical characterizations easier. The chemical recognition phase of electro-grafted NR is characterized by profilometry to determine its thickness, X-ray photoelectron spectrometry (XPS) to determine its chemical composition, infrared spectroscopy to identify its molecular structure, UV-Visible spectroscopy to measure its absorbance. This optical pH probe can find applications for continuous pH measurements and especially for remote measurement in complex aqueous systems. This is the case, for example, of the future Cigeo project which is a deep geological disposal facility for radioactive waste to be built in France the French Geological Disposal will be managed by Andra (French national radioactive waste management agency).

3.4.2   pH water monitoring

For safety reasons, it is very important to survey the quality of water found in the Callovo-Oxfordian (COx) clay by measuring the pH evolution.

Materials present in the storage site (concrete, metals, …) have interactions with the poral water present in the COx. Chemical interactions inside this system may lead to degradation phenomena which can, on a long-time scale, lead to an alteration of the quality of the storage site.

Considering the high-level activity of the nuclear waste stored in Cigeo, a good stability of the storage site is a safety major objective. An Underground Laboratory has been constructed to study the storage possibilities in deep geological clays. In this laboratory, many geochemical, physical and chemical measurements are done. Among them, the pH water monitoring is of primary importance because it is correlated to reactions which can degrade the materials structure.

Although the permeability of the COx is low, poral water can move and have interactions with structure materials. Chemical products issued form degradation reactions are able to migrate in poral water and modify the pH value:

- Acid transient due to the pyrite oxidation,
- Alkaline transient due to carbonatation of concrete.

The pH sensor can be designed either by grafting Neutral Red (NR) on the fiber or on the stainless-steel mirror.

- The optical fiber as metallized glass plate. The objective of the work was to adjust the covalent grafting of Neutral Red to obtain a thick layer to have enough sensitivity for pH measurements. The robustness of the sensor was also tested as well as its reproducibility and time response. Hysteresis tests were also carried out.
- The 316L stainless steel mirror was assimilating with a 316 L stainless steel plate. The grafting on the mirror allows to graft NR on a larger surface than when using the optical fiber.

Various optical configurations are also tested to maximise the optical response. Different light sources, LEDs, spectrometers are used.

3.4.3   Overview of the development team

Most of the work was carried out by Dr. Denis Doizi (CEA) with Dr. Guy Deniau (CEA) for coordination of the work. Organic synthesis was carried out by Dr. Elisabeth Zekri (CEA) and experimental work by

EURAD (Deliverable n° 17.7) - Synthesis report on Innovative and Enhanced Equipment for Repository Monitoring
Dissemination level: PUBLIC
Date of issue of this report: 04/06/2024

Page

Germaine Olorounto during her pHD founded by ANDRA. Johan Bertrand and Vincent Corbas (ANDRA) helped us for fundings and experiments in Bure.

3.4.4 Development steps followed during the MODATS project.

I. **Identification and characterization of suitable acid base indicators for the pH range corresponding to poral water monitoring (4~10).**

II. **Determination of the best analytical conditions for electrochemical grafting and analytical characterizations using various techniques on metallized plates.**

III. **Grafting on the optical fiber and on the stainless-steel mirror.**

IV. **First attempts at the underground Laboratory and REX for future experiments**

Activity	Q4 2021	Q1 2022	Q2 2022	Q3 2022	Q4 2022	Q1 2023	Q2 2023	Q3 2023	Q4 2023	Q1 2024
1. Identification and characterization of suitable acid-base indicators	■	■								
2. Determination of the best analytical conditions			■	■	■					
3. Grafting on the optical fiber and on the mirror						■	■	■	■	
4. First attempts at The Underground Laboratory and REX									■	■

3.4.5 Materials and methods

A white light source is injected into a multimode optical fiber. The fiber carries the light to the measurement location. A mirror, positioned in front of the fiber, sends the light back on a multimode optical fiber to a spectrometer for spectral analysis. A computer software enables the spectral responses processing. The interaction of the immobilized organic layer with the protons contained in a given sample, in the presence of light, leads to variations in optical properties. The chemical recognition phase can be covalently immobilized on the end of the metallized optical fiber or on the 316L stainless steel mirror (Figure 75). These two different optical configurations are studied in this work. The light source (HL 2000-FHSA), the optical fibers with a core diameter of 940 µm and the spectrometer (HR 2000) are supplied by Ocean Insight.

EURAD (Deliverable n° 17.7) - Synthesis report on Innovative and Enhanced Equipment for Repository Monitoring
Dissemination level: PUBLIC
Date of issue of this report: 04/06/2024

Page
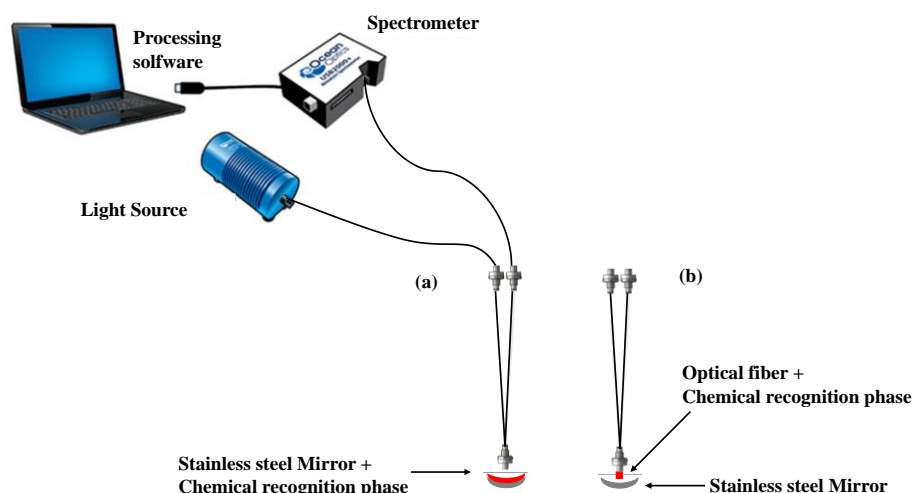
Figure 75***:*** *Schematic diagram of optical pH probe, immobilization of chemical recognition phase on the stainless-steel mirror (a) or on the optical fiber (b).*

The optical fiber is modelized by a glass plate. The glass plates are metallized to provide the conductive surface required for electrochemical grafting using aryl diazonium salt chemistry. The thickness of the metal deposit is low (30 nm) to allow UV-visible transmission measurements. The glass plates are first cleaned in the ultrasonic tank for 5 min in three different solvents: acetone, ethanol, and water respectively. After cleaning, the glass plates are dried with nitrogen to remove any traces of water. The glass plates are placed in the evaporation vacuum chamber (10-7 mbar). 5 nm chromium and 25 nm gold are deposited on the plates. These metallized glass plates are used without further treatment.

The 316L stainless steel mirror is modelized with a 316 L stainless steel plate. It is better to make optimization studies on these 316 L stainless steel plates because of the cost of the mirror and for easier covalent grafting process and analytical characterizations. The 316L stainless steel plate is first polished with different papers containing Struers brand silicon carbide (SiC). The various SiC type papers (P80 to P4000) and grain size papers (200 to 5 μm) were used respectively to obtain identical and optically reflective surfaces. After polishing, the plate is treated with diamond paste ¼ μm then rinsed with ultra-pure water and dried with argon. Then the plate is ultrasonically cleaned in a mixture of water (5 mL), acetone (5 mL) and ethanol (5 mL) for 10 min and then in acetone only for 10 min before being used.

NR grafting is carried out in HCl (0.1M) acidic aqueous medium. An equimolar quantity of NR and sodium nitrite is used to obtain the diazonium salt of the NR. For each concentration, NR is dissolved in acidic HCl (59 mL) and the solution is stirred for 5 min. Sodium nitrite was first dissolved in ultrapure water (1 mL) and then added to the NR solution to transform the aromatic amine into the cation diazonium. The reaction is complete with a 100% yield. The mixture, stirred for 5 min, is then transferred into the three-electrode electrochemical cell.

All experimental tests are performed in a three-electrode electrochemical cell at room temperature using a Biologic SP-300 potentiostat controlled by EC-Lab software. The reference electrode is a silver wire (pseudo-reference), the working electrode is a metallized glass plate (5 nm Cr/ 25 nm Au) held in place with alligator clips, and the counter-electrode is a platinum wire (in the case of the metallized glass plate and metallized optical fiber). For all experiments carried out on 316L stainless steel plates and on the 316L stainless steel mirror, the counter-electrode used is a carbon plate. All voltammograms are recorded at 5 mV/s (in the case of the metallized glass plate and metallized optical fiber) with an inversion potential of -1V. For all experiments carried out on the 316L stainless steel plates and the 316L stainless steel mirror, the scanning speed used is 50 mV/s. The immerged surfaces are ~cm2 for the metallized glass plates, the stainless-steel plates and for the mirror.

All Infrared measurements are performed with a Bruker vertex 70 spectrophotometer controlled by OPUS acquisition software. This FTIR spectrophotometer is equipped with an ATR Pike accessory,

EURAD (Deliverable n° 17.7) - Synthesis report on Innovative and Enhanced Equipment for Repository Monitoring
Dissemination level: PUBLIC
Date of issue of this report: 04/06/2024

Page

enabling measurement in attenuated total reflection (ATR) mode with a DTGS detector. FTIR spectra are recorded in the 600 to 4000 cm-1 wavenumber range with a spectral resolution of 4 cm-1 using 16 scans.

All XPS spectra are recorded using Thermo Scientific's ESCALAB 260Xi X-ray photoelectron spectrometer. This spectrometer offers high sensitivity and resolution, it uses a 1486.6 eV monochromatic Al K-Alpha X-ray source capable of analyzing a 900 µm diameter area of a sample to a depth of 10 nm.

All UV-Visible absorption spectra are recorded in a Hellma 10 mm quartz cell using a Cary 60 spectrophotometer (Agilent technologies) controlled by Cary WinUV software. Absorption spectra are recorded at a speed of 4800 nm/min.

3.4.6   Description on the on-field test used during the project.

The experimental set up is composed of two HL 2000 FHSA 20 W lamps (Oceanview®). A spectrometer Flame 3648 pixels, a multiplexer 2x2 FOS TTL and 600 microns diameter optical fibers, various 940 microns bifurcated optical fibers, SMA/SMA connectors and a labtop with SpectraSuite software have been used on site. A Mirror supports were also realized to test the grafted mirrors. Experiments are carried out in the ACA cabinet which allow pH monitoring of poral water.

3.4.7   Results [107]

3.4.7.1   Study of NR in solution by uv visible spectrophotometry

Prior to any electro-induced covalent functionalization, NR is studied in solution. Its pKa value is 7.1 in acidic medium, it turns to yellow in basic medium (Figure 76).

Figure 77 shows the UV-Visible absorption spectra of NR recorded in buffer solutions of different pH. These spectra show two absorption bands corresponding to its acidic and basic forms. The two bands intersect at a point called the isobestic point (470 nm). This point indicates the presence of an equilibrium between the two forms of NR. The curve of absorbance versus pH measured at 550 nm has a sigmoidal shape. From this curve, we can deduce that NR shows a linear absorbance variation as a function of pH for pH values between 6 and 8 (Figure 78).
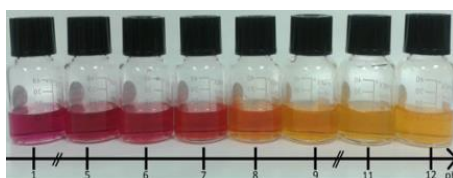
Figure 76: *Evolution of NR color with pH in different buffer solutions.*
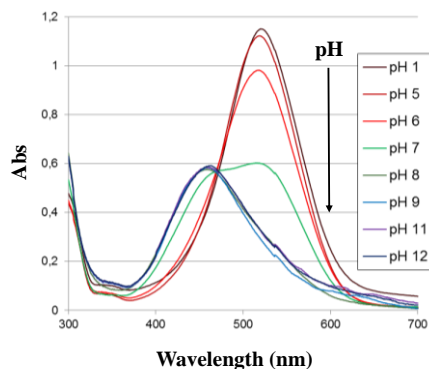
Figure 77: *UV-Visible absorption spectra of NR in solution as a function of pH.*

EURAD (Deliverable n° 17.7) - Synthesis report on Innovative and Enhanced Equipment for Repository Monitoring
Dissemination level: PUBLIC
Date of issue of this report: 04/06/2024

Page
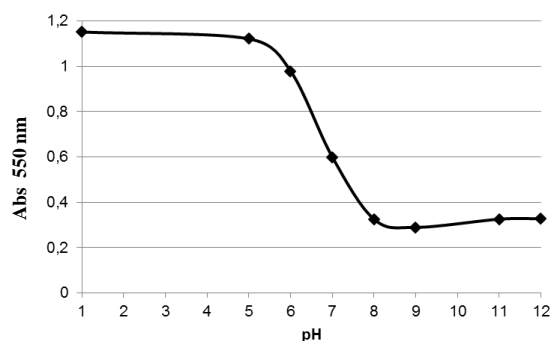
Figure 78: *NR absorbance versus pH curve at 550 nm.*

3.4.7.2 Electro-induced grafting of the diazonium salt of RN onto a metallized glass plate

The diazonium salt of RN is grafted by cathodic reduction onto a metallized glass plate. The electro-grafting reaction is carried out by cyclic voltammetry and sequencing. After each electrografting cycle, a plate washing protocol is applied. The substrate is periodically rinsed with water, then ultrasonically treated in a mixture of water (5 mL) and ethanol (5 mL). This washing protocol between each voltammetric cycle make the film thicker while progressively eliminating the physisorbed part of the indicator. This avoids building up successive layers on the physisorbed parts of the coating under construction. The voltammograms recorded during electro-reduction of NR are shown in Figure 79. The NR reduction peak is observed at around - 0.2 V/Ag and gradually disappears. This electro-induced grafting of NR does not withstand degassing under argon due to bubbles formation. Electro-induced grafting of NR is therefore carried out without argon bubbling.
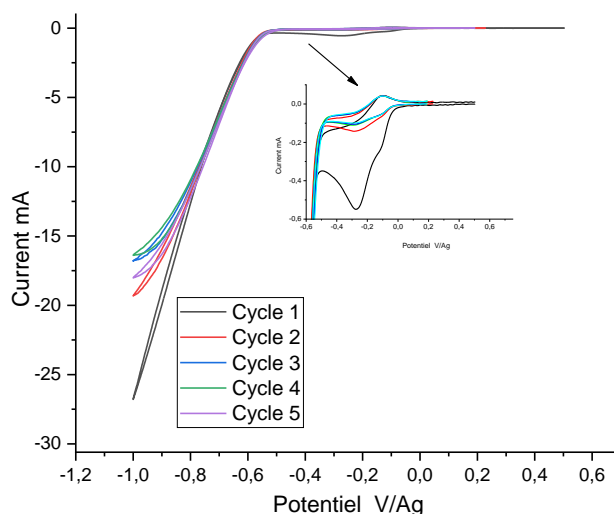
Figure 79: *Voltammograms recorded during electro-reduction of NR on a metallized glass plate, 5 cycles, in HCl 0.1, RN 10 mM and NaNO$_2$ 10 mM.*

3.4.7.3 Optimizing the initial concentration of the diazonium salt of NR on the metallized glass plate

The sensitivity of the pH probe depends significantly on the total amount of indicator grafted onto the metallized substrate. It is therefore important to determine the optimum concentration for effective covalent grafting to obtain a thick film. Five different metallized plates were functionalized at different concentrations of NR: 2.5; 5; 7; 10 and 14 mM. These metallized and grafted glass plates were characterized by UV-Visible, IR-ATR and profilometry.

Figure 80 shows the UV-Visible characterizations carried out in buffer solutions from pH 1 to pH 10. In this figure, the optical response of the NR measured is related to the total quantity immobilized on the metallized glass plate. Thus, the absorbance of grafted NR increases as a function of initial concentration up to a limiting value of 10 mM. The value of 10 mM can therefore be considered as the

EURAD (Deliverable n° 17.7) - Synthesis report on Innovative and Enhanced Equipment for Repository Monitoring
Dissemination level: PUBLIC
Date of issue of this report: 04/06/2024

Page

optimum concentration. However, at higher concentrations, such as 14 mM, too many radicals are generated in the reaction medium. The radical polymerization reaction in solution takes place rather than on the surface. The radicals which are formed dimerize in solution. The kinetics of this reaction varies quadratically with the concentration of these radicals. As a result, as the initial NR concentration increases, reactions in solution are favored, increasing the physisorbed portion of the coating. This results in the loss of radicals available for grafting. Dimerization products physisorbed on the surface are removed during the washing protocol. This may explain the lower quantity of 14 mM NR grafted on the metallized glass plate.

After grafting, the pH range of NR is between pH 4 and pH 6, whereas in solution it is between pH 6 and pH 8. Its pH range is therefore shifted towards acidic pH. This is due to the stacking of NR units to form pyrazines on the metallized surface, and the loss of the amine function during electrochemical reduction. Interestingly, the pH range of grafted NR remains constant, whatever its initial concentration in solution.

Figure 81 shows UV-Visible absorption spectra of NR grafted on a glass plate metallized at 10 mM. This figure presents two absorption bands (acid and basic form) similar as the one observed in solution. The wavelength of the isobestic point moves from 470 in solution to 500 nm for the grafted molecule. The grafting of the NR has therefore led to a modification of its optical characteristics (pKa, pH range, isobestic point).

The thickness of metallized NR-grafted glass plates is determined by profilometry. For concentrations of 2.5, 5, 7, 10 and 14 mM, the estimated thicknesses are of the order of 150, 200, 250, 300 and 250 nm respectively. According to this study, the metallized glass plate grafted with 10 mM is the thickest.

The reproducibility of NR grafting onto metallized glass plates is studied. Three different metallized glass plates from the same batch are grafted with 10 mM NR (Figure 82). The results obtained show that the spectral response of these three grafted glass plates is reproducible.

A cycle of deprotonation and protonation is performed to check for possible hysteresis at 10 mM (Figure 83). The results obtained on the forward and return paths are almost identical. We can therefore conclude that the spectral response of the grafted NR is reversible.

The metallized glass plate grafted with 10 mM NR is characterized by IR-ATR. On this grafted glass plate, 10 different locations are analyzed (Figure 84). The IR-ATR spectra obtained at these different points are almost identical. We can therefore conclude that the grafted NR organic layer is homogeneous.
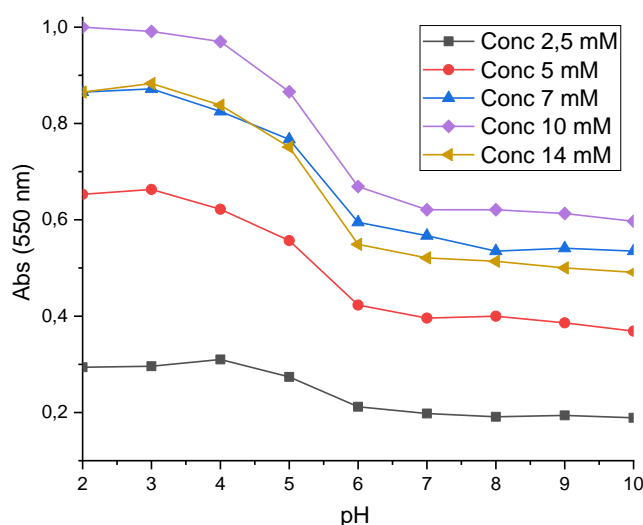
***Figure* 80**: *UV-Visible characterization of five different RN-grafted metallized glass plates as a function of pH.*

EURAD (Deliverable n° 17.7) - Synthesis report on Innovative and Enhanced Equipment for Repository Monitoring
Dissemination level: PUBLIC
Date of issue of this report: 04/06/2024

Page
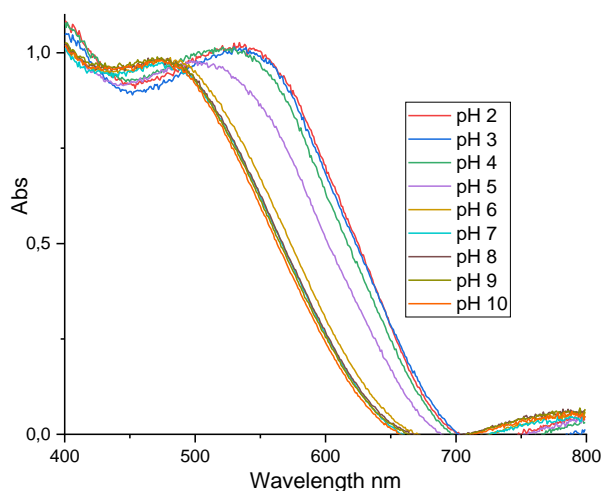
Figure* 81:** *Absorption spectra of the NR film grafted onto the metallized plate at 10 mM and in buffer solutions of different pH.*
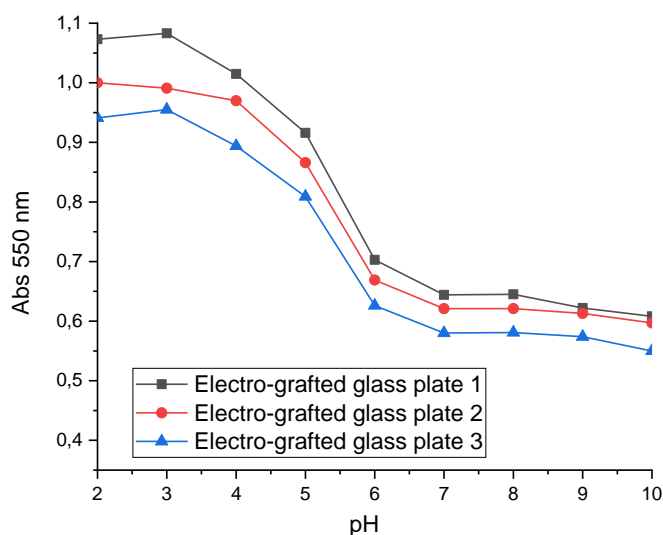
Figure* 82:** *Reproducibility on three different metallized glass plates grafted with NR.*
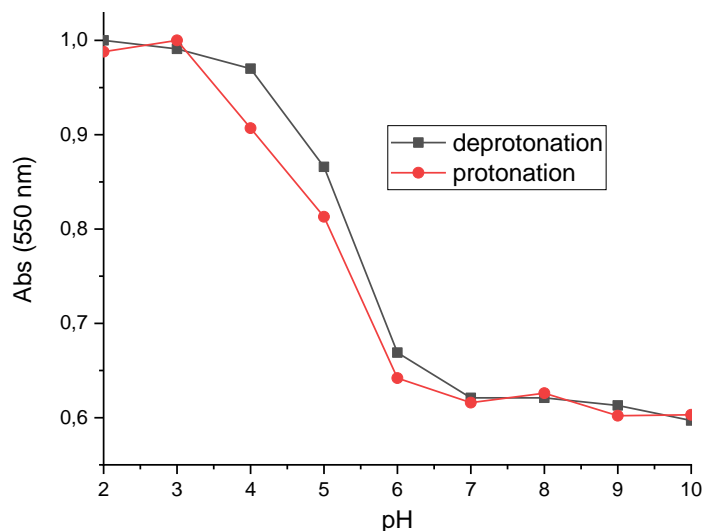
Figure* 83:** *Deprotonation and protonation cycles performed on a metallized glass plate grafted with 10 mM NR.*

EURAD (Deliverable n° 17.7) - Synthesis report on Innovative and Enhanced Equipment for Repository Monitoring
Dissemination level: PUBLIC
Date of issue of this report: 04/06/2024

Page
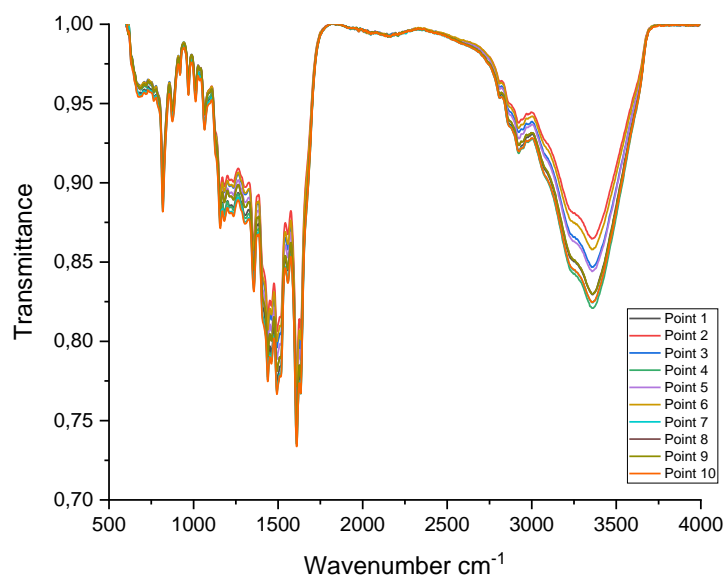
***Figure* 84**: *IR-ATR characterization of the metallized glass plate grafted with 10 mM NR.*

3.4.7.4 Transposition of nr grafting on the metallized optical fiber

The grafting of NR previously studied and optimized on the glass plates was transposed to the end of an optical fiber (diameter 940 µm) after metallization (Figure 85). After grafting, the fiber end exhibits a red color visible to the naked eye. This confirms that grafting has indeed taken place. This NR grafted optical fiber was characterized in a simple experimental setup shown in **Figure 75**(b).

Figure 86 shows the absorption spectra of NR grafted onto the optical fiber as a function of pH. This figure shows two absorption bands at 500 and 550 nm but difficult to detect. The absorption spectra of NR on the optical fiber obtained have a lower sensitivity compared to those obtained on the metallized glass plates. The electro-grafted organic film on the optical fiber is therefore thinner.

The absorption spectra data processing at 550 nm makes it possible to plot the absorption variation curve as a function of pH (Figure 87). The shape of the experimental curve can be modeled with a line of equation $y = (-0.1) x + 1.27$ where x is the pH value and y the optical density measured in the sample. This line has a regression coefficient (0.98) and a slope -0.1 per pH unit. It is important to note that NR grafted on the metallized optical fiber has a pH range between 4 and 8 while that obtained on the metallized and grafted glass plate varies between 4 and 6. The optical characteristics of NR grafted may therefore depend on the geometry of the electrochemical assembly used.

It is also interesting to explore the electro-induced covalent grafting of the same molecule on the 316L stainless steel mirror.

***Figure* 85**: *Grafting of NR on the end of a two-way metallized optical fiber.*

EURAD (Deliverable n° 17.7) - Synthesis report on Innovative and Enhanced Equipment for Repository Monitoring
Dissemination level: PUBLIC
Date of issue of this report: 04/06/2024

Page
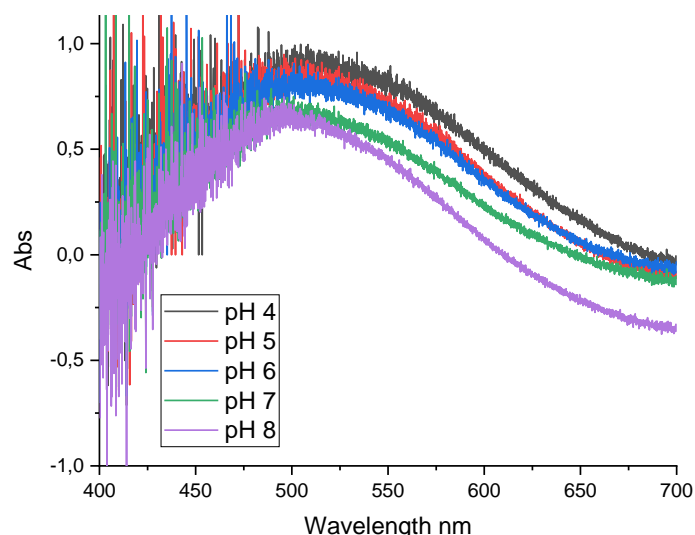
Figure 86: *UV-Visible absorption spectra of NR grafted on the optical fiber in solutions of different pH values.*
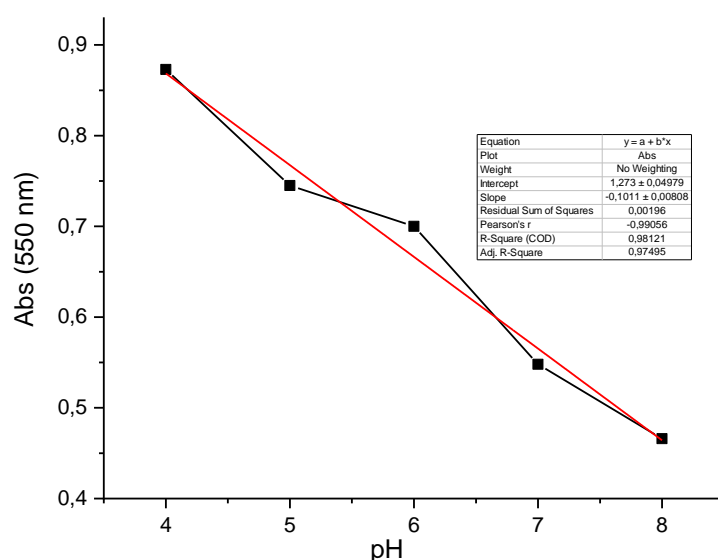
Figure 87: *Absorbance versus pH curves for NR grafted on the optical fiber.*

3.4.7.5 Electro-induced grafting of NR on a 316 L stainless steel mirror

We propose to explore the way of grafting NR on a 316 L stainless steel mirror (Figure 75 (a)). It was chosen because of its corrosion resistance in the presence of a strong acid medium (condition of grafting of NR). The optical design of the stainless-steel mirror requires an optimization of its geometry (diameter, radius of curvature).

Optical calculations are performed using the Zemax/optic studio software. Thanks to this software, different configurations can be studied by varying the diameter of the mirror and its radius of curvature in order to compare the results obtained and to choose the best compromise. This software, based on the tracing of light rays, allows to visualize the light spot after reflection on the mirror. When the mirror geometry is optimal, the light spot after reflection is as homogeneous as possible.

The work carried out shows that, the coupling efficiency is better with mirrors with high radius of curvature at constant diameter. This coupling efficiency corresponds to the ratio between the number of light rays at the input of receiving fiber and the number of rays at the output of transmitting fiber. Figure 88 shows the optical simulation performed for a mirror with a radius of curvature 20 mm and diameter 10 mm. With this mirror R 20 and D 10, a coupling efficiency of 83.2% is obtained and the spot is relatively homogeneous. Based on these simulations, we chose to order stainless steel mirrors with a

EURAD (Deliverable n° 17.7) - Synthesis report on Innovative and Enhanced Equipment for Repository Monitoring
Dissemination level: PUBLIC
Date of issue of this report: 04**/06/2024**

Page

radius of curvature of 24 mm and a diameter of 12.7 mm that have a coupling efficiency of more than 83.2%. These mirrors were manufactured by OPA OPTICAD.

In order to maintain the mirror in front of the fiber in the experimental setup, the design of a mirror holder was carried out. The mirror holder was designed using SolidWorks software and manufactured by Faulcon, Saclay, a company specializing in precision mechanics. The connections for the optical fibers are of SMA type and the mirror is mechanically immobilized in position using a 6-sided screw.

The grafting of NR is carried out by cyclic voltammetry and by sequencing on the 316L stainless steel plate. At the end of each cycle, the stainless-steel plate is removed and then rinsed with water and ultrasound for one minute in a mixture of water (5 mL) and ethanol (5 mL). The grafting cycles are recorded by sequencing on the stainless-steel plate at 50 mV/s.

The analysis of the recorded voltammograms shows that the electro-reduction of NR occurred around – 0.1V/Ag (Figure 89). The evolution of the observed current leads to the formation of a multilayer and thus to the passivation of the stainless-steel surface. The observed decrease in current is related to the formation of an insulating film that passivates the surface of stainless steel.
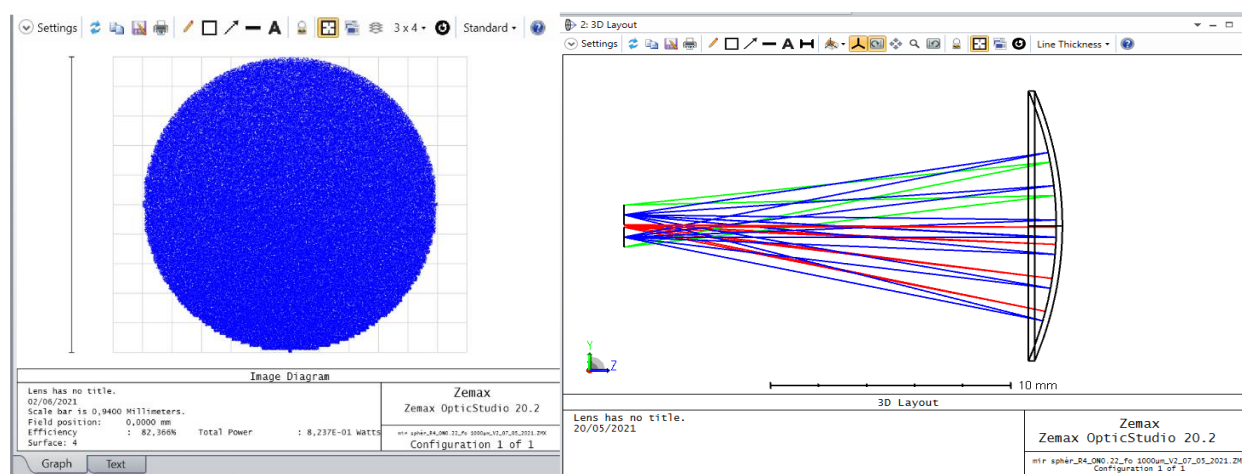
Figure 88: *Spotlight and ray tracing for simulation with a R 20 D10 mirror, using Zemax/optic studio software.*
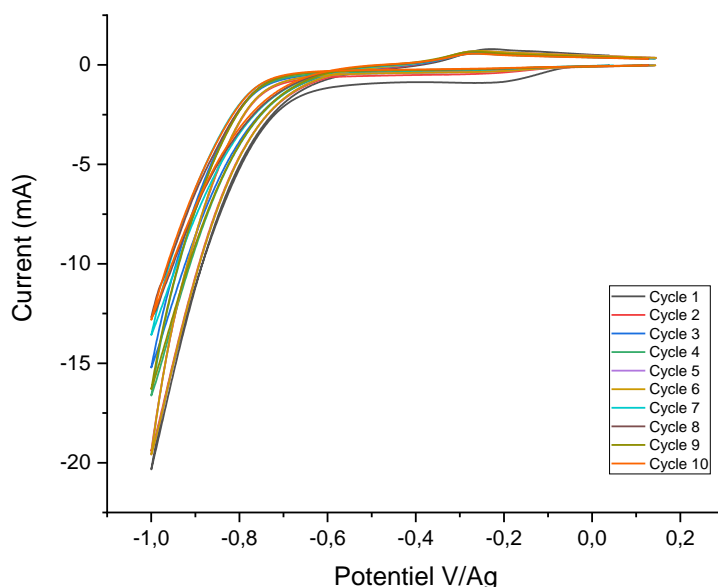
Figure 89: *Voltammograms recorded during electro-grafting of NR 5 mM and 5mM NaNO₂.*

EURAD (Deliverable n° 17.7) - Synthesis report on Innovative and Enhanced Equipment for Repository Monitoring
Dissemination level: PUBLIC
Date of issue of this report: 04/06/2024

Page

3.4.7.6 Optimizing the initial concentration of the diazonium salt of NR on 316L stainless steel plate

Obtaining a thick organic structure grafted on the surface of a substrate requires the optimization of electrochemical conditions, in particular the initial concentration of diazonium salt. Different, concentrations of 5, 10 and 14 mM are studied in 0.1M HCl aqueous medium on the 316L stainless steel substrate.

These different 316L stainless steel plates grafted to NR and with variable concentrations are characterized in XPS (Figure 90). The intensity of the C1s, N1s, O1s and Cr2p peaks is predominant in the non-grafted samples, indicating the presence of these elements in the stainless steel metal substrate [52]. On the three samples, the intensity of the C1s and N1s peaks increases after the functionalization of the surface of the stainless-steel metal substrate. This indicates the presence of organic film on the surface of the stainless-steel metal substrate.

On the first two samples grafted with NR (5 and 10 mM), the signal of the metal substrate in particular that of Cr is visible, which is not the case at 14 mM. The XPS allows the analysis of only about the first 10 nanometers of the sample, this characterization confirms the presence of a thick organic layer of NR on the surface of stainless steel with a thickness greater than 10 nm for this concentration of 14 mM. The film grafted with NR at 14 mM therefore appears thicker. At this concentration, the thickness estimated by profilometry is close to 100 nm.

The covalent grafting of NR 14 mM is therefore transposed on the 316L stainless steel mirror. The fluorine signal observed on the XPS spectra appears to be related to sample contamination.
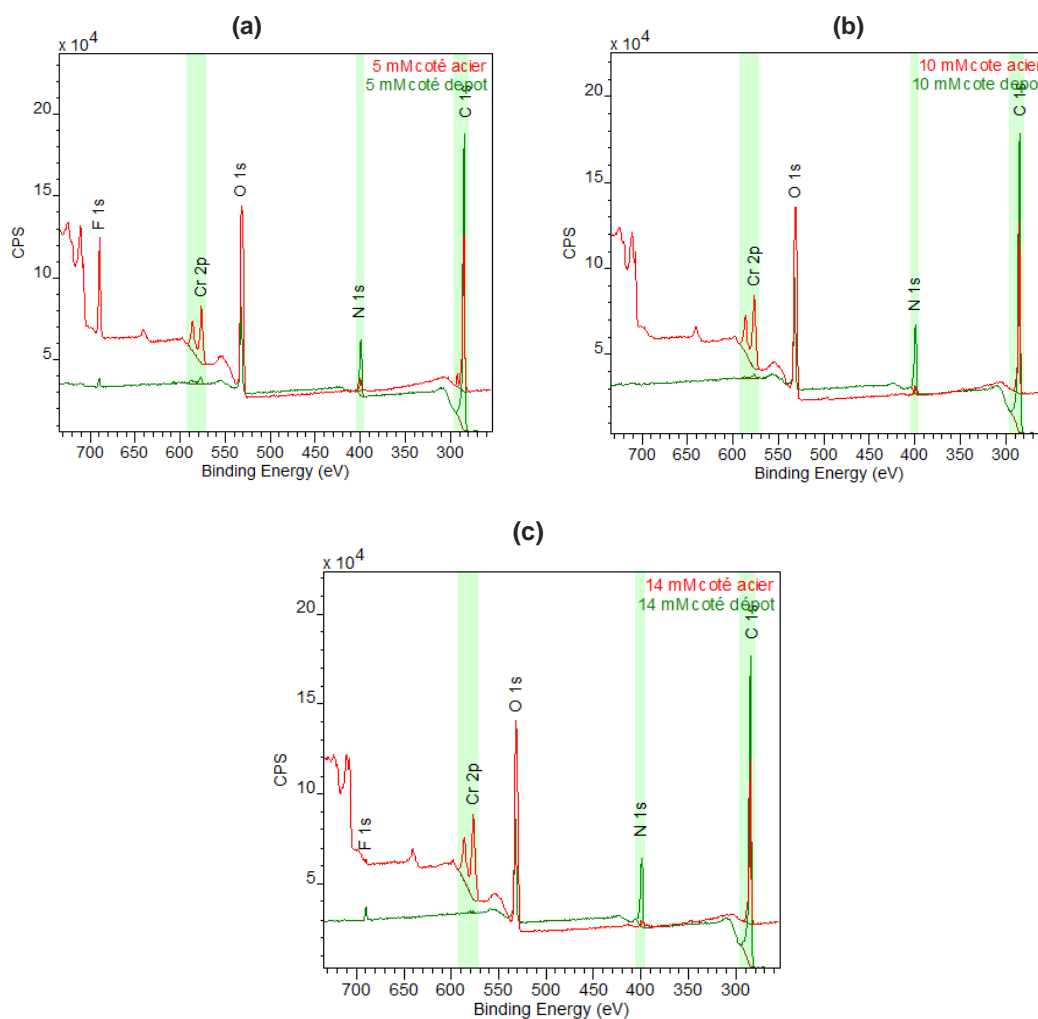
Figure 90: _Overall surface analysis obtained in XPS on stainless steel plates grafted with NR (a) = 5 mM, (b) = 10 mM and (c) = 14 mM._

EURAD (Deliverable n° 17.7) - Synthesis report on Innovative and Enhanced Equipment for Repository Monitoring
Dissemination level: PUBLIC
Date of issue of this report: 04/06/2024

Page

3.4.7.7 Transposition of NR grafting on 316 L stainless steel mirror

The electro-induced grafting procedure of NR studied at 14 mM on 316L stainless steel plates was transposed on the 316L stainless steel mirror. Figure 91 shows two stainless steel mirrors, one grafted and one not. At the end of the grafting, a red color is clearly visible on the mirror. This indicates that the grafting has taken place. We also notice that the organic layer of grafted NR is homogeneous on the mirror.

A two-channel optical configuration (1 reference channel and 1 sample channel) is explored to evaluate the performance of the organic layer of the grafted NR. This configuration uses a single light source (HL-2000-FHSA), a 2x2 FOS TTL multiplexer, a spectrometer (Flame 3648 pixels model), 600 µm diameter optical fibers, two 316 L stainless steel mirrors (one not grafted and a NR grafted) and a computer with SpectraSuite acquisition software.

The UV-Visible absorption spectra recorded in different pH buffer solutions are presented (Figure 92). These spectra have two absorption bands (acid form and basic form) not easy to detect located at 450 and 550 nm respectively. The spectral response of NR obtained is selective but not sufficiently sensitive in the different buffer solutions of different pH. We believe these results from the fact that the organic layer of the grafted NR is not thick enough to deliver a valuable spectral response. These spectra were analyzed at 550 nm in order to plot the absorption variation curve as a function of pH (Figure 93). This curve is modelized with a trend line of equation y = (-0.13) x + 1.7. The regression coefficient of this line is 0.97 with a slope of (-0.13) per pH unit.

Figure 91*: Two stainless steel mirrors, one grafted and the other not grafted.*
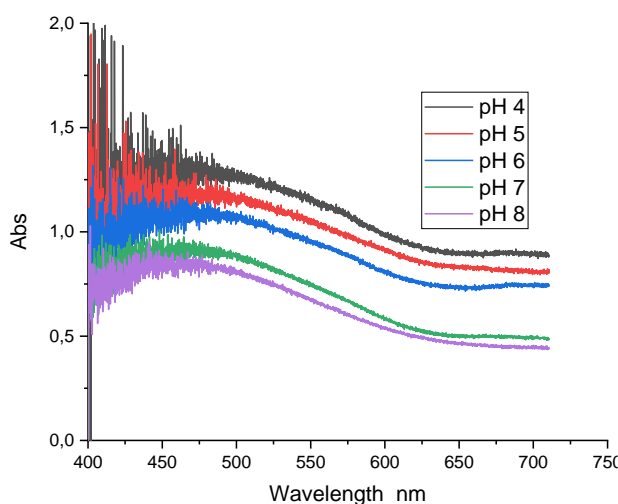
Figure 92*: UV-Visible spectra of NR grafted on a 316L stainless steel mirror in buffer solutions of different pH, optical configuration with two measurement channels and a light source.*

EURAD (Deliverable n° 17.7) - Synthesis report on Innovative and Enhanced Equipment for Repository Monitoring
Dissemination level: PUBLIC
Date of issue of this report: 04/06/2024

Page

Equation	y = a + b*x
Plot	Abs
Weight	No Weighting
Intercept	1,6804 ± 0,07246
Slope	-0,1276 ± 0,01175
Residual Sum of Squares	0,00415
Pearson's r	-0,98751
R-Square (COD)	0,97517
Adj. R-Square	0,9669
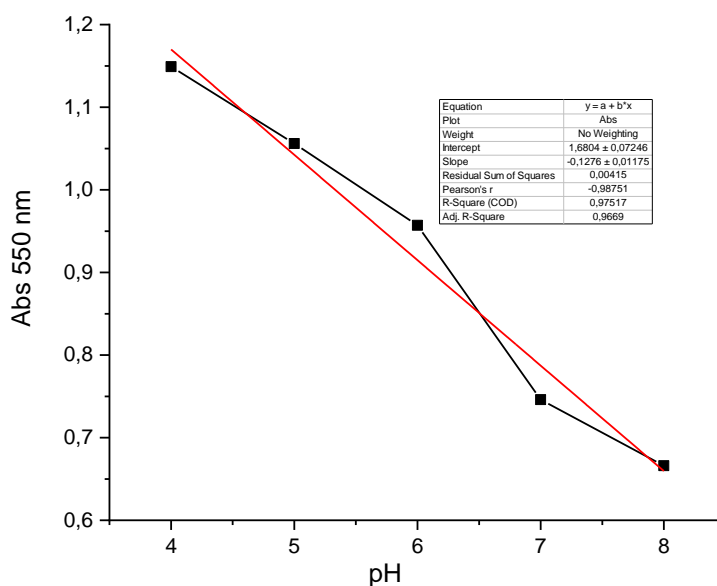
Figure 93: *Absorption variations at 550 nm versus pH of NR grafted on the 316L stainless steel mirror.*

3.4.8   Discussion about the results obtained.

The experimental results obtained in Bure [106] are preliminary results resulting from only three experiments. Nevertheless, the results are promising. Many factors of progress have been identified which will allow. The design of a specially dedicated cabinet for future experiments. The experimental set up using the grafted mirror is easier if an efficient grafting on the mirror can be obtained.

3.4.9   References

[103].   J. Daoudi, S. Betelu, T. Tzedakis, J. Bertrand, et I. Ignatiadis, « A multi-parametric device with innovative solid electrodes for long-term monitoring of pH, redox-potential and conductivity in a nuclear waste repository », Sensors, vol. 17, no 6, p. 1372, 2017.

[104].   G. J. Mohr et O. S. Wolfbeis, « Optical sensors for a wide pH range based on azo dyes immobilized on a novel support », *Anal. Chim. Acta*, vol. 292, no 1, p. 41‑48, juin 1994, doi:10.1016/0003-2670(94)00096-4.

[105].   M. Fages, « Etude du greffage covalent de colorants pour la conception d'une optode pour la mesure du pH », Thèse de doctorat, École polytechnique, Palaiseau, Essonne ; 1795-...., France, 2015.

[106].   Rapport d'installation et de mesures de l'intervention au Laboratoire Souterrain de l'Andra le 11 et 12 juillet 2023 dans le cadre de la thèse de Germaine Olorounto, Référence : ANDRA, DISTEC/DCC/CED/23-0115.

[107].   "Etude et développement d'une sonde optique de mesure du pH pour le projet Cigéo", G. Olorounto, pHD thesis Sorbonne Université, 12/12/2023.

EURAD (Deliverable n° 17.7) - Synthesis report on Innovative and Enhanced Equipment for Repository Monitoring
Dissemination level: PUBLIC
Date of issue of this report: 04**/06/2024**

Page

4. Interactions between Sensors and the Multi-Barrier System

Sub-Task 3.3 of the MODATS WP provides a contribution to addressing that requirement, through the development of a monitoring features, events and processes (FEP) catalogue, referred to herein as a Monitoring FEPs catalogue. The FEP catalogue identifies and describes ways in which monitoring equipment used during the operational phase could impact the post-closure performance of a repository system.

A dedicated report has been elaborated for Deliverable 17.7b: Monitoring FEPs: Potential Impacts of Monitoring Equipment on Post-Closure Safety.

EURAD (Deliverable n° 17.7) - Synthesis report on Innovative and Enhanced Equipment for Repository Monitoring
Dissemination level: PUBLIC
Date of issue of this report: 04/06/2024

Page

5. *Future Needs*

5.1 Objectives

The objectives of this chapter are to identify the monitoring technology issues that need to be addressed before confident implementation of repository monitoring programmes commence, and to define the steps that are required to address these issues. Confidence is a critical consideration because it is recognised that some desired technology performances cannot be proved before their deployment in a repository. This is particularly true for long lifetimes desired for some technologies.

This work aims to provide a monitoring technology RD&D roadmap that can be used to help plan research, targeted enhancements, and/or the development of novel technologies, tailored to the specific demands of the repository. The RD&D roadmap considers what is important for repository monitoring in support of the long-term safety case. By uncovering the gaps between existing monitoring sensor/system capabilities and the repository's requirements, this methodology aims to pave the way for the implementation of more robust, reliable, and tailored monitoring solutions, ensuring the optimal functioning and safety of the repository in the long term.

The main outputs are a list of identified needs and a generic technology development roadmap that defines the required steps to ensure that the required technologies are available for the implementation of repository monitoring when needed[108]. The output is intended to be generic. Therefore, some issues identified may not be an issue for confident deployment of a technology in an environment that is more narrowly constrained than the conditions considered here.

The aim is also to link the output to the Modern2020 Screening Methodology [109]. This is because repository monitoring should be designed to support the safety case.

5.1 Document use.

This document presents a generic RD&D roadmap that is intended to be used as a guide. The generic technology development roadmap is intended to be applied to help understand whether a technology can confidently be implemented in a repository and where the focus may be applied if it cannot be confidently implemented in a repository. The generic roadmap has been applied to some technology examples during its development to ensure it is valuable; the examples are presented in this document demonstrate its value.

The gaps identified between existing monitoring sensor/system capabilities and the repository's requirements are generic. Repository requirements were determined by combining different WMO's anticipated repository requirements. A specific repository is likely to have constrained repository requirements further and so may have fewer technology gaps. However, a specific repository may also have conditions outside of the ranges that were anticipated by the WMOs at the time they were surveyed, e.g., higher salinity groundwater. Therefore, a specific repository may also have gaps that have not been identified here. The methodology may be repeated using different repository conditions and different monitoring programmes to determine a specific set of gaps.

5.2 Methodology

The general methodology was to cross-compare technology performance information with monitoring requirements. Technology performance information was collated from ongoing NWS monitoring strategy research, the survey of URL experiments, and the MODATS Reference Experiments. The repository monitoring requirements were developed in the MoDeRn and Modern2020 projects.

The technology capabilities and limitations are mostly collected from a review led by GSL [112] . We refer to this report as the "Technologies and Methodologies report". The technologies considered in this work were identified in the Technologies and Methodologies report. These were well known technologies that were taken through the Screening Methodology in the NWS Monitoring Strategy report. The expected conditions in the repository are collected from the MoDeRn project Technical Requirements report (D2.1.1)[113].

EURAD (Deliverable n° 17.7) - Synthesis report on Innovative and Enhanced Equipment for Repository Monitoring
Dissemination level: PUBLIC
Date of issue of this report: 04/06/2024

Page

Hereafter, this section details the cross-comparison approach. The section summarizes the content and background of the information used, explains the classification of identified needs, and presents the approach used to elaborate a generic technology development roadmap.

5.3 Matrix analysis for the identification of needs

A square matrix is used to cross-compare technology capabilities and limitations with expected conditions in a repository. For example, in the first diagonal cell, the temperature range that a technology can perform in is compared with the expected temperature in a repository location. The matrix is then repeated for argillaceous and crystalline rocks and different repository locations (described in [113]). For a given technology, this matrix serves as a tool to highlight the RD&D needs of the technology to be implemented with confidence in its performance in the repository at specific locations and in specific rock types [113]

Two types of information are tabulated along the axes of the matrix: physical parameters and data quality parameters. The physical parameters include temperature, mechanical pressure, saturation, salinity, and radiation. Along the x-axis, these physical parameters relate to the capabilities of the technology, i.e., the maximum values that can be sustained by the technology before failure. Along the y-axis, these physical parameters relate to the maximum values of the expected range of parameters in the repository, at different locations, for argillaceous and crystalline rocks. The different locations are derived from the Technical Requirements report and include 'Waste package and buffer', 'Near-field rock', 'Backfill', and 'Seals' (see Section 4).

The data quality parameters include the range of values that can be covered by the considered technology, the assessed lifetime of the technology, its accuracy, and its potential measurement drift. Along the x-axis, these quality parameters relate to the technology capabilities and limitations whereas along the y-axis, they relate to the data quality objectives (DQO) defined by the user (presumably a WMO).

Each of the input X and Y parameters feed into a diagonal cell which is conditionally colour coded using the following rules:

- Green when technology performance > technology requirements.
- Red when technology performance ≤ technology requirements.
- Yellow when the necessary information is insufficient.

Note that for the lower range of measurement capability, accuracy, and drift, the above rules are reversed since in these cases the technology performance is required to be less (better) than the technology requirements for the technology to be suitable for deployment. In all cases, green cells indicate that the technology can withstand the repository conditions and/or fulfil the DQOs.

The needs are identified by red and yellow cells which indicate unsuccessful matches of the available information. Red cells highlight either the failure of the technology to be able to withstand the expected conditions in a repository or in fulfilling the DQOs. Yellow cells highlight a lack of information required to confidently implement the technology.

Only the template is presented here and not the completed matrices because the 36 matrices are too large in total to include here.

Using the developed matrix approach, at first order, the various identified needs can be:

- To improve the robustness of the technology for withstanding repository conditions.
- To improve the performance of the technology, such as its accuracy, to fulfil the DQOs.
- To complete knowledge on the technology capabilities and limitations and/or on the expected conditions at the repository.
- To develop a non-existing technology able to sustain the expected physical conditions and fulfil the DQOs.

Table 10: Template of the matrix developed for the identification of the future needs in repository monitoring technologies. The blue blank cells would contain parameter's values. The crossing white blank cells along the diagonal would be filled in green, red or yellow according to the colour code defined in the text. The x-axis

![eurad logo] European Joint Programme on Radioactive Waste Management

EURAD (Deliverable n° 17.7) - Synthesis report on Innovative and Enhanced Equipment for Repository Monitoring
Dissemination level: PUBLIC
Date of issue of this report: 04/06/2024

Page

abbreviations are T: Temperature; P: Mechanical pressure; Sat (HR): Saturation (Relative Humidity); Sal: Salinity; Rad: Radiation; LR: Lower range of the parameter; UR: Upper range of the parameter; LT: Lifetime; Acc: Accuracy; Dr: Drift. Note that this template shows only ¼ of the whole matrix as it must be applied to the four selected locations in the repository.

EURAD (Deliverable n° 17.7) - Synthesis report on Innovative and Enhanced Equipment for Repository Monitoring
Dissemination level: PUBLIC
Date of issue of this report: 04/06/2024

Page

PARAMETER (e.g., pore pressure, temperature)				TECHNOLOGY (optical fibers, piezometer, thermistor)									
				Max Operating Conditions and Specificities									
				T (°C)	P (MPa)	Sat (RH) (%)	Sal (g/L)	Rad (Gy/hr)	LR	UR	LT (yr)	Acc	Dr
LOCATION (e.g., waste package and buffer, Near-field rock, ...)	Expected Conditions and Requirements	Temperature(°C)	Argillaceous rock										
			Crystalline rock										
		Mechanical Pressure (MPa)	Argillaceous rock										
			Crystalline rock										
		Saturation (RH) (%)	Argillaceous rock										
			Crystalline rock										
		Salinity (g/L)	Argillaceous rock										
			Crystalline rock										
		Radiation (Gy/hr)	Argillaceous rock										
			Crystalline rock										
		Lower Range	Argillaceous rock										
			Crystalline rock										
		Upper Range	Argillaceous rock										
			Crystalline rock										
		Lifetime (yr)	Argillaceous rock										
			Crystalline rock										
		Accuracy	Argillaceous rock										
			Crystalline rock										
		Drift	Argillaceous rock										
			Crystalline rock										

European Joint Programme on Radioactive Waste Management

5.3.1 Identification of monitoring technology capabilities

The Technologies and Methodologies report[112] is a review by GSL. It focuses on the monitoring technologies that might be used in support of the Environmental Safety Case (ESC), which is the UK equivalent of the long-term safety case, but also includes assessment of the environmental safety during the operational period. The workflow is based on the Modern2020 screening methodology, which represents the international good practice in the selection of monitoring parameters for inclusion in a monitoring programme [114].

In the monitoring strategy report [114], the Modern2020 screening Methodology was used to define processes and parameters that could be monitored in support of the ESC. It integrates the possible technologies that could be used to conduct the monitoring of the screened processes and parameters to define PP&T combinations. *Table 11* summarizes the PP&T combinations reviewed in the Technologies and Methodologies report.

Table 11: Summary of the monitoring technologies reviewed in the Technologies and Methodologies report[112].

Process	Parameter	Technology and/or Sensor
Heat transfer	Temperature	Resistance temperature detectors (RTDs)
		Thermistors
		Thermocouples
		Optical fiber sensors
Groundwater flow	Water table level, hydraulic head and/or pore pressure	Vibrating wire piezometers
		Strain gauge piezometers
		Linear variable differential transformer (LVDT) piezometers
		Capacitive piezometers
Groundwater flow and saturation/ desaturation	Volumetric flow rate	Flow loggers
Saturation/ desaturation	Relative humidity	Capacitive hygrometers
	Water matric potential	Tensiometers
		Thermocouple psychrometers
	Water content	Time domain reflectometry (TDR; dielectric probes)
		Electrical resistivity imaging (ERI)

EURAD (Deliverable n° 17.7) - Synthesis report on Innovative and Enhanced Equipment for Repository Monitoring
Dissemination level: PUBLIC
Date of issue of this report: **04/06/2024**

Page

Process	Parameter	Technology and/or Sensor
Deformation (including displacement and rock creep)	Strain	Vibrating wire extensometers
		Optical fiber sensors
	Tilt	Inclinometers
	Excavation profile dimensions and relative position	Photogrammetry
		Terrestrial light detection and ranging (LiDAR)
Fracture initiation and propagation	Fracture aperture and length	Crack meters
	Ultrasonic wave transit time	Embedded ultrasonic sensors
	Ground acceleration	Acoustic emission monitoring
		Micro-seismic monitoring
Swelling, loading and compaction	Mechanical pressure	Vibrating wire pressure cells
		Strain gauge pressure cells
		Capacitive pressure cells
		Piezoelectric pressure cells
		Optical pressure cells
	Density	Cross-hole seismic tomography
	Stress	Stress meters
Reduction and oxidation	Redox potential	Electrodes
	Oxygen concentration	Electrochemical sensors
		Optical sensors
Solid-liquid interactions	Chemical composition of groundwater	Groundwater sampling and inductively coupled plasma mass spectrometry (ICP-MS)

EURAD (Deliverable n° 17.7) - Synthesis report on Innovative and Enhanced Equipment for Repository Monitoring
Dissemination level: PUBLIC
Date of issue of this report: **04/06/2024**

Page

Process	Parameter	Technology and/or Sensor
Gas generation and migration	Gas concentrations (including radioactive and non-radioactive gases)	Gas sampling lines and gas chromatography mass spectrometry (GC-MS)
	Radon concentration	Electronic radon detectors
	Hydrogen concentration	Thermal conductivity sensors
	Waste package colour and shape	Remote-controlled cameras
	Carbon oxide concentrations	Non-dispersive infrared (NDIR) spectroscopy
	Gas pressure	Strain gauges

The Technologies and Methodologies report reviews the capabilities and limitations of monitoring technologies to monitor thermal, hydraulic, mechanical, chemical, and gas processes. By integrating theoretical knowledge with practical experiences, the report assesses the current capabilities of monitoring technologies and identifies gaps that exist. It also offers recommendations based on the findings and provides detailed information on the technologies, experiment data, and sensor failures in the appendices.

Table 12 presents potential operational technologies and their capabilities, which are collated in the Technologies and Methodologies report and are used in the present analysis. This table summarizes maximum operating temperatures and pressures for commercially available underground monitoring technologies, which are quoted from technology data specification sheets.

Table 12: Summary of the maximum operating temperatures and pressures of underground monitoring technologies.

Parameters	Technologies	Maximum Operating Temperature	Maximum Operating Pressure
Temperature	RTDs, thermocouples and optical fiber sensors	2300 °C	Limited information available, but 3.5 MPa stated with respect Geokon thermistors [115] And 6 MPa From the FEBBEX experiment [116][117]

![eurad logo] European Joint Programme on Radioactive Waste Management

EURAD (Deliverable n° 17.7) - Synthesis report on Innovative and Enhanced Equipment for Repository Monitoring
Dissemination level: PUBLIC
Date of issue of this report: **04/06/2024**

Page

Parameters	Technologies	Maximum Operating Temperature	Maximum Operating Pressure
Pore pressure	Piezometers (including pressure transducers)	250 °C	150 MPa
Volumetric flow rate	Flow loggers	70 to 80 °C	20 MPa
Relative humidity	Capacitive hygrometers	200 °C	10 MPa
Water matric potential	Tensiometers and thermocouple psychrometers	50 °C	Not specified
Water content	TDR and ERI	70 °C	Not specified
Displacement (relating to deformation)	Extensometers	100 °C	Not specified
Strain	Optical fiber sensors	2100 °C	100 MPa [118]
Tilt	Tiltmeters	85 °C	4 MPa
Excavation profile dimensions and relative position	TLS and photogrammetry	Not applicable	Not applicable
Fracture aperture and length	Crack meters	80 °C	2 MPa
Ultrasonic wave transit time (for the purposes of fracture mapping)	Ultrasonic pulse velocity	50 °C	Not specified
Ground acceleration (for the purposes of fracture mapping)	Acoustic emission and micro-seismic monitoring	70 °C	6.9 MPa
Mechanical Pressure	Pressure cells (including pressure transducers)	80 to 125 °C	0 to 100 MPa
Density (from the full-waveform inversion of seismic datasets)	Cross-hole seismic surveys	70 °C	Not specified
Stress	Stress meters	200 °C	0 to 70 MPa
Redox potential	Electrodes	80 °C	1 MPa

![EURAD logo] European Joint Programme on Radioactive Waste Management

EURAD (Deliverable n° 17.7) - Synthesis report on Innovative and Enhanced Equipment for Repository Monitoring
Dissemination level: PUBLIC
Date of issue of this report: **04/06/2024**

Page

Parameters	Technologies	Maximum Operating Temperature	Maximum Operating Pressure
Atmospheric oxygen concentration	Electrochemical sensors	50 °C	Not specified
Dissolved oxygen concentration	Optical sensors	85 °C	1.2 MPa
Chemical composition of groundwater	Groundwater sampling and ICP-MS	Not applicable - laboratory based analysis	Not applicable - laboratory based analysis
Non-specific gas concentration	Gas sampling lines and GC-MS	Not applicable - laboratory based analysis	Not applicable - laboratory based analysis
Radon concentration	Electronic radon detectors	45 °C	Not specified
Atmospheric hydrogen concentration	Thermal conductivity sensors	50 °C	0.11 MPa
Hydrogen concentration (in EBS materials)	Miniaturised thermal conductivity sensors	60 °C	0.11 MPa
Concentration of carbon oxide gases	NDIR spectroscopy sensors	60 °C	0.5 MPa
Gas pressure	Strain gauges (including pressure transducers)	150 °C	25 MPa

5.3.2   Identification of generic technical requirements on monitoring technologies

The expected environmental conditions in a repository were derived from the Technical Requirements report [113] of the MoDeRn project. This report aimed to provide an overview of the technical requirements that will likely need to be addressed when developing, selecting and implementing monitoring technologies suitable for the geological disposal of radioactive waste. It is noted that the technical requirements are not to be understood in the sense of being mandatory to implement the technology, but rather in the sense of specifications that might need to be addressed when selecting monitoring technology best suited to respond to technical monitoring objectives. It was based on a reasonable understanding of the environmental conditions and implementation constraints available to the MoDeRn project. It provided enough information and context for this report to provide a first overview of technical requirements to be considered for development, selection and implementation of monitoring technologies.

A questionnaire (initial outline) was distributed to obtain an initial overview of such monitoring requirements and constraints from each project partner. Some of the contributions were based on general wish lists of potential interesting parameters and techniques, while others were the result of considerations regarding feasibility aspects or the relevance within the overall context.

EURAD (Deliverable n° 17.7) - Synthesis report on Innovative and Enhanced Equipment for Repository Monitoring
Dissemination level: PUBLIC
Date of issue of this report: **04/06/2024**

Page

Inputs received considered different host rocks, and requirements were clearly influenced by that constraint. Four inputs considered a repository built in argillaceous rock (Andra, NRG, Euridice and Nagra), another two in salt rock (DBETEC and SANDIA), four in crystalline rock (Enresa, Posiva, Rawra and SKB), one more considered both argillaceous or crystalline rocks (RWMC) and finally one considered all three of those host rocks (NWS).

Five areas for potential monitoring were identified [113]:

The results of the questionnaire indicated that the expected environmental conditions in each of the identified potential monitoring areas can be defined by seven parameters that are most likely to affect the performance of monitoring systems:

- **Temperature (°C):** can be monitored to understand heat transfer processes and the thermal conditions in the repository. In some programmes, monitoring temperature may be used to ensure confidence that it remains within acceptable limits to prevent any adverse effects on the nuclear waste containers or the repository components (e.g., smectite-illite transformation).
- **Mechanical pressure (MPa)**: refers to the physical stress or load applied to the materials and structures in the repository which may result from tunnel convergence, bentonite swelling, other volume change processes, etc. In some programmes, monitoring mechanical pressure may ensure confidence that the waste packages, structural elements, and other repository components are withstanding the pressures without failure or deformation.
- **Hydraulic pressure (MPa):** relates to the pressure of fluids within the repository. In some programmes, monitoring hydraulic pressure may ensure confidence when assessing the integrity of seals, preventing water infiltration into the repository, and/or understanding how it might affect the waste packages and other components.
- **Water saturation (%):** indicates the amount of water present in the repository materials relative to their porosity. It may be monitored in some programmes to ensure confidence in the stability of the repository components and functioning of bentonite barriers.
- **Salinity (g/L):** refers to the concentration of dissolved salts in the groundwater or fluids within the repository. In some programmes, monitoring salinity may ensure confidence that the engineered barrier system (EBS) is behaving as designed and over the lifetime that it is designed for. High salinity can accelerate the corrosion of materials, impacting the long-term integrity of the EBS.
- **Radiation (Gy/hr):** radiation levels should be monitored for operational safety to ensure that they remain within acceptable limits for the safety of personnel working in the repository. They may also be monitored in some programmes to ensure confidence in the longevity of materials and components that may undergo radiation-related degradation.
- **Displacement (m):** refers to the movement or deformation of materials, structures, or components within the repository. Monitoring displacement in some programmes may help confidence in the structural integrity of the waste packages, buffers, seals, and the overall repository, as excessive displacement can lead to damage and potential breaches.

The questionnaire results indicated the necessity, for some partners, of measuring other parameters such as moisture content, pH, Eh, radioactive gases, hydrogen, oxygen, carbon dioxide and methane concentrations in the gas phase, gas pressure, colloidal particle concentrations, alkalinity concentrations, ground-water inflow, and humidity. However, for most of these parameters, the ranges of expected values in repository environment are poorly determined or unknown.

Salt rocks are out of scope for MODATS and not considered here. Salt rocks have significantly different environmental conditions, disposal concepts and likely monitoring requirements. High salinity in these environments may be particularly challenging for monitoring technology longevity. However, the output of this work is generic. The roadmap and gap identification method can be applied to specific host rocks, disposal concepts, and monitoring programmes – including for salt rocks.

EURAD (Deliverable n° 17.7) - Synthesis report on Innovative and Enhanced Equipment for Repository Monitoring
Dissemination level: PUBLIC
Date of issue of this report: **04/06/2024**

Page

5.4 Classification of needs for the roadmap design

In this study, the process used to classify monitoring technology RD&D needs entailed the following steps:

1. Implementation of the matrix approach to evaluate 36 technologies covering 25 parameters, facilitating the identification of specific RD&D needs within underground monitoring technologies.
2. Utilisation of the comprehensive list of identified needs to discern and emphasize several distinct categories, each representing a cluster of requirements and priorities crucial for the advancement of monitoring technologies.
3. Aggregation of these categorised needs into broader, overarching families, allowing for the grouping of related requirements and the identification of common themes and underlying challenges inherent in the development of underground monitoring technologies for geological repositories.
4. Generation of a generic technology development roadmap, structured around the principal generic categories of needs, thereby providing a strategic framework that integrates the identified priorities and requirements essential for the holistic advancement and evolution of monitoring technologies.

This method assumes that the matrix approach will identify the developmental needs of a technology. This assumption is reasonable if the parameters that form the axes of the matrix are comprehensive. It is possible that a specific monitoring location in a specific disposal concept and host rock may have an environmental condition or data quality objective that is not included in the matrix.

5.5 Roadmap development

The methodology for constructing the technology development roadmap for monitoring technologies of radioactive waste geological repositories was founded upon a collaborative approach. A series of workshops were conducted as part of the MODATS project. The initiative commenced with a series of structured meetings between GSL and NWS, aimed at aligning the strategic objectives and vision for the technology development roadmap. These preliminary discussions served as a foundation for identifying the critical technological gaps, safety imperatives, and regulatory considerations pertinent to the monitoring of nuclear waste disposal sites.

Synthesizing the insights from the collaborative engagements and workshop deliberations, the roadmap development process emphasized the integration of multidisciplinary perspectives into a coherent, strategic plan. The amalgamation of inputs from various stakeholders played a pivotal role in creating a technology development roadmap that prioritizes the development of robust monitoring frameworks, safety protocols, and contingency measures to ensure the long-term integrity and security of nuclear waste deep geological repositories.

The generic technology roadmap went through a series of iterations that included applications to a representative range of technologies (fiber optic cables, wireless data transfer, and piezometers). Applying the roadmap was an opportunity to test that it was providing value. Iterative changes were required to ensure that the roadmap was universal and comprehensive.

5.6 Results

The matrix approach was applied to the 36 selected technologies. *Table 13* lists all the technologies that were covered in the analysis and an identification number assigned to each.

EURAD (Deliverable n° 17.7) - Synthesis report on Innovative and Enhanced Equipment for Repository Monitoring
Dissemination level: PUBLIC
Date of issue of this report: **04/06/2024**

Page

Table 13: *List of covered parameters and technologies with assigned numbers.*

Parameters	Technology name	#Tech
Temperature	Optical fibres	1
	Thermistors	2
	RTDs	3
	Thermocouples	4
Porewater pressure	Piezoelectric pressure sensor	5
Relative humidity	Capacitive hygrometers	6
Water matric potential	Electronic tensiometer probe	7
	Thermocouple Psychrometers	8
Water Content	TDR	9
	Electrical resistivity imaging (ERI)	10
Displacement	Capacitive Displacement Measurement Sensors	11
Strain	Optical Fibres	12
Tilt	MEMS Tiltmeters	13
Excavation profile dimensions and relative positions	TLS and Photogrammetry	14
Fracture aperture and length	Vibrating wire Crack meters	15
Fracture Mapping	Ultrasonic pulse velocity	16
	Acoustic emission monitoring	17
	Micro-seismic monitoring	18
Mechanical Pressure	Wire Pressure Transducers	19
	Strain Gauge Pressure Cells	20
	Capacitive Pressure Cells	21
	Piezoelectric Pressure Cells	22
	Optical Pressure Cells	23

EURAD (Deliverable n° 17.7) - Synthesis report on Innovative and Enhanced Equipment for Repository Monitoring
Dissemination level: PUBLIC
Date of issue of this report: **04/06/2024**

Page

Parameters	Technology name	#Tech
Density	Cross-hole seismic surveys - Full Waveform Inversion (FWI)	**24**
Stress	Stress meters	**25**
Atmospheric Oxygen Concentration	Electrochemical sensors	**26**
Dissolved Oxygen Concentration	Optical sensors	**27**
Chemical composition of groundwater	Groundwater sampling and ICP-MS	**28**
Non-specific gas concentration	Gas sampling lines and GC-MS	**29**
Radon concentration	Electronic radon detectors	**30**
Atmospheric hydrogen concentration	Thermal conductivity sensors	**32**
Hydrogen concentration (in EBS materials)	Miniaturised thermal conductivity sensors	**31**
Concentration of carbon oxide gases	NDIR spectroscopy sensors	**33**
Gas pressure	Strain gauges (including pressure transducers)	**34**
Redox potential	Electrodes	**35**
Volumetric flow rate	Flow loggers	**36**

5.6.1   List of needs

From the results of the matrix analysis applied to the 36 technologies and from specific information on the needs in underground monitoring technologies reviewed in the Technologies and Methodologies report, 14 categories of issues were identified.

The issues directly revealed by the matrices fall into three broad categories: the technology being able to withstand the harsh environmental conditions in a repository; the technology being able to fulfil the DQOs; and a lack of information required to determine if the technology can withstand the harsh environmental conditions and/or fulfil the DQOs. When the technology is unable to withstand physical conditions, it means that it lacks the robustness or resilience required to operate effectively in the range of harsh conditions that it may be exposed to within a repository. In this analysis the harsh conditions include exposure to high relative humidity, high salinity, high pressure, high temperature and radiation. The matrix analysis also reveals issues in data quality objectives that include measurement range, assessed lifetime, accuracy, and measurement drift.

EURAD (Deliverable n° 17.7) - Synthesis report on Innovative and Enhanced Equipment for Repository Monitoring
Dissemination level: PUBLIC
Date of issue of this report: **04/06/2024**

Page

In addition, other specific issues are identified from a literature review. It includes unsatisfactory measurement repeatability, unsatisfactory sensor attachment, unsuitable power supply, unsuitable sampling, and the necessity to define tailored calibration procedure and scaling relationships for the interpretation of signal. These fall into another broad category that may be considered as operational suitability.

Table 14 indicates which technologies are impacted by the identified issues. All these issues are generically defined hereafter in this section. Note that this table includes only the technologies for which specific needs were clearly identified.

Table 14: *A summary of the identified issues, the technologies (numbers defined in Table 13) that the issues were identified for, and the broader category within which each of the issues may be considered*

Broad categories of issues	Issues	Tech number in the list
Issues with harsh conditions	Unable to withstand high temperature	7,8, 10, 11, 13, 15, 20, 19, 21, 26, 32, 35, 27, 30, 31, 33
	Unable to withstand high pressure	2, 6, 7,8, 13, 15, 27, 32, 34, 35, 20, 31, 33
	Unable to withstand high relative humidity	6, 26, 32, 31
	Unable to withstand high salinity	6, 9
	Suffer from Radiation induced attenuation	1, 12
Not fulfilling the data quality objectives	Unsuitable Accuracy	1, 23, 25
	Significant Drift	2
	Insufficient Lifetime	26, 35
	Require Specific calibration and constitutive relationships	9, 10, 16, 17, 18, 24
Issues with operational suitability	Unsuitable Sensor attachment	11, 15
	Cannot measure expected range	11, 20
	Unsatisfactory Measurement repeatability	14
	Unsuitable Sampling	28, 29
	Unsuitable Power supply	20, 34
	Require Regular Maintenance	7
Extensive Lack of Knowledge	Extensive Lack of Knowledge	5, 7, 8, 23, 36

EURAD (Deliverable n° 17.7) - Synthesis report on Innovative and Enhanced Equipment for Repository Monitoring
Dissemination level: PUBLIC
Date of issue of this report: **04/06/2024**

Page

Issues identified from the matrix analysis:

Unable to withstand high relative humidity – The technology is not capable of functioning reliably in environments where humidity levels are elevated, typically issues begin >80%. High humidity can pose challenges such as the risk of moisture entering the system, which may lead to corrosion, electrical issues, or other forms of damage.

Unable to withstand high salinity – The technology is not resistant to the corrosive effects of high salinity. Underground environments in geological repositories may have elevated salinity levels either due to their depth or host rock salinity sources. Technologies that are not designed to withstand this condition could experience degradation or damage. This is a known issue for flow loggers and thermocouple psychrometers and is also a likely issue for other technologies, however, the performance data does not exist for them.

Unable to withstand high pressure – The technology is not engineered to endure high-pressure conditions. Underground environments in geological repositories can experience significant pressures and a monitoring system not designed to withstand these pressures may suffer structural failures or malfunctions. Technology performances under elevated pressures are generally well investigated.

Unable to withstand high temperature – The technology is not designed to withstand elevated temperatures. High temperatures can affect the performance and longevity of electronic components, sensors, and other sensitive parts of the monitoring system. This issue affects nearly 40% of the technologies covered in this analysis (***Figure 94***), making it one of the most common challenges to address for future developments. This is partly explained by technology performances under elevated temperatures having been well investigated, therefore, the issues are known.

Undergoes radiation induced attenuation (RIA) – When optical fibers are exposed to gamma radiation, signal attenuation increases through the interaction of the gamma flux with the colour centres or point defects present in SiO_2 in the fiber core. RIA limits the performance of the sensing system. The degree of RIA depends on the fiber chemical composition, the fiber history, and the nature and parameters of the radiation (gamma, neutrons, continuous, pulsed, dose rate, total dose, etc.). This is a known issue for optical fibers and extensometers, and RD&D has been successful in improving specific optical fiber technology's performance in high radiation environments.

Insufficient lifetime – The operational lifetime of a technology refers to the duration over which the technology can effectively perform its intended functions. It is the period during which the technology remains operational, providing the desired level of performance and functionality. Sensor data specification sheets may state the expected operational lifetime of sensors; however, the lifetimes are typically based on laboratory conditions and not the in situ environmental conditions. The quoted lifetimes may not be considered realistic for the repository monitoring purposes owing to the non-standard and extreme environmental conditions in some repository monitoring locations. Information concerning the operational lifetime of monitoring technologies in these locations can be gained from URL experiments. For example, conclusions drawn from URL experiments suggests that THM sensors can operate in test conditions similar to the disposal system for multiple decades; THM sensors were operating for 18 years in the FEBEX Experiment. Knowledge of sensor operational longevity is limited by the relatively short length of URL experiments compared to repository monitoring programmes. In many cases it will not be possible to test a technologies lifetime to the durations that may be desired of it.

Insufficient accuracy – The accuracy of a technology refers to its ability to provide measurements that are close to the true values. It is a measure of how well the technology can produce output that is consistent with a reference standard or the actual state of the measured quantity. Accuracy is usually provided in sensor data specification sheets. However, accuracy requirements of a technology within a monitoring programme are often not yet well defined making it difficult to interpret whether the known accuracies of technologies are sufficient.

EURAD (Deliverable n° 17.7) - Synthesis report on Innovative and Enhanced Equipment for Repository Monitoring
Dissemination level: PUBLIC
Date of issue of this report: **04/06/2024**

Page

Significant drift – Sensors experience measurement drift, which is the difference between the actual value and the measured value; the difference increases over time. Some sensors can experience high measurement drifts that lead to data errors; for example, capacitive hygrometers can experience between 0.25 and 5% relative humidity measurement drift per year. Measurement drift is typically managed through routine manufacturer re-calibration and maintenance processes. However, such processes cannot be performed on sensors emplaced in the EBS where access would negatively affect the EBS and safety case. Drift is often lacking data for both technology performance and/or requirements. It is expected that the issue is more pervasive than identified here and further testing to fill data gaps is required.

Cannot measure expected range – This statement implies that the technology, which is designed to measure certain parameters or conditions, is incapable of covering the full range of values that are anticipated or expected in the specific underground environment. In other words, the monitoring system lacks the capability to capture and accurately represent the entire spectrum of values that may be encountered within the monitored space. The measurements range is usually provided in sensor data specification sheets. An issue may exist at either end of the range; however, this issue has only been identified for the upper bound of extensometers.

Other specific issues identified through the literature review:

Require specific calibration, constitutive relationships – This statement indicates that the technology necessitates precise calibration processes and the establishment of specific constitutive relationships to function accurately. Calibration is the process of adjusting or fine-tuning a measurement device to ensure its readings align with known standards. In this context, the technology requires a tailored calibration procedure. This involves adjusting the system to account for any inherent biases, inaccuracies, or changes in its performance over time. Specific calibration means that the adjustments are uniquely tailored to the characteristics and requirements of the monitoring technology in question. Constitutive relationships refer to the mathematical or empirical relationships between the input and output parameters of a system. In the context of monitoring technologies, these relationships are crucial for translating raw measurements into meaningful data about the monitored environment. Specific constitutive relationships imply that the mathematical models or algorithms used to interpret the data are specialized and customized for the unique characteristics of the technology and the monitored conditions. This is a complex and pervasive issue; it is also somewhat unique in this list in that it relates often to algorithms rather than materials and engineering.

Unsatisfactory measurement repeatability – It refers to a situation where the measurements taken by the technology are not consistent or reproducible when the same conditions are repeated or attempted to be repeated. In other words, if the monitoring system is designed to measure certain parameters or signals over time, unsatisfactory repeatability means that the measurements fluctuate or vary more than expected when the same or similar conditions are replicated. This was identified as an issue for TLS and Photogrammetry for which the issue is typically in the technology operator's ability to successfully replicate the exact conditions present and locations used in previous measurements. A 10.5 m test vault at the Meuse-Haute Marne URL has attached markers to the vault walls that can be easily identified in images so that image tracking is more accurate.

Unsatisfactory sensor attachment – It refers to issues or challenges associated with the physical connection and installation of sensors within the repository. Unsatisfactory sensor attachment may result in misalignment or instability, leading to inaccurate measurements which can compromise the overall effectiveness of the monitoring system. It also may make sensors more susceptible to environmental factors such as moisture, temperature fluctuations, or corrosive substances, affecting their performance. Poorly attached sensors may be more prone to mechanical failure which can result in a loss of data. Poor anchoring or excessive force during installation could potentially cause structural damage over time, and undesired newly created pathways in the EBS with a risk of fluid or gas leakage in the underground environment.

EURAD (Deliverable n° 17.7) - Synthesis report on Innovative and Enhanced Equipment for Repository Monitoring
Dissemination level: PUBLIC
Date of issue of this report: **04/06/2024**

Page

Unsuitable sampling – It refers to the measurements that require in situ sampling, which involves collecting samples directly from the repository. This may be impractical or incompatible with safety requirements of the safety case.

Unsuitable power supply – It refers to issues related to the provision of electrical power to the monitoring equipment and sensors. The power supply is a critical aspect of any monitoring system, as it directly influences the reliability, functionality, and longevity of the equipment. Selected power supply systems must be reliable, durable, safe, and energy-efficient, considering the unique conditions of the deep geological nuclear waste repository. Miniaturised thermal conductivity sensors were identified as having insufficient power supply. Miniaturisation of technologies and conversion to wireless is likely to increase the pervasiveness of this issue.

Figure 3.1 shows that being unable to withstand high temperature and high pressure were the two most frequent issues. This is partly explained by the technology performances under elevated temperatures and pressures being well investigated relative to other harsh conditions. For example, the performance of technologies in high salinity conditions is often unknown and listed as a lack of data issue rather than a performance under harsh conditions issue. Therefore, these other issues may have higher frequencies if they were better investigated.
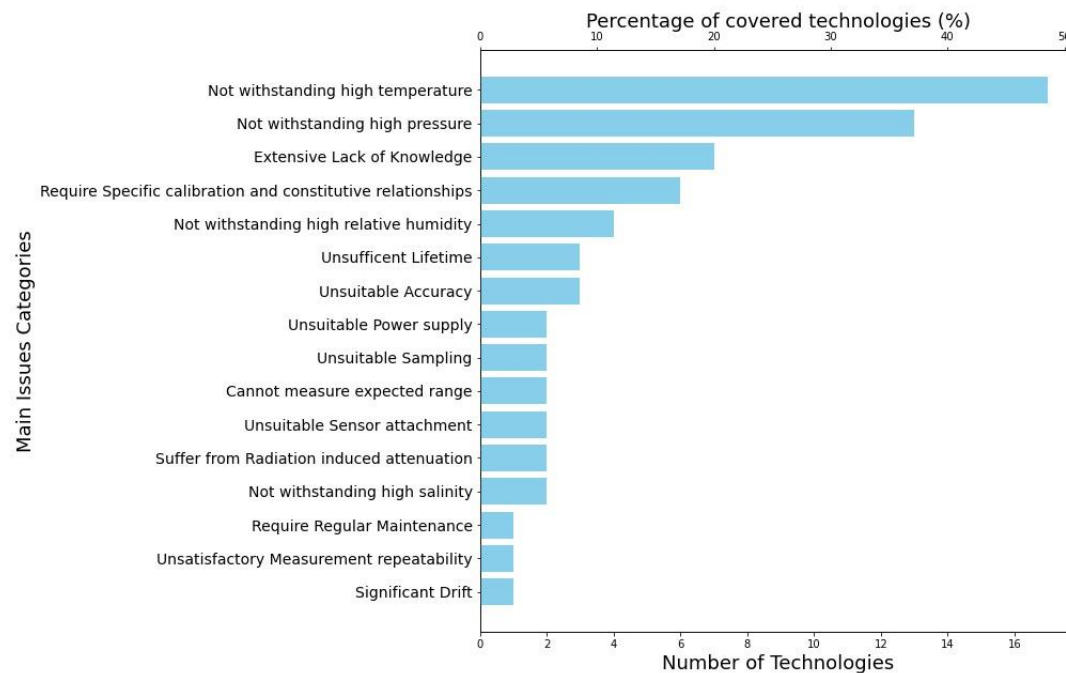
Figure 94: Number of monitoring technologies per identified issues. Some of these issues are likely to be more pervasive if data gaps were filled.

The 14 technology issues have been grouped into three broader categories, representing generic reasons for technology development. These categories were determined _a posteriori_ and aim to summarise the longer list of needs. The three categories relate to the conditions of the environment that the technology will be deployed into; the data quality objectives of the technology; and any potential issues relating to installation and/or operation in the repository.

- The first category contains issues pertaining to the technology not being able to withstand the expected conditions within the repository. It includes:
  - Unable to withstand high relative humidity.
  - unable to withstand high salinity.
  - unable to withstand high pressure.
  - unable to withstand high temperature.

EURAD (Deliverable n° 17.7) - Synthesis report on Innovative and Enhanced Equipment for Repository Monitoring
Dissemination level: PUBLIC
Date of issue of this report: **04/06/2024**

Page

- o Radiation induced attenuation.
- The second category contains issues pertaining to the technology not being able to fulfil the data quality objectives. It includes:
    - o Insufficient lifetime
    - o Insufficient accuracy
    - o Require specific calibration, constitutive relationships.
    - o Significant drift
    - o Unsatisfactory measurement repeatability
    - o Cannot measure expected range.
- The third category contains issues pertaining to the technology not being able to be installed and operated effectively. It includes:
    - o Unsatisfactory sensor attachment
    - o Unsuitable sampling
    - o Unsuitable power supply

5.6.2   The generic technology development roadmap

The technology development roadmap developed here (**Figure 95:** *Generic technology development roadmap for underground repository monitoring technologies. Orange coloured stages are from the Modern2020 screening methodology workflow. Blue stages are assessment gates. Green stages are activities to undertake according to the responses that follow the assessment gates.*) starts from connection to the Modern2020 Screening workflow where the stage PRO6 asks "*Are there sufficient feasible parameters to monitor this process?*". This question reviews whether the process in question can be feasibly monitored. In many cases a single parameter will be sufficient to provide the desired level of information about a process. However, in other cases it is possible that multiple parameters may be needed.

When the answer to PRO6 is no, it leads to stage PRO7 asking, "*How else could this process be monitored?*" If there are not sufficient feasible parameters to monitor the process in question, it is necessary to reconsider:

- The basis for the decision to monitor it.
- Whether a different high-level monitoring strategy could enable the desired parameter(s) to be monitored.
- Whether further R&D on monitoring technologies should be undertaken to develop options for monitoring the desired parameter(s) to a technically feasible level.

The roadmap developed here suggests a workflow that could be followed when the latter option is taken forward. This proposed generic workflow encompasses two main types of stages:

- Blue gates (G) that contain assessments under the form of questions.
- Green activities (A) that provide possible processes to be undertaken according to the answers to the questions asked in the blue gates.

The initial blue gate (G_0) of the roadmap starts with the question "*What was/were the reasons for parking the process, parameter and technology combination?*". The answer to this question can be based on information collated upstream from:

- Databases of sensor performances in URL experiments.
- Discussions with technology manufacturers and operators (e.g., WMOs).
- Documentation from the stage TEC2 of the Modern2020 workflow which states "*Take option forward*" when an option considered to be technically feasible (based on the answers to the sub-questions in TEC1) is identified.

Four possible responses can answer G_0, the PPT combination may have been parked because:

EURAD (Deliverable n° 17.7) - Synthesis report on Innovative and Enhanced Equipment for Repository Monitoring
Dissemination level: PUBLIC
Date of issue of this report: **04/06/2024**

Page

- "The technology has no proof-of-concept". In that case, it is suggested to undertake development of proof-of-concept and in case it fails, the technology is parked. If it is successfully proven, the technology prototype needs to undergo laboratory testing of performances at conditions relevant to the repository which refers to the activity A1 here.
- "Specific monitoring system components require further laboratory testing". In that case, a proof-of-concept is already existing and the laboratory tests of the activity A1 can be undertaken directly. The laboratory testing should target data gaps.
- "The monitoring system is not demonstrated in a repository-like environment". The activity A2 intends to address this issue by conducting demonstration in repository-like environments. It can be done, for example, by conducting experiments in URLs or mines. This activity follows testing of performances of the technology conducted in a standard laboratory at the surface.
- "The monitoring system is not proven in site-specific repository environment". The activity A3 intends to address this issue by conducting demonstration in the site-specific repository environment. It is unlikely that all requirements of a technology can be fully tested within the site-specific repository environment before it is deployed. Therefore, this activity requires an assessment of confidence.

In responses to the question gate G_0, each of the three activities A1, A2, and A3 is followed by a question gate developed from the three main categories of issues identified in section 5.6.1. In those blue gates (G_1, G_2, G_3), the three main issue categories are turned into questions to check if the technology needs further development. Hence, the three questions are:

- Can the technology fulfil the data quality objectives?
- Can the technology be installed and operated?
- Can the technology withstand the relevant expected conditions within the repository?

In G_1, these three questions are based on laboratory work. In G_2, these are based on demonstration in a repository-like environment (e.g., a URL). And in G_3, these are based on demonstration in the site site-specific repository environment.

For each of these gates (G_1, G_2, G_{3b}), the response is considered positive only when all the three questions are answered positively. To answer the assessment gates, a matrix approach like the one we used in this study can be applied.

A negative answer to G_1, G_2 and G_3 leads to development of sub-activities that include sequentially the identification of the reasons for failure, proposition and selection of development options, and development. At these stages of the development, the selected or even developed option can be parked if it is judged as unfeasible based on the conducted research or if an alternative option becomes preferred and is taken forward. In case the development is undertaken below G_1, the workflow reconnects upstream for re-testing of the newly developed technology (A1) and re-assessment where required.

The bottom of the G_2 workflow reconnects upstream to activities in A2. However, it also offers the possibility to go back to standard surface laboratory tests (A1) when the development of the new technology in repository-like conditions significantly changes its design and requires new performance assessments.

A positive answer to G_2 leads to a sub-question gate G_{3a} that aims to evaluate whether the repository-like conditions (e.g., environmental conditions within a URL) significantly differ from the real repository. A positive response to G_{3a} leads to the ultimate stages, including an assessment of confidence (based on evidence) in deploying the technology in the repository and possibly further development of the technology in the repository. A negative response to G_{3a} leads to A3 after which only a positive response to G_3 leads to the final stages.

The roadmap offers the flexibility in the proposed workflow to undertake each of the activities A1, A2, and A3 sequentially or directly. Direct undertaking can be used in case ongoing developments of a

EURAD (Deliverable n° 17.7) - Synthesis report on Innovative and Enhanced Equipment for Repository Monitoring
Dissemination level: PUBLIC
Date of issue of this report: **04/06/2024**

Page

technology have already reached some of the stages proposed here. For example, activities of A2 can be directly conducted when the technology performances have already been successfully tested in standard laboratory at the surface but need to be demonstrated in an underground environment. However, it is unlikely that activities of stage A3 can be reached directly from the gate G_0, as a significant number of gaps are expected for any technology before being able to be demonstrated in a site-specific repository environment.

The final three actions are to develop manufacturing capabilities, produce technical specification documents, and deploy the monitoring system in the repository. Developing the manufacturing capabilities recognises that having confidence in a prototype is not sufficient for deploying the technology and that multiple instances of the technology may be required. Furthermore, confidence is required that components that require maintenance will be available throughout the lifetime of the monitoring period. Producing the technical specification documents ensures that the technology is deployed correctly and appropriately and may assist in its wider use beyond the specific repository. Finally, deploying the system. Deploying the system is the endpoint on the roadmap but is not necessarily the end of monitoring technology RD&D. RD&D may continue after deployment in the repository to improve understanding of drift, for example.

Reporting should be done consistently throughout RD&D and at each stage of the roadmap. There may be future interest in transparency around decision making that might be satisfied by documenting progression and decisions throughout this process.
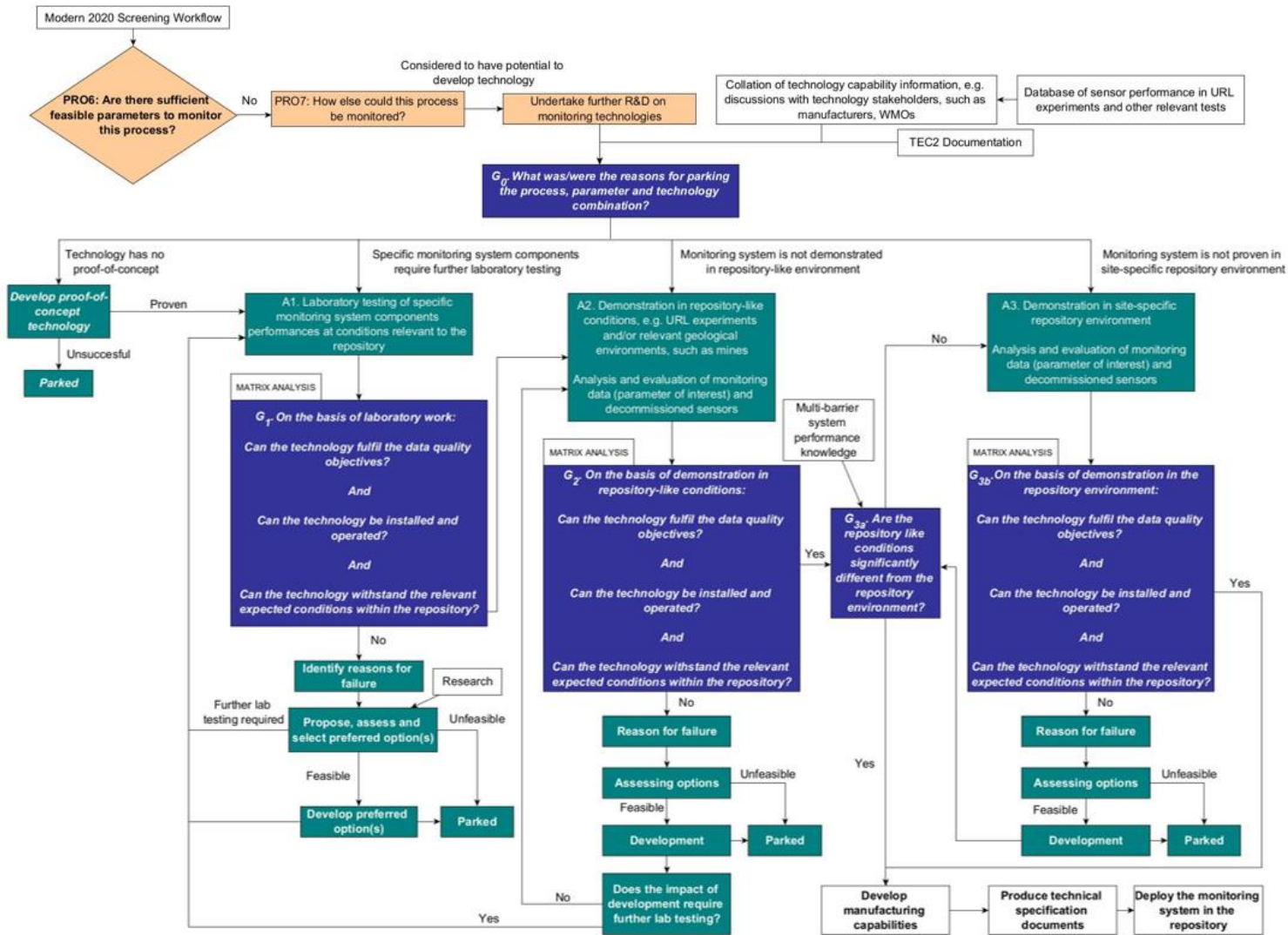
EURAD (Deliverable n° 17.7) - Synthesis report on Innovative and Enhanced Equipment for Repository Monitoring
Dissemination level: PUBLIC
Date of issue of this report: **04/06/2024**

Page

Figure 95: *Generic technology development roadmap for underground repository monitoring technologies. Orange coloured stages are from the Modern2020 screening methodology workflow. Blue stages are assessment gates. Green stages are activities to undertake according to the responses that follow the assessment gates.*

EURAD (Deliverable n° 17.7) - Synthesis report on Innovative and Enhanced Equipment for Repository Monitoring
Dissemination level: PUBLIC
Date of issue of this report: **04/06/2024**

Page

5.7 Discussion

This section discusses the use of the roadmap, emphasizing its relevance in overcoming challenges associated with the design of repository monitoring systems. To aid in the development of the generic roadmap and to ensure that it provides value going forward as well as in the past, the generic roadmap was applied to three different technologies (piezometer, wireless data transfer technology, and fiber optic cables). These technologies were selected because they are at different technology readiness levels and are representative of the range of RD&D issues likely to be encountered in development of repository monitoring technology. In this section, some examples of needed developments are provided, and which were identified from the applications of the proposed generic technology development roadmap.

5.7.1 Application of the roadmap: pore pressure, piezoelectric pressure sensor

The matrix tool highlights several issues that currently compromise the ability to deploy piezoelectric pressure sensor to monitor pore pressure confidently in a repository:

- Lack of knowledge on performances under radiation that may be required for specific programmes.
- Needs more precise performances such less drift for long term measurement.
- Better estimation of the operational lifetime.

Based on these gaps, it is suggested to conduct RD&D activities starting from the stage A1 of the proposed roadmap. A proof-of-concept already exists for piezometers. The performance of piezometers under different possible extreme conditions needs to be determined before undertaking any development that would lead to its deployment in a real repository. Laboratory testing (A1) and tests in underground environment such as URL (A2) would demonstrate fulfilling of the identified issues above and are advisable before an eventual demonstration in a site-specific repository (A3). Furthermore, the performance testing may discover further development needs.

The caveat here is that this is based on the broad, collated, requirements for the technology. A WMO applying the generic roadmap to piezometers for their host rock, disposal concept and monitoring programme might identify different RD&D needs. Not all WMOs will establish a need for piezometers to withstand conditions that they are not known to already be able to withstand.

5.7.2 Application of the roadmap: wireless data transfer technology

Repository monitoring technologies may need wires for power supply and for data transfer. Wires may be undesirable in some locations within a repository environment because they can be preferential transport pathways that bypass repository barriers and affect the safety case. The effect of repository monitoring technologies on the repository safety case has been investigated in another MODATS task by undertaking a features, events, and processes analysis. Wireless data transfer technology presents a potential solution to address the challenges associated with the inaccessibility of sensors and potential negatives of wires in deep geological repository environments.

Wireless data transfer technology has several challenges requiring further RD&D before it can confidently be deployed in a repository. Challenges include signal range limitations, potential interference in underground conditions (depending on the carrier frequency), integrating different frequency systems, and the need for periodic maintenance of battery-powered sensors. The main issues would be:

- Lack of knowledge on performances under high salinity, radiation, temperature, pressure, and humidity.
- Undergoes potential external electromagnetic interferences.
- Not enough secure encryption protocols.

EURAD (Deliverable n° 17.7) - Synthesis report on Innovative and Enhanced Equipment for Repository Monitoring
Dissemination level: PUBLIC
Date of issue of this report: **04/06/2024**

Page

- Unknown operational lifetime.

Wireless data transfer is a newly developed technology. RD&D activities to be undertaken would start in the proposed roadmap by the development of a proof-of-concept, sequentially followed by the sub-workflow of the activities A1, A2 and A3.

5.7.3   Application of the roadmap: fiber optic cables

In this example, fiber optic systems have been identified as a potential technology suitable for development and application to repository monitoring for measuring strain to understand tunnel convergence. It should be noted that fiber optic cables can measure other parameters, e.g., temperature.

Applying the generic roadmap to fiber optic cables resulted in two different outputs. One was a roadmap that identified the earlier technology readiness development needs which included testing under expected extreme repository conditions, similar to the examples above. The other output was a roadmap onto which RD&D on fiber optic cables to date were mapped. This showed, and was seen for other technologies, that some RD&D has been successfully carried out in repository-like environments despite there still being data gaps in technology performance that could be determined by (surface) laboratory experiments simulating expected extreme conditions. Indeed, undertaking RD&D underground is good practice because it commonly identifies unknown issues and is useful for generating requirements.

The juxtaposition can partly be explained by the method presented here being generic and using the wider, collated ranges of extreme conditions across different potential repositories. In this method, data gaps are more likely to exist. However, a WMO with a URL may have a narrower range of expected conditions in which they may deploy fiber optic cables and fewer or no data gaps. Therefore, they may move to demonstration in repository-like conditions (A2). Therefore, the ongoing and undertaken RD&D for fiber optic system technology is an example that illustrates how the proposed generic roadmap reflects a workflow consistent with a way that has been successfully conducted *Figure 96* describes various RD&D activities that have been conducted to address challenges that may be encountered with fiber optic systems in repository environments.

Laboratory tests of performances (A1) revealed that radiation may impact a fiber optic system. Because of its interaction with the fiber core, radiation degrades optical fiber properties through three different mechanisms: radiation-induced attenuation (RIA), radiation-induced emission, and compaction. Research conducted on potential options of development indicated that pure silica core fibers with fluorine dopants in the cladding are the most radiation resistant fibers [93]. Based on these results and undertaken developments, the next stage involved new tests in a laboratory (i.e., looping back to A1), this time on a surface mock-up.

In situ demonstration using 2D test measurements was then conducted in the Meuse/Haute Marne URL [119] (consistent with suggested A2 activities). Results of these URL tests indicated that distributed strain sensing with Brillouin or Rayleigh scattering associated to a parametric identification calculation were an efficient method to monitor the convergence of tunnel. This analysis on performance in repository-like conditions also concluded that fiber optic sensors can be used in harsh environments in which the radiation dose is expected to be close to 1 MGy after 100 years and the temperature close to 80°C [119].

After this successful series of RD&D, the proposed roadmap here would suggest addressing the gate G_{3a} prior to the ultimate stages of demonstration in the site-specific repository (A3) and deployment in the repository. This would evaluate whether the repository-like conditions in which the tests have been conducted significantly differ from the real repository. For example, in the case of the future application in radioactive waste repositories, the temperature is expected to be spatially uniform with a slow temporal evolution. According to [119], the temperature variations were negligible in the URL tests performed here, so not significantly different from the expected temperature distribution in a repository.

EURAD (Deliverable n° 17.7) - Synthesis report on Innovative and Enhanced Equipment for Repository Monitoring
Dissemination level: PUBLIC
Date of issue of this report: **04/06/2024**

Page

The temperature variation is important for measuring strain with fiber optic cables because the fiber optic measurements are sensitive to temperature (the Neubrex fiber optic unit uses Brillouin scattering to jointly measure temperature and strain). Having negligible temperature variations across the sensor overcomes the potential issue of needing to decorrelate the effects of temperature and strain. Or having Pt100 type temperature sensors or Smartec or Silixa fiber optic units which use Raman scattering to measure temperature could be sufficient to perform this decorrelation. However, it is likely that a negative answer to G_{3a} would be relevant here for several reasons.

Firstly, the mock-up used in the surface laboratory and in the URL provides 2D measurements as it represents tunnel cross section measurements with a steel ring (762 mm outer diameter, 10 mm thickness and 200 mm width). Further 3D tests, i.e., along a longer tunnel section would be suitable to increase confidence for deployment in a repository. Secondly, the proposed method here is well adapted to galleries with a steel lining, but a concrete tunnel liner may be used for intermediate level long lived waste. Its implementation on galleries with a concrete lining is expected to be more complex because of the effects of the evolution of the concrete and the adhesion of the cable in the structure. It implies that further tests on various types of lining would be needed before demonstration and deployment in a repository.
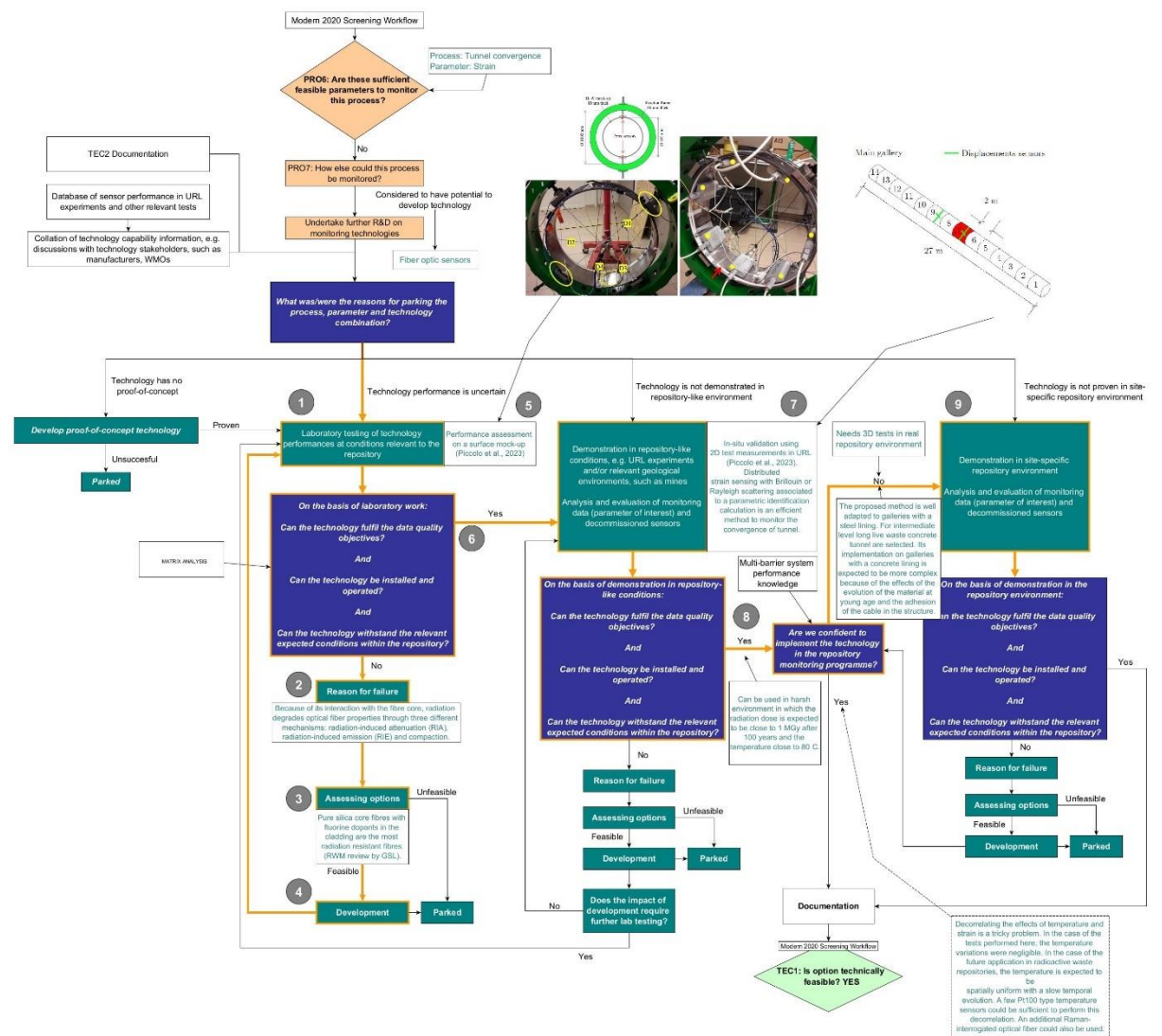
Figure 96: An illustrated *example of application of the generic roadmap to a review of the RD&D that has been conducted by various groups to improve fiber optic cable technology. The roadmap is shown to be a useful template for mapping previous and ongoing RD&D of repository monitoring technologies.*

EURAD (Deliverable n° 17.7) - Synthesis report on Innovative and Enhanced Equipment for Repository Monitoring
Dissemination level: PUBLIC
Date of issue of this report: **04/06/2024**

Page

5.7.4 Building on Modern2020

The roadmap provides a structured approach to navigate monitoring system design for underground deep geological repositories for nuclear wastes. By starting with the fundamental question of parameter feasibility through connection to the Modern2020 screening methodology workflow (PRO6), it directs users to assess the complexity of monitoring processes and ascertain the adequacy of selected parameters. It builds on previous work for developing best practices for parameter screening and monitoring system design.

The transition to the Modern2020 stage PRO7 ("*How else could this process be monitored?*") marks a crucial point where the roadmap addresses uncertainties. This step prompts users to reconsider their monitoring strategies, fostering adaptability in the face of evolving technological landscapes and emerging challenges.

The roadmap initiates with a detailed examination of past decisions regarding the parking of specific process, parameter, and technology combinations (G_0). Drawing insights from databases, manufacturer discussions, and documentation, users gain a comprehensive understanding of historical choices, providing a solid foundation for future decision-making.

5.8 Summary

This study aims to develop a comprehensive approach for undertaking RD&D on repository monitoring technologies. This encompasses identifying challenges in monitoring technologies and defining the required RD&D steps to undertake before their deployment in a repository.

The methodology employs a multifaceted strategy, utilizing a matrix approach for cross-comparing technology capabilities and limitations and technical requirements for 36 technology/parameter combinations. This approach led to the identification of specific developmental needs within underground monitoring technology. These needs were grouped into 14 categories and aggregated into 3 overarching families, forming the basis for a generic technology development roadmap.

The culmination of this methodology results in a versatile generic roadmap that provides a strategic and adaptable framework for advancing monitoring technologies in radioactive waste geological repositories. Beginning with the Modern2020 Screening methodology, the roadmap addresses the crucial question of parameter feasibility for monitoring a specific process. The roadmap's flexibility is evident in its two main components: Assessment gates (G), that raise questions, and Activities (A), suggesting processes based on answers to the questions.

The first gate, G_0, initiates with the question, "*What were the reasons for parking the process, parameter, and technology combination?*". Informed by upstream information from sensor performance databases, discussions with stakeholders, and Modern2020 workflow documentation. G_0 leads to four possible responses. Each response triggers specific activities and subsequent question gates that assess further technology development. Each main G/A couple acts as a sub-workflow, the first one devoted to standard laboratory testing of technology performances, the second one to demonstration in repository-like environment, e.g., a URL, and the third one to demonstration in a site-specific repository.

Assessment gates evaluate technology development based on three critical questions: "*Can the technology fulfil data quality objectives? Can the technology be installed and operated? Can the technology withstand relevant expected conditions within the repository?*". Positive responses lead to subsequent stages and, ultimately, confident deployment in a repository. Negative responses initiate sub-activities, including identification of reasons for failure, proposition and selection of development options, and actual development, with the possibility of reconnection upstream for re-testing and re-assessment. The option can be parked if the development options are deemed unfeasible.

The roadmap's flexibility allows sequential or direct undertaking of activities based on ongoing technology developments. It accommodates scalability, enabling direct progression when technology

EURAD (Deliverable n° 17.7) - Synthesis report on Innovative and Enhanced Equipment for Repository Monitoring
Dissemination level: PUBLIC
Date of issue of this report: **04/06/2024**

Page

performances have been tested in standard laboratory conditions but need demonstration in an underground environment.

Acknowledging diverse technology development stages, the roadmap offers flexibility in workflow execution, allowing for adaptation to ongoing advancements. Incorporating assessment gates ensures a meticulous evaluation of key issues, and iterative development processes foster continuous improvement.

The absence of a fixed timeline underscores a commitment to practicality and realism, allowing WMOs to tailor the roadmap to their unique needs and navigate the complexities of technology development effectively. Recognizing diverse contexts and programmatic intricacies, the generic roadmap serves as a framework, encouraging WMOs to tailor its implementation to their specific programme timelines. Acknowledging challenges corresponding to project size, WMOs can use the roadmap as a guideline, adapting the pace and intensity of each stage to the demands of their programmes.

5.9   References

[108].   EC (2004). Thematic Network on the Role of Monitoring in a Phased Approach to Geological Disposal of Radioactive Waste. European Commission Project Report EUR 21025 EN.

[109].   Modern2020 (2017). Repository Monitoring Strategies and Screening Methodologies. Modern2020 Work Package 2, Deliverable D2.1.

[110].   M. White (2013). Monitoring During the Stages Implementation of Geological Disposal: The MoDeRn Project Synthesis. MoDeRn Deliverable D6.1.

[111].   . M. White and S. Scourfield (2019). Modern2020 Project Synthesis Repository Monitoring: Strategies, Technologies and Implementation. Work Package 6, Deliverable No D6.5.

[112].   T.J. Haines and M.J. White. Technologies and Methods for Monitoring the Geological Disposal Facility during Construction and Operation in Support of the Environmental Safety Case. 2020-3, Version1, 2022.

[113].   MoDeRn (2011). Technical Requirements Report. MoDeRn Project Deliverable D-2.1.1, www.modern-fp7.eu.

[114].   .Modern2020. Work Package 6, Modern2020 Project Synthesis Repository Monitoring: Strategies, Technologies and Implementation. Deliverable D6.5, 2019.

[115].   Geokon. Model 3800/ 3810 Thermistors and Thermistor Strings Installation Manual. www.geokon.com, 2020.

[116].   García Siñeriz, JL. Et al. 2006 FEBEXII Project. Pos tmortem Analysis : Instruments .ENRESA,TechnicalReport05-4/2006.

[117].   Rey. M.et al l. 2016. FEBEX DP : Post mortem analysis : Sensors . Nagra Arbeits bereicht NAB16-20. Wettingen, 122pp

[118].   .Smart Fibres. Technology Overview of Distributed Pressure and Temperature Sensing with Fiber Bragg Grating Technology. 4.10.10.13 Iss I, 2018.

[119].   .A. Piccolo, Y. Lecieux, S. Lesoille, P. Teixeira, J. Bertrand, D. Leduc. Performance Assessment of Distributed Strain Sensing Techniques for Convergence Monitoring of Radioactive Waste Repository. Sensors 2023, 23, 398. https://doi.org/10.3390/s23010398

EURAD (Deliverable n° 17.7) - Synthesis report on Innovative and Enhanced Equipment for Repository Monitoring
Dissemination level: PUBLIC
Date of issue of this report: **04/06/2024**

Page

EURAD (Deliverable n° 17.7) - Synthesis report on Innovative and Enhanced Equipment for Repository Monitoring
Dissemination level: PUBLIC
Date of issue of this report: **04/06/2024**

Page

Appendix A. Technology Data sheet summary

EURAD (Deliverable n° 17.7) - Synthesis report on Innovative and Enhanced Equipment for Repository Monitoring
Dissemination level: PUBLIC
Date of issue of this report: **04/06/2024**

Page

Joint inversion of various geophysical data **Partners involved: ETH, Nagra**	eurad European Joint Programme on Radioactive Waste Management

Rationale:

For monitoring the state of radioactive waste repositories, knowledge of the spatial and temporal variations of key parameters, such as temperature, pressure, water content, porosity, etc. is preferred. In principle, this can be obtained with a dense sensor network, with which all these parameters can be measured directly. However, this imposes several problems. First, the placement of the sensors may affect the integrity of the repository barriers. Furthermore, the placement of a sensor may locally disturb the embedding material, and the measurements may therefore not be representative. Finally, the sensor data represent only point information, which may not be representative for the entire volume of interest.

With geophysical methods, the problems mentioned above can be addressed. They can be performed in a non-destructive and non-intrusive fashion. Therefore, the integrity of the barriers remains unaffected, and the embedding material is not disturbed locally. Most importantly, repeated geophysical measurements allow spatial and temporal changes to be monitored over larger volumes.

In this work we assessed the feasibility of extracting tomographic images of a geotechnical parameter in full-scale emplacement (FE) experiment (Müller et al., 2017) by using geophysical measurements.

Description of the technology:

In FE there are > 1500-point sensors that measure parameters such as temperature, pressure, relative humidity. Additionally, there are two fibreglass pipes (Figure 97) installed within the granular bentonite mixture (GBM) for geophysical measurements (cross-hole seismic

and GPR measurements and single hole GPR, gamma-gamma and neutron log). We used crosshole seismic and GPR measurements. With the help of structural similarity constraint one can improve the resolution of tomographic images (seismic velocities, GPR velocities and GPR attenuation). With the help of machine learning, out of the geophysical tomograms and point relative humidity sensors in one case and neutron log in the other we were able to obtain tomographic images of relative humidity and water content distribution, respectively. Our analysis shows that these images are qualitatively correct. Without detailed calibration work it will not be possible to obtain quantitative values.
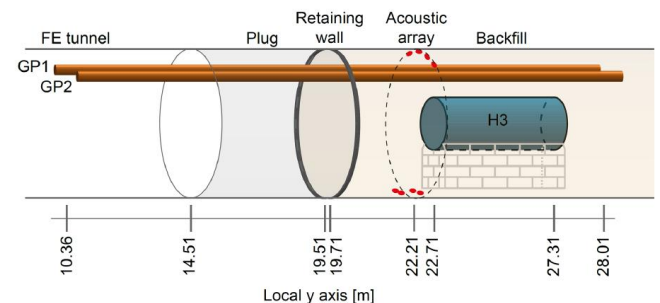
***Figure 97:** Side-view of the FE experiment. GP1 and GP2 are the two geophysical pipes within which crosshole seismic and GPR data is acquired. H3 marks the position of the third heater. Permanently installed acoustic sensors are marked in red.*

Specifications:

EURAD (Deliverable n° 17.7) - Synthesis report on Innovative and Enhanced Equipment for Repository Monitoring
Dissemination level: PUBLIC
Date of issue of this report: **04/06/2024**

Page

Technology	Applicability to Test site (Mont Terri FE experiment)	General applicability to radioactive waste repositories
Seismic full waveform inversion	Not applicable (low signal-to-noise ratio, 3D effects)	Applicable, with an appropriate experimental setup
Coda wave interferometry	Successfully tested	Applicable to resolve subtle temporal changes, but limited applicability for high spatial resolution
Joint inversions of various geophysical data sets	Successfully tested	Applicable and highly recommended
Machine learning for transferring geophysical to geotechnical parameters	Successfully tested	Applicable, supposed that suitable training data sets would be available

What are Technology Readiness Levels of the technology?

Technology	Initial TRL	TRL after completion of MODATS
Seismic full waveform inversion	7-8	7-8
Coda wave interferometry	6-7	7
Joint inversions of various geophysical data sets	5-6	6-7
Machine learning for transferring geophysical to geotechnical parameters	3-4	5

Results

We have shown that with the help of machine learning one can combine geophysical measurements and local humidity information to

obtain tomographic images of humidity distribution in granular bentonite mixture.
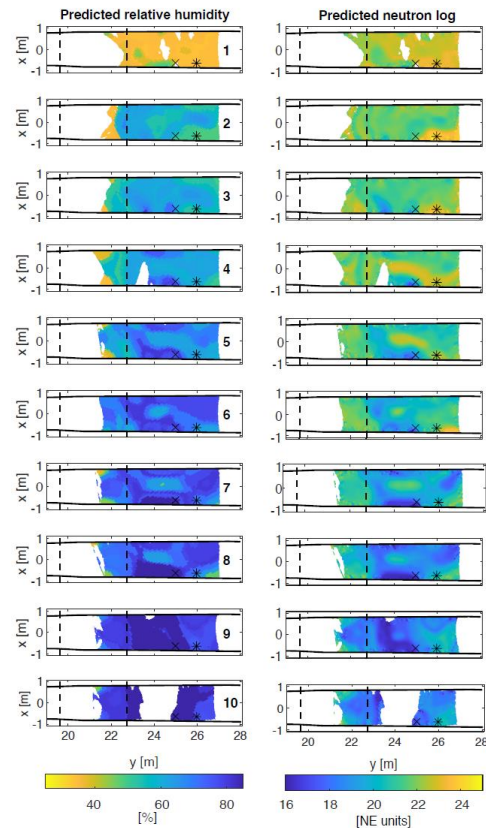
Figure 98: Estimated distribution of relative humidity (left) and virtual neutron log measurements (right) predicted from jointly inverted geophysical tomograms using a machine learning model.

Existing alternatives to this technique (if any):

·   **none**

·   Advantages

The main advantage of the geophysical technologies, further developed within MODATS, is the volumetric information on relevant geotechnical parameters (in contrast to point information, obtained with traditional sensors)

EURAD (Deliverable n° 17.7) - Synthesis report on Innovative and Enhanced Equipment for Repository Monitoring
Dissemination level: PUBLIC
Date of issue of this report: **04/06/2024**

Page

Spectral Induced Polarisation SIP **Partner: IRSN**	**eurad** European Joint Programme on Radioactive Waste Management

Rationale:

This development can be designed in a (i) non-intrusive manner, (ii) sensitive to variations in water and clay content, (iii)allows dynamic phenomena to be monitored over time, (iv)allows local anomalies to be captured those isolated sensors cannot detect and (v)is also sensitive to mineralogical and chemical variability of pore water.

Description of the technology:

<u>Principal of Spectral Induced Polarisation</u>

The Induced Polarization (IP) characterizes the ability of a medium to store charges reversibly under a slowly alternating electrical field. In the time-domain, this effect will show as a delay between the extinction of the injected current and that of the measured voltage (see *Figure 1a*).
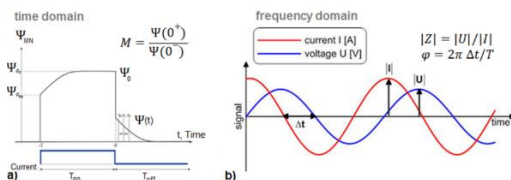
Figure 1 – Typical induced polarization observations in a) the time-domain with ΨMN the voltage between measuring electrodes M-N, b) the frequency domain (modified from Duvillard et al. 2018 and Madsen 2019).

In a controlled environment, the capacitive properties of the medium can also be investigated using a frequency sweep to characterize the polarization dependence on frequency. This investigation method is known as Spectral Induced Polarization (SIP); the effect will appear as an amplitude modulation and a phase shift between injected current and measured voltage sinusoids (see Figure 1b). This method developed for laboratory investigations, is still ill-adapted to field scale, where large cable length easily picks extensive electromagnetic (EM) induction noise spoiling the SIP data.

Polarization observations may have different origins: polarizable electrodes, membranes effect (associated to bottleneck in the porous medium), interfaces effects also known as Maxwell-Wagner (occurring at phases interfaces in heterogeneous media) and finally the electrical double layer (EDL).

Our interest lies in this last type of polarization, characteristic of frequencies below the kHz range, and typically caused by the interaction of the pore fluid (electrolyte) with electrically charged mineral surfaces, where the so-called EDL is formed. A schematic description of the electrical double layer is given in Figure 2: the EDL is composed of the thin Stern layer, where fluid counter ions may be adsorbed, and the diffuse layer with an accumulation of fluid counter ions, yet not physically bound. Beyond the diffuse layer the fluid phase complies with electroneutrality.

When an external electric field is applied, charges located in the Stern and diffuse layers may move tangentially to the grain surface and polarize the grain. At current extinction, the charges move back to their initial places (retro-diffusion) with a relaxation time in connection to the grain diameter.

EURAD (Deliverable n° 17.7) - Synthesis report on Innovative and Enhanced Equipment for Repository Monitoring
Dissemination level: PUBLIC
Date of issue of this report: **04/06/2024**

Page
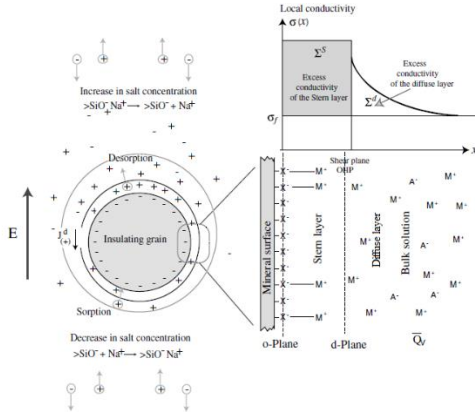
Figure 2 - Polarization at the EDL of an insulating grain and schematic description of the EDL constitution (after Proix et al. 2015).

Polarization measurements assess the complex impedance of the medium Z* defined as

$$Z^* = |Z| . e^{i\Phi} \tag{1}$$

We convert this value into a complex conductivity σ*:

$$\sigma^* = G . \frac{1}{Z^*} \tag{2}$$

where G is a geometrical factor, specific of the measuring geometry.

We can write σ* as the sum of its real part σ' and imaginary part σ'':

$$\sigma^* = \sigma' + i\,\sigma'' = \frac{G . e^{-i\Phi}}{|Z|} \tag{3}$$

$$\sigma' = \frac{G . \cos\Phi}{|Z|} \quad , \quad \sigma'' = -\frac{G . \sin\Phi}{|Z|} \tag{4}$$

The real part σ' is also known as the in-phase component of complex conductivity σ*. It bears the conduction contribution from the fluid within the poral system, as well as the surface conduction σ_S occurring at the EDL.

$$\sigma' = \frac{\sigma_w}{F} + \sigma_S \tag{5}$$

where σ_W is the fluid electrical conductivity and F is the formation factor that characterizes the pore space connectivity. In an electric analogue of the medium, the in-phase component is represented by two resistances in parallel (see Figure 3a).

The imaginary part σ'' is also known as the out-of-phase component of complex conductivity σ*. It supports the polarization contribution

originating from the EDL and, as such, appears as a capacitor in the electric analogue scheme. For natural materials, Promentilla at al. 2010 gave following relation:

$$\sigma'' \approx -\frac{M_n}{\alpha} \tag{6}$$

where α = 8.1 is a constant and Mn is the normalized chargeability, one major parameter for polarization characterization defined as $M_n = \sigma_\infty - \sigma_0$, with σ_∞ the instantaneous conductivity and σ_0 the DC conductivity. As a matter of fact, M_n is exactly the difference between high-frequency surface conductivity and the low-frequency surface conductivity. As such, it may also be expressed as a combination of EDL properties and hydraulic parameters:

$$M_n = \left(\frac{1}{F . \varphi}\right) \rho_g\, \beta_{(+)}^s\, f\, CEC \tag{7}$$

where φ is the connected porosity, ρ_g is the grain density, CEC is the cation exchange capacity that evaluates the number of adsorbing sites at the EDL in $C.kg^{-1}$, $\beta^s_{(+)}$ is a ion mobility in the diffuse layer and f is the partition coefficient expressing the fraction of counter ions within the Stern layer, vs the whole EDL. Apart from these last two parameters, which should be taken from literature, we aim at determining all parameters by direct experimental measurements. The CEC may also be approached from the angle of the specific surface area (SSA). Thus, an alteration of the sample should produce a change in SSA and have a SIP expression. Furthermore, the linear dependence of quadrature conductivity σ'' to the CEC (Revil et al. 1998) provides us with a tool to test the validity of our experimental observations.
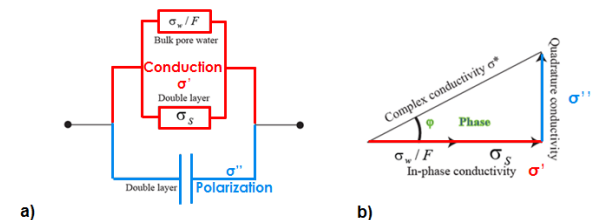
Figure 3 - a) Electric analogue scheme and b) trigonometric representation to the complex conductivity of a porous medium. (Revil et al. 1998).

Specifications:

EURAD (Deliverable n° 17.7) - Synthesis report on Innovative and Enhanced Equipment for Repository Monitoring
Dissemination level: PUBLIC
Date of issue of this report: **04/06/2024**

Page

Measuring range	1 mHz to 45 kHz
Accuracy	0.005%
Measured parameters	real (in-phase) and imaginary (quadrature or out-of-phase) conductivity components
Material used	MX80 bentonite, Fontainebleau sand, deionised water and hyperalkaline solution (pH 13.5)
Petrophysical parameters investigated and their ranges	Water content (0.15 - 1.25), saturation (0.4 - 1), dry (0.6 -2) and bulk (1.1 – 2.2) density, bentonite (10 - 100%) and sand ratios (0 - 90%), pore water chemistry (pH 7 and 13.5)
Operation temperature	10 - +60°C
Sample size	Cylinder 5 x 5 cm
Lifetime	> 1 month

What are Technology Readiness Levels of the technology?

The TRL of the technology is 4 (technology validated in a lab). Our initial goal was to reach a TRL of 5 (technology validated in a relevant environment (industrially relevant environment in the case of key enabling technologies) however, we have yet to obtain satisfactory results at a metric-scale.

Results

For pure MX80 bentonite: (1) both the in-phase conductivity and quadrature conductivity exhibit a power law dependence with the volumetric water content; (2) the prefactor coefficients for these power laws can be determined from the theory, particularly from the CEC of the bentonite alone and (3) the values of the two power-law exponents $m = 4.5$ and $p = 3.1 \pm 0.1$ are consistent with the expression $p = m - 1$.

For MX80 bentonite and sand mixtures with deionised water: (1) at a given saturation, the in-phase conductivity linearly depends on the bentonite content because of the increase of the cation exchange capacity with the amount of smectite; (2) both the in-phase and quadrature conductivities depend on the water content according to power law relationships with a power-law exponent of $m = 2.3$ for the in-phase conductivity and $p = m + 1 = 3.3$ for the quadrature conductivity. Therefore, the relationship between the two exponents (for the in-phase and quadrature conductivities) does not agree with the prediction of the classical dynamic Stern layer model ($p = m-1$), (3) the in-phase and quadrature conductivities linearly depend on temperature in the temperature range 10-60°C.

For MX80 bentonite and sand mixtures with an hyperalkaline solution: (1) static experiments show an increase of the in-phase and quadrature conductivity with the presence of the hyperalkaline solutions with respect to the spectra at near-neutral pH conditions, (2) the relationships established for MX80 and sand mixtures regarding the dependence of the in-phase and quadrature conductivity with respect to the water content and saturation remains however valid; (3) for the time-lapse experiments, we observed at the opposite with respect to the static experiments a decrease of both the in-phase and quadrature conductivities over time. These data can be fitted using an exponential decay function. This evolution may be explained by the illitization process of the smectite contained in the bentonite thanks to the presence of potassium in the pore water solution.

Existing alternatives to this technique:

• Electrical resistivity

Advantages

Spectral Induced Polarisation (SIP) is not only sensitive to variations in water content but also to the mineralogical and chemical variability of the water. Furthermore, it is possible to relate the parameters from SIP to permeability and thus offers a new method to image in 4D the permeability of porous media

![eurad logo] European Joint Programme on Radioactive Waste Management

EURAD (Deliverable n° 17.7) - Synthesis report on Innovative and Enhanced Equipment for Repository Monitoring
Dissemination level: PUBLIC
Date of issue of this report: **04/06/2024**

Page

Acoustic Emission (AE) monitoring in clay/shale formations **Partners involved: GFZ, IRSN**	eurad **European Joint Programme on Radioactive Waste Management**

Rationale:

Attenuation in clay-rich material is often high, prohibiting the detection of acoustic emissions resulting from crack formation or reactivation beyond a few meters distance from the source. Existing high-frequency sensors with a defined instrument response function are often not sensitive enough to detect weak signals. Piezoelectric acoustic emission sensors operate in near-resonance mode, which results in significantly more sensitive instruments (Plenkers et al., 2022). However, the instrument response of piezoelectric acoustic emission sensors is complex because the amplitude response is not flat over their frequency bandwidth due to sensor specific resonant frequencies (Ohtsu and Aggelis, 2022, Plenkers et al., 2022) and coupling plays a key role for installation of the sensor. There are a few companies that develop this kind of instrumentation and there are ongoing efforts in the science community to develop an in-situ calibration.

We test detection distances, frequency characteristics and attenuation of acoustic emission events in clay/shale rocks as there is a lack of these measurements and experience in these environments.

Description of the technology:

The AE sensors of type *GMuGMABLr-7-70* comprise a piezoelectric disk of PZT ceramic and are single component, side-view sensors. AE sensors are operated with a preamplifier GMuG VV30 that amplifies the signal by 30dB. Preamplifiers were located within 0.3 m distance to the sensor. The sensors were operated with analogue 1 kHz high-pass filters. The sensors are embedded in a brass housing, suitable for pressures up to 1 MPa, and are pneumatically pressed to the borehole wall. The

sensor's main sensitivity is perpendicular (±90°) to the borehole orientation in the direction of sensor orientation. Functionality of the sensor is intellectual property of the manufacturer GMuG. Figure 1 shows the construction of the borehole sledge containing the sensor.
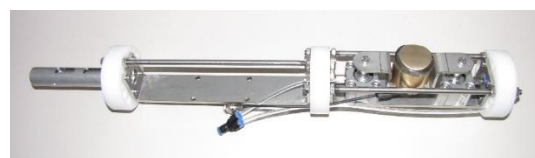
Figure 99 : 1-component AE sensor on sledge for borehole installation.

Specifications:

Measuring range	1-100 kHz
Main resonance frequency	70 kHz
AD resolution/Filter	16 bit/analogue 1kHz
Sensor type	GMuG-MA-Blr-7-70
Power supply	GMuG SPV20
Operation temperature	0 - +75°C
Preamplifier (+ internal gain)	30 dB (+10 dB)
Lifetime	10+ years

What are Technology Readiness Levels of the technology?

TRL is considered to have improved from TRL 5 to TRL 6 for AE monitoring in shale rocks, because in the past AE studies in these environments have been rare and often unsuccessful, however this is now more commonly done and instrumentation has increased sufficiently in sensitivity to allow for AE monitoring in highly attenuative settings.

On field test or advanced test example:

EURAD (Deliverable n° 17.7) - Synthesis report on Innovative and Enhanced Equipment for Repository Monitoring
Dissemination level: PUBLIC
Date of issue of this report: 04/06/2024

Page

Set up

We installed 12 AE sensors in boreholes at distances up to 5 meters from the stimulation interval (Figure 2). In addition, two HAE (Hydrophone-like AE) sensors were placed in horizontal boreholes used regularly for crosshole seismic tomography measurements. The latter were pushed into the boreholes with rods and will be pulled out again if the boreholes are required for other purposes. We want to test the performance of these HAE sensors, which are slightly more sensitive due to a reduced bandwidth but are less-well coupled due to the installation (coupled only by gravitational pull and contact with the borehole wall). The coupling quality of the pneumatically pressed AE sensors was checked one year after installation, showing that only one of the sensors has decreased waveform quality. Active ultrasonic transmission measurements using the transmitter source GMuG-Blw-Tr40 from borehole BH8 were generated during the installation to test the transmission of high-frequency source signals with dominant frequency content higher than that commonly associated with AE events. Hammer and bolt hits were used to recently examine sensor performance, because BH8 now hosts two AE sensors as well.

The AE sensors record continuously since 13 Dezember 2023, when the heating system was turned to full heating in the study area. By design we want to take advantage of the quiet site conditions during the Christmas mine closure to obtain low noise reference data. During everyday operation there are strong site specific noises, especially of electric origin. The AE sensors are ready to record data of the planned injection experiment once a suitable temperature is reached in the injection chamber. During the experiment, we will supplement the network with 3–4 broadband seismic sensors to extend the frequency range to low frequency monitoring. This may also allow to monitor any slow deformation associated with the experiment.
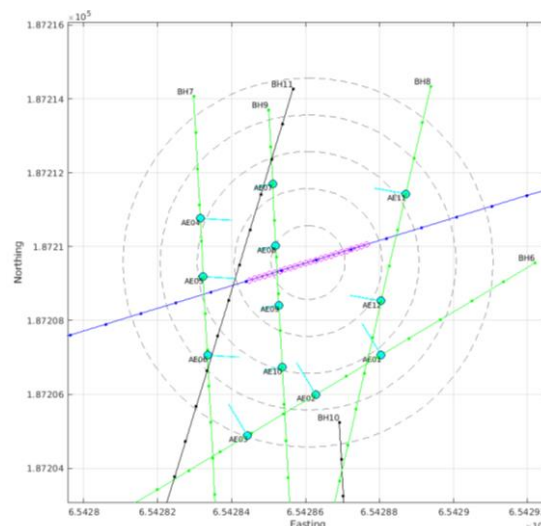
Figure 100: Instrumentation of AE sensors (light blue dots in green monitoring boreholes) surrounding the injection chamber (pink circles along BH1 in blue) in the East gallery 03 in Tournemire. The direction in which the 1-component sensor is facing is shown. Dashed circles indicate distance from the centre of the injection chamber in 1 m intervals.

Results

The AE sensors recorded natural seismic activity during the mine closure due to the Christmas vacation 2022. These events were seldom detected, coinciding with lower-than-average noise conditions while the system was set up in trigger mode. High and systematically occurring electrical noise spikes frequently trigger the system and may mask natural events. This is one reason why the system was switched from triggered mode to continuous recording, so that trigger setting may be tuned during postprocessing to detect these signals. The natural events are currently being located to test detection ranges of the recording system. Frequency characteristics show a limited frequency content with a peak at 11 kHz (see Figure 3 below). These records illustrate that the recording system is up and running and currently being tuned to the site conditions.
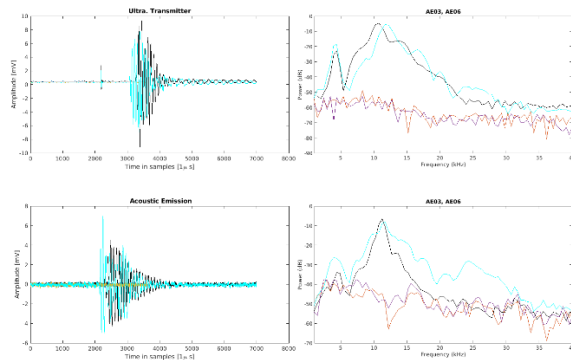
EURAD (Deliverable n° 17.7) - Synthesis report on Innovative and Enhanced Equipment for Repository Monitoring
Dissemination level: PUBLIC
Date of issue of this report: **04/06/2024**

Page

Figure 101: Waveform examples of an ultrasonic transmission signal generated in BH8 at 12.5 m depth and recorded by two AE sensors (AE03, black; AE06, blue) and an AE event of unknown location recorded by the same sensors (left panel). The spectra on the right show that the frequency content is highly attenuated (ultrasonic transmission source signal has energy up to 40 kHz) and limited to frequencies around 10 kHz for the AE event

Existing alternatives to this technique (if any):

During the Faults&Fluids project at the Tournemire URL, accelerometers PCB 356B18 sensitive in a frequency range between 2 Hz and 4 kHz were installed in boreholes within the same fault zone (deBarros et al., 2016).

High-frequency hydrophones were used during the EGS Collab experiment at the Sanford Underground Research Facility to monitor stimulation experiments in phyllitic rocks (Schoenball et al. 2020).

Advantages

The main advantage of the AE sensors, applied in this study, over sensors used previously, is the wider bandwidth and the higher sensitivity. This may allow to detect and record smaller acoustic emission events of lower magnitudes, which occur more frequently and exhibit higher frequency content. The spectra of both active ultrasonic transmission signals and passive AE events show clear peaks at 10 – 15 kHz, much higher than previously resolved at the site. In addition, detection ranges may be improved for recording in highly attenuative settings due to the increase sensitivity. During previous experiments isolated seismic events were recorded but their relationship with the measured deformation in the injection chamber remained inconclusive. By increasing the

sensitivity of the system more acoustic emissions may be recorded to better understand their spatio-temporal relationship with the injection

EURAD (Deliverable n° 17.7) - Synthesis report on Innovative and Enhanced Equipment for Repository Monitoring
Dissemination level: PUBLIC
Date of issue of this report: **04/06/2024**

Page

Automatic passive seismic Partners involved: Institute of Mine Seismology, AFRY	eurad European Joint Programme on Radioactive Waste Management

Rationale:

Amount of recorded seismic events in and around an active final disposal facility can reach tens of thousands annually. To ease the burden of human seismologists, an automated system for reliable event classification is required.

Description of the technology:

Automatic classification algorithm is developed by Institute of Mine Seismology (IMS). It utilizes machine learning algorithms that are intellectual property of IMS. The algorithm is part of IMS's processing services, and it is used with their seismic analysis software "IMS Combined".

What are Technology Readiness Levels of the technology?

Technology Readiness Level (TRL)	initial	final
Basic and applied research (TRL : 1-4)	⚫	🔴
Development (TRL : 5-7)	🔴	⚫
Manufacturing (TRL : 8-9)	🔴	⚫

Results

The automatic classifier was able to correctly accept 97% of manually accepted events form database containing ONKALO's seismic events from 2021 to 2023. The number of false positives, i.e. falsely accepted events, is still quite high with only 77% of manually rejected events being correctly rejected by the classifier. Further training of the classifier is required

before full integration to daily analysis routines, but overall, the results so far show promise.

Existing alternatives to this technique:

As the automatic classifier for Posiva's purposes must work with established analysis programs produced by Institute of Mine Seismology, no other viable alternatives are available for this particular project. However, other solutions may exist for others depending on their choice of seismic monitoring equipment and software suppliers.

Advantages

Automation of seismic event classification eases the workload of human seismologists.

EURAD (Deliverable n° 17.7) - Synthesis report on Innovative and Enhanced Equipment for Repository Monitoring
Dissemination level: PUBLIC
Date of issue of this report: **04/06/2024**

Page

Water leakage mapping Partners involved: Posiva	eurad European Joint Programme on Radioactive Waste Management

Rationale:

In addition to continuous leakage measurements, Posiva has monitored groundwater leakage on tunnel walls and roof by regular visual mapping surveys in the underground facility ONKALO® since 2005. The leakage mapping survey is based on visual observation of groundwater leakage on tunnel walls and roof. The tunnel surface is mapped using five different "moisture condition" classes from dry to flowing. Digitalised results are statistically examined, interpreted and reported annually.

Along with the underground leakage measurement network, leakage mapping provides more detailed information about the surface area and location of leakages. Observation and monitoring of leakages into the underground facilities supports understanding of the hydrogeological conditions, enables detection of local fracture-scale leakages and provides feedback for construction as it enables evaluation of the success of grouting operations.

The selection criteria for methodology selected for field test was based on the practical aspects: economically feasible, fast and easy to use, suitability in underground conditions.

Description of the technology:

Task for Automatic Digital Mapping of Leakages is initiated to develop and test a technical application that could be used to ease the present mapping method that is time-consuming and hard to validate, as visual mapping is always a subjective interpretation of the performing person.

After determination of specific requirements for reliability and performance of the technology, a search for potential technologies and contractors were carried out. Selection of method type and contractor for co-operation to conduct method development were completed by November 2022. Method development

continued to testing of the technology in various tunnel conditions in Olkiluoto, Finland. The final deliverable of the task is a memorandum describing the selected method, test arrangements and results of the performed tests, as well as an assessment of suitability of the method for tunnel leakage mapping.

The most promising and feasible for underground field testing was judged to be standard thermal imaging to start with to be able to see the possibility to detect different type of inflows in conditions where different structures like shotcrete, steel mesh reinforcement and other tunnel infra may disturb the results.

Specifications:

The commercial IR-camera used in the field test specifications.

FLIR IR-CAMERA	Model T865
Wavelength range	7.5 - 14 µm
Thermal sensitivity	<30 mK @ 30°C (42° lens)
Image Frequency	30 Hz
Power supply	0, 6.0 – 16.0V
Weight	1.4 kg (3.1 lbs)
Operating Temperature Range	-15°C to 50°C
Battery Operating Time (Li-ion)	4 hours

What are Technology Readiness Levels of the technology?

The TRL system measures a technology's maturity, from Level 1 (Concept Evaluation) to Level 9 (Successful Deployment) https://horizoneuropencpportal.eu/sites/default/

eurad
European Joint Programme
on Radioactive Waste Management

EURAD (Deliverable n° 17.7) - Synthesis report on Innovative and Enhanced Equipment for Repository Monitoring
Dissemination level: PUBLIC
Date of issue of this report: **04/06/2024**

Page

files/2022-12/trl-assessment-tool-guide-final.pdf.

On field test or advanced test example:

Set up

A field test was conducted in ONKALO®. An IR-camera was used to scan tunnels and to detect water leakages. The results of IR-imaging were compared with the manual leakage maps.

Results

An automatic water leakage digitizing system is possible to develop but achieving accuracy on par with human will be challenging.

Some problems include achieving accurate location information especially in variable tunnel profiles, determining the amount of water, detecting point like anomalies and detecting anomalies behind objects. Also the fact that water temperature varies depending on the depth in ONKALO® and also the temperature increase is expected during the operational phase it might be difficult to achieve a library which can take into account these facts.

Advantages

Even though the thermal imaging has some challenges, it could be applied to assist human logger. IR-image/recording could be used to automatically identify the leakages and to digitize them. In practice, this would mean taking IR-images and using photogrammetry (Huang et al. 2020) and pattern recognition to map the anomalies to tunnel profile. Even this would provide significant help, though. After anomalies are digitized, the logging personnel could then determine the amount of water (five different classes) in each anomaly by other means, for example by visual observation (which is the procedure currently anyway).

EURAD (Deliverable n° 17.7) - Synthesis report on Innovative and Enhanced Equipment for Repository Monitoring
Dissemination level: PUBLIC
Date of issue of this report: **04/06/2024**

Page

Optical Fiber Sensors **Partners involved: LabHC, ANDRA.**	

Rationale:

Optical fiber-based monitoring technologies for temperature and strain monitoring offer real time measurements of both T and ε with a cm spatial resolution along nuclear waste cell. In addition, optical fiber sensor design through: its composition, manufacturing process and interrogation techniques, offers a high variety of monitoring application to either perform dose-deposition measurement with radio-sensitive fibers or other monitoring processes (temperature, strain, gas concentrations, etc.) using radiation hardened optical fibers.

The objective of this work is to analyse the influence of radiation on a distributed optical fiber sensor and to propose a measurement strategy for monitoring a structure hosting radioactive waste over a period of 100 years. For Gamma irradiation, the observed degradations are solely caused by ionization mechanisms, and mitigation techniques have been implemented at the material, component, or system level to reduce the risk associated with high cumulative doses.

Under neutron radiation, the mechanisms become more complex, as atomic displacement effects are added to the ionization mechanisms. The impact of these new mechanisms, especially from the perspective of measurement and optical fiber sensors, remains to be explored for the neutron fluxes and fluences considered for Cigéo.

Description of the technology:

The temperature and strain monitoring depend on measuring both Rayleigh and Brillouin light scattering signatures occurring inside the optical fiber core and cladding. Both phenomena exhibit linear sensitivity to temperature and strain (refer to (1) and (2)). An

interrogator sends light pulses into the fiber, and based on the light scattering phenomena, the light is backscattered and analysed. Rayleigh scattering is a result of local refractive index inhomogeneity within the fiber core, leading to light backscattering. Brillouin scattering, on the other hand, results from the interaction between acoustic waves in the fiber core and cladding and the incident light pulse. Local changes in refractive index due to density inhomogeneities from the propagation of acoustic waves lead to the backscattering of the light pulse, carrying the Brillouin spectrum signature of the local state of the optical fiber. In most distributed optical fiber-based techniques, the time delay between pulse emission and backscattered light reception is used to determine the location inside the fiber.
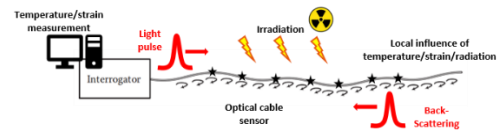
Figure 102: Principle scheme of temperature and strain measurement with optical fibers under in a radiation-rich environment

.

The technology selected by ANDRA for the simultaneous monitoring of strain and temperature involves the measurement of both light scattering phenomena using the Neubrescope instrument (NBX-7020) from Neubrex. The frequencies of both Rayleigh and Brillouin scattering (ν_R, ν_B) are measured, enabling the resolution of the two unknowns and two equations system by introducing a decorrelation of temperature (T) and strain (ε).

$$\Delta\nu_B = C_{T,B}.\Delta T + C_{\varepsilon,B}.\Delta\varepsilon \qquad (1)$$

$$\Delta\nu_R = C_{T,R}.\Delta T + C_{\varepsilon,R}.\Delta\varepsilon \qquad (2)$$

EURAD (Deliverable n° 17.7) - Synthesis report on Innovative and Enhanced Equipment for Repository Monitoring
Dissemination level: PUBLIC
Date of issue of this report: **04/06/2024**

Page

Where $C_{T,B}$, $C_{T,R}$, $C_{\varepsilon,B}$ and $C_{\varepsilon,R}$ represent the temperature and strain sensitivity coefficients for Brillouin (B) and Rayleigh (R) scattering, respectively. This technology undergoes testing under various conditions to evaluate its performance in neutron and gamma-rich environments during and after irradiation runs. The study focuses on the optical fiber, considering its composition, type, and response (including losses, Brillouin, and Rayleigh properties) under diverse harsh environments. Additionally, the research explores the integration of the optical fiber into different cable structures (with varying compositions) and examines the effects of coating on monitoring capabilities.

Specifications:

In Tables 1 and 2, we present general specifications regarding the optical fiber requirements, Neubrescope performances, and optical cable requirements up to the current date.

Table 15: Cigéo specification for optical fiber-based temperature and strain monitoring

Table 16: Up to this day Optical fiber cable specification with Neubrescope NBX-7020.

Technology specification	
Spatial resolution	10 cm (modulable with NBX-7020)
Time resolution	From 1min to 1h (depending on the application requirements and sampling)
Temperature accuracy	< 1 °C
Strain accuracy	< 20 µε
Temperature measurement range	From -80°C to +80°C
Strain measurement range	From 0µε to 5000µε
Fiber Specification	• Radiation hardened grade (Pure silica core + Fluorine doped cladding fiber) • Polyimide coated to withstand higher temperatures (+80°C) • Carbon coated to limit H_2 diffusion inside the fiber core
Cable Specification	• No gel allowed inside the cable (release of additional H_2) • Strain and temperature sensitive ($C_{T,B}$, $C_{T,R}$ and $C_{\varepsilon,B}$, $C_{\varepsilon,R}$ values) • No mechanical degradation after irradiation

What are Technology Readiness Levels of the technology?

The project was launched through a collaboration between ANDRA and LabHC, focusing on the study of the effects of gamma irradiation on radiation-hardened optical fibers. Initially, the project was in development,

primarily concentrating on fiber-based studies through applied research. Currently, the development has progressed to include the consideration of neutron effects in addition to gamma effects, as well as the exploration of cable coatings. ANDRA is actively involved in developing new cables specifically designed for this application. It's important to note that this work is still in the development phase.

On field test or advanced test example:

We conducted irradiation campaigns to test seven different cable types under gamma irradiation and a mixed field neutron/gamma campaign. These tests aim to study the radiation effects on both optical fibers and optical fiber cables, as well as on Rayleigh and Brillouin scattering signatures. Online measurements are carried out for RIA, Brillouin,

Cigéo specifications	
Radiation	• Dose-rate from 1 to 10Gy/h • Total accumulated dose: 0.8 MGy for MA-VL cells (after 100 years) • Total accumulated dose: 10 MGy for HA cells (after 100 years) • Mixed field (gamma + neutrons)
Temperature	• HA cells: T= 90 °C • MA-VL cells: T= 50 °C • Temperature accuracy of 1°C
Strain accuracy	20 µε
Spatial resolution	< 1 m
Gaz	Presence of H_2 due to radiolysis of organic matter contained in wastes
Cell length	• HA cells: 100m long • MA-VL cells: 500m long
Sensing range	> 1 km
Time	Real time measurement
Lifetime	100 years

and Rayleigh using an OTDR (Optical Time Domain Reflectometer) and the Neubrescope NBX-7020, respectively. Figure 2 presents two examples, illustrating the installed samples around the source support for: (left) the irradiation campaign at IRSN-IRMA (^{60}Co source) in September 2023, and (right) the irradiation at CVRez (^{252}Cf source) in Czech Republic in September 2022. The setup will be detail in the "Type of technology section".

EURAD (Deliverable n° 17.7) - Synthesis report on Innovative and Enhanced Equipment for Repository Monitoring
Dissemination level: PUBLIC
Date of issue of this report: **04/06/2024**

Page
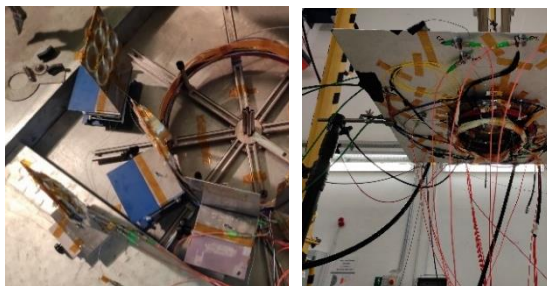
Figure 103: *Instrumentation of two irradiation campaigns for optical fiber cable testing at IRSN-IRMA (^{60}Co) source and (left) installed sample before irradiation with the optical cable coil in the middle around the source holder and optical fiber spools on aluminium plates placed at different dose-rates. (right) the irradiation at CVRez (^{252}Cf source) in Czech Republic in September 2022.*

Results

Based on the data obtained from past irradiation campaigns, online measurements and post-irradiation characterizations have been employed to identify the most and least suitable candidates for temperature and strain monitoring in the challenging environments of both Cigéo (HA and MA-VL). The assessment involves analysing RIA levels, RI-BFS, and RI-RFS from online measurements of the seven tested cables during the two irradiation campaigns. Furthermore, pre and post-mortem evaluations have been conducted based on multiple criteria, as outlined in Table 4. Detailed results will be provided in the "Type of technology" section.

resulting from the two irradiation campaigns (at IRSN-IRMA and at CVRez).

Advantages

Optical fibers offer many advantages comparted to previous point sensors. It offers a distributed, deported and time resolved measurement with high spatial resolution allowing to place the sensors in harsh environment. It's versatility by tuning its composition and structure make it possible to fit the sensors capabilities to the desired application requirements. In addition, placing optical fibers around any geometrical form (such as nuclear waste canisters) enables a 3D-mapping of the temperature and strain (measured here) at the location of the optical fiber depending on the spatial resolution of the interrogation technique.

Tested cables	FN1	FN2	CBT	CBS	CFB	NE	PEEK
Robust (installation)	🟥	🟧	🟩	🟩	🟧	🟩	🟧
Temperature sensitive	🟩	🟩	🟧	🟩	🟩	🟩	🟩
Temperature coefficient stability	🟥	🟩	🟧	🟧	🟥	🟧	🟩
Strain sensitive	🟩	🟩	🟥	🟩	🟩	🟥	🟩
RI-BFS tolerance	🟩	🟩	🟥	🟥	🟧	🟩	🟩
RI-RFS tolerance	🟩	🟩	🟥	🟥	🟩	🟥	🟩
Degradation	🟧	🟩	🟩	🟩	🟩	🟩	🟩
RIA levels	🟩	🟩	🟥	🟥	🟩	🟥	🟩

Table 4. Comparative table of criteria satisfaction of the 7 tested optical fiber cables during and after irradiation

EURAD (Deliverable n° 17.7) - Synthesis report on Innovative and Enhanced Equipment for Repository Monitoring
Dissemination level: PUBLIC
Date of issue of this report: **04/06/2024**

Page

Optical pH sensor **Partners involved: CEA**	eurad European Joint Programme on Radioactive Waste Management

Rationale:

The development and use of analytical tools for on-site measurements are of major importance in several applications, in particular for environmental water quality monitoring in complex aqueous systems .

Among measurable quantities, knowledge of pH value is fundamental because it governs a lot of chemical reactions that can induce important modifications in a complex aqueous system .

Alternative to electrochemical measurements:

- No need to use a reference electrode periodically controlled,
- Real time and remote measurement allowed.

Description of the technology:

The development of these optical probes is based on a simple concept involving the immobilization of a chemical recognition phase sensitive to pH variation on a surface part of the optical chain.

OPTICAL SENSOR EXPERIMENTAL SETUP
A white light source is injected into a multimode optical fiber. The fiber carries the light to the measurement location. A mirror, positioned in front of the fiber, sends the light back on a multimode
optical fiber to a spectrometer for spectral analysis. A computer software enables the spectral responses processing. The interaction of the immobilized organic layer with the protons contained in a given sample, in the presence of light, leads to variations in optical properties. The chemical recognition phase
can be covalently immobilized on the end of the metallized optical fiber or on the 316L stainless steel mirror (Figure 1). These two different optical configurations are studied in this work. The light source

(HL 2000-FHSA), the optical fibers with a core diameter of 940 µm and the spectrometer (HR 2000) are supplied by Ocean Insight..
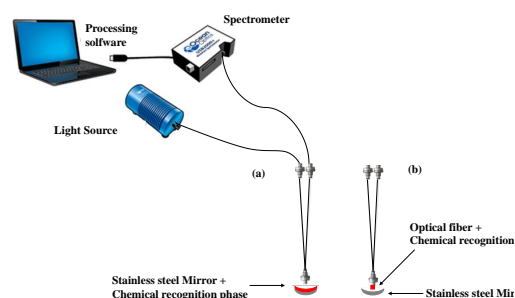
Figure 104: Two different optical set up for the optical sensor: grafting on the optical fiber, grafting on the mirror.

Specifications:

Measuring range	4 < pH < 8 for Neutral Red
Accuracy	0.2 pH units
Response time	~1s
Repeatability	~5%
Operation temperature	+20 - +60°C
Lifetime	> 6 months

What are Technology Readiness Levels of the technology?

The TRL of the sensor starts from Level 1 (Concept Evaluation and Basic research) at the beginning of MODATS project and ends at a final Level 4 (First applied research) at the end of the project.

Optimization of experimental grafting conditions has been realized using thin metallized semi-transparent plates for cost reasons and

EURAD (Deliverable n° 17.7) - Synthesis report on Innovative and Enhanced Equipment for Repository Monitoring
Dissemination level: PUBLIC
Date of issue of this report: **04/06/2024**

Page

easiness of analytical measurements at the laboratory.

First attempts of fiber and mirror grafting have been then realized at the laboratory and then tested at the Underground Laboratory in Bure.

On field test example: Set up.

First experiments have been conducted at the Underground Laboratory in Bure. The two optical set up (fiber and mirror grafting) have been tested for the measurement of the pH of poral water in the ACA dedicated cabinet.

Figure 105: Experimental setup of the optical pH sensor prototype in the ACA cabinet located in the GED gallery in Bure

Results

The first results obtained in Bure for the two optical set up lead to a measured value of pH~6 for poral water. These preliminary results are very encouraging because they are independent of the localization of the grafting (fiber or mirror) and are very close to the value pH ~7 measured by conventional on site pH sensors.

Existing alternatives to this technique

• Electrochemical measurements with their drawbacks

• Optical bragg grating fiber which needs to be evaluated

Advantages

Real time and remote measurements without any electromagnetic interferences. No need for a periodically controlled reference electrode. Robust technology thanks to covalent grafting.

EURAD (Deliverable n° 17.7) - Synthesis report on Innovative and Enhanced Equipment for Repository Monitoring
Dissemination level: PUBLIC
Date of issue of this report: **04/06/2024**

Page

Distributed Temperature Sensors (DTS) and Thermal Characterization of Rocks (TLS-50) **Partners involved: GFZ, IRSN**	eurad European Joint Programme on Radioactive Waste Management

Rationale:

Clay-dominated geomaterials are often characterized by lower thermal conductivities values compared to other siliciclastic rocks and may show, due to the dominance of oriented sheet minerals, a relevant thermal anisotropy affecting the thermal field. In addition, the low permeable rocks may suffer damage due to thermal-mechanical stresses causing the formation of fractures and pathways for fluid transport. Clay sheet minerals may retain larger volumes of water that may be released at elevated temperatures. Thus, in order to describe the temperature field and its evolution, the initial thermal properties need to be known and a respective measurement technique be installed.

Description of the technology:

DTS: Optical fibre based distributed temperature sensor

Optical fibres are well suited for deployment in tunnels and boreholes as they tolerate harsh environmental conditions, i.e. high pressures and temperatures, or corrosive media, and are immune to electromagnetic interference. Distributed fibre-optic sensing methods allow to record data with high spatial and temporal resolution along a fibre of up to several 10s of km length. Optical fibres are made from amorphous quartz glass (SiO_2). The light scattered back from the fibre optic contains three different spectral shares: Rayleigh scattering, Brillouin scattering and Raman scattering. The Raman scattering is characterized by two maxima („stokes" peak and anti-„stokes" peak). The anti-„stokes" peak is temperature dependent. By division of both amplitudes the temperature at the place of

back-scattering can be calculated because the velocity of propagation within the fibre is known for each amplitude and the doubled travel time of the light until the place of scattering is known (Raman optical scattering, Figure **1**). For more details see Hartog, 2017.
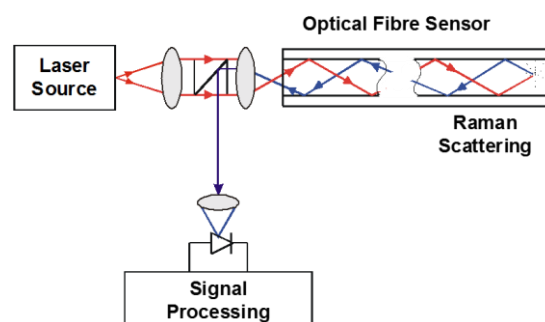
Figure 1 : DTS measurement principle

TLS-50: Transient Line Source 50 mm with measurement platform MP-2

The Measurement Platform-2 (MP-2) of Thermtest is used with a transient thermal conductivity sensor. The sensor wire is heated using a constant current source and the temperature rise is recorded by monitoring the change in electrical resistance of the temperature detector. For samples of high thermal conductivity, resistance increases more slowly over time; for samples of low thermal conductivity, resistance increases more quickly over time. The measurement principle follows the modified ASTM D5334-14 standard.

Specifications:

DTS cable:

The optical cable installed in the project consists of a small, armored fibre optic temperature sensing cable with stainless steel loose tube, stainless steel strength members, fast thermal response, for one polyimide coated optical fibre (Figure 2). It consists of a gel free

eurad
European Joint Programme
on Radioactive Waste Management

EURAD (Deliverable n° 17.7) - Synthesis report on Innovative and Enhanced Equipment for Repository Monitoring
Dissemination level: PUBLIC
Date of issue of this report: **04/06/2024**

Page

central metal loose tube with up to two fibres, shows a high tensile strength and high crush resistance and excellent rodent protection. It is laterally watertight and of compact design, high flexibility, and shows a small bending radius as well as a fast temperature response.
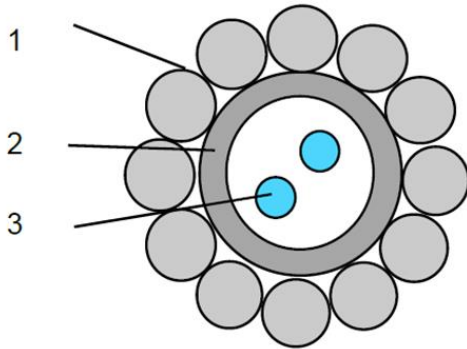
Figure 2 : Fibre Optic Cable of Brugg Sensing Technologies: 1 – stainless steel wires, 2 – stainless steel loose tube, 3 - optical fibres with polyimide primary coating. Diameter of the cable: 2.8 mm

DTS measuring unit

Schlumberger DTS Ultra with the following specifications:

Measuring range	Up to 300°C (limited by cable design)
Temperature resolution	0.02°C
Spatial resolution	0.5m
Temporal resolution	~70s
No. of Channels	4
maximum length	12km
Power supply	230V

TLS-50:

The thermal line source 50 shows a needle length of 50 mm and can be used for testing concrete, rocks, and polymers. The specification of the sensor are as follows:

Measurement Capabilities	Bulk properties
Thermal conductivity (W/m·K)	0.3 to 5
Thermal resistivity (mK/W)	0.2 to 3.3

Measurement Time	3 minutes
Smallest sample size	50 mm in length, 50 mm in diameter
Largest sample size	Unlimited
Accuracy	5%
Reproducibility	2%
Temperature (°C)	-40 to 100°C

What are Technology Readiness Levels of the technology?

Technology Readiness Level (TRL)	initial	final
Basic and applied research (TRL : 1-4)	⚫	⚫
Development (TRL : 5-7)	⚫	⚫
Manufacturing (TRL : 8-9)	🔴	🔴

On field test or advanced test example:

Set up

The DTS cable was installed in 5 boreholes in total. Figure 3 shows the set-up of the cable that was introduced in a lateral borehole section from the tunnel wall and connected to the measuring unit.

A 100 m-breakout cable was connected before and after every well to have a proper connection to the interrogator. To perform a length correlation on the fibre traces, reference temperature spots were set at the well entrance. DTS (distributed temperature sensing) Interrogator, readout computer and an Uninterruptable Power Supply (UPS) were installed in a small cabinet that protects the electronics. Because five boreholes were equipped with optical fibres but the measurement unit covers only four channels, BH1 and BH5 are looped together in one channel.

Beside the preparation of the fibre optic monitoring, the thermal conductivity of the rocks forming the tunnel wall was measured at several points by drilling a small hole into the wall and by placing the needle. Near the ground level, also some measurements perpendicular

EURAD (Deliverable n° 17.7) - Synthesis report on Innovative and Enhanced Equipment for Repository Monitoring
Dissemination level: PUBLIC
Date of issue of this report: **04/06/2024**

Page

to the stratification was possible. In addition, we took samples for laboratory measurements of thermal rock properties.
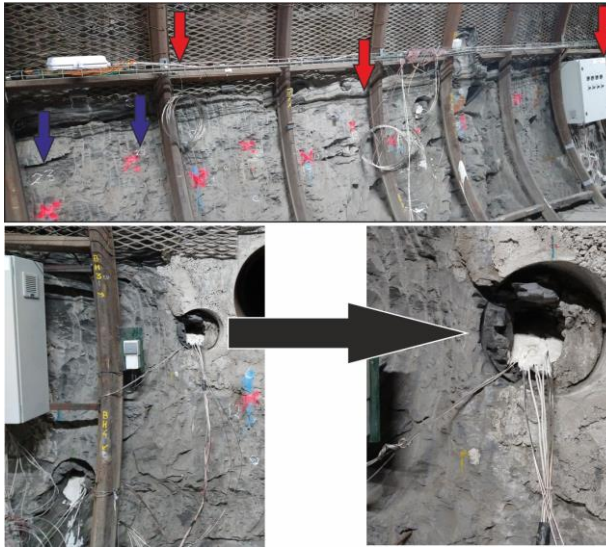
Figure 3: Instrumentation of the DTS cable (red arrows) and measurement points of TLS-50 (blue arrows as example)

Results

The cables were installed in 09/2022 and are recording data since then continuously, providing a long-running baseline for the actual heating experiment (for example see Figure 4). Every T-profile has an integration time of ~70s. As the wells are measured one after another, new T-profiles are recorded every 4:30min for every borehole.
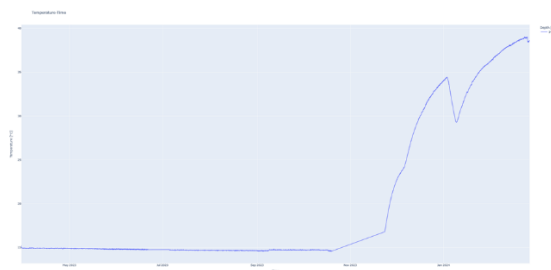
Figure 4: Temperature-Time plot for an 11month period in Borehole BH3, Tournemire. The shown data point is located 14m inside the borehole.

Existing alternatives to this technique (if any):

Advantages

- continuous distributed temperature recording

- detection of small changes
- allows to draw conclusions about involved processes if thermal baseline characterization is given.

Definitions:

Hartog, Arthur H. (2017). <u>An introduction to distributed optical fibre sensors</u>. *Boca Raton.* <u>ISBN</u> <u>978-1-138-08269-4</u>

EURAD (Deliverable n° 17.7) - Synthesis report on Innovative and Enhanced Equipment for Repository Monitoring
Dissemination level: PUBLIC
Date of issue of this report: **04/06/2024**

Page

PART B: Monitoring FEPs: Potential Impacts of Monitoring Equipment on Post-Closure Safety

EURAD (Deliverable n° 17.7) - Synthesis report on Innovative and Enhanced Equipment for Repository Monitoring
Dissemination level: Public
Date of issue of this report: **04/06/2024**

Page i

Executive Summary

Repository monitoring is motivated by the desire to inform decision making, strengthen understanding of system behaviour and to build further confidence in the repository safety case. During the operational period of repository implementation, some waste management organisations (WMOs) might install sensors within the multi-barrier system to conduct such monitoring.

Monitoring Equipment and Data Treatment for Safe Repository Operation and Staged Closure (MODATS) is Work Package (WP) 17 of the European Joint Programme on Radioactive Waste Management (EURAD). The objective of the MODATS WP is to consolidate the implementation strategy for monitoring systems by developing methods through which confidence can be demonstrated in the data acquired and benefits derived for repository implementation.

The EURAD Strategic Research Agenda (SRA) Theme 5 topic calls for an activity "to investigate the impact of monitoring technology on the performance of a range of disposal systems". Sub-Task 3.3 of the MODATS WP provides a contribution to addressing that requirement, through the development of a monitoring features, events and processes (FEP) catalogue, referred to herein as a Monitoring FEPs catalogue. The FEP catalogue identifies and describes ways in which monitoring equipment used during the operational phase could impact the post-closure performance of a repository system.

Monitoring FEPs are expected to have several uses that include:

- Informing the monitoring strategy and design by giving arguments to justify the choice of monitoring system in order to mitigate the potential impacts of monitoring equipment on post-closure safety.
- Providing knowledge to support the development of scenarios involving Monitoring FEPs in order to make robust argumentation in a safety case.
- Identifying future research needs, such as novel monitoring technologies e.g., wireless sensors or monitoring technology test facilities to quantify monitoring FEP impacts.

Owing to the current maturity of monitoring programmes, and differences in monitoring strategies between different repository programmes, the Monitoring FEPs catalogue is generic. Therefore, no conclusion is made on the significance of any of the potential impacts. Given the current expectation that repository monitoring will not involve the intensive instrumentation of the engineered barrier system typically used in underground research experiments, it is envisaged that the Monitoring FEPs identified in this report will not result in impacts on post-closure safety. The Monitoring FEPs will need to be considered during the design of monitoring systems.

The development of the Monitoring FEPs catalogue used a structured process undertaken by experts from WMOs and research entities:

1. Identification of generic monitoring components on the basis of their size, location, distribution, and composition.
2. Consideration of each generic monitoring component to identify possible thermal, hydraulic, mechanical, chemical, gas generation and migration, biological and electromagnetic impacts of the component on post-closure safety.
3. Description of each Monitoring FEP using a standard template.

Eighteen Monitoring FEPs were identified through this process as captured in the matrix presented in Table E.1. As noted above, the impact of monitoring equipment on post-closure performance will ultimately depend on the specific disposal concept and the needs of monitoring as defined by a WMO. The Monitoring FEPs catalogue provides support for the design of monitoring systems, and provides knowledge and information that can be used in the development of programme-specific monitoring FEPs and scenarios associated with the impacts of monitoring equipment left in situ following repository closure.

EURAD (Deliverable n° 17.7) - Synthesis report on Innovative and Enhanced Equipment for Repository Monitoring
Dissemination level: Public
Date of issue of this report: **04/06/2024**

Page ii

Table E-1 Matrix illustrating the Monitoring FEPs and relevant monitoring system components.

Monitoring System Component	Thermal	Hydraulic	Mechanical	Chemical	Biological	Gas	Electromagnetic
Cuboidal and Cylindrical Centimetre-Scale Sensors			7. Void Introduction 8. Volume Change	10. Corrosion of Monitoring System Components 11. Electrochemical Effects 12. Degradation 14. Chemical Interactions 15. Contamination	16. Microbial Activity	13. Gas Generation	
Metre-Scale Linear Sensors	1. Heat Transfer			10. Corrosion of Monitoring System Components 11. Electrochemical Effects 12. Degradation 14. Chemical Interactions			
Fibre Optic Cables		3. Pathway Generation 4. Liquid Transport				5. Gas Transport 13. Gas Generation	
Accelerometers and Geophones						13. Gas Generation	
Sound Waves			17. Sound Wave Propagation				
Electrodes			7. Void Introduction 8. Volume Change	10. Corrosion of Monitoring System Components 11. Electrochemical Effects 12. Degradation 14. Chemical Interactions	16. Microbial Activity	13. Gas Generation	
Electromagnetic Waves							18. Electromagnetic Wave Propagation

EURAD (Deliverable n° 17.7) - Synthesis report on Innovative and Enhanced Equipment for Repository Monitoring
Dissemination level: Public
Date of issue of this report: **04/06/2024**

Page iii

Monitoring System Component	Thermal	Hydraulic	Mechanical	Chemical	Biological	Gas	Electromagnetic
Data Transmission Cables			7. Void Introduction 8. Volume Change	10. Corrosion of Monitoring System Components 11. Electrochemical Effects 12. Degradation 14. Chemical Interactions	16. Microbial Activity		
Wireless Nodes							
Sampling Systems							
Borehole Sampling System		6. Pressure Reduction					
Solid Chemical Batteries				10. Corrosion of Monitoring System Components 11. Electrochemical Effects 12. Degradation 14. Chemical Interactions 15. Contamination		13. Gas Generation	
Thermoelectric Generators	2. Heat Generation						
Electromagnetic Antennae				10. Corrosion of Monitoring System Components 11. Electrochemical Effects 12. Degradation 14. Chemical Interactions			
Power Transmission Cables		3. Pathway Generation 4. Liquid Transport				5. Gas Transport 13. Gas Generation	
Data Transmission Cables							
Data Loggers			9. Collapse			13. Gas Generation	

EURAD (Deliverable n° 17.7) - Synthesis report on Innovative and Enhanced Equipment for Repository Monitoring
Dissemination level: Public
Date of issue of this report: **04/06/2024**

Page iv

Table of Contents

EURAD (Deliverable n° 17.7) - Synthesis report on Innovative and Enhanced Equipment for Repository Monitoring
Dissemination level: Public
Date of issue of this report: **04/06/2024**

Page v

EURAD (Deliverable n° 17.7) - Synthesis report on Innovative and Enhanced Equipment for Repository Monitoring
Dissemination level: Public
Date of issue of this report: **04/06/2024**

Page vi

List of Figures

EURAD (Deliverable n° 17.7) - Synthesis report on Innovative and Enhanced Equipment for Repository Monitoring
Dissemination level: Public
Date of issue of this report: **04/06/2024**

Page vii

EURAD Deliverable 17.7 – Synthesis report on Innovative and Enhanced Equipment for Repository Monitoring

List of Tables

EURAD (Deliverable n° 17.7) - Synthesis report on Innovative and Enhanced Equipment for Repository Monitoring
Dissemination level: Public
Date of issue of this report: **04/06/2024**

Page viii

Acronyms

EBS	Engineered barrier system
ERI	Electrical resistivity imaging
EURAD	European Joint Programme on Radioactive Waste Management
FE	Full-Scale Emplacement
FEP	Features, events and processes
GAST	Gas-Permeable Seal Test
IFEP	International features, events and processes
MODATS	Monitoring Equipment and Data Treatment for Safe Repository Operation and Staged Closure
NEA	Nuclear Energy Agency
POPLU	Posiva Plug Experiment
PVC	Polyvinyl chloride
RTG	Radioisotope thermoelectric generator
SRA	Strategic Research Agenda
TDR	Time-domain reflectometer
URL	Underground research laboratory
WMO	Waste management organisation
WP	Work package
WTB	Wireless Test Bench

EURAD (Deliverable n° 17.7) - Synthesis report on Innovative and Enhanced Equipment for Repository Monitoring
Dissemination level: Public
Date of issue of this report: **04/06/2024**

Page ix

6. Introduction

6.1 Background

Repository monitoring is motivated by the desire to inform decision making, strengthen understanding of system behaviour and to build further confidence in the repository safety case [1]. During the operational period of repository implementation, some waste management organisations (WMOs) might install sensors within the multi-barrier system to conduct such monitoring.

Monitoring Equipment and Data Treatment for Safe Repository Operation and Staged Closure (MODATS) is Work Package (WP) 17 of the European Joint Programme on Radioactive Waste Management (EURAD). The objective of the MODATS WP is to consolidate the implementation strategy for monitoring systems by developing methods through which confidence can be demonstrated in the data acquired and benefits derived for repository implementation. The EURAD Strategic Research Agenda (SRA) Theme 5 topic calls for an activity "to investigate the impact of monitoring technology on the performance of a range of disposal systems" [2]. Sub-Task 3.3 of the MODATS WP provides a contribution to addressing that requirement, through the development of a monitoring features, events and processes (FEP) catalogue, referred to herein as a Monitoring FEPs catalogue.

6.2 Report Objectives

This report presents the Monitoring FEPs catalogue developed with MODATS. It also provides the context to the catalogue, including:

- The approach used to develop the catalogue.
- A commentary on the ways in which the Monitoring FEPs catalogue might be used in repository programmes going forward.

6.3 Scope

It has been recognised for a long time that monitoring, especially the installation of monitoring equipment within the near field has the potential to affect the processes occurring underground. Although not systematically documented, there has been observations made during underground research laboratory (URL) experiments of monitoring equipment impacting near-field processes. Examples include the equipment acting as a conduit for water movement, interactions between host materials and the monitoring equipment corrosion products, and the development of microbial growths on monitoring equipment. The potential for monitoring equipment to have an impact on processes operating underground is exacerbated by the possibility that some equipment could be used for several decades with little or no ability to intervene or otherwise maintain it. The understanding that monitoring equipment could impact processes in the near field has driven technology developments such as wireless transmission of data and development of advanced geophysical monitoring methods for non-intrusive monitoring [1]. In addition, the potential for monitoring equipment to impact post-closure performance is taken into account in monitoring system design [1].

The scope of this work is to capture generic understanding of the way in which monitoring technology and equipment could impact repository post-closure performance. The work is generic because the impact of any particular monitoring system component on repository performance would depend on the relevant safety case, including, for example, the radionuclide inventory considered, the nature of the geological environment, and the disposal concept adopted. Generic understanding is captured in a Monitoring FEPs catalogue as this is considered to be consistent with structured approaches used in post-closure safety assessment in repository programmes.

Furthermore, each repository monitoring programme is developing tailored solutions for monitoring during the operational period that respond to both the safety case and other aspects of the national context, such as the regulatory framework (e.g. requirement for monitoring in a pilot repository in Switzerland [3]). These repository monitoring programmes are under development; detailed plans for

EURAD (Deliverable n° 17.7) - Synthesis report on Innovative and Enhanced Equipment for Repository Monitoring
Dissemination level: Public
Date of issue of this report: **04/06/2024**

Page 1

monitoring of the multi-barrier system, especially the engineered barrier system (EBS), are not yet mature. It is also recognised that different types of monitoring systems will be deployed in different repository programmes. For example, whilst most programmes will use boreholes during site investigation to characterise the geosphere and may extend the use of the boreholes into the monitoring programme, Andra will not drill boreholes from the surface footprint of the repository and, therefore, will not conduct monitoring from surface-drilled boreholes in that surface footprint.

The Monitoring FEPs catalogue provides a first attempt at understanding the potential impacts of monitoring equipment on post-closure safety using a systematic approach. It is anticipated that the generic analysis presented herein could underpin repository programme-specific analyses of the way in which monitoring systems could impact disposal system performance. It is envisaged that use of structured approaches would provide greater underpinning to design, for developing a structured argumentation for use in a safety case, and would support licensing decisions. To serve this purpose, the Monitoring FEPs catalogue aims to be comprehensive and identify all events and processes that might be driven by the presence or use of monitoring equipment.

Although the term "FEPs" has been adopted in this document, it is recognised that there are some differences between the intent and purpose of the Monitoring FEPs catalogue and existing FEP catalogues, for example the Nuclear Energy Agency (NEA) International FEP (IFEP) catalogue [4]. Existing FEP lists are focused on safety assessment, for example, for the identification and development of scenarios and/or conceptual models for performance assessment; to check the completeness of scenarios, conceptual models and/or their implementation in software tools for a particular safety assessment; and as an audit tool to check the completeness of FEP lists developed independently of each other [4].

The FEPs provided in the Monitoring FEPs catalogue could be used in this way. However, a key requirement on monitoring programmes is that they have to be designed and implemented so as not to reduce the overall level of safety of the facility after closure [5]; any potential impacts would be mitigated through design of the monitoring system. Therefore, it is envisaged that the Monitoring FEPs catalogue will mainly be used as a tool to support the design of repository monitoring systems, for example to provide arguments to justify choices made in repository monitoring plans. The structure and content of the Monitoring FEPs catalogue has therefore been developed with this purpose in mind, as explained later in this report.

The scope of this study is the operational period of the repository lifecycle, and the potential impacts of monitoring technology on the multi-barrier systems following their emplacement in the repository. The study assumes that monitoring technology is left in situ. It is recognised that some monitoring equipment could be decommissioned and removed from the repository at the end of the monitoring period, but this study identifies the potential consequences of not doing so, in order to inform design decisions to be made by specific programmes.

This study does not cover system evolutions triggered by undertaking monitoring inconsistent with the design (which could, for example, result in the introduction of different materials to those envisaged in the design) or the implementation plan (e.g., not following quality assurance procedures correctly). It contributes to the development of strategies for repository monitoring and for designing monitoring systems.

No conclusion is made on the significance of the potential impacts because the descriptions of the potential impacts identified during this study are not linked to specific safety cases. As indicated above, there are a wide range of ways that repositories could be monitored. In addition to the specifics of the repository programme mentioned above, any impacts from use of a particular piece of monitoring equipment would depend on how it was used, what period the monitoring covered, and the intensity of monitoring (how much equipment is deployed). However, as the Monitoring FEPs catalogue is comprehensive, there are some FEPs that are included in the catalogue that are unlikely to affect post-closure performance and this is highlighted in the text.

EURAD (Deliverable n° 17.7) - Synthesis report on Innovative and Enhanced Equipment for Repository Monitoring
Dissemination level: Public
Date of issue of this report: **04/06/2024**

Page 2

6.4   Approach

The development of the Monitoring FEPs catalogue used a structured process undertaken by experts from WMOs and research entities:

1. Identification of generic monitoring components on the basis of their size, location, distribution, and composition.
2. Consideration of each generic monitoring component to identify possible thermal, hydraulic, mechanical, chemical, gas generation and migration, biological and electromagnetic impacts of the component on post-closure safety.
3. Description of each Monitoring FEP using a standard template.

The potential impact of monitoring equipment on post-closure safety is likely to be similar for equipment with the same dimensions, distribution within the repository, and composition. Therefore, generic monitoring technologies were identified as a basis for identifying potential impacts.

An initial Monitoring FEP catalogue was developed and presented, discussed, and revised at a three-day dedicated workshop held in Oakham, UK, in April 2023. The workshop was led by Nuclear Waste Services and Galson Sciences Limited, with attendance from Andra and SKB. During the workshop, the initial Monitoring FEP catalogue was restructured and revised extensively, and the catalogue presented in this report was developed. The catalogue has been further enhanced through peer review of this document.

6.5   Document Structure

The remainder of this report is structured as follows:

- Section 2 (Monitoring Systems) presents a generic description of the equipment that could be used to monitor radioactive waste repositories. The description includes the scale and likely materials used in each component of monitoring systems.
- Section 3 (Monitoring FEPs) introduces the Monitoring FEPs catalogue, describes the structure of the catalogue entries and provides a brief description of each Monitoring FEP identified in this work.
- Section 4 (Discussion) section provides a discussion of the FEP catalogue, with some suggestions for the use of the catalogue in developing strategies and designs for monitoring systems, and for assessing any potential impacts of monitoring equipment on post-closure performance.
- Section 5 (Summary) provides a summary of the work.
- Appendix A (Monitoring FEPs Catalogue) presents the Monitoring FEPs catalogue.

EURAD (Deliverable n° 17.7) - Synthesis report on Innovative and Enhanced Equipment for Repository Monitoring
Dissemination level: Public
Date of issue of this report: **04/06/2024**

Page 3

7. Generic Monitoring Systems

This section provides a generic description of monitoring system technology for which Monitoring FEPs can be identified. There is a large range of equipment that could potentially be used in repository monitoring systems. Therefore, each type of technology has been grouped to define a generic list of repository monitoring system components. This simplifies the identification of Monitoring FEPs. Each generic component is summarised in Table 7-1 and subsequently described in greater detail under four categories of equipment:

- **Data acquisition equipment:** the technologies used to acquire monitoring data through conversion of phenomena into a recordable variable (e.g., a voltage). Data acquisition technologies are described in Section 2.1.
- **Power equipment:** the technologies used to provide the power for operation of sensors, data transmission systems and data loggers. Power technologies are described in Section 7.2.
- **Data transmission equipment:** the technologies used to relay raw data to data loggers. Data transmission technologies are described in Section 7.3.
- **Data loggers:** data loggers receive monitoring data and translate the data into parameters. Data logger technologies are described in Section 7.4.

Monitoring equipment includes the materials used to fix the equipment in the required location, such as screws, bolts, glues and resins, and these materials were also considered in the identification of Monitoring FEPs. Monitoring system component descriptions consider the assumed size, geometry, and materials of each generic component. They also consider the expected positioning of sensors and discuss whether they are likely to span multiple barriers of the multi-barrier system. Descriptions were developed from reviews of monitoring technologies that were developed in previous international monitoring projects such as MoDeRn [6] and Modern2020 [1], including the state-of-the-art review of monitoring technologies [7], and in research undertaken in repository programmes (e.g., [8]). Readers are referred to these reports, especially [8], for further details of the monitoring technologies.

Table 7-1: Generic monitoring system components as defined in this study.

Category	Monitoring System Component	Definition	Example
Data Acquisition Equipment	Cuboidal / Cylindrical Centimetre-Scale Sensors	Typically fabricated from metals e.g., stainless steel and various plastics. This categorisation covers sensors installed in a point like fashion. Sensors are typically up to several decimetres in dimension.	Total pressure sensor
	Linear Metre-Scale Sensors	Typically fabricated from metals and plastics. This technology grouping covers linear sensors of a similar scale to the width or diameter of multi-barrier system components from several decimetres up to a few metres.	Extensometer
	Optical Fibre Sensors[1]	A flexible fibre manufactured from plastics or glass that may span several components of the multi-barrier system with a length of up to several kilometres. The diameter of the sensing element is typically less than a millimetre with variable internal structure. Generally, fibre sensors are "packaged" similarly to electrical cables, with several protective layers around the sub-millimetre fibre.	Distributed temperature sensing

EURAD (Deliverable n° 17.7) - Synthesis report on Innovative and Enhanced Equipment for Repository Monitoring
Dissemination level: Public
Date of issue of this report: **04/06/2024**

Page 4

Category	Monitoring System Component	Definition	Example
	Accelerometers and Geophones (Seismic Techniques)	This technology is typically comprised of metals and plastics. Individual components are on the order of decimetres in dimension and are distributed as a connected array and typically installed in a borehole. This technology is used to measure passive and actively generated seismic waves and may also be used to generate seismic waves.	Borehole seismometer
	Sound Waves	Pressure waves which travel through gaseous, liquid, and solid media, and which is generated by active monitoring.	Seismic tomography
	Electrodes (Geoelectric Techniques)	Electrodes are typically made from copper, stainless steel, and plastics. Individual electrodes are a few centimetres to decimetres in scale and arrays may span several metres to decimetres with a few tens of electrodes. This technology grouping is typically used in electromagnetic surveys.	Time domain reflectometry (TDR)
	Electromagnetic Waves	Waves in the electromagnetic field (including lasers and other optical techniques) that may arise from electrodes and other measurement techniques, and from power transmission or data transmission technologies.	Wireless data transmission
	Sampling Systems	Metals and plastics are typically used to manufacture sampling systems; tubes may be a few millimetres to centimetres in diameter with a length of tens of metres and pumps are on the order of a few centimetres in dimension. A sampling system is used to collect either gas or fluid from a component of the multi-barrier system.	Gas sampling system
	Borehole Samplers	Typically fabricated from plastic or stainless steel and attached to a metal support cable. Sampling vials may be a few millimetres to a few decimetres in scale and cabling maybe a few millimetres in diameter and several hundreds of metres in length. This technology may be inserted into a borehole to sample groundwaters or gases.	Groundwater sampler
Power Technologies	Power Transmission Cables[2]	Power transmission cables are typically made from copper and encapsulated in plastics and may be several millimetres to centimetres in diameter and may be up to several hundreds of metres in length. This technology is used to supply power to repository monitoring components.	Power supply cable
	Solid Chemical Batteries	A solid chemical battery typically includes lithium polymers and other metal salts and oxides.	Lithium-ion battery

EURAD (Deliverable n° 17.7) - Synthesis report on Innovative and Enhanced Equipment for Repository Monitoring
Dissemination level: Public
Date of issue of this report: **04/06/2024**

Page 5

Category	Monitoring System Component	Definition	Example
		Chemical batteries have a typical dimension of a few decimetres up to the metre scale. This technology provides electrical power using electrochemical phenomena. It is currently assumed that liquid batteries (e.g., lead batteries), would be excluded from use in monitoring systems.	
	Thermoelectric Generators	Fabricated from stainless steels and a thermocouple material e.g., bismuth telluride. RTGs will also integrate a radioactive source e.g., Americium-241 as a heat source. Thermoelectric generators are expected to be several centimetres to a few metres in dimension. This technology generates electrical power from a temperature gradient and exploits the electromotive force.	Radioisotope thermoelectric generator (RTG)
	Electromagnetic Antennae	Typically comprised of copper, graphite, and plastics. Antenna may could have dimensions of a few metres to a few decimetres depending on the application. This technology can be used to transmit or receive electromagnetic waves.	Electromagnetic power transmission
Data Transmission Technologies	Data Transmission Wires[2]	Data transmission wires are typically made from copper and encapsulated in plastics. They are typically a few millimetres to centimetres in diameter and may be many tens to hundreds of metres in length. This technology is used to transmit electrical signals from a data acquisition technology to a data logger.	Cabling from a sensor to a data logger
	Optical Fibres[1]	A flexible fibre manufactured from plastics or glass that may span several components of the multi-barrier system with a length of up to several kilometres.	Telecom fibres
	Wireless Nodes	Wireless nodes incorporate a range of metals and plastics and have a typical dimension of a few decimetres to a metre. This technology is used to wirelessly transmit data, and include a power supply, electromagnetic antenna, electronic hardware, and data acquisition technologies.	Wireless data logger
Data Loggers	Data Loggers	Data loggers are housed in cabinets and are made from a range of metals and plastics and are on the scale of a few decimetres up to a few metres. This technology used to digitise and store sensor data.	Potentiosat

[1] Optical fibres used for sensing and for data transmission are similar.

[2] Wires used for power transmission and data transmission are similar.

EURAD (Deliverable n° 17.7) - Synthesis report on Innovative and Enhanced Equipment for Repository Monitoring
Dissemination level: Public
Date of issue of this report: **04/06/2024**

Page 6

EURAD (Deliverable n° 17.7) - Synthesis report on Innovative and Enhanced Equipment for Repository Monitoring
Dissemination level: Public
Date of issue of this report: **04/06/2024**

Page 7

7.1 Data Acquisition Equipment

There are a broad range of data acquisition technologies that might be used in repository monitoring (Figure 7-1). Monitoring technologies have been used widely in many URL experiments. The range of technologies and the various ways that these technologies have been applied are summarised in the literature, including [8] and [9]. In this report selected examples are provided to illustrate some ways in which monitoring technologies might be used during repository monitoring.

For this study, the sensors of greatest interest are underground sensors that may be in direct contact with the multi-barrier system, as these are likely to have the most significant impacts on post-closure safety. Examples include resistance temperature detectors and thermocouples for measuring temperature, piezometers for measuring pore pressure, and hygrometers for measuring relative humidity. These sensors are typically made of many different types of metals, ceramics, and plastic components, and have dimensions that are relatively small relative to the scale of the multi-barrier system components in which they are placed (e.g., mm-scale to cm-scale). Some sensors, such as extensometers may have a scale comparable to the multi-barrier system component in which they are placed (e.g., metre-scale sensors).

Other data acquisition technologies that are of interest to repository monitoring include optical fibre systems, geophysical techniques (i.e., seismic, and electromagnetic techniques, which include both the waves and the equipment used to produce and detect them), borehole samplers and sampling systems.

Aerial and surface technologies were not considered in this study as they would not be able to impact post-closure behaviour.
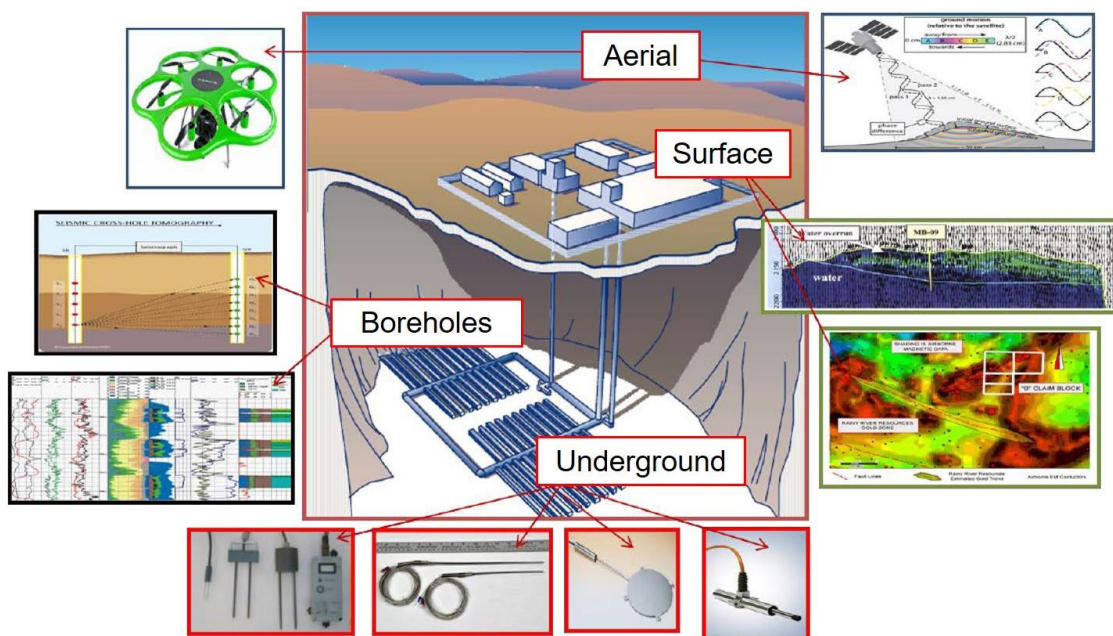
Figure 7-1 - The locations of sensors used for repository monitoring. Note, whilst the majority of programmes will use boreholes during the site investigation programme, Andra will not drill boreholes from the surface within the repository footprint.

7.1.1 Cuboidal and Cylindrical Centimetre-Scale Point Sensors

Cuboidal and cylindrical centimetre-scale point sensors measure a wide range of parameters including temperature, pressure, chemical concentration, saturation and strain. A range of physical phenomena are exploited to measure parameters, e.g., temperature-dependant resistivity, and resonant frequency to measure pressure. Typically, several tens to many hundreds of these sensors maybe deployed in the repository based on experience from URL experiments.

EURAD (Deliverable n° 17.7) - Synthesis report on Innovative and Enhanced Equipment for Repository Monitoring
Dissemination level: Public
Date of issue of this report: **04/06/2024**

Page 8

These types of sensors are typically enclosed in a corrosion-resistant stainless steel or superalloy housing, sometimes the housing includes a filter made of ceramic or plastic (e.g., polytetrafluoroethylene). Internal components are typically fabricated from plastic, silicon (semiconductors and circuit boards), glasses, ceramics, and various metals (e.g., copper, stainless steel, platinum). In some cases, fluids such as oil maybe used as a pressure transmission medium to protect delicate components. Cylindrical sensors typically have a diameter of several millimetres to several centimetres and can be up to tens of centimetres in length, cuboidal sensors are often tens of centimetres in dimension. Centimetre-scale sensors could be placed wholly within the EBS or host rock, or at the interfaces between EBS components or between the EBS and host rock.

7.1.2   Metre-Scale Linear Sensors

Metre-scale sensors are generally used to measure a few parameters that include groundwater flow rate, strain using extensometers, and water matric pressures. Metre-scale potentiometric displacement sensors were deployed in the Full-Scale Emplacement (FE) Experiment (Mont Terri Rock Laboratory, Switzerland, Nagra) to measure the displacement of the heaters [10].

Metre-scale linear sensors are typically housed in stainless steel and may integrate plastics and other metals to facilitate the sealing and motion of sensing components. Internal components are typically constructed from metals such as stainless steel, various alloys, plastics, and fibre glass. Metre-scale linear sensors are those which could traverse multiple components of the EBS and/or the host rock. The length of these sensors is typically from half-a-metre up to a few metres with a diameter of centimetres.

Figure 7-2 Photograph of extensometers used to measure the displacement of heaters in the FE Experiment [10].

![eurad logo] European Joint Programme on Radioactive Waste Management

EURAD (Deliverable n° 17.7) - Synthesis report on Innovative and Enhanced Equipment for Repository Monitoring
Dissemination level: Public
Date of issue of this report: **04/06/2024**

Page 9

7.1.3   Fibre Optic Cables

Fibre optic systems are mainly used to make distributed measurements of temperature and strain, although other uses for fibre optic cables have been or are being developed. Andra has extensively developed and used fibre optic cables during the course of underground heating experiments [11]. The primary use of fibre optic sensors in these experiments was to measure temperature and strain along the external boundaries of simulated waste packages, e.g., during the ALC1605 experiment (Bure, France, Andra) [12].

Materials used to construct fibre optic cables may include glasses and plastics. Fibre optic cables are often installed along an interface of the multi-barrier system and may traverse components of the multi-barrier system. They are typically less than a millimetre in diameter (but they can be installed as a bundle) and may be many hundreds of metres in length, interrogator boxes are typically on the order of tens of centimetres in dimension.

7.1.4   Accelerometers and Geophones

In addition to use for characterising rock, these sensors are used to monitor micro-seismicity that might result from excavation and emplacement activities as well as activity resulting from nearby faults and fractures. Micro-seismic monitoring has been deployed in the ONKALO® excavation in Finland, in particular to monitor possible events relating to the intersection of excavations with faults [13, 14].

These sensors are typically housed in components fabricated from metal, for example stainless steel and will include an internal assembly fabricated from various metals, for example nickel, plastics, and other materials. Accelerometers and geophones are expected to be positioned in boreholes drilled from the surface or underground. This category of sensor is distinct from centimetre-scale sensors since they are typically organised in arrays distributed within a borehole over scales of tens-to-hundreds of metres. Individual sensors are typically less than a decimetre in diameter and may be up to approximately a metre in length.

7.1.5   Sound Waves

Sound waves are used as part of non-invasive seismic surveying which may be used to investigate the velocity structure of a repository. Soundwaves have been used in the Grimsel Test Site URL in Switzerland to investigate the saturation of bentonite buffers based on the inverted velocity structure [15].

Sound waves can be generated using a range of technologies. They are expected to pass through all components of the facility. They are included as a data acquisition technology since they arise as part of active seismological site surveys relating to accelerometers and geophones. Sound waves result from object vibrations and produce pressure waves, these may be actively produced by geophones or vibratory pads mounted on surface vehicles. They may also be associated to arrays of geophones that may be installed in boreholes which are drilled at an angle to the main disposal borehole. Frequencies of 10^2-10^5 Hz are typically associated to in situ active monitoring, corresponding to wavelengths of metre-to-centimetre scale.

7.1.6   Electrodes

Examples of the use of electrodes include TDR, electrical resistivity imaging (ERI) and spectral induced polarisation, providing information on water saturation states. TDR has been used by Nagra to investigate the saturation of bentonite backfill materials in the FE Experiment [16].

Electrodes are normally fabricated from metal rods, typically copper or stainless steel, that may be supported by plastic housing e.g., polyvinyl chloride (PVC), and connected to a monitor, the monitor is typically constructed from a combination of plastics and metal components. Electrodes may be used within various locations within or around the multibarrier system, in particular buffer materials. These systems consist of a sensing element (electrodes) with a typical dimension of tens-of-millimetres to tens-

EURAD (Deliverable n° 17.7) - Synthesis report on Innovative and Enhanced Equipment for Repository Monitoring
Dissemination level: Public
Date of issue of this report: **04/06/2024**

Page 10

of-centimetres in length, electrodes are attached to a monitor which may be on the order of few decimetres in dimension. Electrodes are distinct from Cuboidal and Cylindrical Centimetre-Scale Point Sensors as they typically organised in arrays which may span many metres to tens of metres.

7.1.7 Electromagnetic Waves

Electromagnetic waves would arise in a multi barrier system as part of investigation techniques such as TDR [16], or due to power or wireless data transmission [17]. They are included in data acquisition technologies as they form part of electromagnetic survey techniques. These waves are expected to penetrate all components of the disposal facility. TDR and ERI pass current through a repository generating electromagnetic waves and wireless data and power transmission use electromagnetic waves to transmit data or power.

7.1.8 Sampling Systems

Sampling systems can be used to obtain samples of gas and water, which are typically removed from site for further analysis using laboratory techniques. A sampling system has been deployed in the GAST experiment at the Grimsel Test Facility to monitor gas migration, with sampling tubes passing through a simulated seal in a hypothetical waste repository [18] (see Figure 7-3).

Sampling systems are likely to be plastic based, although they could be made from stainless steel or other metals, valves and pumps are constructed from metals and plastics, filters may be made from porous stainless steel, plastics, or ceramics. Sampling systems are likely to pass through various components of a multi-barrier system and may also be installed within the host rock. Sampling systems comprise tubing of up to a few millimetres in diameter and may also be connected to centimetre-scale cylindrical and cuboidal components which include filters, pumps, and valves (Figure 7-3). Tubes may be bundled together to access multiple sampling points (e.g., as shown in Figure 2-3) which will increase the overall diameter up to the centimetre scale.
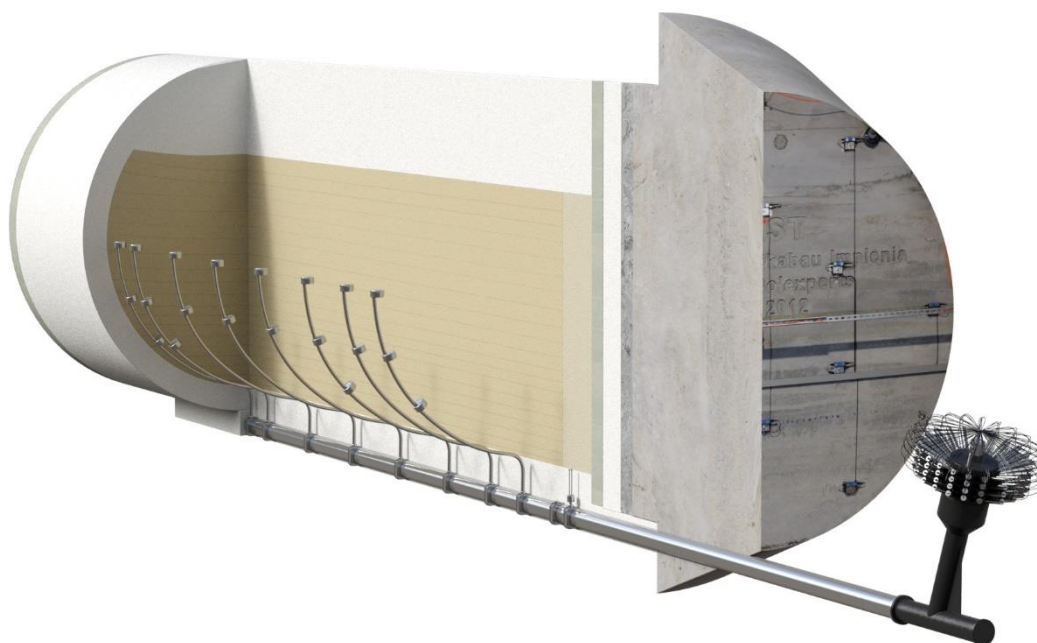
Figure 7-3 CAD image of Gas Permeable Seal Test (GAST) at the Grimsel test facility, the sampling system is distributed throughout the experimental plug [18].

EURAD (Deliverable n° 17.7) - Synthesis report on Innovative and Enhanced Equipment for Repository Monitoring
Dissemination level: Public
Date of issue of this report: **04/06/2024**

Page 11

7.1.9 Borehole Sampling Systems

Sections of boreholes used for sampling are sometimes lined with metal and cement to maintain borehole dimensions, especially in weaker rocks such as claystones. Typical sampling systems are manufactured from stainless steel, plastics that may be lowered and then retrieved from boreholes accessing the geological disposal facility (Figure 7-4). Borehole sampling systems are expected to be contained within the geological barrier. Borehole sampling will vary depending on the repository characteristics and may involve retrieval of gas, groundwater or rock samples which will be taken offsite for further analysis; repository monitoring is most likely to focus on sampling of gas and water, with rock sampling undertaken during characterisation activities. Borehole sampling systems will originate from the ground surface above a repository or underground within a repository and may be on the order of a few metres up to a kilometre in length. Boreholes used for sampling are likely to have a diameter of less than a metre and may be as small as a few centimetres in diameter.

As mentioned above, different types of monitoring systems will be deployed in different repository programmes. For example, Andra will not drill boreholes from the surface footprint of the repository (and, therefore, will not conduct monitoring from surface-drilled boreholes), whereas the monitoring programme of Posiva includes monitoring from boreholes drilled from the surface.

Figure 7-4 Example of a borehole sampling system to retrieve ground water samples[1].

7.2 Power Supply Technologies

The power required to operate sensors is traditionally supplied by power transmission cables or solid chemical batteries, e.g., sodium-ion, lithium-ion, and lithium-thionyl-chloride batteries. Alternatives that have been considered within recent European collaborative research include thermoelectric generators and wireless energy transfer using electromagnetic induction as part of MoDeRn [19] and Modern2020 [20]. This section does not consider diesel power generation as it is considered unlikely to be used in repository monitoring systems (no such proposal is known to the authors).

7.2.1 Power Transmission Cables

Power transmission cables have been used in a wide range of multi-barrier experiments and are used to power a wide range of data acquisition technology, from computers and data loggers through to sensor excitation.

---

[1] Image taken from https://www.rshydro.co.uk/groundwater-monitoring-sampling-equipment/disposable-bailers-discrete-sampling/point-source-bailer/solinst-429-point-source-bailer/ on 17/05/2023

EURAD (Deliverable n° 17.7) - Synthesis report on Innovative and Enhanced Equipment for Repository Monitoring
Dissemination level: Public
Date of issue of this report: **04/06/2024**

Page 12

Power transmission cables are normally fabricated from a copper core which is sheathed in a wide range of plastics (e.g., polyvinyl chloride, fluorinated ethylene propylene), and may be supported by glues (e.g., epoxy), metal trays and plastic or metal cable ties. Power transmission cables will span multiple components of the multi-barrier system. Depending on power requirements an individual cable diameter may range from a few millimetres up to a few centimetres, when cables are bundled together their total cross section may be up to tens of centimetres. Support components such as glues and cable trays may further increase the cross-sectional area.

7.2.2   Solid Chemical Batteries

Solid chemical batteries have been used to provide power to sensors and associated data acquisition technologies and may also form part of other power supply systems. Solid chemical batteries were used to power prototype wireless transmitters as part of both MoDeRn and Modern2020, which were integrated with a range of sensor elements and data acquisition technologies [17, 19].

Solid chemical batteries are expected to contain a metal oxide, graphite, and metal salts (typically lithium based) in an organic solvent which are encased in a combination of plastics and metals. Solid chemical batteries are expected to be positioned close to sensors or associated acquisition equipment and as such may be found in range of locations within the multi-barrier system. They may have a size up to tens of centimetres and will come in range of geometries depending on the application.

7.2.3   Thermoelectric Generators

Thermoelectric generators are electrical generators that exploit thermal gradients to generate electrical power. Temperature gradients may be actively generated by a radioactive source i.e., a radioisotope thermoelectric generator (RTG), or they may passively harvest heat generated from emplaced wastes.

Thermoelectric generators are likely to be housed in stainless steel and may include bismuth telluride as the thermocouple material although other alloys could be considered. For an RTG, americium-241 has been identified as a candidate radioactive source.

Thermoelectric generators are proposed to be installed in close proximity to waste packages, and due to installation requirements, they may traverse the multibarrier system (Figure 7-5). The estimated RTG size would comprise a cylinder or cuboidal unit with a dimension of several decimetres which would be attached to cooling plates that may be up to a few metres in length and a few cm's in thickness [20].

Modelling exercises and device prototyping (without radioactive sources) formed part of MoDeRn2020 [20] as a power source for wireless instrumentation and achieved a proof-of-principle (Figure 7-5). RTG's have been successfully deployed in space missions using Plutonium-238 as the fuel source [21] and are subject to ongoing research in some repository programmes (Figure 7-6).
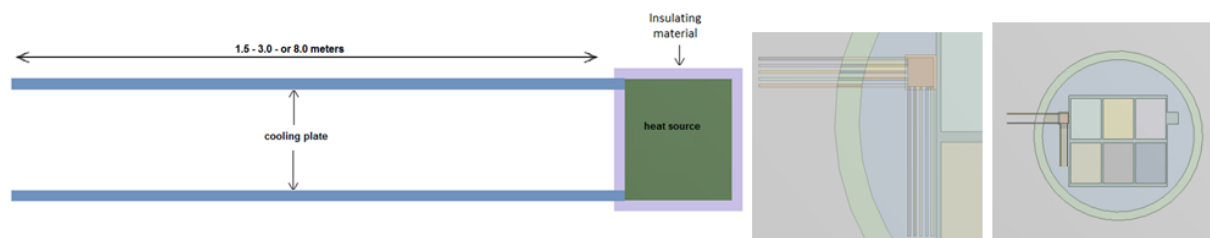
Figure 7-5 Hypothetical RTG installation developed as part of Modern2020 [20]

EURAD (Deliverable n° 17.7) - Synthesis report on Innovative and Enhanced Equipment for Repository Monitoring
Dissemination level: Public
Date of issue of this report: **04/06/2024**

Page 13
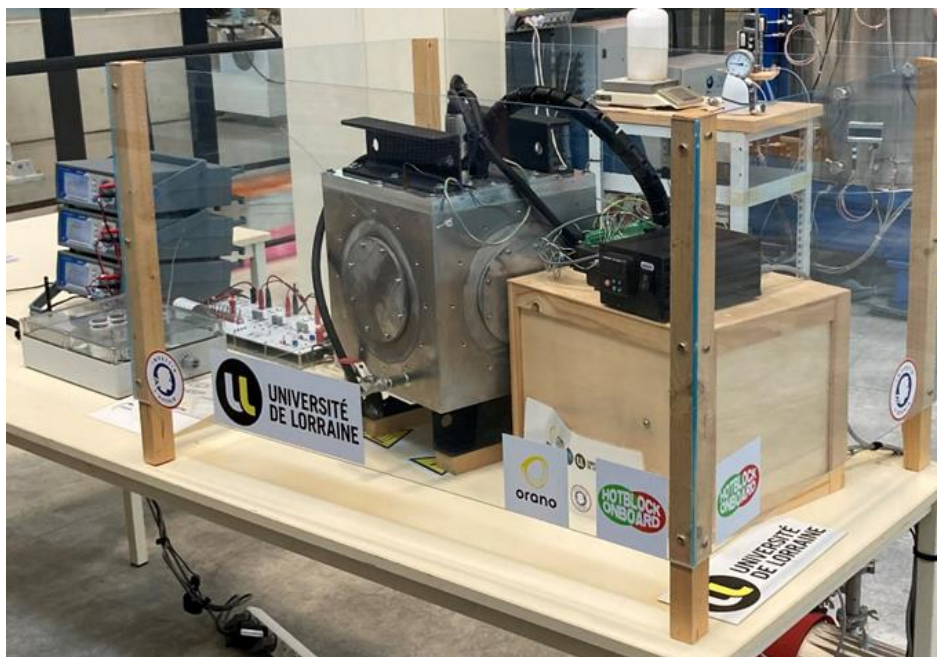
Figure 7-6 Prototype Radioisotope Thermoelectric Generator on display at the ANDRA Technological Exhibition Facility.

7.2.4 Electromagnetic Antennae

Antennae are typically made from copper and may be encased in plastics (e.g., PVC) and are connected to electronic hardware and circuitry which will contain a wide range of materials. Electromagnetic antennae are expected to be found directly behind plugs and seals or within an accessway beyond a plug or seal, they are unlikely to span multiple barriers. Depending on the requisite application they may be anywhere from a few centimetres up to a few decimetres in length or diameter and will take the form of a ring, cylinder, or a single rod of a few millimetres in diameter (Figure 7-7).

EURAD (Deliverable n° 17.7) - Synthesis report on Innovative and Enhanced Equipment for Repository Monitoring
Dissemination level: Public
Date of issue of this report: **04/06/2024**

Page 14

Figure 7-7: Prototype wireless antenna installed in the Tournemire URL (France) as part of Modern2020 [17]

Electromagnetic antenna can be used for two purposes, wireless data transfer or wireless power transfer. Wireless power transmission is currently in a prototype phase. Several underground tests of the technology have been undertaken, for example in Finland [20], but not within a multi-barrier system. Wireless data transmission has also been successfully tested underground, including, for example, within a simulated multi-barrier system in Tournemire URL, France as part of Modern2020 [17] (Figure 7-7).

7.3 Data Transmission Technologies

Data transmission covers any physical hardware used to transmit data between data acquisition technologies and data loggers. These may be wired or wireless and will be found in various locations throughout the multi barrier system and are likely to remain in place after repository closure. Optical fibres are also used to transmit data but the description as described in Section 2.1.3.

7.3.1 Data Transmission Cable

Data transmission cables are used to transmit analogue or digital signals from sensors to various data acquisition technologies. This technology has been widely deployed in a wide range of multi-barrier systems, in the POPLU experiment (Onkalo, Finland, Posiva), stainless steel tubing was used to provide additional protection to data transmission cables (Figure 7-8) [22]. Data transmission cables are typically of a multicore construction with copper cores surrounded by layers of plastic insulation (e.g., PVC), and possibly meshed copper to act as shielding. In some cases, wiring may be housed in stainless steel tubing to provide further protection from the multi-barrier system. Data transmission cables may, in the absence of wireless technologies, cross multiple EBS components. Data transmission cable will have a total cross-sectional diameter of a few millimetres up to a few centimetres and may be bundled together which further increase the total diameter.

EURAD (Deliverable n° 17.7) - Synthesis report on Innovative and Enhanced Equipment for Repository Monitoring
Dissemination level: Public
Date of issue of this report: **04/06/2024**

Page 15
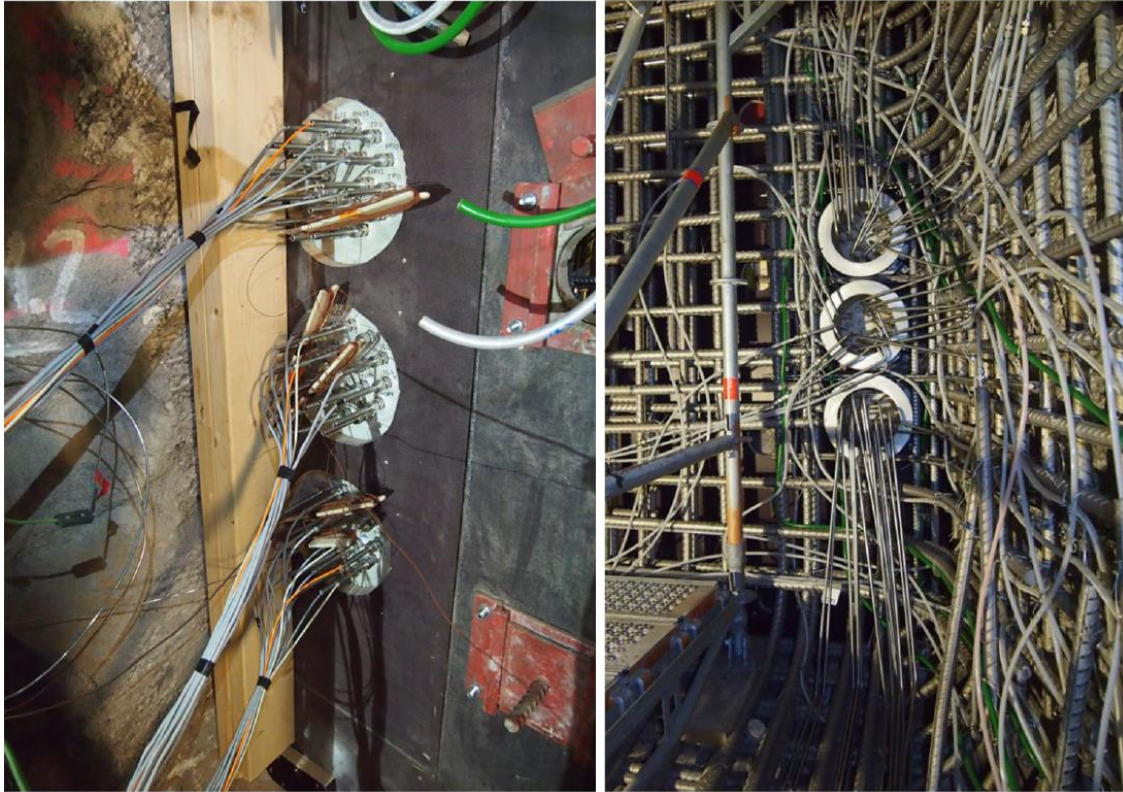
Figure 7-8 Data transmission cables installed as part of the POPLU experiment in ONKALO, Finland [22]

7.3.2   Wireless Node

Wireless nodes are used to replace the need for wired data transmission cables that traverse the multi-barrier system and may integrate a wide range of point sensing components e.g., thermocouples, pressure, relative humidity. Wireless nodes have been deployed in a range of multi-barrier systems including the Wireless Test Bench (WTB) experiment [16] in the Tournemire URL in France. In the WTB experiment a prototype wireless node was used to measure and transmit measurements of humidity (psychrometer) and temperature for a period of 6 months.

Devices in this category may include materials such as stainless steel, copper, plastics, and lithium-polymer batteries, in particular plastic has been used as the enclosure medium in previous prototype devices. Wireless nodes may be placed within a single component of the multi-barrier system, or at an interface between two components of the multi-barrier system and could remain in place after repository closure. Typical wireless nodes constitute a sensor, power supply and an antenna enclosed within housing of an overall length scale of several decimetres to metres, existing designs have used a cylinder with a diameter on the order of several centimetres (see Figure 7-9).

EURAD (Deliverable n° 17.7) - Synthesis report on Innovative and Enhanced Equipment for Repository Monitoring
Dissemination level: Public
Date of issue of this report: **04/06/2024**

Page 16
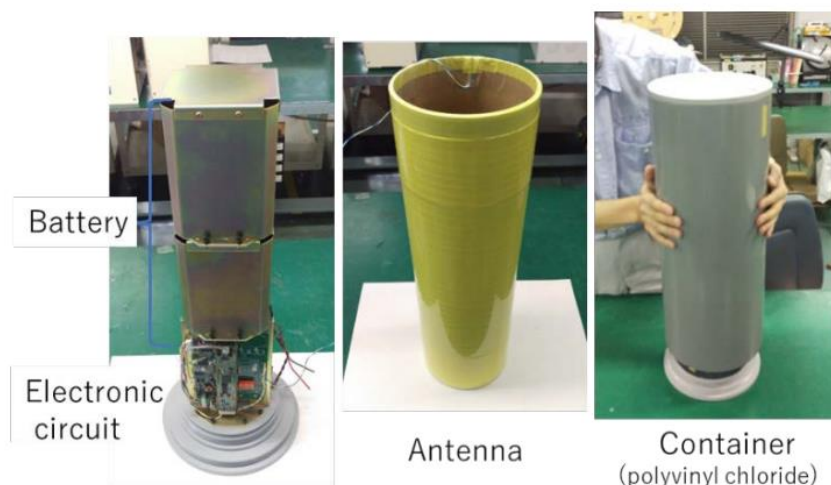
Figure 7-9 Example of a prototype wireless node deployed in the Tournemire URL, France. After Modern2020 [17].

7.4 Data Loggers

Data logging is done in an accessible location, but there might be a case made in the future to dispose of the data logger underground.

7.4.1 Data Logger

Data loggers are used to temporarily store raw data from sensors installed in the multi-barrier system and will be connected to data communication cables and power supply cables. There may be greater use of wireless technologies in the future. All underground monitoring systems are likely to include a data logging system, although they may become redundant with the emergence of novel technologies. For this study, we include optical fibre system interrogators in this category.

Data loggers are typically fabricated from metals (e.g., aluminium) and plastics, electrical hardware made from a wide range of materials including metals (e.g., copper, iron, aluminium) and plastics, additional peripheral devices such as monitors may also be considered. In addition, uninterruptible power supplies containing chemical batteries could form part of the data logger. Data loggers could be placed within access galleries, centrally within the repository or at the surface. Although it is currently envisaged that data loggers would be removed during the closure of the repository (or before), there is a possibility that they may be left in place. In the general case, data loggers comprise electrical hardware in cabinets of the order of tens of centimetres up to a few metres scale.

EURAD (Deliverable n° 17.7) - Synthesis report on Innovative and Enhanced Equipment for Repository Monitoring
Dissemination level: Public
Date of issue of this report: **04/06/2024**

Page 17

8.   Monitoring FEPs

The Monitoring FEPs catalogue that is included in this report follows a consistent structure as defined in Table 8-1. Each FEP is given a sequential identification number and short title, categorised as a feature, event or process, and defined by a high-level description which outlines the key characteristics of the FEP. Monitoring system components relevant to the FEP are identified alongside examples of the FEP occurring or not occurring within real-world monitoring programmes, and mitigation strategies to minimise or eliminate the FEP described. Finally, a row is provided for any salient comments and references are provided.

Table 8-1 Structure and content of Monitoring FEP descriptions as developed in this study.

Title	A short title describing the FEP.
Category	Identify if FEP is a feature, event, or process.
Description	A general description of the feature, event of process. This is a fundamental physical, chemical, biological, or other category of description. The description includes details of what the FEP is, what conditions are required for the FEP to occur, and what components of the multi-barrier system the FEP interacts with.
Relevant Monitoring System Components	A generic description, supported by examples, of the monitoring system component that could cause the FEP to exist or occur. This description could include description of relevant dimensions, compositions, and structure of the monitoring system component.
Potential Relevance to Performance and Long-Term Safety	Description of how the monitoring system component might affect long-term system performance or safety, including uncertainties and concept specific issues where identified.
Examples of the FEP	Examples of the FEP occurring or not occurring. Examples are largely from URL experiments, but other analogues could be included, i.e., groundwater abstraction, mining, and tunnelling.
Mitigations	Description of how any potential impact of the FEP could be mitigated through selection of monitoring component (e.g., use of different materials in the sensor), design of the monitoring system (e.g., sensor positioning) or changes to the multi-barrier system.
Comments	Any other information that may be relevant to the FEP.
References	Any references used to develop the FEP description.

Eighteen monitoring FEPs were identified using the approach described in Section 6.4. The Monitoring FEP catalogue is presented in Appendix A. The description of each FEP is provided below. Additionally, Table 8-2 provides a matrix to illustrate the Monitoring FEPs that are relevant to each generic monitoring system component.

EURAD (Deliverable n° 17.7) - Synthesis report on Innovative and Enhanced Equipment for Repository Monitoring
Dissemination level: Public
Date of issue of this report: **04/06/2024**

Page 18

Table 8-2 Matrix illustrating the Monitoring FEPs and relevant monitoring system components.

Monitoring System Component	Thermal	Hydraulic	Mechanical	Chemical	Biological	Gas	Electromagnetic
Cuboidal and Cylindrical Centimetre-Scale Sensors			7. Void Introduction 8. Volume Change	10. Corrosion of Monitoring System Components 11. Electrochemical Effects 12. Degradation 14. Chemical Interactions 15. Contamination	16. Microbial Activity	13. Gas Generation	
Metre-Scale Linear Sensors	1. Heat Transfer			10. Corrosion of Monitoring System Components 11. Electrochemical Effects 12. Degradation 14. Chemical Interactions			
Fibre Optic Cables		3. Pathway Generation 4. Liquid Transport				5. Gas Transport 13. Gas Generation	
Accelerometers and Geophones						13. Gas Generation	
Sound Waves			17. Sound Wave Propagation				
Electrodes			7. Void Introduction 8. Volume Change	10. Corrosion of Monitoring System Components 11. Electrochemical Effects 12. Degradation 14. Chemical Interactions	16. Microbial Activity	13. Gas Generation	
Electromagnetic Waves							18. Electromagnetic Wave Propagation

EURAD (Deliverable n° 17.10) - Monitoring FEPs: Potential Impacts of Monitoring Equipment on Post-Closure Safety
Dissemination level: Public
Date of issue of this report: **xx/xx/2024**

Page 19

Monitoring System Component	Thermal	Hydraulic	Mechanical	Chemical	Biological	Gas	Electromagnetic
Data Transmission Cables			7. Void Introduction 8. Volume Change	10. Corrosion of Monitoring System Components 11. Electrochemical Effects 12. Degradation 14. Chemical Interactions	16. Microbial Activity		
Wireless Nodes							
Sampling Systems							
Borehole Sampling System		6. Pressure Reduction					
Solid Chemical Batteries				10. Corrosion of Monitoring System Components 11. Electrochemical Effects 12. Degradation 14. Chemical Interactions 15. Contamination		13. Gas Generation	
Thermoelectric Generators	2. Heat Generation						
Electromagnetic Antennae				10. Corrosion of Monitoring System Components 11. Electrochemical Effects 12. Degradation 14. Chemical Interactions			
Power Transmission Cables		3. Pathway Generation 4. Liquid Transport				5. Gas Transport 13. Gas Generation	
Data Transmission Cables							
Data Loggers			9. Collapse			13. Gas Generation	

EURAD (Deliverable n° 17.10) - Monitoring FEPs: Potential Impacts of Monitoring Equipment on Post-Closure Safety
Dissemination level: Public
Date of issue of this report: **xx/xx/2024**

Page 20

During the process of identifying and developing monitoring FEPs, several were discounted as they were considered to be out of scope. These are:

- Cross contamination.
- Density reduction.
- Hydrogen donor.

Cross contamination is a process that describes mixing of groundwaters within a borehole that intersect formations with distinct groundwater compositions. This FEP is already considered in the existing IFEP list (Borehole Sealing FEP 3.1.4) [4] and, therefore, was not also considered here.

Density reduction is a process that describes the reduction in density of an engineered material e.g., bentonite buffer, by the inclusion of a monitoring system component. This monitoring FEP has not been included in the final catalogue as considered to be covered by FEP 7 Void Introduction (see Section 8.7).

The FEP Hydrogen Donor describes compounds that contain abstractable atoms of hydrogen which can lead to the corrosion of multi-barrier system components. This monitoring FEP was not considered further as it is considered within the scope of FEP 14 Chemical Interactions (see 8.14).

8.1   Heat Transfer

Heat transfer is a process that describes the movement of thermal energy along a temperature gradient from high to low temperature. Heat transfer is relevant to linear metre-scale sensors which have a thermal conductivity at least an order of magnitude higher than natural materials (e.g., rock). Linear metre-scale sensors would be relevant if these are positioned close to a heat source e.g., a container of spent nuclear fuel, and transfer heat across multiple barriers. Their impact is dependent on their thermal conductivity, size, location, and the number of installed sensors. The increase in thermal conductivity from a barrier material to a monitoring system component material could be large, and heat transfer could be accelerated, but the monitoring system components are small, therefore, the amount of heat transfer is unlikely to be significant. Increased thermal conductivity would not increase the overall thermal input to the system, and is likely to only result in minor changes to local temperatures. If the use of linear metre-scale sensors was extensive, the effects might have to be taken into account in coupled thermal-hydraulic-mechanical modelling.

8.2   Heat Generation

Heat generation is the process of increasing thermal energy which results in an increase in temperature. This FEP considers monitoring system components that generate heat. RTGs exploit temperature gradients created by radioactive decay to generate electricity. The use of RTGs has been frequently proposed as a solution to energy supply for monitoring equipment and conceptual designs for RTGs have been developed within the Modern2020 project [1]. The placement of a heat-generating RTG may result in heating of the EBS or host rock. Temperature increases would be dependent on the scale at which RTGs would be used. Modelling of RTGs in a proof-of-principle study indicated that temperature increases of ~5 C might occur around an intermediate-level waste vault [20]. Localised temperature increases may drive coupled processes and accelerate gas generation in the vicinity of an RTG that might need to be considered in the safety case. However, the use of RTGs is only conceptual at present; should large-scale use of RTGs be proposed, the temperature impacts on performance would have to be understood. Other sources of heat generation, such as joule heating relating to power consumption in sensors (which is in the milliwatt regime) and exothermic chemical reactions resulting from degradation and corrosion are considered to generate negligible heat.

EURAD (Deliverable n° 17.10) - Monitoring FEPs: Potential Impacts of Monitoring Equipment on Post-Closure Safety
Dissemination level: Public
Date of issue of this report: **04/06/2024**

Page 21

8.3   Pathway Generation

Pathway generation is a process resulting in the creation of a significant, continuous, and discrete relative permeability increase with respect to the surrounding medium. Pathways could be formed by additional holes, power cables, data cables, tubing and fibre optic cables. The potential relevance of the pathway would depend on its length, the materials along the pathway, the expected evolution of the pathway, and the pathway position with respect to radionuclide transport pathways. Creation of pathways has the potential to create radionuclide transport pathways and to decrease travel times. It is expected that pathway generation would be taken into account during design of a repository monitoring system – no potentially significant pathways should be introduced during implementation of monitoring.

8.4   Liquid Transport

Liquid transport describes the process of movement of a liquid phase through connected pore space under a pressure gradient (advection) or by chemical potential (diffusion). Liquid transport can be single phase or multiphase when acting in conjunction with gas transport (see Section 8.5). Relevant monitoring system components are power cables, data cables, tubing and fibre optic cables, i.e., any long linear materials that could connect or create pathways (Monitoring FEP 3). Liquid transport could occur along:

- Corroded or degraded material.
- Gaps in equipment.
- Gaps between equipment and host media.

The potential impact of liquid transport would depend on the location of the pathway and system conductivity. Localised pathways, unconnected to the system would not result in connected transport through the repository system. As for Pathway Generation (Monitoring FEP 3), it is expected that pathway generation would be taken into account during design of a repository monitoring system, and that no potentially significant pathways should be introduced during implementation of monitoring. Mitigation through sealing of pathways would have to consider the potential lifetime of sealing materials.

8.5   Gas Transport

Gas transport is the process of the movement of a gaseous phase and can be single phase or multiphase when coupled to fluid transport (see Section 8.4). This FEP considers gas transport driven by monitoring technology groups, which are, data transmission cables, power cables, borehole sampling systems (tubing) and fibre optic cables. The relevant monitoring equipment, potential impacts and mitigations are the same as for Liquid Transport (Monitoring FEP 4).

8.6   Pressure Change

Pressure change refers to the process whereby pressure is reduced by the removal of fluids during groundwater and pore water sampling, or increased owing to the introduction of mass during borehole testing (e.g. slug tests). Pressure reduction arises in borehole sampling systems and may impact repository function by altering the fluid flow regime in the vicinity of the sample site. However, reduction in pressures would be expected to be negligible compared to the reduction in pressures associated with repository construction and operation, and changes in pressures associated with natural processes, such as significant climate variations during the assessment period (e.g. glaciations). The period over which any pressure reduction would occur would be limited to the monitoring period plus the time that the system would take to recover from any perturbation. The most significant impact is likely to be the potential to introduce cross-flows along boreholes or between boreholes, and this could be mitigated through design of any borehole sampling programme and the use of packer systems to isolate borehole sections.

EURAD (Deliverable n° 17.10) - Monitoring FEPs: Potential Impacts of Monitoring Equipment on Post-Closure Safety
Dissemination level: Public
Date of issue of this report: **04/06/2024**

Page 22

8.7   Void Introduction

Void introduction is the process of increasing the total porosity within a system. This FEP can be associated with all monitoring technologies as nearly all monitoring technologies contain voids. The void space in any single sensor is usually small, although some prototype sensors and transmission antennae do have more significant void space (see Figure 7-9). Therefore, the significance of this FEP is dependent on the number of devices used and their location within the multi-barrier system. Potential impacts would be to cause pathway formation or other mechanical damage, to host favourable locations for microbial activity, or to reduce density of components of the multi-barrier system (e.g. bentonite buffer). Placement within a buffer with tight requirements on density would require significant miniaturisation and specific placement, and would need to be carefully assessed in the safety case. However, the small void space of many sensors is unlikely to cause significant impacts if located appropriately.

8.8   Volume Change

Volume change refers to the process of volume evolution of monitoring equipment, which can increase e.g., through the generation of expansive iron corrosion products, or decrease e.g., mass loss through dissolution. The potential impact on system performance would be to cause deformation of surrounding materials (expansion) of the formation of voids (reduction). This FEP is applicable to all monitoring system components as they all have the potential to corrode or degrade. Expansion is most relevant to iron-based metals, which corrode under anaerobic conditions to form magnetite, which has a greater volume than iron or steel. The loads in the repository would likely counter much, if not all, expansion and expansion could also be accommodated by voids within monitoring equipment. The impact of volume reduction would have to be considered during the design and is dependent on the number of sensors used, the materials of which they are composed, and their distribution in the repository.

8.9   Collapse

Collapse is an event describing mechanical failure, characterised by displacement of a medium, in particular, the collapse of the EBS or host rock. This FEP is most likely to be driven by the presence of data loggers in the repository following closure or the collapse of boreholes. Data loggers and their associated cabinets could have significant internal void space. Should they be left *in situ* following closure, rather than being removed the potential for their collapse and the propagation of the collapse into other components of the near-field could lead to the generation of pathways. However, these pathways are most likely to be separated from the waste owing to the location of data loggers in accessible locations during repository operation. The potential for borehole collapse is expected to be mitigated through borehole backfilling and sealing.

8.10   Corrosion of Monitoring System Components

Corrosion of monitoring system components refers to the process whereby a metal surface undergoes mass loss caused by chemical or electrochemical action from the surrounding medium under non-equilibrium conditions. This FEP can be applied to any metallic component installed in a repository and is therefore likely to apply to all monitoring technologies excluding sound waves and electromagnetic waves.

Corrosion could cause Volume Change (Monitoring FEP 8), Gas Generation (Monitoring FEP 13), and Chemical Interactions (Monitoring FEP 14). The potential for corrosion to drive these processes sufficiently to impact safety needs to be taken into account during design and is linked to the rates at which corrosion might occur and the mass of monitoring materials left *in situ* (e.g., high rates of corrosion of large amounts of monitoring equipment could create a gas phase). However, this FEP is readily mitigated through design, including appropriate distribution of monitoring equipment and choice of

EURAD (Deliverable n° 17.10) - Monitoring FEPs: Potential Impacts of Monitoring Equipment on Post-Closure Safety
Dissemination level: Public
Date of issue of this report: **04/06/2024**

Page 23

materials (e.g., use of sensors constructed from titanium or nickel if considered appropriate and use of coatings).

8.11   Electrochemical Effects

This process considers two electrochemical effects:

- Galvanic coupling between metals with differing oxidisation potential, which can enhance corrosion. Galvanic corrosion occurs when different metals are in contact with each other, allowing the free flow of electric current between the two; the corrosion rate of the most reactive metal is enhanced due to the formation of a macroscopic electrochemical ('galvanic') cell with the less reactive material supporting the cathodic reaction.
- The introduction of electrical current into the multi-barrier system, which can alter redox conditions.

Galvanic coupling can be driven by the presence of monitoring technologies with metallic components that are installed within the multi-barrier system. Similarly, a wide range of monitoring equipment is operated using electrical currents and is therefore relevant to this FEP. This FEP could impact the safety case if it causes a significant effect on multi-barrier corrosion or on groundwater chemistry, but it is envisaged that effects will be small, localized, and (in the case of flow of electrical currents) time-limited to the operation of the monitoring system. Therefore, there is expected to be little significance to post-closure safety.

8.12   Degradation

Degradation refers to the process of breakdown of non-metallic materials within the monitoring system, which can generate acids and gases. Monitoring systems could contain organic materials e.g., polymers used in cabling and glues used for fixing of monitoring equipment in place, both of which could be left in a repository on closure. Degradation of cables could lead to pathway formation and could result in the formation of:

- Gases, for example CO_2 or methane.
- Acids, which could react with cementitious materials.
- Complexants (e.g. acetate), which could degrade further giving rise to gas and/or influence radionuclide mobility by modifying sorption and solubility.
- Nutrients for microbial activity (for example, the degradation of plastic pipes might enhance microbial activity).
- Degradation may increase or decrease the volume of the system.

As the mass of materials introduced by the monitoring system is anticipated to be small, and the materials distributed, it is not anticipated that this FEP would impact the post-closure safety case, but the FEP would have to be considered during design.

8.13   Gas Generation

This FEP refers to the process of gas generation resulting from corrosion and degradation of monitoring system components and also to radiolytic gas generation. Gas generation resulting from corrosion and degradation may be driven by all monitoring system components. Radiolytic gas generation may be driven by the use of RTGs. The significance of any gas generation to the safety case would depend on number of monitoring sensors used and their distribution. Gas generation can be mitigated during design of the monitoring system through the use of alternative materials or metals (e.g., replacing steel with titanium or nickel, and using coatings on organic materials such as cable insulation.

EURAD (Deliverable n° 17.10) - Monitoring FEPs: Potential Impacts of Monitoring Equipment on Post-Closure Safety
Dissemination level: Public
Date of issue of this report: **04/06/2024**

Page 24

8.14   Chemical Interactions

Chemical interactions could occur between the corrosion or degradation products of monitoring system components, and other repository components e.g., waste forms, EBS and the host rock. This FEP could be driven by all repository monitoring components and covers complexation, the generation of corrodents (e.g., H_2S through microbial processes and degradation of organic compounds) and alteration (e.g., redox reactions, mineralogical changes, and dissolution). This FEP could impact the safety case if the products generated enhance radionuclide migration significantly. As for Gas Generation (Monitoring FEP 13), mitigation would be to use appropriate use materials.

8.15   Contamination

Contamination is the addition of a hazardous material for a monitoring purpose. Hazardous materials that could be introduced in the monitoring system include, for example:

- Cadmium, lead, zinc, manganese, nickel, silver, mercury and lithium, which could be included in batteries.
- Oils in certain sensors (e.g. total pressure sensors).
- Radionuclides in RTGs.

The frequency, location and concentration of introduced sources needs to be considered with regards to each safety case; localised use of materials may be acceptable if justified. Any materials that threaten the safety case if used above a certain quantity only be used in the monitoring system in limited amounts.

8.16   Microbial Activity

The process of microbial activity describes the growth and decline of microbes in the repository, with growth requiring energy and nutrient sources, and the action of these microscopic organisms on the materials used in the monitoring system. Monitoring equipment could introduce organic materials such as cellulose and polymers into the repository, which would provide nutrients for metabolism of microbes if they degrade. Furthermore, microbial activity could be driven by all repository components that lead to, or are susceptible to, Void Introduction (Monitoring FEP 7), Corrosion (Monitoring FEP 10), and Degradation (Monitoring FEP 12).

Possible impacts of microbial activity include:

- Degradation of organic materials and the subsequent generation of gases.
- Microbially-influenced corrosion, for example, localised corrosion resulting from generation of aggressive species such as sulphides from microbial activity.
- Controlling the redox potential of environments relevant to the geological disposal of radioactive waste by iron(III)-reducing species.
- Changes to the chemical form of some radioelements, such as uranium, technetium, neptunium and plutonium and for certain radionuclides such as carbon-14.

The potential impact of microbial activity should be limited in design of the monitoring system and assessed in the safety case.

8.17   Sound Wave Propagation

Sound wave propagation is the transmission of pressure through a medium as it travels away from a mechanical perturbation leading to acceleration of the medium through which the perturbation propagates. Acceleration could lead to shaking, redistribution of materials (e.g., settling of granular materials) and/or collapse (e.g., collapse of waste packages in vaults that have not been backfilled). However, the amplitudes of within-rock motions as a result of the passage of waves are small, and significantly smaller than micro-seismic events that the disposal facilities will be designed to withstand. This FEP is therefore not considered significant.

EURAD (Deliverable n° 17.10) - Monitoring FEPs: Potential Impacts of Monitoring Equipment on Post-Closure Safety
Dissemination level: Public
Date of issue of this report: **04/06/2024**

Page 25

8.18   Electromagnetic Wave Propagation

Electromagnetic wave propagation is the propagation of electric fields (generated by coupled oscillations of electrical and magnetic fields) through a medium in order to transfer data or power. This FEP is driven by electromagnetic waves which are actively generated as part of monitoring activities and are linked to electrodes, electromagnetic antennas and wireless nodes. The presence of the electric fields could lead to the generation of electrical currents (see Monitoring FEP 11), and electrical currents can drive the diffusion of contaminants. The use of electric fields for contaminated land remediation is common but electric fields that would be generated in a repository monitoring system are expected to be weaker. Furthermore, the monitoring period is expected to coincide with the period when contaminants are isolated and contained within the engineered barrier system. Therefore, this FEP is unlikely to be significant to the safety case.

EURAD (Deliverable n° 17.10) - Monitoring FEPs: Potential Impacts of Monitoring Equipment on Post-Closure Safety
Dissemination level: Public
Date of issue of this report: **04/06/2024**

Page 26

9.   Summary and Discussion

This study was a first of a kind analysis, which introduced the concept of a monitoring FEP and has systematically identified the FEPs through which monitoring equipment used during the operational phase could impact the post-closure performance of a repository system. Many of the potential impacts have previously been recognised, and have affected decisions on monitoring research, development, and demonstration. For example, providing a driver for the development of wireless data transfer technologies, optical fibre systems and the miniaturisation of sensors.

In most cases, previous recognition of potential monitoring equipment impacts on post-closure performance has not been underpinned by systematic identification and description of Monitoring FEPs. The structured work undertaken herein provides a sound basis upon which to develop robust and comprehensive argumentation within the safety case and to develop an adequate monitoring programme that will have no significant impact on the post-closure performance of the disposal system. It can also be used to provide a transparent and traceable approach to assessing the potential impacts from leaving monitoring equipment *in situ* following closure. It is anticipated that use of structured approaches would provide greater underpinning to design and support to licensing decisions.

Eighteen Monitoring FEPs were identified through which monitoring could affect post-closure performance. For each FEP, the catalogue entry provides a description of the FEP, it's potential impact and possible approaches to mitigate these impacts. The potential impacts of monitoring FEPs depend on a specific disposal concept. The structured nature of the catalogue descriptions, including the discussion of how the materials used, the density of monitoring equipment used, the location in which sensors might be placed and decisions on decommissioning monitoring equipment, provides a good basis for programme-specific investigations of the impact of monitoring technology on the performance of a range of disposal systems as called for in the EURAD SRA Theme 5 topic.

It should also be noted that many of the processes identified in the Monitoring FEPs catalogue will occur even if a monitoring system is not present. Consideration of the potential impact of monitoring processes should evaluate whether the monitoring equipment would cause any significant increase to the impact of these processes (in many cases, the monitoring equipment and its use would not cause a significant increase). Also, it should be recognised that the impact of monitoring equipment and its use is both localised and time-limited, which will reduce the potential impacts on system performance.

It is envisaged that the Monitoring FEPs catalogue will provide a starting point for WMOs to evaluate proposed monitoring system designs and to determine if the equipment defined in the design could impact post-closure performance. If potentially significant detrimental impacts are identified, it is expected that the WMO would refine its monitoring strategy in order to mitigate the impacts. Monitoring programmes have to be designed and implemented so as not to reduce the overall level of safety of the facility after closure [5]. Refinements could include changing the positioning of monitoring technologies in order to avoid placing them at critical locations, using different technologies, changing the materials used in monitoring equipment or changing the extent to which monitoring was undertaken. Mitigation strategies could be developed on the basis of Monitoring FEPs, and these are included in individual FEP catalogue entries.

EURAD (Deliverable n° 17.10) - Monitoring FEPs: Potential Impacts of Monitoring Equipment on Post-Closure Safety
Dissemination level: Public
Date of issue of this report: **04/06/2024**

Page 27

Appendix B. Catalogue of Monitoring FEPs

Title	**1. Heat transfer**
Category	Process
Description	Heat transfer is the movement of thermal energy (joules). The process always occurs from a region of higher temperature to a region of lower temperature, as described in the second law of thermodynamics. The most relevant mechanism for heat transfer associated with monitoring system components is thermal conduction. The differential form of the law of heat conduction (Fourier's law) shows that the local heat flux density, q, (the amount of energy that flows through a unit area per unit time) is equal to the product of thermal conductivity, k, and the negative local temperature gradient, $-\nabla T$. $$q = -k\nabla T$$
Relevant Monitoring System Components	**Relevant Monitoring System Components: Linear metre scale sensors.** Relevant monitoring system components are linear metre scale sensors, in particular if located near a heat source and spanning an entire barrier that has insulating properties significant to the disposal concept, for example a barrier with a heat buffer safety function. For example, metallic extensometers may span disposal vaults. Thermistors may have stainless steel sheaths 6 mm in diameter and 135 mm in length. The thermal conductivity of monitoring system components is typically higher than of rock and engineered barriers. Therefore, monitoring system components may provide preferential pathways for heat transfer. **Their potential relevance is dependent on their thermal conductivity, size, location and number of devices (or density of placement).** Stainless steel thermal conductivity is 15 W/(mK) which is relatively low for a metal but an order of magnitude higher than a representative value for rock. Copper thermal conductivity is 380-400 W/(mK). Location is important because it determines the potential temperature gradient across a component. Significant temperature gradients may exist in heat generating waste disposal areas.
Potential Relevance to Performance and Long-Term Safety	**The potential impact is an increase in temperature of the engineered barrier and host rock above a threshold.** Maximum temperature requirements/constraints may exist. For example, bentonite buffer safety function may be impaired by high temperatures. Thermal dimensioning is the process of positioning heat generating waste to achieve maximum temperature limits. Thermal dimensioning may need to account for the monitoring system components increasing its complexity. Depending on location the effect could be an advantage or a disadvantage, if the temperature constraint is on the waste then it may be an advantage but if the constraint is on the engineered material or rock then it may be a disadvantage. **However, it is unlikely to be significant.** The increase in thermal conductivity from a barrier material to a monitoring system component material may be large but the monitoring system components are small, therefore, the amount of heat transfer is unlikely to be significant. Long features are likely to be thin, therefore, extra heat transfer along them will be dissipated radially like a 2D line source/loading condition.

EURAD (Deliverable n° 17.10) - Monitoring FEPs: Potential Impacts of Monitoring Equipment on Post-Closure Safety
Dissemination level: Public
Date of issue of this report: **04/06/2024**

Page 28

Examples of the FEP	Extensometres in the FE Experiment bridged the heater to the host rock across the bentonite backfill (Figure A1). Thermal modelling of the FE experiment did not need to include the extensometres to fit the temperature profile.

FE instrumentation phase 3b (heater)
- Fibre optical cable
- Temperature / Humidity
- Thermal conductivity
- Pressure cell
- Extensometer
- Gas sampling port / gas sensors
- Corrosion coupons
- Fixation
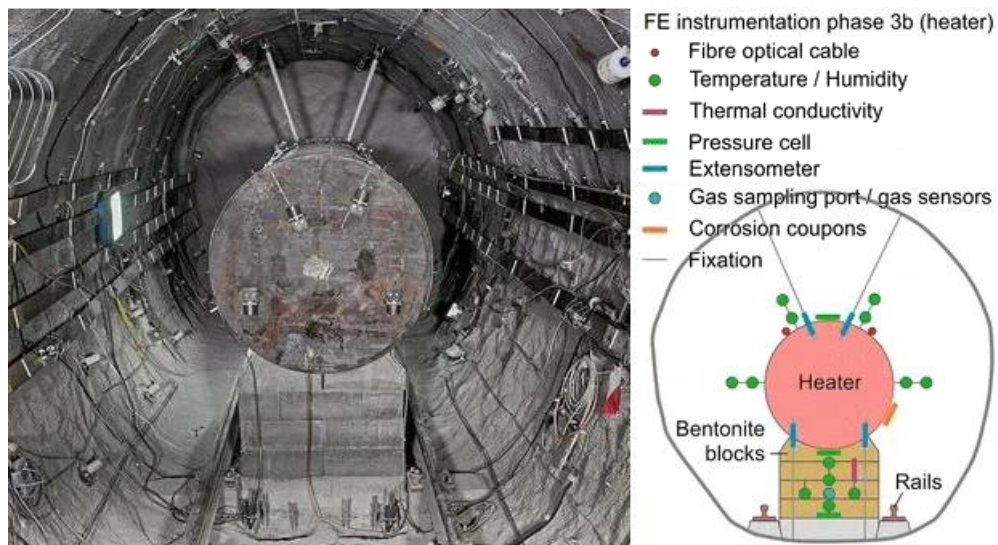
Figure 10 (Nagra, 2019) photo of a bentonite block pedestal supporting a heavily instrumented heater in the FE tunnel. Right: illustration of the FE heater instrumentation showing the location of the extensometers and their fixations. The fixations can be seen in the photo bridging the heater to the host rock across the bentonite barrier.

Mitigations	Not needed with the current understanding based on experience from MODATS, because there is not currently anticipated to be extensive numbers of linear metre scale sensors that cross these barriers.
Links to other FEPs	None because the extent of this process is unlikely to drive coupled processes.
Comments	
References	Nagra, 2019. Implementation of the Full-scale Emplacement Experiment at Mont Terri: Design, Construction and Preliminary Results, Technical Report NTB 15-02.
Title	**2. Heat generation**
Category	Process
Description	Heat generation describes the process of increasing thermal energy and is measured in watts (W), defined as one joule per second. An increase in temperature is associated with heating. Heating is observed when a body generates heat energy (joules) and when a body is the recipient of heat transfer. This FEP considers monitoring system components that generate heat, whereas heat transfer is considered in FEP 1.
Relevant Monitoring System Components	**Relevant Monitoring System Components: radioisotope thermoelectric generators** The monitoring system components identified as potentially generating significant heat are power technologies, specifically radioisotope thermoelectric generators. Thermoelectric generators generate electrical power almost directly proportional to the temperature difference between their hot and cold sides.

EURAD (Deliverable n° 17.10) - Monitoring FEPs: Potential Impacts of Monitoring Equipment on Post-Closure Safety
Dissemination level: Public
Date of issue of this report: **04/06/2024**

Page 29

A temperature gradient of at least 6.9 °C is needed to generate electricity by an RTG.

The normal power consumption of sensors is in the milliwatt range so can be dismissed. Similarly the heat generation from exothermic chemical reactions (degradation and corrosion) is negligible.
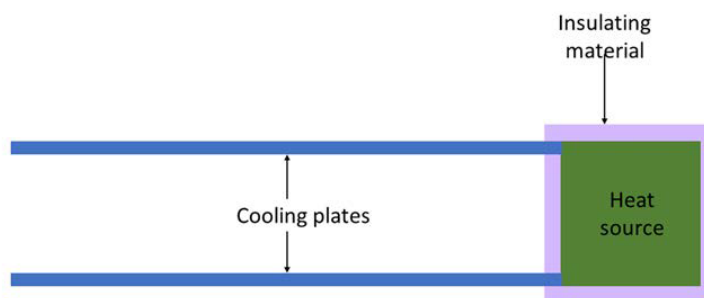
Figure 11 Schematic view of a radioisotope thermoelectric generator. Cooling plates may be composed of a compound such as bismuth telluride (Modern2020. 2019).

Potential Relevance to Performance and Long-Term Safety	Heating associated with a thermoelectric generator needs to be taken into account to ensure that maximum temperature limits on engineered materials and host rock are not exceeded. If installed within the thermal field of heat generating waste then the heating of a thermoelectric generator would be additive to the heating of the waste. However, the extent of high temperatures associated with a thermoelectric generator is likely to be minimal.
	This temperature gradient would drive coupled processes on a localised scale within the repository. However, these are unlikely to be significant as they would be localised and not likely to be emplaced near to high heat generating waste, to be additive.
Examples of the FEP	None observed noting that radioisotope thermoelectric generators are not standard technology for monitoring at present.
Mitigations	Not needed with the current understanding based on experience from MODATS.
Links to other FEPs	None because the extent of this process is unlikely to drive coupled processes. An increase in temperature may affect all other processes but the increase will not be significant.
Comments	Radioisotope thermoelectric generators are not standard technology for monitoring at present. They have been considered as a power supply for wireless data transfer and proof of principle was developed in Modern 2020 but significant further research would be required before these can be deployed.
	The additive effect of heating associated with waste might be mitigated by combining a thermoelectric generator module with an energy management device. The resultant technology is a thermoelectric harvester. Feasibility analysis conducted in the Modern2020 project showed that it is possible to use the heat generated by radioactive decay in high level waste to supply power to wireless sensing units in the EBS.
References	Modern2020. 2019. Project Synthesis – Repository Monitoring: Strategies, Technologies and Implementation (Deliverable D6.5)

Title	**3. Pathway generation**
Category	Process
Description	Generating a significantly continuous and discrete increase in permeability relative to the surroundings. This could be represented as an open aperture or a region with

EURAD (Deliverable n° 17.10) - Monitoring FEPs: Potential Impacts of Monitoring Equipment on Post-Closure Safety
Dissemination level: Public
Date of issue of this report: **04/06/2024**

Page 30

higher permeability. These pathways may be formed by tubes, wires, cables, internal and external interfaces, removal, degradation, failure.

Relevant Monitoring System Components	**Relevant Monitoring System Components: power and data cables, tubing, fibre optic.** The potential relevance is related to the component length, materials (in particular interfaces), expected evolution (including degradation and removal), and location. These can be installed as single entities or bundles and bundles may be more relevant. Figure 12 Data transmission cables installed as part of the POPLU experiment in ONKALO, Finland (DOPAS 2016).
Potential Relevance to Performance and Long-Term Safety	Relevant monitoring system components could change the travel pathway and travel time for radionuclides. Bundles are more likely to generate significant pathways. A pathway may undergo self-healing if within swelling (e.g. clay host rock, bentonite) or creeping (e.g. evaporite) materials which may decrease the relevance.
Examples of the FEP	The Sandwich Seal Experiment at the Mont Terri Rock Laboratory observed leakage within wire insulation between June and August 2021. Water bypassed barrier layers within the experiment because of the size and location of the cables.
Mitigations	Wireless data transmission may remove the need for the components. Decommissioning, removal of the sampling system and plug installation may seal the pathway. Resealing after removal of bundles.
Links to other FEPs	This FEP is strongly linked to FEP 4 Liquid transport and FEP 5 Gas transport. It is also linked to FEP 7 Void introduction and formation and FEP 8 Volume change.
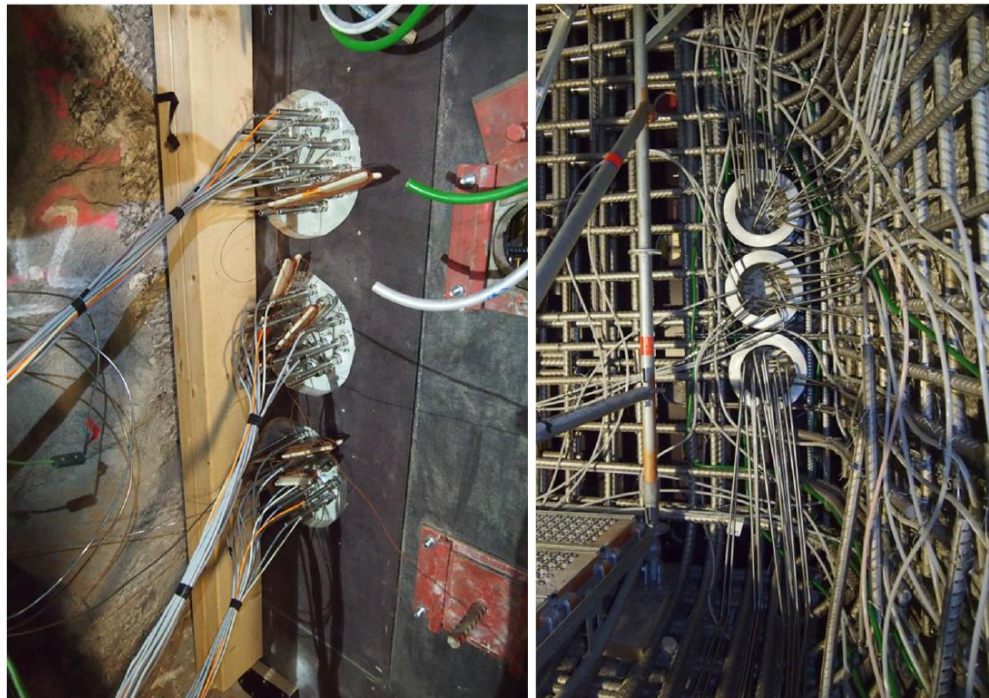
EURAD (Deliverable n° 17.10) - Monitoring FEPs: Potential Impacts of Monitoring Equipment on Post-Closure Safety
Dissemination level: Public
Date of issue of this report: **04/06/2024**

Page 31

Comments	There is a possible feedback loop whereby the engineered materials or host rock could affect the monitoring system component (e.g. mechanical failure of tubing) and then that generates a pathway.
References	K. Wieczorek, K. Emmerich, R. Schuhmann, J. Hesser, M. Furche, D. Jaeggi, S. Schefer, J. Aurich, J.C. Mayor, S. Norris, K. Birch, M. Sentis, J.L. García-Siñeriz, F. Königer, U. Glaubach, C. Rölke, and R. Diedel 6(2021). Large-scale testing of a sandwich shaft-sealing system at the Mont Terri rock laboratory. SaND Conference Abstract, 1, 133–135,. https://doi.org/10.5194/sand-1-133-2021.

Title	**4. Liquid transport**
Category	Process
Description	Liquid transport is the movement of a liquid phase. This may occur as single phase flow in a fully saturated condition or in conjunction with gas transport (FEP 4) in a partially saturated condition. Single phase flow in a porous medium can be modelled using the Darcy fluid flux, q_f, equation: $$q_f = -\frac{k}{\mu}(\nabla p_f - \rho g)$$ where k is permeability, μ is fluid viscosity, ∇p_f is the pore pressure gradient, ρ is fluid density and g is acceleration due to gravity. Darcy's law is valid for viscous flow, in particular flow with a Reynold's number <1 but up to 10 may still be considered using Darcy fluid flux. Liquid transport may also occur by diffusion from a region of higher concentration to a region of lower concentration, i.e., across a gradient in Gibbs free energy or chemical potential. This FEP considers preferential liquid transport pathways associated with monitoring system components. The source could be groundwater or derived from waste or engineered barrier system materials e.g. from corrosion.
Relevant Monitoring System Components	**Relevant Monitoring System Components: Data transmission wires, energy transmission wires, sampling tubing and fibre optic cables.** The potential relevance of a monitoring system component is dependent on its permeability, size and location. The permeability must be higher than the medium in which it is installed which is likely because engineered barrier materials and host rocks are typically characterised by low permeability. The size must be of significance as a pathway. The location is important because it determines the potential pore pressure gradient across a component and could combine with the size to bypass a barrier. Data transmission wires, energy transmission wires, sampling tubing and fibre optic cables may have a relatively high permeability and be significantly long. Transport may occur within the wire itself, e.g. within the wire insulation, and/or at the interface between the wire and the engineered barrier system material or host rock. Wires connecting piezometers might be expected to be within a pressure gradient and wires connecting thermocouples are likely to span thermally pressurised gradients.
Potential Relevance to Performance and Long-Term Safety	Enhanced liquid transport along a pathway may increase the amount of radionuclide transport. A worst case scenario is component size and location combining to create a preferential pathway that bypasses a barrier entirely. A pathway through a clay host rock and engineered barrier materials is likely to be added to diffusion. In crystalline rock the pathway would only be relevant if it connected with the fracture network in at least two locations otherwise it is isolated.

EURAD (Deliverable n° 17.10) - Monitoring FEPs: Potential Impacts of Monitoring Equipment on Post-Closure Safety
Dissemination level: Public
Date of issue of this report: **04/06/2024**

Page 32

Examples of the FEP	The Sandwich Seal Experiment at the Mont Terri Rock Laboratory observed leakage within large electrical resistivity tomography cable insulation between June and August 2021. Water bypassed barrier layers within the experiment because the size and location of the cables.
Mitigations	This FEP can be mitigated by mitigating the pathway generation FEP in the first place.
	Alternatively this FEP can be mitigated by sealing the pathway ends by installing plugs or segmenting the pathway using connectors and/or cable clamps to limit flow.
	The Sandwich Seal Experiment at the Mont Terri Rock Laboratory successfully mitigated water transport within wire insulation by filling the inside of cables with synthetic resin. This method was tested and found to have an upper pressure limit of 2.3 MPa, above which the cables were found to burst.
Links to other FEPs	This FEP is strongly linked to FEP 3 Pathway generation and FEP 5 Gas transport.
Comments	Single phase flow is the flow of one state of matter, regardless of the composition, such as vapor, liquid or gas. A fully saturated condition is required for single phase flow. Liquid transport and gas transport are likely to occur coevally in a partially saturated porous medium.
	This FEP has covered pressure driven flow. It is also possible to have buoyancy driven liquid flow driven by chemical coupling and density gradients.
References	
Title	**5. Gas transport**
Category	Process
Description	Gas transport is the movement of a gas phase. This may occur as single phase flow in a fully desaturated condition or in conjunction with liquid transport (FEP 3) in a partially saturated condition.
	Gas transport may occur by advection (Darcy flow, see FEP 4 Liquid transport) and/or diffusion. Diffusion from a region of higher concentration to a region of lower concentration, i.e., across a gradient in Gibbs free energy or chemical potential. For gas diffusion, Fick's law relates the diffusive flux to the gradient of the concentration: $$q_g = -D \frac{\partial C}{\partial z}$$ where q_g is the gas flux, D is the gas diffusion coefficient, C is the gas concentration, and z is the depth.
	This FEP considers preferential gas transport pathways associated with monitoring system components. The source could be groundwater or derived from waste or EBS materials during e.g. corrosion. The flow may be driven by pressure gradients or buoyancy/density-gradient driven.
Relevant Monitoring System Components	**Relevant Monitoring System Components: Data transmission wires, energy transmission wires, sampling tubing and fibre optic cables.**
	The potential relevance of a monitoring system component is dependent on its permeability, size and location. The permeability must be higher than the medium in which it is installed which is likely because engineered barrier materials and host rocks are typically characterised by low permeability. The size must be of significance as a pathway. The location is important because it determines the potential pressure

EURAD (Deliverable n° 17.10) - Monitoring FEPs: Potential Impacts of Monitoring Equipment on Post-Closure Safety
Dissemination level: Public
Date of issue of this report: **04/06/2024**

Page 33

	and density gradient across a component and could combine with the size to span multiple barrier components and bypass a barrier.
Potential Relevance to Performance and Long-Term Safety	Enhanced gas transport along a pathway (FEP 3 Pathway generation) may increase the amount of radionuclide transport. A worst case scenario is component size and location combining to create a preferential pathway that bypasses a barrier entirely.
	A pathway through a clay host rock and engineered barrier materials is likely to be added to diffusion and interact with liquid transport. In crystalline rock the pathway could only be relevant if it connected with the fracture network in at least two locations.
	The gas transport along a pathway can also increase inflow of gases from ventilated areas into seals. This is mainly relevant during the operation phase and during partial saturation.
Examples of the FEP	In LASGIT (Cuss et al 2022) implementation the monitoring system was designed to prevent this FEP, since the objective was to study gas migration in an undisturbed bentonite barrier. The measures taken were successful and no gas transfer to place in sensors or cables.
Mitigations	This FEP can be mitigated by mitigating the pathway generation FEP in the first place, e.g. wireless data transmission.
	Alternatively this FEP can be mitigated by sealing the pathway ends by installing plugs or segmenting the pathway using connectors and/or cable clamps to limit flow.
	The Sandwich Seal Experiment at the Mont Terri Rock Laboratory successfully mitigated fluid (including gas) pathways within wire insulation by filling the inside of cables with synthetic resin. This method was tested and found to have an upper pressure limit of 2.3 MPa, above which the cables were found to burst.
Links to other FEPs	This FEP is strongly linked to FEP 3 Pathway generation and FEP 4 Liquid transport.
Comments	Single phase flow is the flow of one state of matter, regardless of the composition, such as vapor, liquid or gas. A fully saturated condition is required for single phase flow. Liquid transport and gas transport are likely to occur coevally in a partially saturated porous medium.
References	

Title	**6. Pressure Reduction**
Category	Feature/Event
Description	Groundwater sampling has been proposed in some programmes via boreholes to monitor the evolution of the groundwater chemistry and flow regime in the disposal system, however, in other programmes the use of boreholes in this way is ruled out. This FEP is describing a transient pressure reduction caused by groundwater sampling.
	Withdrawal of groundwater from the system during the conduct of monitoring activities will reduce the groundwater pressures and can have an impact on flow. It may take time for the groundwater conditions at the local disturbance to equilibrate.
Relevant Monitoring System Components	**Relevant Monitoring System Components: borehole sampling system.**
	The potential relevance of a monitoring borehole is related to the geological environment and total sample volume. Boreholes can be from the surface or underground. These boreholes are drilled and can be drained and sampled.

EURAD (Deliverable n° 17.10) - Monitoring FEPs: Potential Impacts of Monitoring Equipment on Post-Closure Safety
Dissemination level: Public
Date of issue of this report: **04/06/2024**

Page 34

Potential Relevance to Performance and Long-Term Safety	This could change the flow field by changing direction and slope of pressure gradients. This may be significant if the disturbances are large, however, this is unlikely.
	The potential significance of boreholes to affect the geological environment is related to strategy – design, placement, sealing, etc.
	This FEP completely excludes human intrusion.
Examples of the FEP	Posiva active monitoring programme at Olkiluoto. At Olkiluoto changes in the flow regime have been identified, however, these have been predominantly driven by excavation of the underground.
Mitigations	The impact of this FEP is mitigated by the design and placement of the boreholes and any sampling strategy conducted within them.
Links to other FEPs	This is related to cross-contamination/short-circuiting which was determined to be out of scope as a FEP since it is related to boreholes generally rather than monitoring.
Comments	
References	
Title	**7. Void introduction and formation**
Category	Process
Description	Void introduction and formation is an increase in total porosity within a system. The new porosity may be inherent within a monitoring system component or created as part of the installation process.
Relevant Monitoring System Components	**Relevant Monitoring System Components: all components installed underground.**
	The installation of any monitoring system components is expected to introduce voids in the disposal system. These are likely to be small volume. They can occur between the monitoring equipment and the multi-barrier system or host rock, e.g. behind sensors fixed on an interface. They can also occur within the monitoring equipment itself, e.g. within protective sensor housing or inherently within filters which are voids by definition.
Figure 13 Components of a vibrating wire piezometer (Geokon, 2021). There are inherent voids within the filter and filter housing at the end of the equipment and surrounding the vibrating wire. There may be additional voids not represented in this illustration that relate to manufacturing.
Potential Relevance to	Quantities and sizes of voids associated with monitoring equipment are unlikely to be significant. However, their potential relevance to performance and long-term safety is
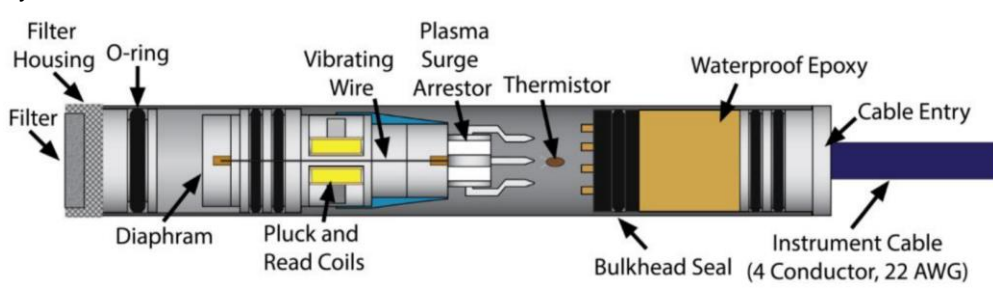
EURAD (Deliverable n° 17.10) - Monitoring FEPs: Potential Impacts of Monitoring Equipment on Post-Closure Safety
Dissemination level: Public
Date of issue of this report: **04/06/2024**

Page 35

Performance and Long-Term Safety	causing increased permeability, decreased mechanical stability, and/or increased microbial activity (FEP 16).
	Increased permeability can be understood by considering the Kozeny-Carman equation (Carman, 1956) for absolute (single phase) permeability:
	$$\kappa = \Phi_s^2 \frac{\epsilon^3 D_p^2}{180(1-\epsilon)^2}$$
	where κ (m^2) is absolute permeability, Φ_s is the sphericity of the particles, ϵ is porosity, and D_p is the average diameter of the particles. Increasing porosity will generally cause increasing permeability. Additionally, the size and shape of the porosity is important, considered in the equation as the diameter and sphericity of particles. Larger voids with smoother capillaries contribute to increased permeability.
	Voids may undergo structural changes due to waste related perturbations (e.g., heat generation) and/or time dependent deformation (e.g., visco-plastic behaviour). Void migration is the concern that distributed voids within a disposal vault could migrate towards interfaces and coalesce, thereby, reducing the mechanical support that a barrier may be providing to another barrier or the host rock. In turn, this could inhibit the closing of excavation damage zone fractures.
	Voids may undergo self-healing if within swelling (e.g., clay host rock, bentonite) or creeping (e.g., evaporite) materials. Self-healing is similar to undergoing structural changes but distinguished here by the absence of the void migrating elsewhere. Self-healing will decrease the relevance of voids towards permeability and microbial activity.
Examples of the FEP	This FEP is pervasive. All monitoring systems are expected to introduce voids. However, this is typically small volume and not studied.
Mitigations	Monitoring system component design will inherently avoid unnecessary void space within the monitoring system components where it is reasonably achievable. If this FEP requires mitigating then there is a motive to further reduce void space within monitoring system components, therefore, making more changes reasonably achievable. This could include miniaturisation of monitoring system components to reduce the internal void space.
	Furthermore, mitigations are possible for when voids are introduced surrounding the monitoring equipment during installation. These include improving installation strategies to reduce the size and frequency of voids being introduced alongside the monitoring system components. Similarly reducing voids after they are formed by grouting during installation. Miniaturisation of monitoring system components may also reduce the void space introduced during installation.
Links to other FEPs	This is related to FEP 3 Pathway generation, FEP 8 Volume change, FEP 9 Collapse, FEP 10 Corrosion, FEP 12 degradation, and FEP 16 Microbial Activity.
Comments	
References	P.C. Carman, "Flow of gases through porous media." Butterworths, London, 1956.
	Geokon, Model 4500 Series Vibrating Wire Piezometer Instruction Manual. www.geokon.com, 2021.
Title	**8. Volume Change**
Category	Process

EURAD (Deliverable n° 17.10) - Monitoring FEPs: Potential Impacts of Monitoring Equipment on Post-Closure Safety
Dissemination level: Public
Date of issue of this report: **04/06/2024**

Page 36

Description	Volume change is related to the volume evolution of monitoring system components. This may be an increase or decrease in volume. Volume expansion is anticipated to be caused by less dense corrosion and degradation products, e.g., expansive corrosion products of iron-based materials (Fe304, Fe(OH)2, Fe304). Volume reduction is anticipated to be caused by mass loss, corrosion, degradation, and mechanical effects.
Relevant Monitoring System Components	**Relevant Monitoring System Components: all components installed underground.** The potential relevance of a monitoring system component is related to its expected evolution on repository timescales.
Potential Relevance to Performance and Long-Term Safety	Volume reduction may lead to expansion of the clay rock or bentonite into the void and, therefore, density reduction and/or pathway formation. Density reduction may be related to loss of strength and pathway formation may be related to a potential increase in radionuclide transport. Volume expansion may lead to pressurisation. Pressurisation is particularly important for concrete because it may cause cracking.
Examples of the FEP	FEBEX pressure cells were placed between bentonite blocks and subsequently failed under high stress caused by bentonite swelling (García-Siñeriz et al., 2019). In this example the volume change being considered is the pressure cells failing and undergoing some compaction rather than the bentonite swelling which is the cause of the failure. The pressure cell failure will have released some of the bentonite swelling pressure although it is unlikely to have been significant.
Mitigations	The significance of volume change can be mitigated by having a preference for using materials that are stable over repository timescales (e.g. titanium). Risks associated to loss of strength or pressurisation can be mitigated during design of the monitoring system, by placing sensors in locations with anticipated low strain if mechanical failure is a risk or not within concrete if pressurisation is a risk.
Links to other FEPs	Links to FEP 7 Void introduction and formation, FEP 3 Pathway generation, FEP 10 Corrosion, and FEP 12 Degradation.
Comments	
References	José Luis García-Siñeriz, María Rey Mazón, Florian Kober, Toshihiro Sakaki. Performance of THM monitoring instrumentation in FEBEX bentonite barrier after 18 years of operation under repository-like conditions. Geomechanics for Energy and the Environment. Volume 17, March 2019, Pages 75-89.
Title	**9. Collapse**
Category	Event
Description	Collapse is a mechanical failure event that can be characterised by the displacement of material. This FEP considers collapse of the engineered barrier or host rock. Corral et al. (2022) presents mechanical modelling for void migration in a generic geological disposal facility. Figure A5 illustrates this concept for waste package voidage, however, this FEP considers the possibility of a similar evolution scenario arising from monitoring system voidage. Small monitoring system components may collapse but are described in FEP 8 Volume change. Collapse is loosely used to include propagation and opening of fractures.

EURAD (Deliverable n° 17.10) - Monitoring FEPs: Potential Impacts of Monitoring Equipment on Post-Closure Safety
Dissemination level: Public
Date of issue of this report: **04/06/2024**

Page 37
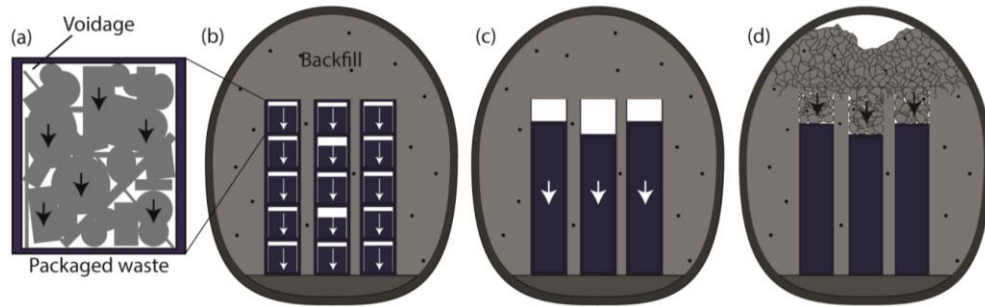
Figure 14 Schematic diagram showing an evolution scenario being considered by NWS for the migration of in-package voidage towards the crown space of a disposal vault. (a) in-package voidage; (b) collapse of waste packages; (c) collapse of waste package stacks; (d) crown voidage caused by backfill failure (Corral et al., 2022). The relevance to monitoring considered here is relating to data loggers.

Relevant Monitoring System Components	**Relevant Monitoring System Components: data loggers.**
	The potential relevance of a monitoring system component is dependent on its size, compressibility, and degradation products. The size, compressibility and degradation products may be considered together as void potential. The component must have the potential to cause a significant void to be relevant. Only a data logger is determined to be significantly large to potentially cause a collapse. Data loggers size varies from several centimetres to up to a metre in width and height. Corrosion and degradation may reduce the strength of the data logger components. In order to be relevant, a data logger must have been left in-situ during backfilling (see mitigations).
Potential Relevance to Performance and Long-Term Safety	A collapse event is characterised by initiation, propagation, coalescence and opening of fractures and migration of voids. A collapse event can affect engineered barriers and host rock overlying the original location of the data logger. The extent to which fractures propagate during collapse will be related to the void potential of the data logger, mechanical properties of the engineered barriers and host rock, and texture of the engineered barriers and host rock (e.g., bedding). It is unlikely that fractures will propagate to and affect overburden rock because of the limited size and compressibility of data loggers.
	A collapse event may be treated like an excavated damage zone. Indeed a collapse is likely to interact with existing excavation damage zones. Therefore, the relevance to long-term safety is a likely increase in permeability. Collapse may also offset an entire barrier such that a fast pathway diverges past that barrier (see FEP 3 Pathway generation).
Examples of the FEP	No known examples. An example is unlikely to arise during experimentation because there is no need to backfill around a data logger and leave it for a duration over which a collapse is likely.
Mitigations	Collapse as a consequence of a data logger can be mitigated by removing the data logger prior to backfilling. However, the data logger may still be required to collect data after backfilling. Alternatively, the data logger may be moved to the surface, possibly assisted by wireless technologies. This would remove the need to have a void for the data logger altogether. If a data logger is going to be left underground, then miniaturisation to reduce the void potential would reduce the risk of collapse. Similarly using a bentonite backfill around the data logger could also reduce the risk of collapse by swelling into the void, however, the swelling could cause the (partially mitigated) collapse to occur sooner.
Links to other FEPs	Links to FEP 3 Pathway generation and FEP 8 Volume change.

EURAD (Deliverable n° 17.10) - Monitoring FEPs: Potential Impacts of Monitoring Equipment on Post-Closure Safety
Dissemination level: Public
Date of issue of this report: **04/06/2024**

Page 38

Comments	
References	J. Corral, F. Dedecker, M. Tovey, P. Main, M. Camusso, and D. Holton (2022). Consideration of Voidage in the GDF and Related Potential Implications: Further Studies: Phase 2 modelling report. Issue 0.1, 208261WN / P2MR.
Title	**10. Corrosion of monitoring system components**
Category	Process
Description	Corrosion is the evolution of metals under non-equilibrium conditions. Example chemical reactions in the metal anaerobic corrosion process*:* • *$3Fe + 4H_2O \rightarrow Fe_3O_4 + 4H_2$* • *$Fe + 2H_2O \rightarrow Fe(OH)_2 + H_2$* • *$3Fe(OH)_2 \rightarrow Fe_3O_4 + 2H_2O + H_2$*
Relevant Monitoring System Components	**Relevant Monitoring System Components: all metallic components installed underground.** Of particular interest to monitoring system evolution is the corrosion of ferric based components under anaerobic conditions. Accelerometers and electrodes placed surrounding a barrier in significant number and size (cm—dm per unit and including several materials, e.g. aluminium, steel, nickel) may be particularly relevant. Thin components will have a high rate of corrosion but low total production of corrosion products because they have a high surface area to mass ratio.
Potential Relevance to Performance and Long-Term Safety	Corrosion will cause volume change (FEP 8), generate gas (FEP 13) and cause chemical interactions (FEP 14). Corrosion rate is dependent on the material and overall conditions. The overall materials list must be considered. Corrosion products can be seen in the vicinity of the source, i.e., they are not restricted to the metallic source. However, corrosion products on a barrier are unlikely to have an impact on its long-term safety.
Examples of the FEP	Corrosion has been observed related to the FEBEX experiment but is limited due to low supply of water. Retrieved sensors showed good conditions in general but a few had external corrosion signs (Rey et al. 2016). Figure A6 shows corrosion in different areas on and in the vicinity of the extensometer anchorage. Corrosion of monitoring system components has also been observed within the Prototype repository.

EURAD (Deliverable n° 17.10) - Monitoring FEPs: Potential Impacts of Monitoring Equipment on Post-Closure Safety
Dissemination level: Public
Date of issue of this report: **04/06/2024**

Page 39

Figure 15 Photograph showing corrosion areas on and in the vicinity of an extensometer anchorage used in the FEBEX experiment (García-Siñeriz et al., 2016).

Mitigations	Choosing particular grades of ferric materials or alternative metals, e.g. titanium, nickel according to the expected conditions. Coatings designed to protect the underlying material.
Links to other FEPs	FEP 3 Pathway generation, FEP 8 Volume change, FEP 13 Gas generation, and FEP 14 Chemical interactions.
Comments	
References	J.L. García-Siñeriz, M.R. Mazón, F. Kober, T. Sakaki, 2019. Performance of THM monitoring instrumentation in FEBEX bentonite barrier after 18 years of operation under repository-like conditions, *Geomechanics for Energy and the Environment*, **17**, 75–89, ISSN 2352-3808, https://doi.org/10.1016/j.gete.2018.09.008. J.L. García-Siñeriz, H. Abós, V. Martínez,C. De la Rosa, U. Mäder and F. Kobe (2016). FEBEX DP: Dismantling of heater 2at the FEBEX "in situ" test. Description of operations. Arbeitsbericht NAB 16-11.
Title	**11. Electrochemical effects**
Category	Process
Description	Three electrochemical effects are considered: galvanic corrosion, electrical treeing, and electricity releases. Galvanic corrosion is an electrochemical process in which one metal corrodes preferentially when it is in electrical contact with another, in the presence of an electrolyte. When metals with different electrode potentials and an electrolyte are in contact, the metal that is more reactive acts as an anode and the metal that is less reactive acts as a cathode. The electropotential difference between the reactions at the two electrodes is the driving force for an electrochemical attack on the anode metal, which dissolves into the electrolyte. This leads to the metal at the anode experiencing an enhanced corrosion rate. The presence of an electrolyte and an electrical conducting path between the metals is essential for galvanic corrosion to occur. High voltage loads with partial discharges can damage insulating materials such as dielectrics, which degrade via electrical treeing caused by prolonged electrical field

EURAD (Deliverable n° 17.10) - Monitoring FEPs: Potential Impacts of Monitoring Equipment on Post-Closure Safety
Dissemination level: Public
Date of issue of this report: **04/06/2024**

Page 40

stress. Electrical treeing progresses through the stressed dielectric insulation in a path resembling the branches/roots of a tree.

Thirdly, introducing electricity into the system which could affect redox conditions.

Relevant Monitoring System Components	**Relevant Monitoring System Components: all metallic components installed underground, power and data transmission cables and electrical sources.** Galvanic materials and those which introduce electricity into the system. Galvanic coupling between different metallic materials can be internal within a monitoring system or external between the monitoring system and other metal components.
Potential Relevance to Performance and Long-Term Safety	Galvanic coupling between different metallic materials could increase corrosion rates (FEP 10). Small currents related to monitoring system components are not expected to be significant but are an unknown. Treeing of solid high-voltage cable insulation is a common breakdown mechanism and source of electrical faults in underground power cables. Electrochemically enhanced degradation of cables can lead to pathway generation (FEP 3) as covered in FEP 12 Degradation.
Examples of the FEP	No known examples.
Mitigations	This process is typically mitigated by material selection and fit for purpose cabling systems. Steel and iron components can be galvanized (applying a protective zinc coating) to prevent corrosion.
Links to other FEPs	FEP 10 Corrosion, FEP 12 Degradation and FEP 14 Chemical interactions.
Comments	
References	
Title	**12. Degradation**
Category	Process
Description	Degradation is the breakdown of non-metallic materials within the monitoring system. This is likely to be include an inherent volume change (FEP 8). The degradation products may include reactive chemicals, e.g., acids, that may contribute to contamination (FEP 15) and/or gases (FEP 13). Plastic polymer degradation is the reduction in the physical properties (e.g., strength, malleability) of a polymer caused by changes in its chemical composition. Polymers are subject to degradation at all stages of their life cycle. The rate of this degradation varies significantly; biodegradation can take decades. Heat, light, air and water are significant factors in the degradation of polymers. The major chemical changes are oxidation and chain scission, leading to a reduction in the molecular weight and degree of polymerization of the polymer. Heating polymers can cause damaging chemical changes (thermal degradation) usually starting with chain scission. PVC is the most thermally sensitive common polymer, with major degradation occurring from ~250 °C. Many electric items, e.g., high-voltage cables, operate at elevated temperatures for years which can cause low-level but continuous thermal oxidation. This can be

EURAD (Deliverable n° 17.10) - Monitoring FEPs: Potential Impacts of Monitoring Equipment on Post-Closure Safety
Dissemination level: Public
Date of issue of this report: **04/06/2024**

Page 41

	exacerbated by direct contact with metals, which can promote the formation of free-radicals (Fenton reactions).
Relevant Monitoring System Components	**Relevant Monitoring System Components: all non-metallic components in the system.**
	Primarily refers to organic materials, e.g. polymers, plastics, resins, glue, PVC, but also for example glass. Organic materials are contained in cable insulation. This FEP includes materials used during installation of monitoring systems and which are left in the repository.
Potential Relevance to Performance and Long-Term Safety	Degradation of cable insulation may cause pathway generation. In particular if the cable degradation is accompanied by a volume decrease (FEP 8) or if the degradation products are mobile, then the original cable location is likely to become a pathway.
	Degradation may create an additional gas (e.g., CO_2, methane) source term (FEP 13).
	Chemical interactions can form acids and a range of complexants. Acids could for example react with cementitious materials affecting porosity. Complexants (e.g. acetate) could themselves degrade further giving rise to gas and/or influencing radionuclide mobility (changing sorption and solubility).
	Degradation products may act as a nutrient for microbial activity (FEP 16).
	Degradation may increase or decrease the volume of the system (FEP 8).
	In each case except pathway generation the relevance is dependent on the amount of degradation (mass balance). In the case of pathway generation the relevance is also dependent on whether barriers are bypassed by the pathway.
Examples of the FEP	Plastic components were interpreted to provide nutrients for microbial activity in the MINICAN experiment at Aspo Hard Rock Laboratory, which is a high sulphate environment (TR-12-09).
	H_2S observed in boreholes has also been interpreted to be related to increased microbial activity.
Mitigations	Degradation risks can be mitigated by choice of materials fit for the environment. For example, preference towards slow kinetics materials.
	Technologies have been developed to both inhibit or promote degradation. Polymer stabilizers extend the useful lifespans of plastics. Conversely, biodegradable additives accelerate the degradation of plastics.
Links to other FEPs	Links to FEP 3 Pathway generation, FEP 8 Volume change, FEP 13 Gas generation, FEP 14 Chemical interactions (e.g. complexation), FEP 15 Contamination, and FEP 16 Microbial activity.
Comments	
References	Amec Foster Wheeler, 2015. Determination of G-values for use in SMOGG gas generation calculations. RWMD/03/037.
	N. Smart, A. Rance, B. Reddy, P. Fennell, R. Winsley, 2012. Analysis of SKB MiniCan. Experiment 3. SKB TR-12-09.
Title	**13. Gas Generation**
Category	Process

EURAD (Deliverable n° 17.10) - Monitoring FEPs: Potential Impacts of Monitoring Equipment on Post-Closure Safety
Dissemination level: Public
Date of issue of this report: **04/06/2024**

Page 42

Description	Gas generation relating to corrosion and degradation of monitoring system components and radiolytic gas generation. The gases generated depend on the materials undergoing corrosion and degradation. Example chemical reactions in the metal anaerobic corrosion process*:*
	$3Fe + 4H_2O \rightarrow Fe_3O_4 + 4H_2$ $Fe + 2H_2O \rightarrow Fe(OH)_2 + H_2$ $3Fe(OH)_2 \rightarrow Fe_3O_4 + 2H_2O + H_2$
Relevant Monitoring System Components	**Relevant Monitoring System Components: all components installed underground.** For example, centimetre-scale sensors, metre scale sensors, accelerometers and geophones, and electrodes are identified as potential source terms for gas generation. Radiolytic gas generation is related to radioisotope thermoelectric generators.
Potential Relevance to Performance and Long-Term Safety	Gas generation is an important consideration for the performance and long-term safety of a geological disposal facility since it can lead to the release of radioactive gases, chemically toxic gases, and flammable gases. Furthermore, gas generation can lead to the pressurisation of a geological disposal facility after closure, however, the potential volumes of gas generated from monitoring components will be small and associated pressurisation is unlikely to be relevant.
Examples of the FEP	No known examples. It is likely to be difficult to detect gas generation due to the relatively short durations of field experiments compared to relevant (e.g. corrosion) rates.
Mitigations	Choice of materials, e.g. using slow kinetics materials. Choosing particular grades of ferric materials or alternative metals, e.g. titanium, nickel according to the expected conditions. Using coatings designed to protect the underlying material, including for example, applying a protective zinc coating to iron and steel components (galvanisation).
Links to other FEPs	Related to FEP 5 Gas Transport, FEP 10 Corrosion, FEP 12 Degradation, and FEP 16 Microbial activity.
Comments	
References	
Title	**14. Chemical Interactions**
Category	Process
Description	Chemical interactions are defined as those between corrosion and degradation products of monitoring system components with other components of the repository including wasteform, engineered barriers and host rock. Examples could be:
	- Complexation, the process of forming an ion or an electrically neutral molecule. Complexation is of particular interest if it involves radionuclides or chemically toxic substances. - Generation of corrodents, typically hydrogen sulphide through microbial processes and degradation of organic compounds. - Alteration, including redox reactions, mineralogical changes through acid formation, dissolution.

![eurad logo] European Joint Programme on Radioactive Waste Management

EURAD (Deliverable n° 17.10) - Monitoring FEPs: Potential Impacts of Monitoring Equipment on Post-Closure Safety
Dissemination level: Public
Date of issue of this report: **04/06/2024**

Page 43

Relevant Monitoring System Components	**Relevant Monitoring System Components: all components installed underground.** Similar to for FEP 10 Corrosion and FEP 12 Degradation. Of particular interest to monitoring system evolution is ferric based components under anaerobic conditions and organic materials. This FEP includes materials used during installation of monitoring systems and which are left in the repository.
Potential Relevance to Performance and Long-Term Safety	Complexation may affect radionuclide and chemically toxic substance transport and of particular interest may increase mobility. Corrodents may have reduced durability (see FEP 10 Corrosion). Alteration may affect barriers and host rock, e.g. change porosity, change of swelling properties, change of hydro-mechanical properties, change sorption capacity. All materials list for system must be considered, however, in consideration of the monitoring system components these effects are likely to be small. This is strongly linked to the overall environmental condition and repository concept.
Examples of the FEP	It is likely to be difficult to detect examples of chemical interactions due to low rates and relatively short duration field experiments.
Mitigations	Choice and mass of materials. Choosing particular grades of ferric materials or alternative metals, e.g. titanium, nickel according to the expected conditions. Mitigations must be fit for the environmental conditions.
Links to other FEPs	FEP 10 Corrosion, FEP 12 Degradation, and FEP 16 Microbial Activity.
Comments	Iron-bentonite interaction halos were observed in the FEBEX experiment, however, in this example the iron source was not monitoring system components.
References	

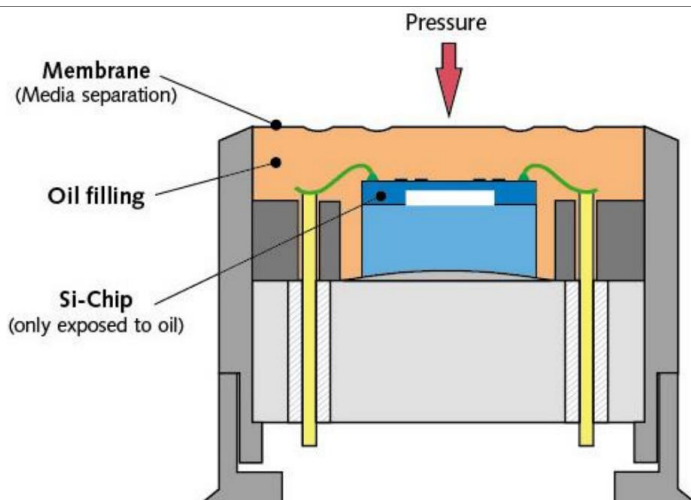|	
Title	**15. Contamination**
Category	Feature
Description	Contamination is considered here as the addition of a hazardous material for a monitoring purpose. For example, the hazardous material may be a working component of the monitoring technology. The hazardous material may initially be fully encapsulated within the monitoring system but have a risk of being released over safety case timescales due to volume change (FEP 8), corrosion (FEP 10) and/or degradation (FEP 12) of the monitoring system. A hazardous material may be radioactive or non-radioactive, chemically toxic.
Relevant Monitoring System Components	**Relevant Monitoring System Components: Batteries, RTGs, cm scale sensors.** Chemical batteries may contain toxic metals, such as antimony, arsenic, cadmium, mercury, nickel, selenium, silver, and zinc. They may also contain reactive chemicals, such as sulfuric acid, solvents, acids, caustic chemicals, and electrolytes. RTGs contain radioisotopes by definition, such as americium-241. Total pressure sensors (cm scale sensors) contain liquids that may be considered to be groundwater contaminants, such as oil as illustrated in Figure A7. In some disposal programmes there is currently a requirement that there are no free liquids introduced into the repository. In these disposal programmes the relevant monitoring system components may be extended to all of those that contain liquids.

EURAD (Deliverable n° 17.10) - Monitoring FEPs: Potential Impacts of Monitoring Equipment on Post-Closure Safety
Dissemination level: Public
Date of issue of this report: **04/06/2024**

Page 44

Figure 16 Simplified diagram of a strain gauge sensor (Haines et al., 2020).

Potential Relevance to Performance and Long-Term Safety	Providing a source for potential releases of radiological and non-radiological, chemically toxic substances to the environment. The frequency, location and volume/mass of introduced sources needs to be considered with regards to each safety case.
	These monitoring system components may be a source term for hazardous wastes that might otherwise not have existed in a location within the geological disposal facility, or otherwise may have additive effects to sources of hazardous wastes within a facility. A safety case built around a waste source and pathways from the waste source may risk overlooking these sources with potentially shorter pathways. The bypassing of barriers due to the original location of these sources is potentially significant and could require additional work within safety cases. However, the source terms are unlikely to have significant volumes.
Examples of the FEP	No known examples of contamination from a monitoring system component. The source within monitoring system components for potential contamination should be well characterised. Furthermore the release of those sources from the original housing may be assumed over safety case timescales.
Mitigations	The significance of this FEP is dependent on the choice of materials and their volumes/mass. The FEP may be mitigated by removing toxic metal and reactive chemical components from monitoring system technologies where possible. This may require further research and development to find suitable replacements. The FEP may also be mitigated by reducing the volume/mass of those materials either within a monitoring system component by research and development of the technology or by reducing the total number of those monitoring system components within the monitoring system design.
Links to other FEPs	FEP 14 Chemical interactions.
Comments	
References	Thomas Haines, Matt White, Erik Johansson, Taina Karvonen, José Luis Garcia-Sineriz, Bernd Frieg, Andreas Reinicke, Herwig Müller, Sophie Haapalehto, Tuomas Pere (2021). GDF Monitoring Technologies and Methods in Support of the ESC Monitoring Programme. RWM310.
Title	**16. Microbial Activity**

EURAD (Deliverable n° 17.10) - Monitoring FEPs: Potential Impacts of Monitoring Equipment on Post-Closure Safety
Dissemination level: Public
Date of issue of this report: **04/06/2024**

Page 45

Category	Process
Description	Microbes are ubiquitous and will exist naturally in the far-field rock and in the groundwater. However, the activity of microorganisms in, for example, undisturbed Opalinus Clay is limited by the very low porosity, the low water activity, and the largely recalcitrant nature of organic matter in the claystone formation.
	The process is included here because interactions with monitoring system components may be a new source of drivers (energy and space) for microbial activity. Additionally, microbes can be introduced directly via monitoring system components, but this is unlikely to be significant. Other microbes will be introduced on construction materials and in the air during repository excavation, operation and closure procedures.
	These microbes may affect chemical conditions in the repository and can affect the rates of some reactions. They may also directly affect radionuclide transport by acting as organic colloids. See general FEP description for FEP 3.2.5: Biological processes (IFEP List).
Relevant Monitoring System Components	**Relevant Monitoring System Components: all components installed underground.**
	Stainless steel components are likely to be relatively small hydrogen donors compared to organic components that could be quickly degraded (dependent on size in each case).
	Voids (see FEP 7 Void formation and FEP 8 Volume change) could be preferential sites for microbial activity by providing trapped oxygen.
Potential Relevance to Performance and Long-Term Safety	Microbes may affect chemical conditions in the repository and can affect the rates of some reactions. They may also directly affect radionuclide transport by acting as organic colloids. Results from nearly 15 years of research at the Mont Terri rock laboratory have shown that microorganisms can potentially affect the environment of a repository by influencing redox conditions, metal corrosion and gas production and consumption under favourable conditions (Leupin et al., 2017).
	Reactions are not different to what we might expect for other reasons. However, the location of these will be different to the locations existing for other reasons.
Examples of the FEP	The presence of microorganisms in numerous experiments at the Mont Terri rock laboratory has suggested that excavation activities and perturbation of the host rock combined with additional contamination during the installation of experiments in boreholes create favourable conditions for microbial activity by providing increased space, water and substrates. Thus, effects resulting from microbial activity might be expected in the proximity of a geological repository i.e., in the excavation damaged zone, the engineered barriers, and first containments.

OTU #	BIC-A1/1	BPC-2/1	BDR-T1/1	BDR-T1/2	Taxonomic affiliation	Metabolism type	Reference
0	1.25E-04	0.5124	1.48E-04	1.08E-04	*Desulfocapsa*	Sulfate-reducing bacteria	Kuever *et al.*, 2005
1	1.10E-04	7.05E-05	8.12E-05	7.19E-05	*Novispirillum*	O_2 and NO_3^- respiring bacteria	Yoon *et al.*, 2007
2	0.2594	0.0056	0.0007	0.0006	*Pseudomonas*	O_2 and NO_3^- respiring bacteria	Moore *et al.*, 2006
3	7.05E-05	1.06E-04	4.43E-05	5.03E-05	Rhodobacteraceae	Metabolically diverse	Garrity *et al.*, 2005
4	1.57E-05	5.28E-05	7.38E-06	4.31E-05	Xanthomonadaceae	O_2 respiring bacteria	Saddler and Bradbury, 2005
5	1.57E-05	5.28E-05	0.5684	0.5258	*Pleomorphomonas*	O_2 respiring or fermenting bacteria	Xie and Yokota, 2005
6	0.0416	0.0095	0.2667	0.2824	*Desulfosporosinus*	Sulfate-reducing bacteria	Spring and Rosenzweig, 2006
7	0.0165	1.76E-05	1.48E-05	0.00E+00	*Desulfotomaculum*	Sulfate-reducing bacteria	Auello *et al.*, 2013
9	0.5717	0.0184	0.0083	0.0079	*Desulfotomaculum*	Sulfate-reducing bacteria	Auello *et al.*, 2013
13	7.84E-06	1.76E-05	7.38E-06	2.87E-05	*Methyloversatilis*	Metabolically diverse	Kalyuzhnaya *et al.*, 2006
15	3.92E-05	0.0033	8.86E-05	2.87E-05	*Pseudomonas*	O_2 and NO_3^- respiring bacteria	Moore *et al.*, 2006
17	7.84E-06	0.0018	1.48E-05	7.19E-06	*Thiobacillus*	O_2 and NO_3^- respiring bacteria	Kelly *et al.*, 2005
36	0.0317	0.1268	0.00E+00	4.66E-04	*Desulfosporosinus*	Sulfate-reducing bacteria	Spring and Rosenzweig, 2006
SUM	0.9213	0.6781	0.8446	0.8175			

color scale
1.0000
0.0100
0.0000

Table A1 shows the contribution of each of the 13 microorganisms ubiquitous in Mont Terri rock laboratory borehole waters to the microbial communities in four anoxic

EURAD (Deliverable n° 17.10) - Monitoring FEPs: Potential Impacts of Monitoring Equipment on Post-Closure Safety
Dissemination level: Public
Date of issue of this report: **04/06/2024**

Page 46

boreholes (BIC-A1, BPC-2, BDR-T1/1 and BDRT1/2). For instance, ubiquitous microbes represented more than 92% of the microbial community in BIC-A1, the borehole in which the IC-A experiment was conducted.

Contribution of ubiquitous Operational Taxonomic Units (OTUs) to the microbial communities from borehole water collected from four anoxic boreholes in the Opalinus Clay at the Mont Terri rock laboratory. Taxonomic affiliation and expected metabolism type are indicated. Total contribution of the 13 ubiquitous OTU's to each borehole community is indicated for each sample (last row). Colours indicate the fraction of the OTU's in each borehole (green 0.5–1.0; yellow 0.01–0.5; red 0–0.01) (Modified from Bagnoud (2015))

In addition to Mont Terri, reducing organisms were also found in boreholes at Bure and their activity was interpreted to be caused by cable coating. Furthermore, in the MINICAN experiment, a monitoring equipment plastic holder was interpreted to have provided nutrients for sulphate production.

Mitigations	Choice of materials similar to mitigations for chemical interactions.
Links to other FEPs	FEP 7 Void formation, FEP 8 Volume change, FEP 10 Corrosion, FEP 12 Degradation, and FEP 14 Chemical interaction.
Comments	The scope of these FEPs is to consider how monitoring system components could impact repository performance. However, it should be noted that biofilm associated with microbial activity may interrupt sensor capability.
References	Capouet, Manuel, Carter, Alexander, & Ciambrella, Massimo (2019). International Features, Events and Processes (IFEP) List for the Deep Geological Disposal of Radioactive Waste Version 30 (NEA-RWM-R--2019-1). Nuclear Energy Agency of the OECD (NEA) Olivier X. Leupin, Rizlan Bernier-Latmani, Alexandre Bagnoud, Hugo Moors, Natalie Leys, Katinka Wouters, Simcha Stroes-Gascoyne. Fifteen years of microbiological investigation in Opalinus Clay at the Mont Terri rock laboratory (Switzerland). Swiss J Geosci (2017) 110:343–354. DOI 10.1007/s00015-016-0255-y.
Title	**17. Sound wave propagation**
Category	Process
Description	A sound wave is the pattern of disturbance caused by the movement of energy traveling through a medium (such as air, water or any other liquid or solid matter) as it propagates away from the source of the sound. Sound waves are created by object vibrations and produce pressure waves. This FEP considers an acceleration of the disposal system media caused by sound waves generated at the surface or underground for monitoring but not natural events or construction activities. All frequency ranges and geophysical sources (seismic tomography, seismic, refraction, reflection) are considered. In this context sound waves are typically called seismic waves and categorised by the particle movement associated with them. P-wave particle motion is parallel to the direction of wave propagation. S-wave particle motion is perpendicular to the direction of wave propagation and can be either vertical (S-V) or horizontal (S-H). Surface waves are similar, however, they are strongest at the surface and decay with depth. Love wave particle motion has an S-H component and Rayleigh wave particle motion has P and S-V components. The velocity of P-waves in an elastic, homogeneous, and isotropic medium is:

EURAD (Deliverable n° 17.10) - Monitoring FEPs: Potential Impacts of Monitoring Equipment on Post-Closure Safety
Dissemination level: Public
Date of issue of this report: **04/06/2024**

Page 47

$$v_p = \sqrt{\frac{\lambda + 2\mu}{\rho}}$$

where v_p is P-wave velocity, λ and μ are the Lamé parameters, ρ is density of the medium. The Lamé parameters can be converted to bulk modulus and shear modulus or Young's modulus and Poisson's ratio.

Wave paths may experience reflection or refraction at interfaces between materials that have significantly different acoustic impedances.

Relevant Monitoring System Components	**Relevant Monitoring System Components: seismic source monitoring components.** All active seismic monitoring, e.g., vibroseis trucks, air guns, seismic surveys and underground seismic tomography. Larger sources (e.g., vibroseis trucks and seismic survey air guns) are typically used further away from the GDF. It is not expected that any monitoring system components will generate significant vibrations causing sound waves as an unintentional output. Large bundles of power cables can generate sound waves but it is generally a very small effect. This discharge of energy occurs when the electrical field strength on the conductor surface is greater than the breakdown strength (the field intensity necessary to start a flow of electric current) of the medium surrounding the conductor. This discharge is also related to corona loss (FEP 18 Electromagnetic wave propagation).
Potential Relevance to Performance and Long-Term Safety	The impacts are presumed to be insignificant. The total energy from seismic source monitoring equipment is relatively low compared to other sources, e.g., surface vehicles driving nearby, trains, operations etc. This is in part due to the more frequent nature of those other sources. Furthermore, the effects of seismicity are greater at the surface than underground. Vibrational settling is theoretically possible as a consequence of sound waves but is unlikely given the sources involved.
Examples of the FEP	There have been numerous seismic tomography experiments from which no meaningful effects have been observed.
Mitigations	No mitigations are anticipated to be needed based on the current understanding of the impact.
Links to other FEPs	None.
Comments	
References	

Title	**18. Electromagnetic wave propagation**
Category	Process
Description	Electromagnetic waves are created as a result of vibrations/oscillations between an electric field and a magnetic field. Electromagnetic waves will propagate through a medium such as air, water or any other liquid or solid matter. The electrical conductivity, σ, range of crystalline rock is µS/m to mS/m and of argillaceous rock is mS/m to S/m. The porosity and pore fluid composition of the geological media or EBS component influences the conductivity. The electric conductivity of fresh water is around 10 mS/m to 1 S/m, and the conductivity of saline water can be as high as 1 to 10 S/m.

EURAD (Deliverable n° 17.10) - Monitoring FEPs: Potential Impacts of Monitoring Equipment on Post-Closure Safety
Dissemination level: Public
Date of issue of this report: **04/06/2024**

Page 48

Skin depth, δ, estimates the distance at which a signal is attenuated by a factor of 1/e:

$$\delta[m] = \frac{1}{\sqrt{\pi \cdot f \cdot \sigma \cdot \mu_0}}$$

where f is frequency and μ_0 is the permeability constant (1.257·10⁻⁶ V·s/A·m).

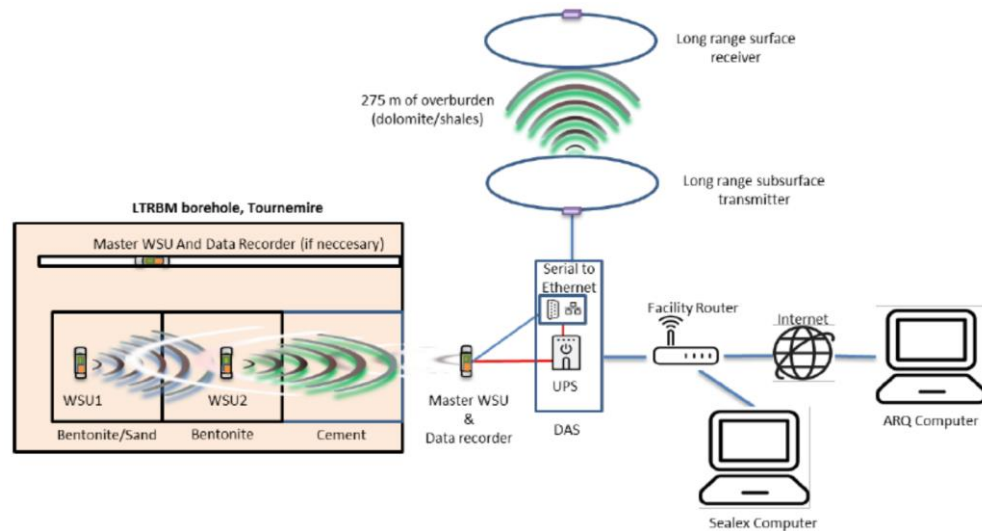|	
Relevant Monitoring System Components	**Relevant Monitoring System Components: Electrical resistivity tomography, wireless data transmission (Figure A8), wireless power transmission.**
	Modern and Modern2020 research on power and data transmission indicates that the most significant effect would be high power requirements for monitoring post-closure but these are not currently included in any known programme. These are emerging technologies with low technology readiness levels (TRLs).,
	Figure 17 Integrated short-range and long-range wireless data transmission from the LTRBM borehole (Tournemire) to the surface (Modern2020, 2019).
Potential Relevance to Performance and Long-Term Safety	This is an emerging technology for which we do not know the impacts. The impacts are presumed to be insignificant.
	The total energy is small for localised activity such as electrical resistivity tomography or small distance wireless data transfer. However, through the earth transmission from the repository horizons to the surface would require larger total energy.
	Transport of species by diffusion in an electric field is likely to be insignificant compared to other advection and diffusion drivers.
Examples of the FEP	No consequences have been evaluated from limited deployments.
Mitigations	No mitigations are anticipated to be needed based on the current understanding of the impact.
Links to other FEPs	FEP 2 Heat generation and FEP 11 Electrochemical effects.
Comments	
References	Modern2020. 2019. Project Synthesis – Repository Monitoring: Strategies, Technologies and Implementation (Deliverable D6.5)

EURAD (Deliverable n° 17.10) - Monitoring FEPs: Potential Impacts of Monitoring Equipment on Post-Closure Safety
Dissemination level: Public
Date of issue of this report: **04/06/2024**

Page 49

EURAD (Deliverable n° 17.10) - Monitoring FEPs: Potential Impacts of Monitoring Equipment on Post-Closure Safety
Dissemination level: Public
Date of issue of this report: **04/06/2024**

Page 50

References

1   Modern2020 (2019). Modern2020 Project Synthesis Repository Monitoring: Strategies, Technologies and Implementation. Work Package 6, Deliverable No D6.5.

2   EURAD Bureau (2023). Update of the EURAD Strategic Research and Knowledge Management Agenda (SRA), of deliverable D1.9 of the HORIZON 2020 project EURAD. EC Grant agreement no: 847593.

3   Nagra (2023). Pilot Repository Monitoring: First Concept Report. Nagra Arbeitsbericht [Working Report] NAB 21-11.

4   NEA (2019). International Features, Events and Processes (IFEP) List for the Deep Geological Disposal of Radioactive Waste. Version 3.0, NEA/RWM/R(2019)1.

5   IAEA (2011). Disposal of Radioactive Waste. Specific Safety Requirements No. SSR-5.

6   MoDeRn (2013). Monitoring During the Stages Implementation of Geological Disposal: The MoDeRn Project Synthesis. MoDeRn Deliverable D6.1.

7   MoDeRn (2013). State of Art Report on Monitoring Technology. MoDeRn Deliverable D2.2.2.

8   T. Haines, M. White, E. Johansson, T. Karvonen, J. Garcia-Sineriz, B. Frieg, A. Reinicke, H. Muller, S. Haapalehto and T. Pere (2023). Technologies and Methods for Monitoring the Geological Disposal Facility during Construction and Operation in Support of the Environmental Safety Case. Galson Sciences Report 2020-3.

9   T. Haines and M. White. (2022): Lessons for Repository Monitoring from Underground Research Laboratory Experiments. Deliverable D17.3 of the HORIZON 2020 project EURAD. EC Grant agreement no: 847593.

10   Nagra (2019). Implementation of the Full-scale Emplacement Experiment at Mont Terri: Design, Construction and Preliminary Results. Nagra Technical Report 15-02.

11   J. Betrand (2015). New Sensors for Repository Monitoring. Modern2020 Deliverable D3.4.

12   J. Betrand (2021). ALC1605 Experiment URL Survey Response. EURAD Work Package 17: MODATS. Final Version.

13   J. Saari and M. Malm (2014). Seismic Network at the Olkiluoto Site and Microearthquake Observations in 2002 – 2013. Working Report 2014-20.

14   S. Haapelehto, M. Malm, O. Kaisko, S. Marila, and V. Saarinen (2020). Results of Monitoring at Olkiluoto in 2019. Rock mechanics. Posiva Working Report 2020-47.

15   ETH Zurich and NDA (2013). Seismic Tomography at Grimsel Test Site. MoDeRn Deliverable D3.2.1.

16   K. Schuster, M. Furche, H. Shao, J. Hesser, J. M. Hertzsch, W. Graesle and D. Rebscher (2019). Understanding the Evolution of Nuclear Waste Repositories by Performing Appropriate Experiments – Selected Investigations at Mont Terri Rock Laboratory. Advances in Geosciences, Volume 49, Pages 175-186.

17   T.J. Schröder, E. Rosca-Bocancea, J.L. García-Siñeriz, G. Hermand, H.L. Abós Gracia, J.C. Mayor Zurdo, J. Verstricht, P. Dick, J. Eto, M Sipilä and J.-M. Saari (2019). Wireless data Transmission Systems for Repository Monitoring. Modern2020 Deliverable D3.2.

18   A. Reinicke (2021). GAST – Gas Permeable Seal Test URL Survey Response. EURAD Work Package 17: MODATS. Final Version.

19   MoDeRn (2013). Development Report of Monitoring Technology. MoDeRn Deliverable D2.3.1.

20   E. Strömmer, H. L. Abós Gracia, F. Alvarez, P. Forbes, E. Rosca-Bocancea and T. Schröder (2018). Long-Term Power Supply Sources for Repository Monitoring. Modern2020 Deliverable D3.3.

EURAD (Deliverable n° 17.10) - Monitoring FEPs: Potential Impacts of Monitoring Equipment on Post-Closure Safety
Dissemination level: Public
Date of issue of this report: **04/06/2024**

Page 51

21   A. W. Fihelly and C. F. Baxter (1970). The SNAP-19 Radioisotope Thermoelectric Generator Experiment. IEEE Transactions on Geoscience Electronics, Vol. GE-8, No. 4.

22   DOPAS (2016). POPLU Experimental Summary Report. DOPAS Deliverable D4.5.

EURAD (Deliverable n° 17.10) - Monitoring FEPs: Potential Impacts of Monitoring Equipment on Post-Closure Safety
Dissemination level: Public
Date of issue of this report: **04/06/2024**

Page 52